PRATHAM
IIT BOMBAY STUDENT SATELLITE

Report
Critical Design Review

By

Pratham Team

Department of Aerospace Engineering,

Indian Institute of Technology, Bombay

December 2015

Contents

List of Tables

List of Figures

Chapter 1

Introduction

1.1 Vital Statistics about Pratham

Pratham is the first Student Satellite being built under the IIT Bombay Student Satellite Project. Some of the vital statistics about the Satellite are as follows:

- Mass: 9.7 kg (without FE Ring of mass 0.6 kg)
- Size: 29.4 cm X 31.5 cm X 46.0 cm (Including Pre-deployed monopoles)
- LVI from VSSC (IBL230V2)
- Solar Panels (4 sides)
- Orbit: 10:30 polar sun-synchronous
- Material of side panel: AL6061-T6
- Downlink at frequency 437.455 MHz
- Beacon at frequency 145.98 MHz
- Uplink at frequency 437.455 MHz
- Completely autonomous (except reset and kill switch)

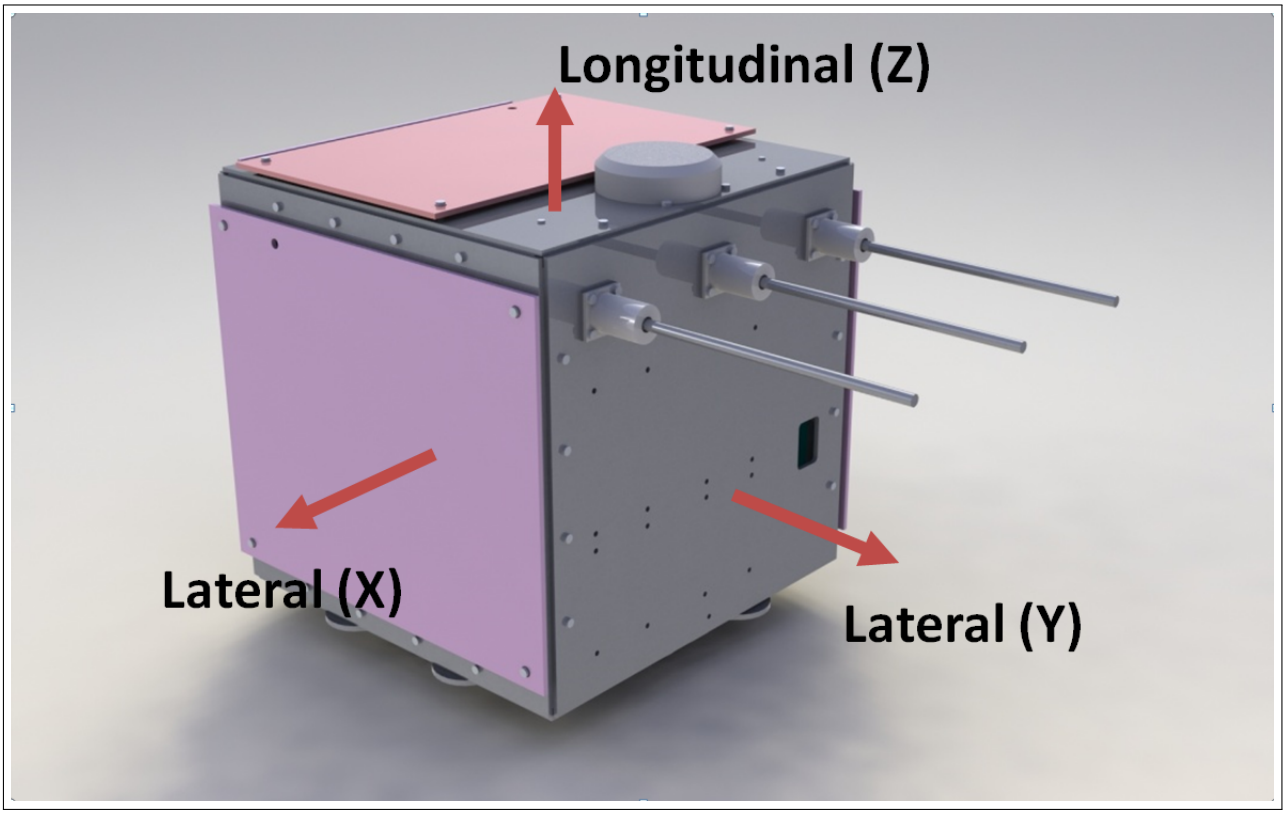

Figure 1.1: Pratham's Engineering Drawing with Axis Definition of Testing

Axes	Simulation	Testing
X	Lagging to Leading	Leading to Lagging
Y	Nadir to Zenith	Anti-sunside to Sunside
Z	Sunside to Anti-sunside	Nadir to Zenith

Table 1.1: Axis Definition

Chapter 2

Mission Statement for Pratham

2.1 Mission Statement and Success Criterion

The Mission for Pratham, IIT Bombay's First Student Satellite is:

1. Acquiring knowledge in the field of Satellite and Space Technology
2. Have the Satellite entirely designed by the student body of IIT Bombay
3. Have the satellite launched, Measure TEC of the Ionosphere above IITB
4. Involve students from other universities in our Satellite project

When all the 4 mission statements are fully satisfied, we can call our satellite to a complete success (100%). The IITB Student Satellite Team has attached a lot of importance to all the mission statements. The Success Criterion for the Project is shown in table 2.1.

Description	Mission Success
Flight Model ready	85%
Beacon Signal received	90%
TEC measurements at IITB	95%
Satellite functional for 4 months	100%

Table 2.1: Success Criterion

Chapter 3

Payload Subsystem

3.1 Introduction

TEC is the Total Electron Count of the Ionosphere. It refers to the total number of electrons in a cylinder of unit area of cross section extending from the ground station up to our satellite in space. TEC values are one of the most prominent sources of information for understanding the structure and dynamic behavior of the ionosphere. However, since there is a fraction of the ionosphere (about 5%) above the altitude of our satellite, what we wish to measure is known as the Ionosphere Electron Count.

3.2 Importance of TEC

- Error correction for GPS systems
- Tsunami warning

3.3 Techniques for measurement of TEC from LEO satellite

3.3.1 Measurement of Faraday rotation of polarization angle

When a linearly polarized radio wave passes through an ionized medium with a magnetic field in the direction of propagation, the plane of polarization rotates. This effect is called Faraday rotation. The relation between the rotation angle and the TEC is given by:

$$\Delta\phi = 4.87 \times 10^4 f^{-2} \int_{h_1}^{h_2} NB\ cos\theta\ dl \tag{3.1}$$

where N = electron density, B = magnetic field of earth, θ = angle between the radio wave and line of sight, $\Delta\phi$ = angle of rotation, f = frequency of the wave

Measurement process: In order to radiate linearly polarized waves from the satellite, we plan to use a monopole antenna. We will be measuring the angle of polarization at the ground station by using a crossed Yagi antenna and measuring the intensities of the signals at the two feeds. The ratio of these intensities will give us the polarization angle.

Measurement of phase angle by AD8302: We plan to measure relative intensities of the radio waves by an Analog Devices chip AD8302. This IC takes two inputs INPA and INPB and gives a voltage o/p proportional to the level ratio of these signals in dB.

In addition the pin VPHS gives the phase difference between the signals at the INPA and INPB. The output of the AD8302 is given by:

$$V = 20 \log_{10} \tan\theta \tag{3.2}$$

where, θ is the plane of polarization

$$\theta = \tan^{-1}(10^{\mathrm{V}/20}) \tag{3.3}$$

OR

$$\theta = \pi - \tan^{-1}(10^{\mathrm{V}/20}) \tag{3.4}$$

To resolve this ambiguity, we need to use the phase difference information.

- If the output is close to 30 mV then (3.3) is true.
- If the output is close to 1.8 V then (3.4) is true.

This chip gives ± 0.3 dB error for magnitude ratios within ± 20 dB.

3.3.2 Simulations

Here we describe the simulations for determining the value of Faraday rotation of polarization due to a typical ionosphere. We know that the Faraday rotation of a linearly polarized wave propagating through the ionosphere is given by:

$$\Delta\phi = 4.87 \times 10^4 f^{-2} \int_{h_1}^{h_2} NB\ cos\theta\ dl \tag{3.5}$$

where N = electron density, B = magnetic field of earth, $\hat{\mathrm{I}}_{\text{›}}$ = angle between the radio wave and line of sight, θ = angle of rotation, f = frequency of the wave
The magnetic field values were obtained from
http://www.ngdc.noaa.gov/geomagmodels/IGRFWMM.jsp

We assumed the vertical profile of electron density also to be the same over all the places. This gave us the following graphs of rotation angles vs. elevation angle and angle with the east direction respectively.

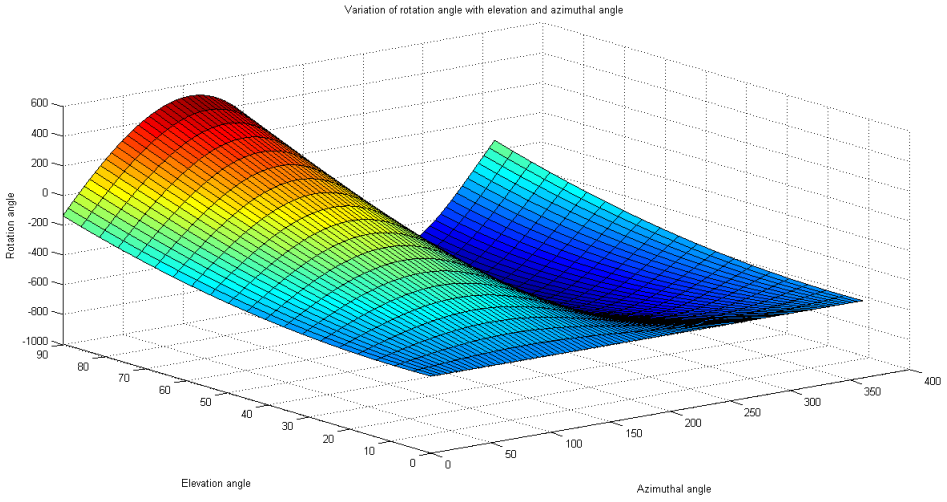

Figure 3.1: 3-D plot showing variation with respect to phi and theta

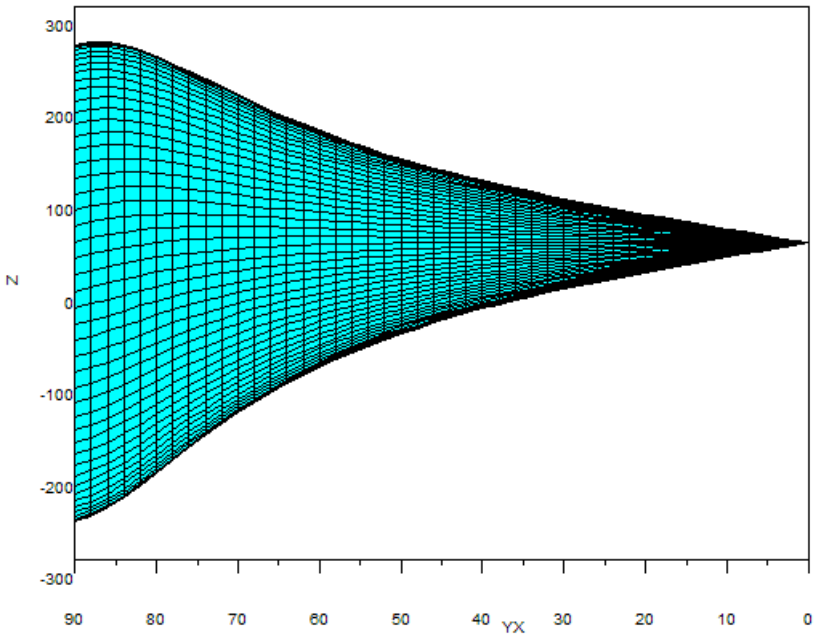

Figure 3.2: Constant phi plots (Phi contours)

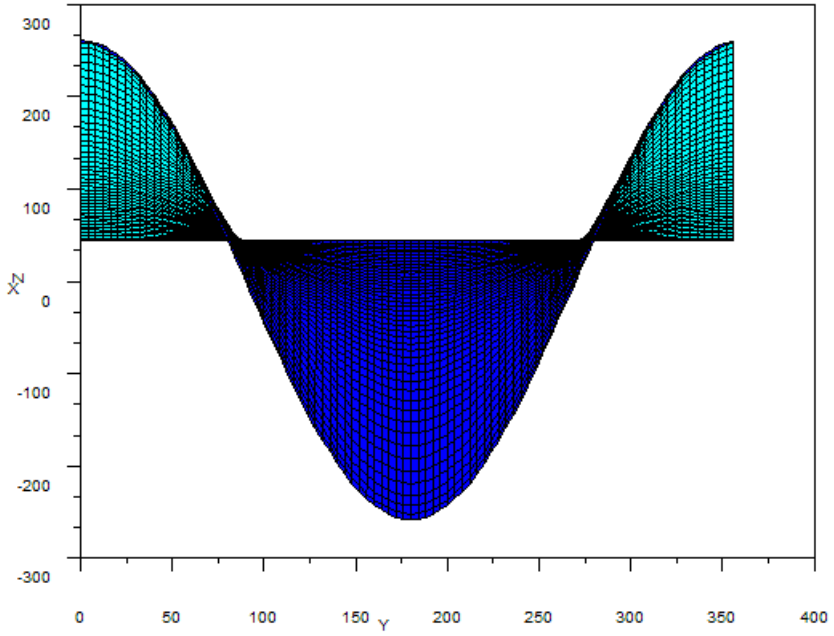

Figure 3.3: Constant theta plots

Chapter 4

Configuation and Layout

The internal and external configuration of the satellite is shown in Figure 4.1 and Figure 4.2 respectively.

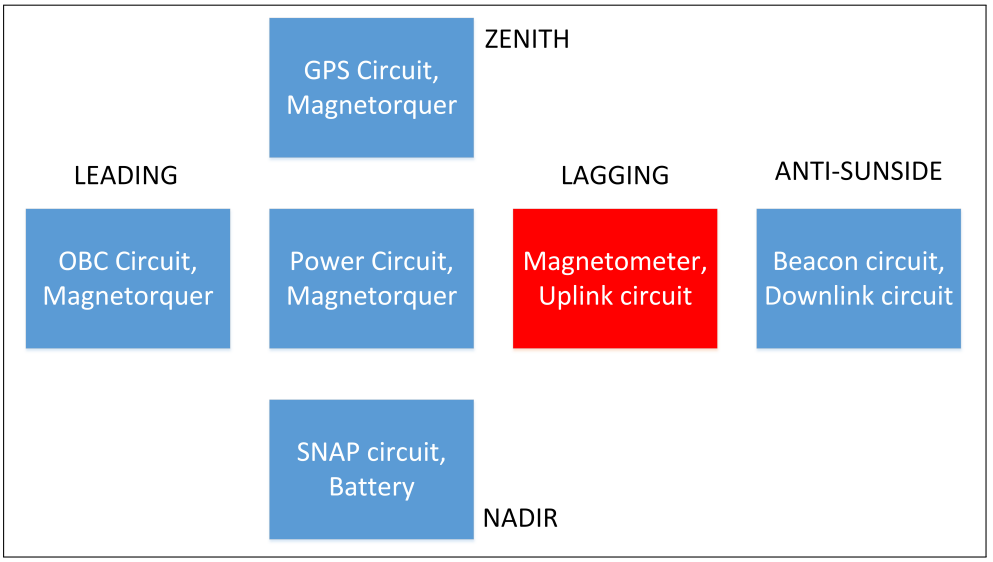

Figure 4.1: Internal Configuration Layout

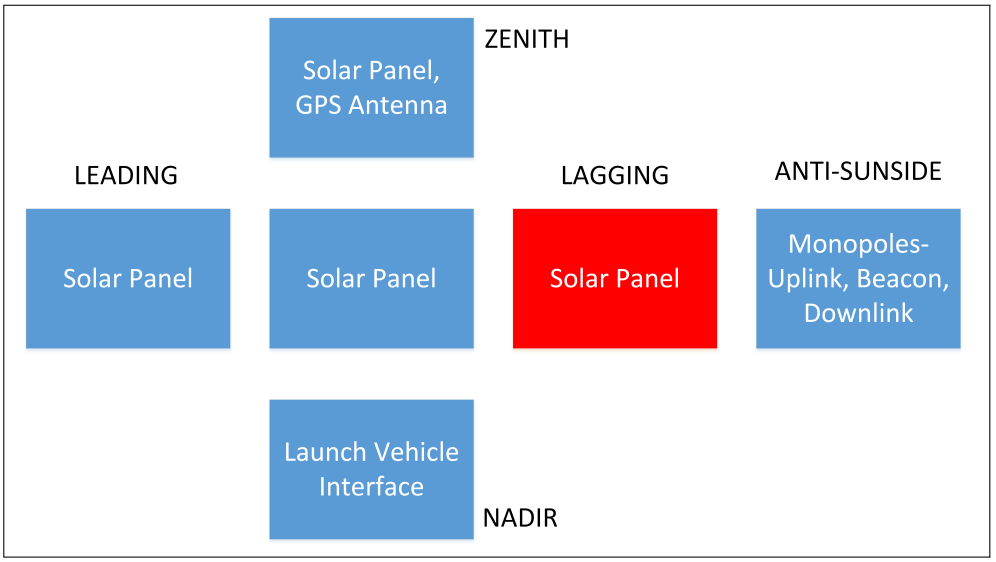

Figure 4.2: External Configuration Layout

The entire satellite structure was modeled in CAD software. The inside view is shown in Figures 4.3 and 4.4.

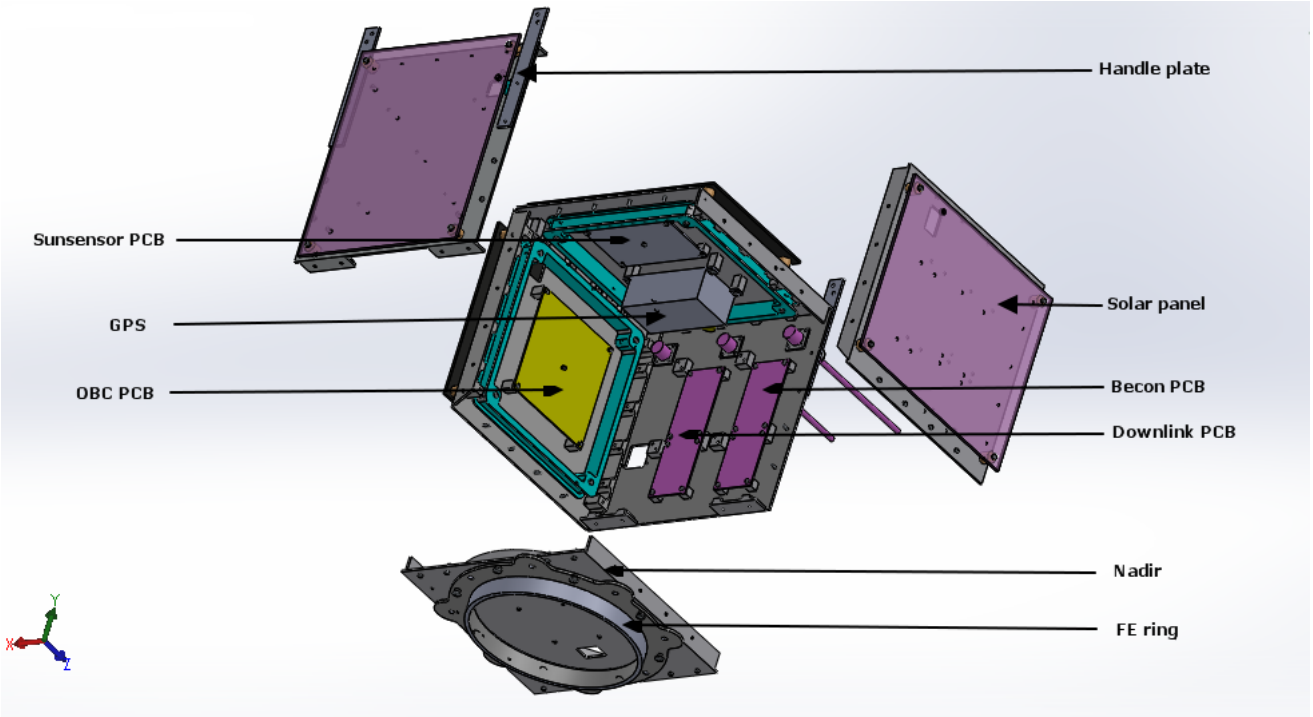

Figure 4.3: Satellite Model: Exploded View

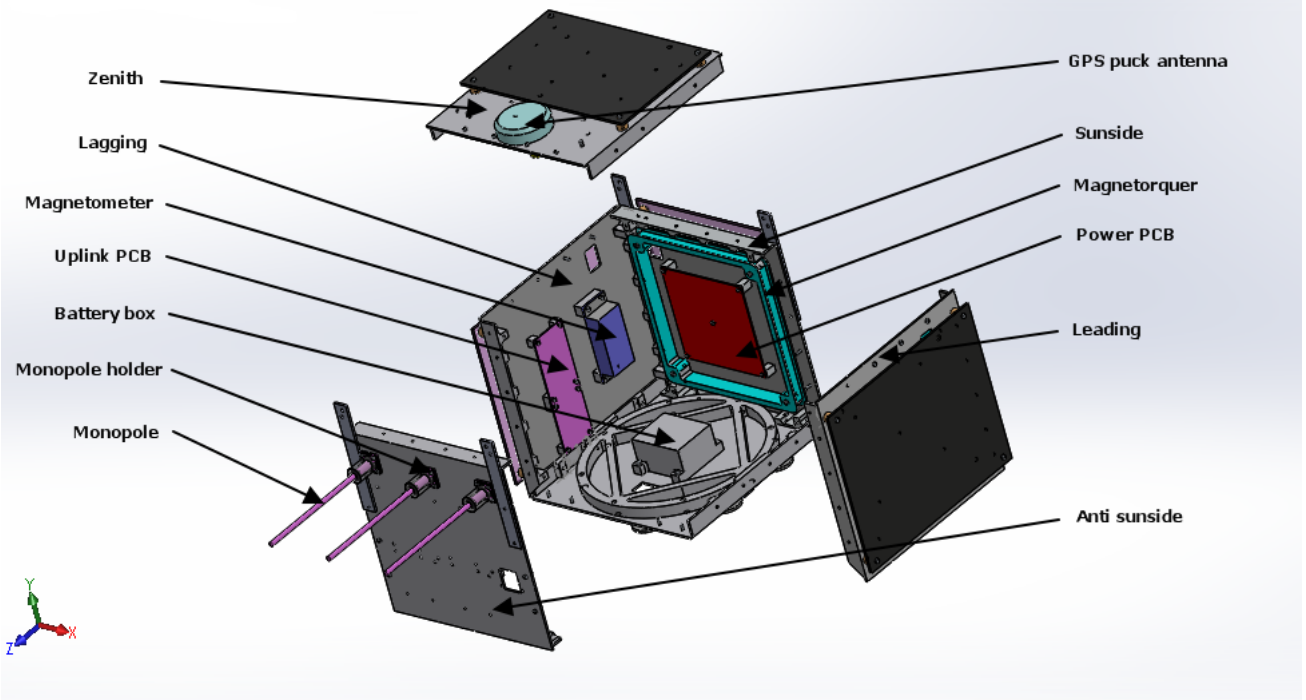

Figure 4.4: Satellite Model: Exploded View

Chapter 5

System and Sub-System Requirements

A V-Model, as shown in Fig. 5.1, was used to find the System and Sub-System Requirements.

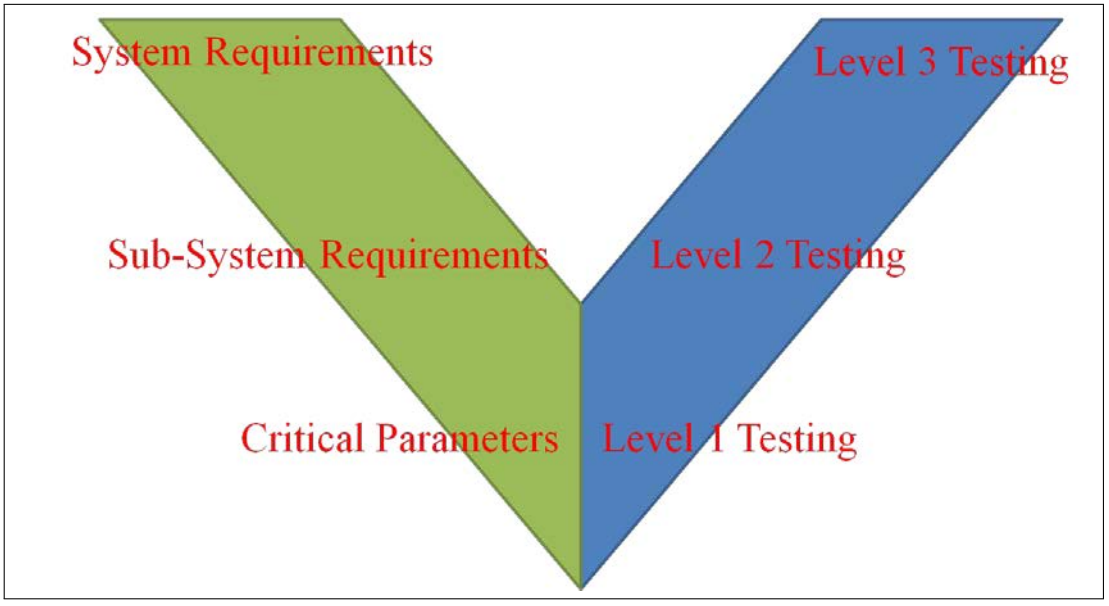

Figure 5.1: V Model

The mission statement and the environment (space, launch vehicle, etc.) give rise to system requirements. These system requirements are handed down to the individual sub-systems. The sub-systems also interact with each other to give sub-system requirements. Finally from all these requirements come the critical parameters which the individual sub-systems have to design and satisfy. similarly, the critical parameters are tested by the sub-systems in level 1 testing. 2-3 sub-systems get together and do level 2 testing where the interactions between these sub-systems are checked. The final satellite level testing is done in level 3 testing like vibration testing, etc.

5.1 System Requirements on the Sub-Systems

The System Requirements on the individual sub-systems is written below

Requirements on the Payload Sub-System from the System

- Payload sub-system shall measure the Total Electron Count (TEC) of Ionosphere above IIT Bombay with 0.1 TEC units accuracy.

Requirements on the Communication and Ground Station Sub-System from the System

- Communication sub-system shall transmit with the 1st monopole (Beacon) all over the world at a certain duty cycle (50%).
- They shall transmit data from the Satellite over India, using the 2nd monopole to the ground station at 1.2 kbps.
- They shall setup a ground station at IIT Bombay.
- They shall design low-cost ground stations for other universities.

Requirements on the Attitude Determination and Controls Sub-System from the System

- Attitude Determination and Controls sub-system shall stabilize the attitude within $\pm 10^o$ accuracy along all axes.
- They shall measure the instantaneous position of the Satellite in orbit to 1 kilometers accuracy.

Requirements on the On Board Computer Sub-System from the System

- On Board Computer sub-system shall carry out pre-launch checks of the Satellite before launch.
- They shall store the telemetry data on-board the Satellite when in orbit. The telemetry data shall contain:
  - Position data
  - Voltages and currents of critical components
  - Temperature data of hot-spots

Requirements on the Power Sub-System from the System

- Power sub-systems shall recharge the batteries before launch using external charger.
- They shall detect the deployment of the satellite into orbit using the deployment switch.
- They shall trap the solar power falling on the satellite and store it in batteries.

Requirements on the Structures Sub-System from the System

- Structures sub-system shall make the satellite frame such that it can withstand the launch loads (Tables 14.2 and 14.3)
- They shall make the satellite frame such that it can withstand the orbital thermal loading.

Requirements on the Mechanism Sub-System from the System

- Mechanisms sub-system shall make/use the Launch Vehicle Interface to be provided by VSSC and attach it to the main frame of the Satellite.
- They shall detect the separation of the satellite and the launch vehicle using the deployment Switch (SNAP circuit) which will switch on the power circuit.
  - The SNAP circuit should draw very low current (∼10microA)
  - The SNAP circuit should not trigger on due to the launch vibrations

Requirements on the Integration Sub-System from the System

- The integration team shall provide the following ports necessary for the pre-flight checks, charging the batteries and during deployment of the satellite:
  - Access Port
  - Battery Charger

5.2 Requirements on one Sub-System from another Sub-System

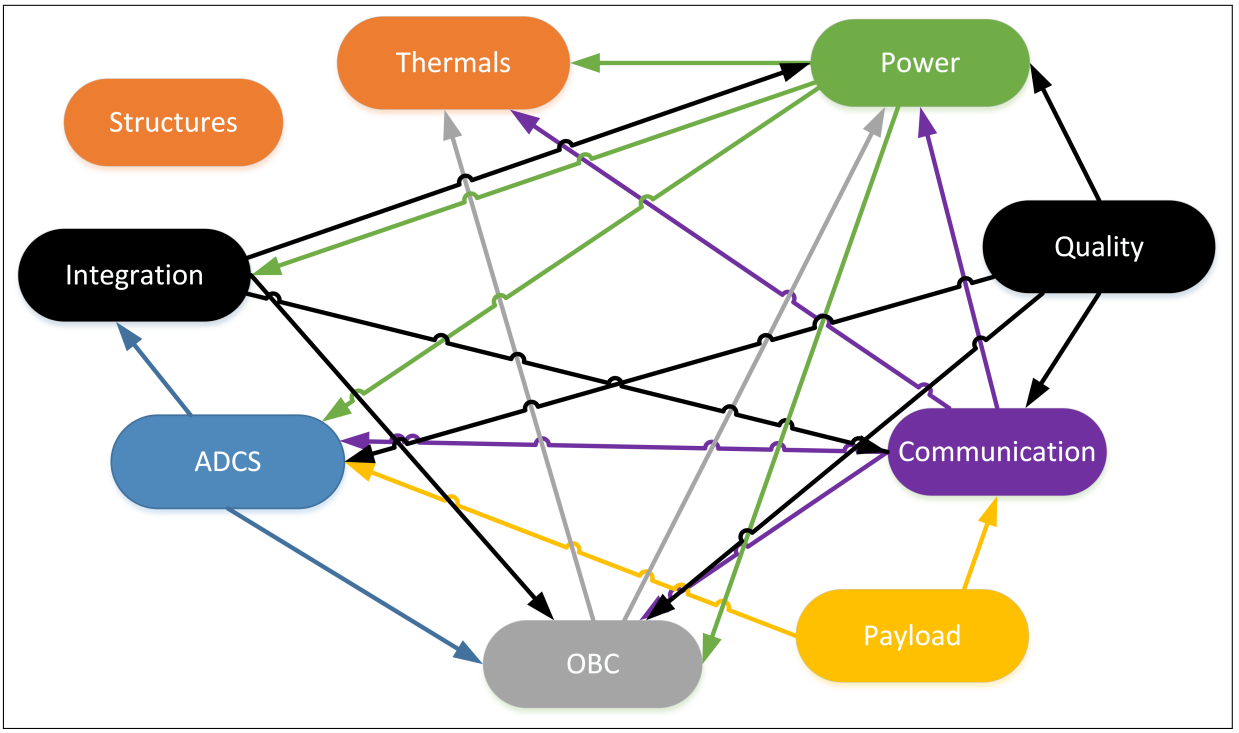

Figure 5.2: Sub-System to Sub-System Requirements

Chapter 6

Structure Subsystem

6.1 Modeling

1. The entire satellite structure, including the body, panels and other components on-board, was modeled using CAD software.

2. The joints were modeled using the "mate" function. In this model, the contact were assumed only at the position of screws, but in actual case some portion around the screws is also coupled. This model provides a worst case representation of the structure.

3. Only the board of the PCBs were modeled. The components on the PCBs were not modeled. The density of boards were changed to compensate for the mass.

4. The co-ordinate system used in the analysis is the Cartesian co-ordinate system with origin at the base of the Nadir of the satellite. The longitudinal axis used for this analysis is along Y axis (axis joining Nadir and Zenith). X axis is from Lagging to Leading sides. Z axis is from Sun-side to Anti Sun-side

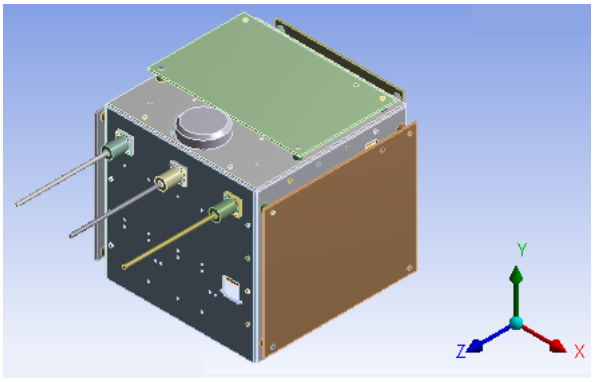

Figure 6.1: Satellite model in ANSYS

The types of Contacts and Joints used in simulating the loads are as follows

1. **Bonded Contacts:** - All degrees of freedom are constrained.

2. **Fixed Joint:** - All degrees of freedom are constrained. But the bodies that are constrained needn't be in contact.

Ansys has a Trim Tolerance of 1.16 mm i.e if any two surfaces are less than 1.16 mm apart then Ansys defines a contact between the two surfaces. By default Ansys treats all the contacts as Bonded.

6.2 Simulations and results

All simulations have been done on the following model-

1. In this model all the contacts have been suppressed except those between GPS puck antenna and zenith and between battery pack and battery box.
2. All the screws have been suppressed and the corresponding screw holes were joined by “Fixed Joint”.
3. The remaining contacts have been suppressed.

Presented in the subsequent sections are the simulations and results of each of the above models

6.3 Static analysis

1. **Aim of analysis**: To determine the stress developed when a static load is applied.
2. **Type of analysis**: Static
3. **Material properties**: As given in section A.1
4. **Constraints applied**: The FE ring, attached to the base of the Nadir was constrained for movement in all directions. All the screw joints are rigidly linked.
5. **Loads applied**: The loads as specified in table 14.1 were applied in different combinations on the model. The results are presented in tables 6.1, 6.3

Top two values of stress at particular component is highlighted in the table below

Sl. No.	Material							
	Al 6061 T6							
	Side Panel		FE Ring		Magnetorquer		Monopole+Holder	
	Max Eq. Stress (MPa)	FOS	Max Eq. Stress (MPa)	FOS	Max Eq. Stress (MPa)	FOS	Max Eq. Stress	FOS
1	15.925	17.331	**55.179**	5.002	0.788	350.298	**5.939**	46.474
2	17.651	15.637	48.739	5.663	0.797	346.386	5.805	47.544
3	11.114	24.834	38.153	7.234	0.517	533.436	4.199	65.733
4	10.530	26.211	42.806	6.448	0.511	540.012	4.332	63.712
5	34.547	7.989	32.689	8.443	0.647	426.782	4.004	68.933
6	41.189	6.701	31.789	8.682	0.588	469.627	3.932	70.193
7	41.189	6.701	31.789	8.682	0.588	469.627	3.932	70.193
8	34.547	7.989	32.689	8.443	0.647	426.782	4.004	68.933
9	46.846	5.892	27.230	10.136	0.845	326.666	4.191	65.857
10	**49.066**	5.625	28.795	9.585	**0.969**	284.756	4.259	64.805
11	41.522	6.647	41.522	6.647	0.711	387.918	2.147	128.575
12	41.568	6.640	21.938	12.581	0.587	470.027	2.107	130.979
13	42.383	6.512	55.518	4.971	0.976	282.816	5.903	46.758
14	49.145	5.616	**55.914**	4.936	1.158	238.404	**5.975**	46.192
15	**51.768**	5.331	52.589	5.248	0.779	354.300	5.679	48.597
16	49.544	5.571	49.462	5.580	**1.206**	228.856	5.841	47.253
17	42.037	6.566	39.403	7.005	0.926	297.960	4.233	65.200
18	46.478	5.938	42.142	6.549	0.629	439.001	4.198	65.742
19	41.664	6.624	43.670	6.320	0.881	313.458	4.368	63.182
20	38.137	7.237	43.323	6.371	0.867	318.523	4.296	64.247

Table 6.1: Static Simulation Results

Sl. No.	Material				
	Al 6061-T6		**FR 04**		**GFRP**
	Solar Panel		**PCB**		**Washer**
	Max Eq. Stress (MPa)	**FOS**	**Max Eq. Stress (MPa)**	**FOS**	**Max Eq. Stress (MPa)**
1	30.448	9.065	7.087	17.639	0.005
2	30.202	9.138	6.975	17.921	0.005
3	30.257	9.122	6.833	18.294	0.004
4	30.379	9.085	6.846	18.260	0.004
5	35.156	7.851	7.339	17.033	0.004
6	37.415	7.377	7.343	17.023	0.004
7	37.415	7.377	7.343	17.023	0.004
8	35.156	7.851	7.339	17.033	0.004
9	31.831	8.671	6.962	17.956	0.005
10	40.744	6.774	7.588	16.474	0.005
11	38.506	7.168	7.316	17.087	0.004
12	34.048	8.106	6.805	18.369	0.004
13	32.228	8.564	7.107	17.589	0.005
14	**41.903**	6.587	**7.890**	15.842	0.005
15	32.950	8.376	6.975	17.922	0.005
16	39.606	6.969	7.851	15.921	0.005
17	37.378	7.384	7.595	16.458	0.005
18	35.179	7.846	7.069	17.682	0.005
19	39.656	6.960	7.617	16.412	0.005
20	32.944	8.378	7.082	17.649	0.005

Sl. No.	**X (g)**	**Y (g)**	**Z (g)**
1	6	-7	0
2	-6	-7	0
3	6	3.5	0
4	-6	3.5	0
5	6	0	6
6	6	0	-6
7	-6	0	6
8	-6	0	-6
9	0	-7	6
10	0	-7	-6
11	0	3.5	6
12	0	3.5	-6
13	6	-7	6
14	6	-7	-6
15	-6	-7	6
16	-6	-7	-6
17	6	3.5	6
18	6	3.5	-6
19	-6	3.5	6
20	-6	3.5	-6

Table 6.2: Simulation No. v/s Load

Note: The last 8 simulations corresponding to loads along all 3 axes are extreme case scenarios which hardly occur. But they have been included to show that, the satellite can sustain even these loads.

Screenshots of Simulations:

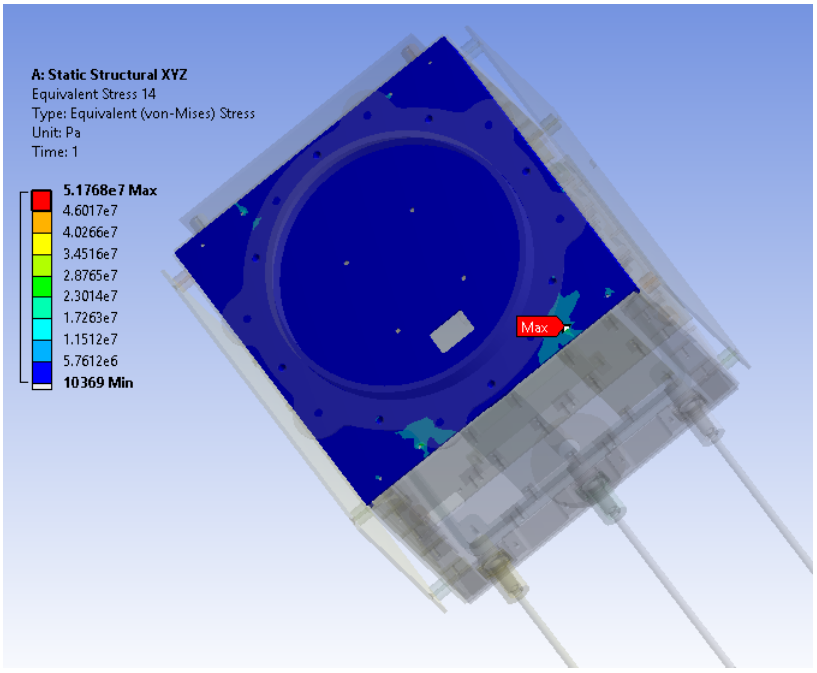

Figure 6.2: Max Eq. Stress on Nadir for loading -6g(X), -7g(Y), 6g(Z)

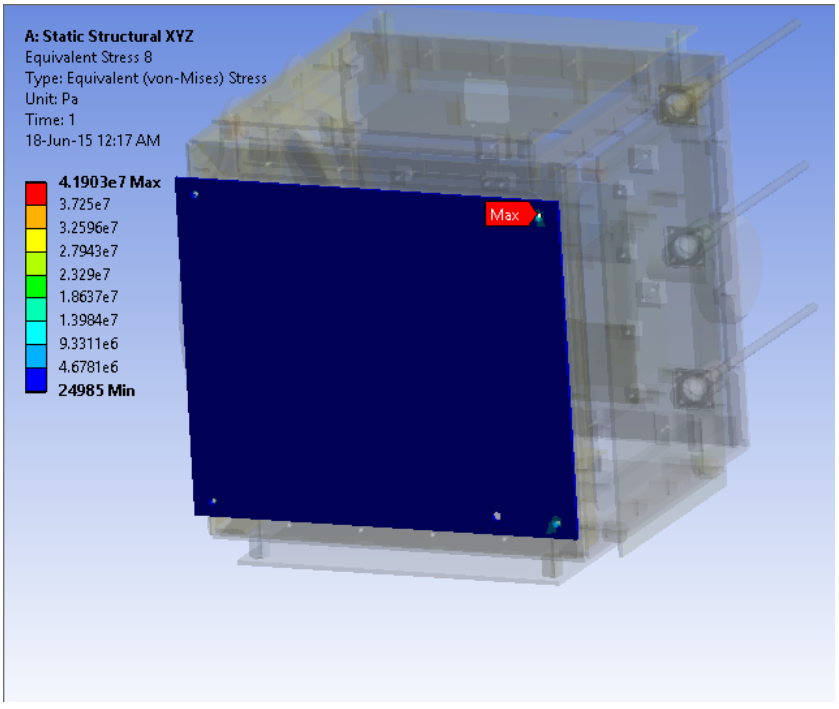

Figure 6.3: Max Eq. stress on Sunside Solar Panel for loading 6g(X), -7g(Y), -6g(Z)

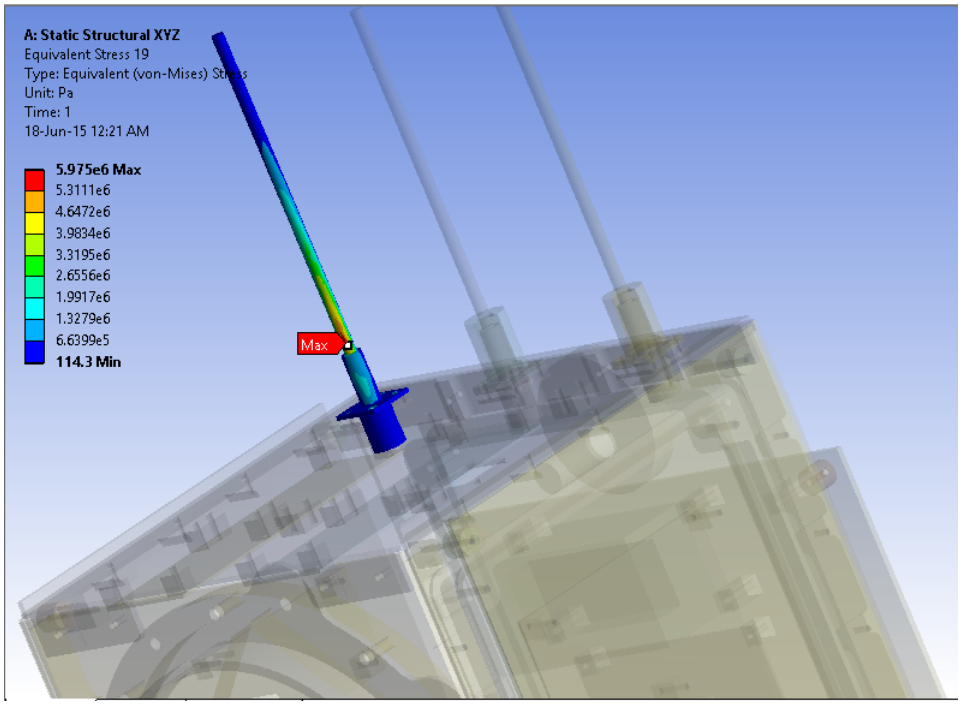

Figure 6.4: Max Eq. stress on Monopole for loading 6g(X), -7g(Y), -6g(Z)

Interpretation of results:

1. The maximum stress on the Side panels is 51.768 MPa (FOS: 5.3)
2. The maximum stress on the FE ring is 55.914 MPa (FOS: 4.9)
3. The maximum stress on the Solar Panel is 41.903 MPa (FOS: 6.5)
4. The maximum stress in the PCB is 7.890 MPa (FOS: 15.8)
5. The maximum stress on monopole is 5.975 MPa (FOS: 46.1)

The maximum stress-points observed in the simulation is located near the hole in majority of cases. Since washer is not taken into account in the simulation. Therefore we need to observe the stress outside the 6 mm diameter circle concentric to holes. Observed stress values in mentioned location is much less than the max stress value mentioned in the table.

Conclusion: Simulations for all possible worst case scenarios of static loading has been done. Stresses developed in these simulations are well within yield limit with high factor of safety. Stress values mentioned in above interpretation is of the simulation in which static load in all the directions are applied simultaneously. Since such case of loading is very unlikely during launch, therefore this design is safe for static loading.

6.4 Modal Analysis

Two kinds of Modal analysis have been done. One with constraining bottom of FE ring as fixed and other with a heavy point mass attached on FE ring. The first kind of Modal analysis is used for Harmonic simulation. As suggested by Murali dhar sir, second kind of Modal simulation is more accurate.

1. **Aim of analysis:** To determine the fundamental frequencies of the structure.
2. **Type of analysis:** Modal
3. **Material properties:** As given in section A.1
4. **Constraints applied:** The FE ring, attached to the base of the Nadir was constrained for movement in all directions. All the screw joints are rigidly linked.
5. **Loads applied:** NIL
6. **No. of modes extracted:** 80

Screenshots of Simulations: The images given below is only useful to observe the mode shape. The given deformation values are not to the scale.

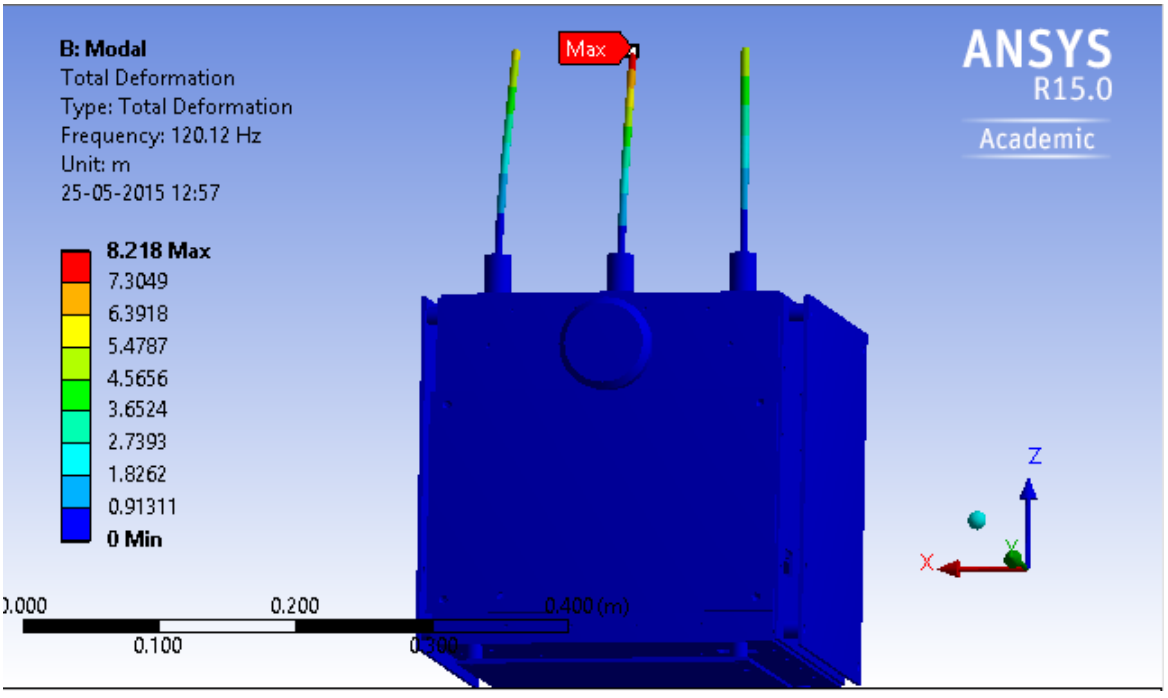

Figure 6.5: 1st mode of satellite (antenna mode)

Mode	Frequency (Hz)	Mode	Frequency (Hz)
1	120.12	41	493.56
2	123.86	42	497.81
3	124.9	43	499.29
4	126.28	44	509.21
5	126.53	45	521.85
6	127.22	46	557.13
7	129.78	47	564.19
8	152.6	48	575.28
9	160.47	49	581.01
10	166.91	50	583.07
11	187.99	51	583.39
12	200.57	52	590.06
13	231.5	53	593.74
14	239.01	54	598.37
15	251.83	55	604.87
16	252.35	56	608.45
17	253.02	57	610.07
18	254.09	58	618.42
19	266.58	59	634.32
20	267.6	60	636.06
21	277.72	61	640.93
22	280.48	62	656.12
23	280.57	63	663.5
24	283.08	64	666.74
25	308.24	65	677.56
26	319.61	66	682.67
27	321.92	67	688.04
28	327.61	68	697.66
29	330.5	69	708.06
30	338.19	70	710.09
31	356.14	71	720.61
32	357.04	72	724.08
33	357.05	73	733.08
34	402.15	74	735.37
35	423.66	75	737.08
36	442.04	76	742.92
37	444.58	77	752.15
38	457.55	78	755.48
39	462.14	79	757.1
40	490.37	80	776.42

Table 6.3: Result of Modal Analysis: Fixed FE Ring

Mode	Frequency [Hz]	Mode	Frequency [Hz]
1	0	41	423.63
2	9.35E-08	42	440.04
3	3.52E-07	43	444.31
4	9.33E-04	44	456.51
5	9.36E-04	45	457.48
6	1.05E-03	46	490.08
7	121.50	47	493.32
8	122.73	48	497.79
9	124.87	49	499.24
10	126.25	50	508.87
11	126.42	51	521.81
12	127.05	52	556.97
13	128.39	53	564
14	146.36	54	574.97
15	160.47	55	580.82
16	166.18	56	582.99
17	186.22	57	583.28
18	186.64	58	589.86
19	230.9	59	592.67
20	236.57	60	593.79
21	251.83	61	604.25
22	252.15	62	608.36
23	252.95	63	609.67
24	254.08	64	617.81
25	260.74	65	632.8
26	266.59	66	635.73
27	267.61	67	639.92
28	280.46	68	656.01
29	280.52	69	663.47
30	282.43	70	666.67
31	307.85	71	676.43
32	319.52	72	682.45
33	321.54	73	687.81
34	324.16	74	697.24
35	330.03	75	707.88
36	338.09	76	709.95
37	350.71	77	720.57
38	356.14	78	723.93
39	356.99	79	732.33
40	357.05	80	734.84

Table 6.4: Results of Modal Analysis: Remote Point

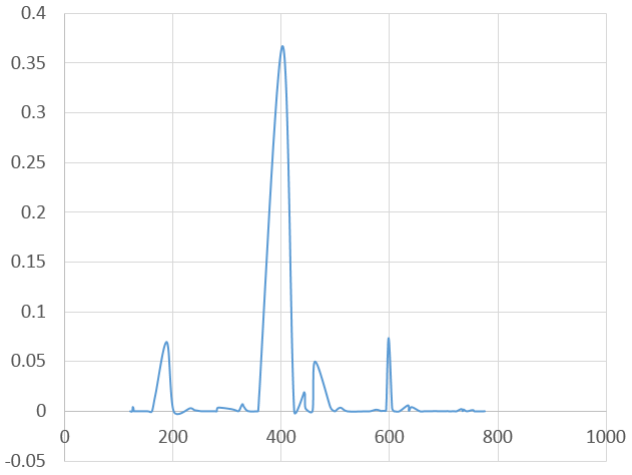

Figure 6.6: Effective Mass Participation Vs Frequency Response in X-direction

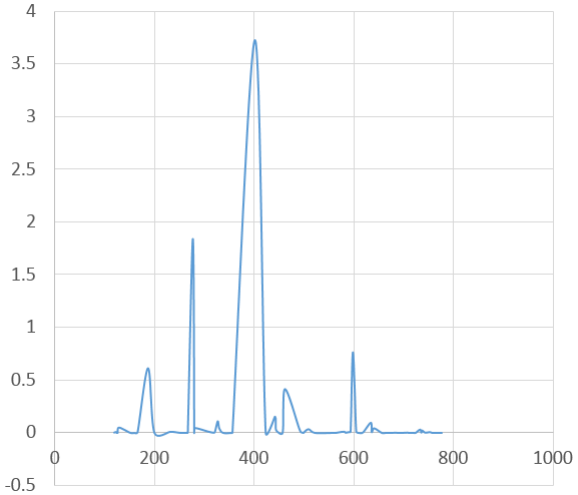

Figure 6.7: Effective Mass Participation Vs Frequency Response in Y-direction

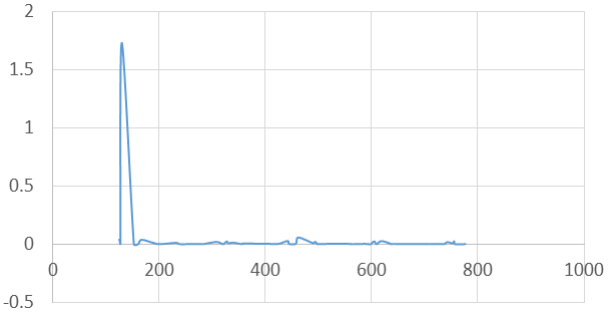

Figure 6.8: Effective Mass Participation Vs Frequency Response in Z-direction

Interpretation: Graphs plotted for modal frequency vs effective mass participated

in all three direction. The peak in the graphs show the different modal frequencies in separate directions.

1. 1st peak in the graph for X direction shows the global mode for X direction is around **150 Hz**.
2. 1st peak in the graph for Y direction shows the global mode for Y direction is around **120 Hz**.
3. 1st peak in the graph for Z direction shows the global mode for Z direction is around **180 Hz**.

Modal analysis is done for 80 modes and mass participation for different direction is given in the table below

Direction	**Mass Participation (%)**
X	86.02
Y	94.50
Z	87.10

Table 6.5: Mass Participation for Modal Analysis of first kind

Mass participation table for X, Y and Z are given in the appendix.

Interpretation of results:

1. Modal analysis of first kind
   (a) The 1^{st} mode of the satellite is 120.12 Hz.
   (b) 1-6 modes are antenna modes.
   (c) The 1^{st} Solar Panel mode is the 7^{th} mode of satellite i.e 160.64 Hz.
   (d) The modes of the PCBs start from the 11^{th} mode of the satellite i.e 229.83 Hz.
   (e) No dominant side modes within the first 34 modes of the satellite(440.04 Hz).
2. Modal analysis of second kind
   (a) 1^{st} six modes are rigid body mode. Therefore, they are approximately zero.
   (b) This result will be used for Harmonic Analysis because it helps us to analyze more actual scenario by assuming PSLV as point mass.
   (c) Mass Participation values for this kind is not valid, since first six modes are rigid body mode.

Conclusion: There is no satellite mode below 90 Hz as required according to PSLV manual. First mode of the satellite should be antenna mode, which can be easily verified as the monopoles are the only part of satellite similar to cantilever. Solar panels, PCBs and satellite sides are like plate. Solar panels and PCBs are connected at four corners by screws whereas satellite sides are connected by flanges. So, Solar panels and PCBs have lower mode than satellite sides, but higher than antenna.

6.5 Harmonic Response

Harmonic Simulation is done separately for three directions and also for combined loading taken two directions at a time.

1. **Aim of analysis:** To obtain the stress developed and frequency response of the structure when subjected to sinusoidal loads.
2. **Type of analysis:** Harmonic
3. **Material properties:** As given in section A.1
4. **Constraints applied:** The base of the FE ring is rigidly attached to a heavy point mass of 10^8 kg.
5. **Loads applied:** The harmonic loads are taken from the PSLV manual. To simulate the base acceleration part, a heavy point mass was rigidly attached to the base of the FE ring and a remote force was applied on the point mass that gives the required acceleration

Sl. No.	Material	Component Type	Component	X= 3g, Y= 0, Z= 0	X= 0, Y= 4.5g, Z= 0	X= 0, Y= 0, Z= 6g
				Max (MPa)	Max (MPa)	Max (MPa)
1			Whole body	12.728	24.004	12.989
2	FR 04	PCBs	Downlink	0.1748	0.95811	0.9978
3			Beacon	0.1183	0.891	0.9145
4			Uplink	0.8162	0.6956	0.1957
5			Power	0.3504	0.6788	2.3263
6			OBC	2.2285	0.6971	0.4227
7			Sunsensor Board	0.1697	2.5041	0.7414
8	Al 6061-T6	Solar Panel	Solar Panel Sunside	0.3848	6.5617	12.989
9			Solar Panel Lagging	12.728	1.7201	1.0338
10			Solar Panel Leading	11.311	1.7061	0.5479
11			Solar Panel Zenith	1.1918	24.004	2.4473
12		Side Panels	Sunside	0.7674	5.526	1.2056
13			Leading	1.1017	7.0665	0.411
14			Nadir	0.4518	21.768	1.335
15			Lagging	1.428	6.1221	0.3327
16			Antisunside	0.7068	6.7205	1.857
17			Zenith	2.1166	5.431	2.4306
18		Monopole Holder	Outercover+ Antenna(leading 1st)	2.0617	8.5901	5.3029
19			Outercover+ Antenna(lagging 1st)	2.0098	8.6115	5.1472
20			Outer cover +Antennna(middle)	0.7826	8.6474	6.0691
21		Battery	Battery Box	0.2478	0.2033	0.22465
22		Torquer	Torquer sunside	0.03028	0.4884	0.1002
23			Torquer Leading	0.0504	0.4859	0.0327
24			Torquer Zenith	0.0321	0.2528	0.03887
25		FE Ring	FE Ring	0.1589	9.3578	0.21998
26	GFRP	Washer	All washers	0.000394	0.00261	0.000597

Table 6.6: Harmonic Simulation Results for Loads in Separate Direction

6. **Screenshots of simulation:**

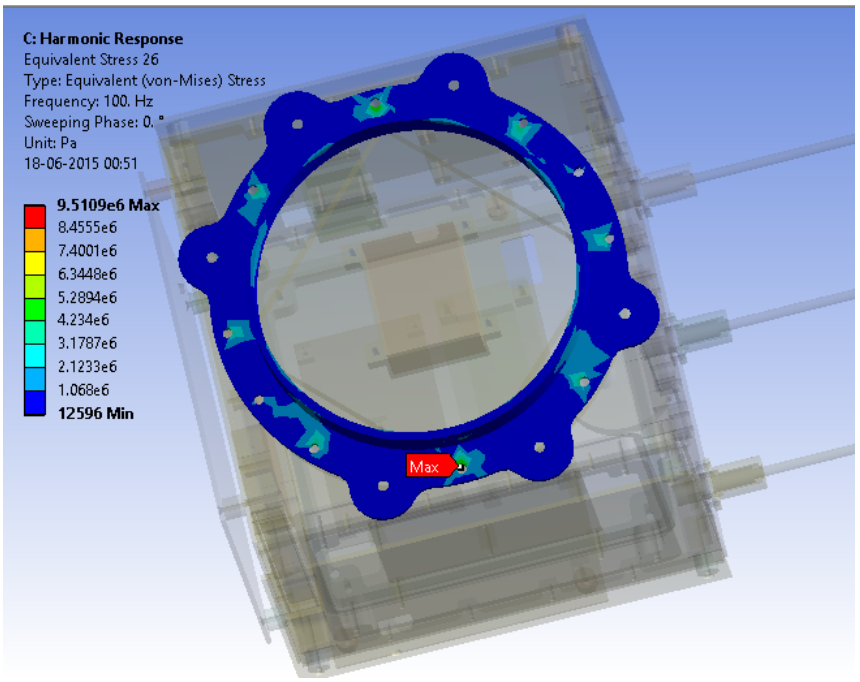

Figure 6.9: Max Eq. Stress: FE Ring (Combined X, Y Harmonic)

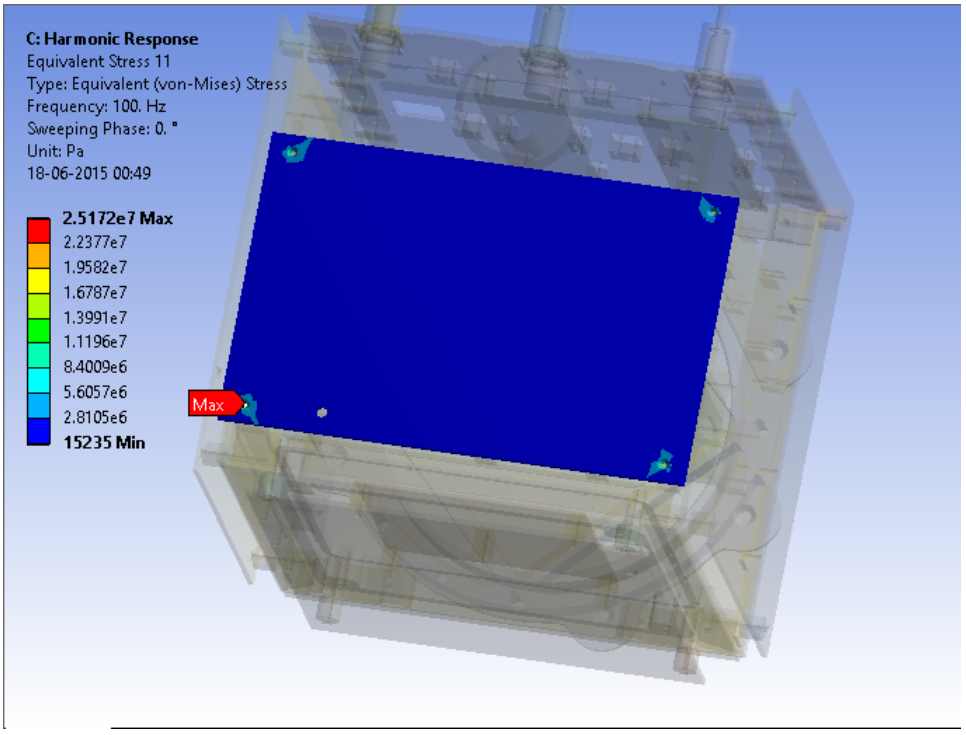

Figure 6.10: Max Eq. Stress: Zenith Solar Panel (Combined X, Y Harmonic)

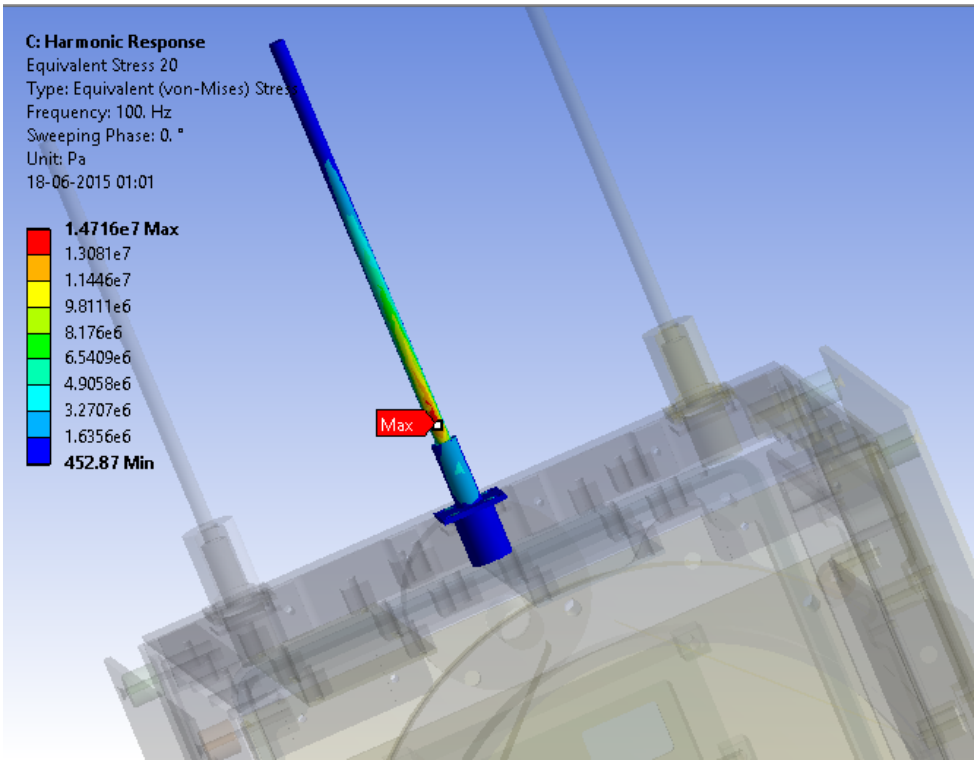

Figure 6.11: Max Eq. Stress: Middle Antenna (Combined Y, Z Harmonic)

Acceleration Frequency Response at different locations and its direction:

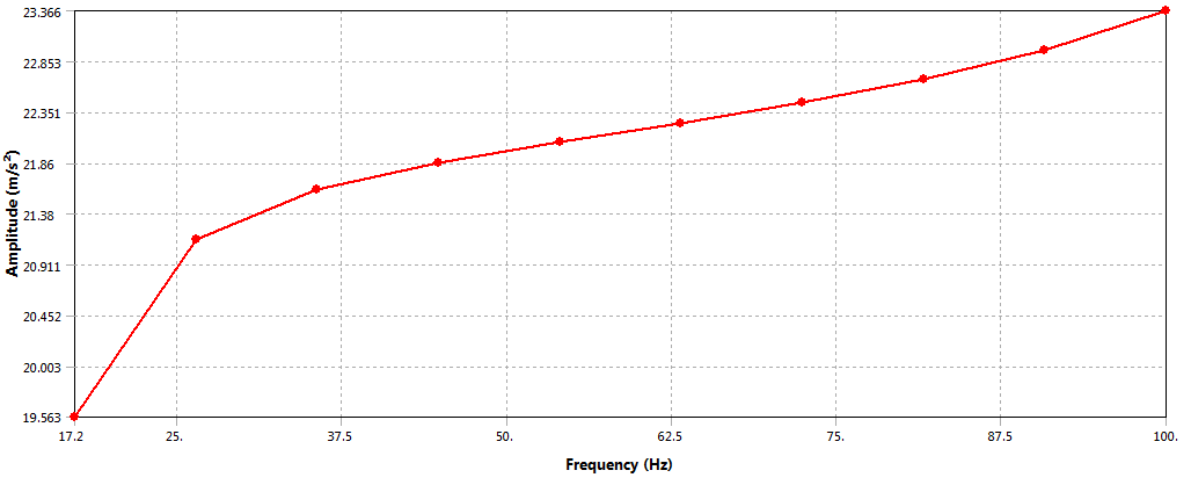

Figure 6.12: Bottom of Anti-sunside in Z-direction

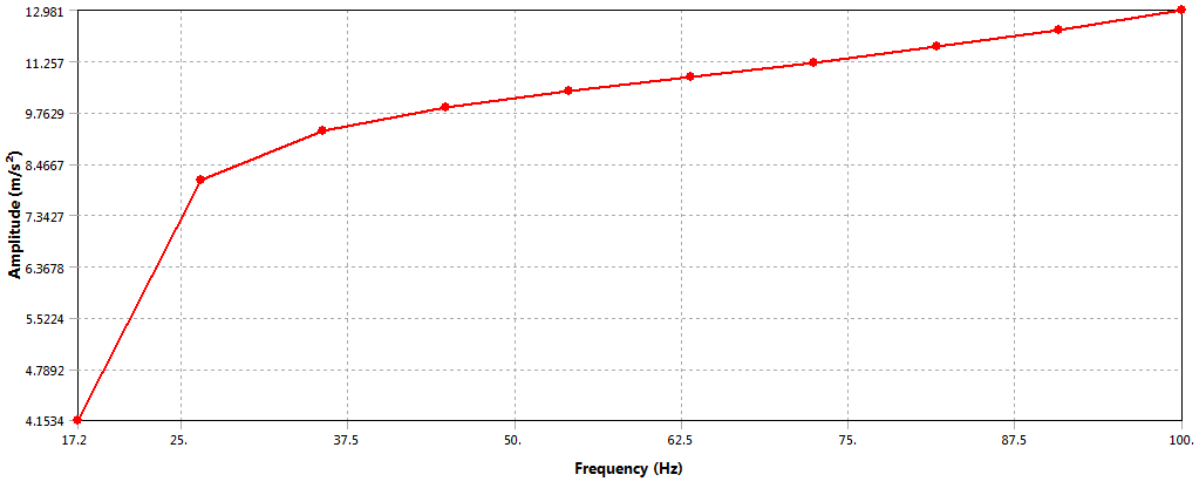

Figure 6.13: Power Board in Z-direction

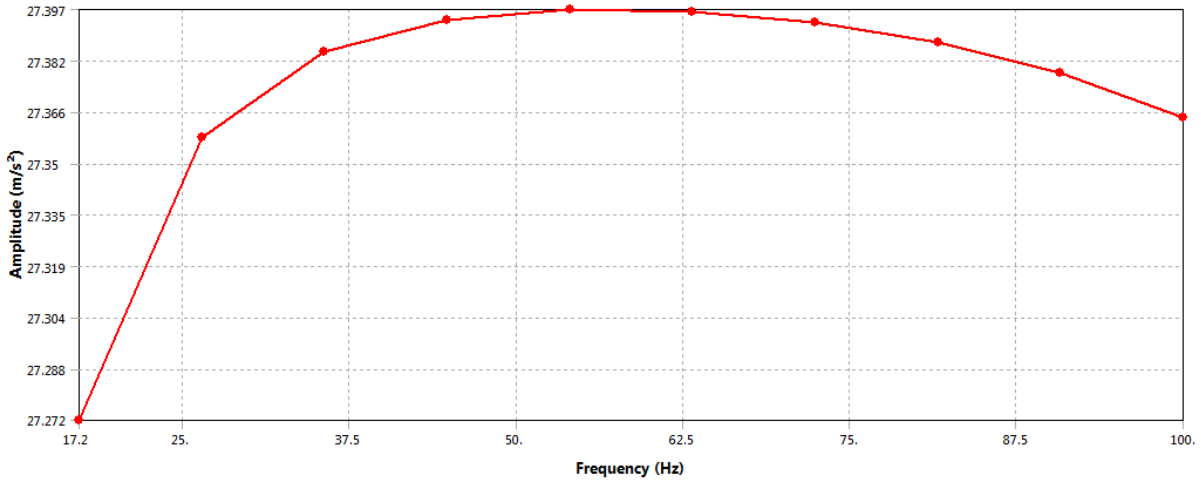

Figure 6.14: On Fixture near Leding Side in X-direction

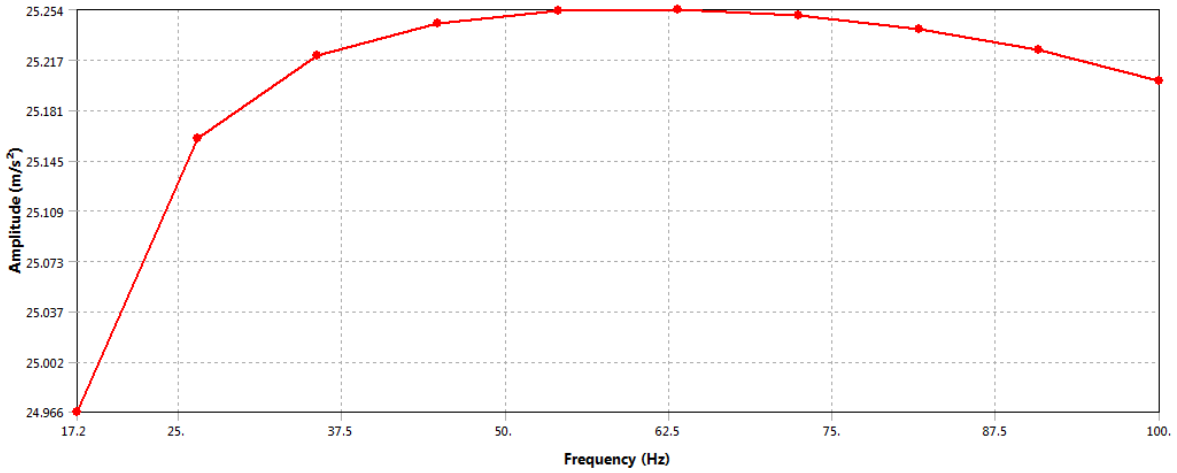

Figure 6.15: Bottom of Leading Side in X-direction

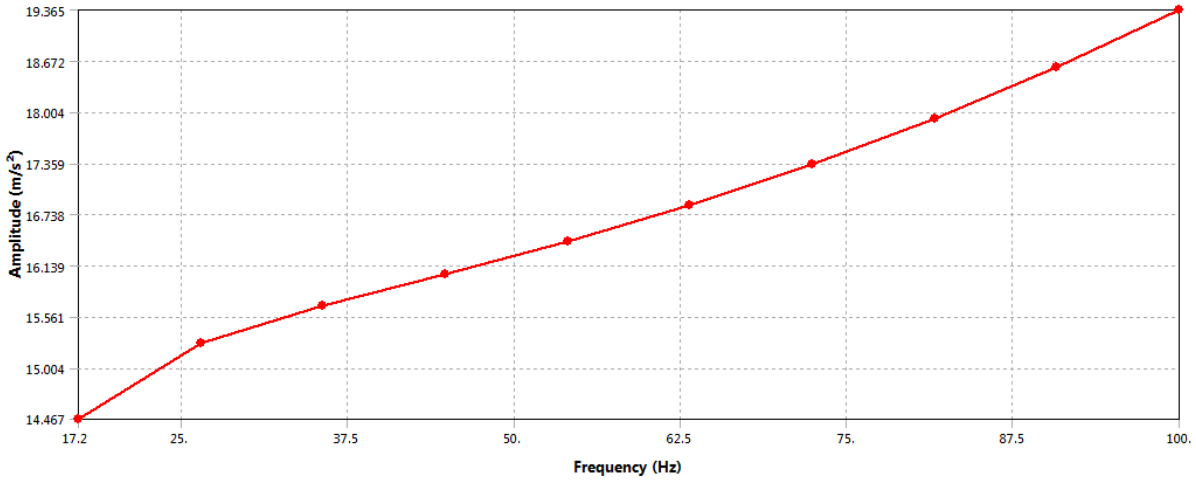

Figure 6.16: OBC Board in X-direction

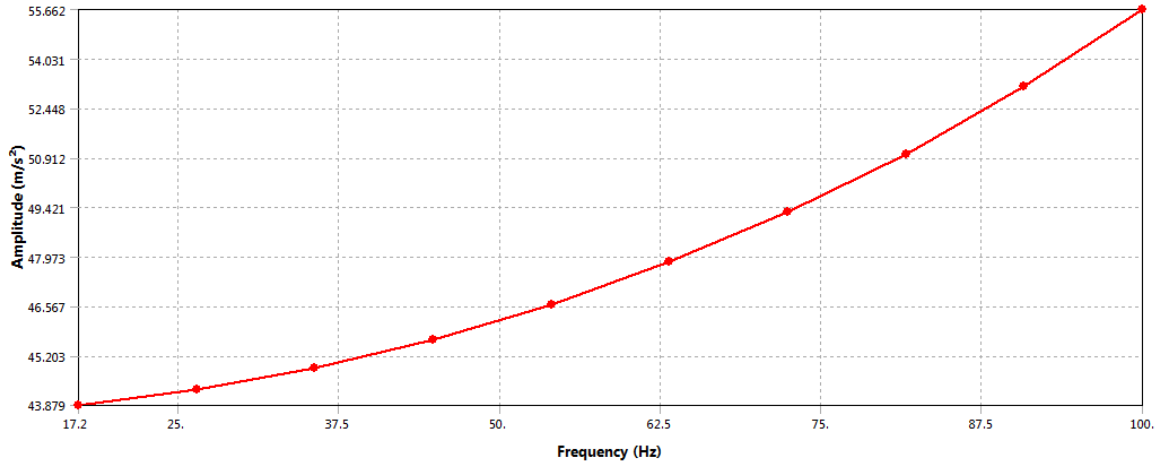

Figure 6.17: Sun-sensor Board in Y-direction

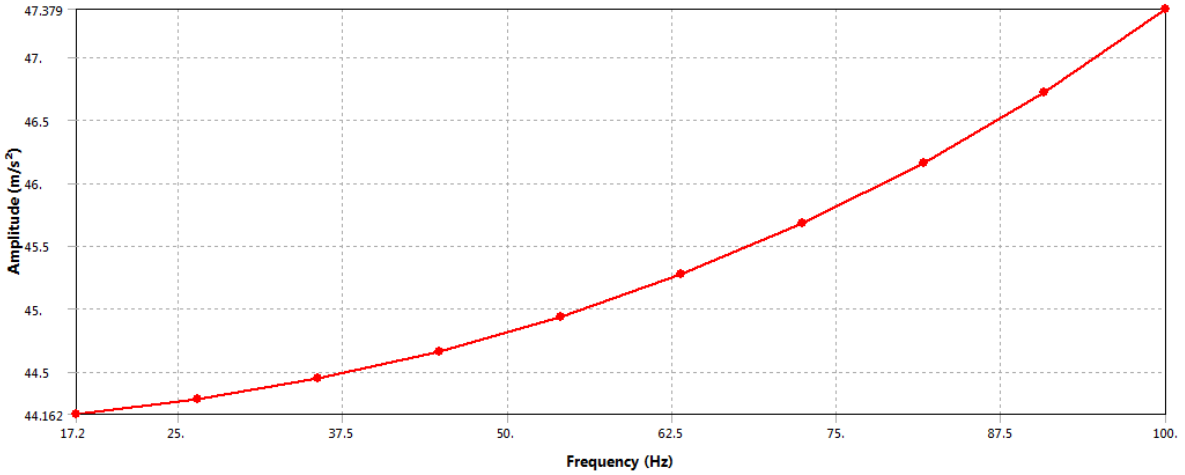

Figure 6.18: On Fixture near Leading Side in Y-direction

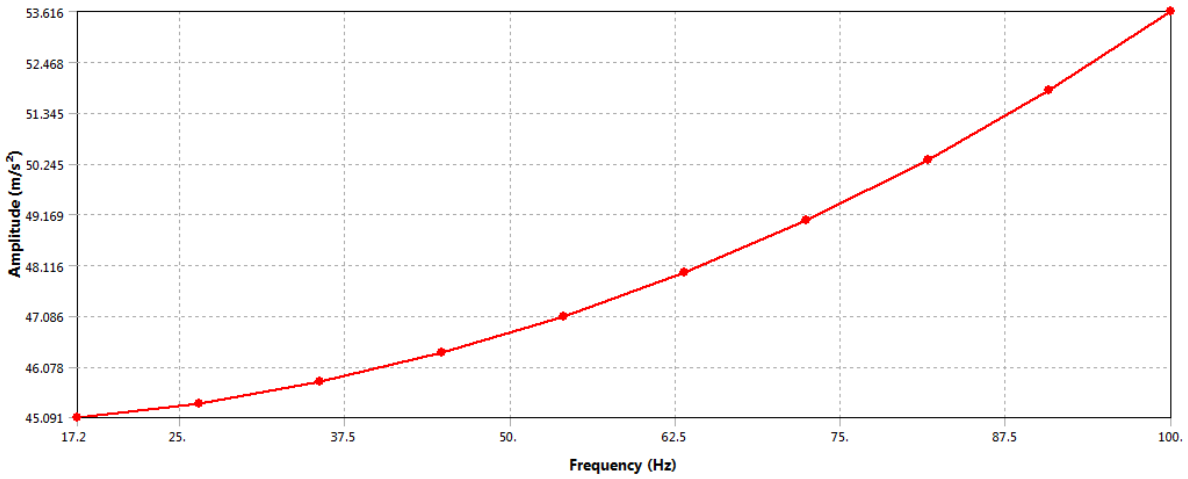

Figure 6.19: Zenith Side Panel in Y-direction

7. **Interpretation of results:**

   (a) The maximum stress in PCBs is 2.5014 MPa (FOS: 50)

   (b) The maximum stress on Solar Panel is 24.004 MPa (FOS: 11.5)

   (c) The maximum stress on Side Panel is 21.7680 MPa (FOS: 12.7)

   (d) The maximum stress on Monopole+Holder is 8.6474 MPa (FOS: 32)

   (e) The maximum stress on FE Ring is 9.3578 MPa (FOS: 29.5)

   Frequency Response of normal stress for Harmonic loading is continuously increasing in range 8-100 Hz and max value of stress is at 100 Hz. Therefore, there is no fundamental mode in between these range. The image above frequency response shows the corresponding normal stress plot on the body.
   The maximum stress-points observed in the simulation is located near the hole in majority of cases. Since washer is not taken into account in the simulation. Therefore we need to observe the stress outside the 6 mm diameter circle concentric to holes. Observed stress values in mentioned location is much less than the max stress value mentioned in the table.
   Conclusion: No peak in the frequency range (5-100 Hz) specified by PSLV manual shows no failure of satellite.

6.6 Random Vibration Analysis

1. **Aim of analysis:** To determine the stress developed and PSD response when structure is subjected to Random loading.

2. **Type of analysis:** Random
3. **Material properties:** As given in section A.1
4. **Constraints applied:** The modal analysis results with fixed constraint on FE RING is used.
5. **Loads applied:** PSD base excitation are taken from PSLV manual and simulated for all the three directions separately
6. **No. of modes used for analysis:** 300 modes - Till 2000 Hz
7. **Constant damping ratio:** 1%
8. **Scale factor:** 3 sigma
9. **Probability:** 99.73%

Sl. No.	Material	Component Type	Component	X	Y	Z
				Max (MPa)	Max (MPa)	Max (MPa)
1			All body	**266.55**	**194.28**	**102.71**
2	FR 04	PCBs	Downlink	13.907	75.863	19.435
3			Becon	11.79	36.466	16.375
4			Uplink	29.029	28.234	22.922
5			Power	21.696	39.604	31.337
6			OBC	**103.42**	31.787	27.245
7			Sunsensor Board	18.838	**156.04**	**50.781**
8	AL 6061 T6	Solar Pannels	Solar Panel Sunside	22.652	131.46	**102.71**
9			Solar Pannel Lagging	**266.55**	69.292	35
10			Solar Pannel Leading	243.84	41.521	29.824
11			Solar Pannel Zenith	42.397	**194.28**	40.879
12		Side Pannels	Sunside	33.177	52.962	26.682
13			Leading	49.607	55.565	34.28
14			Nadir	**55.873**	**121.85**	**69.838**
15			Lagging	38.639	59.635	29.26
16			Anti-Sunside	26.081	42.821	24.925
17			Zenith	18.002	98.51	27.362
18		Monopole+ Holder	Outercover-1+ Antenna(leading 1st)	23.102	14.051	87.89
19			Outercover-2+ Antenna(lagging 1st)	25.118	14.272	**88.248**
20			Outer cover-3+ Antennna(middle)	**25.863**	**21.953**	75.522
21		Battery	Battery Box	4.1955	10.365	4.2045
22		Torquers	Torquer Sunside	8.2399	6.2715	6.3412
23			Torquer Leading	7.4512	5.5474	6.7048
24			Torquer Zenith	6.6203	5.2276	7.3923
25		FE Ring	FE Ring	**144.04**	**171.25**	**38.584**
26	GRPF	Washer	All washers	0.0415	0.03831	0.03857

Table 6.7: Random Vibration Results

NOTE: The numbers shown in bold are higher stress values in the corresponding components.

10. **Screenshot of contour plot obtained:**

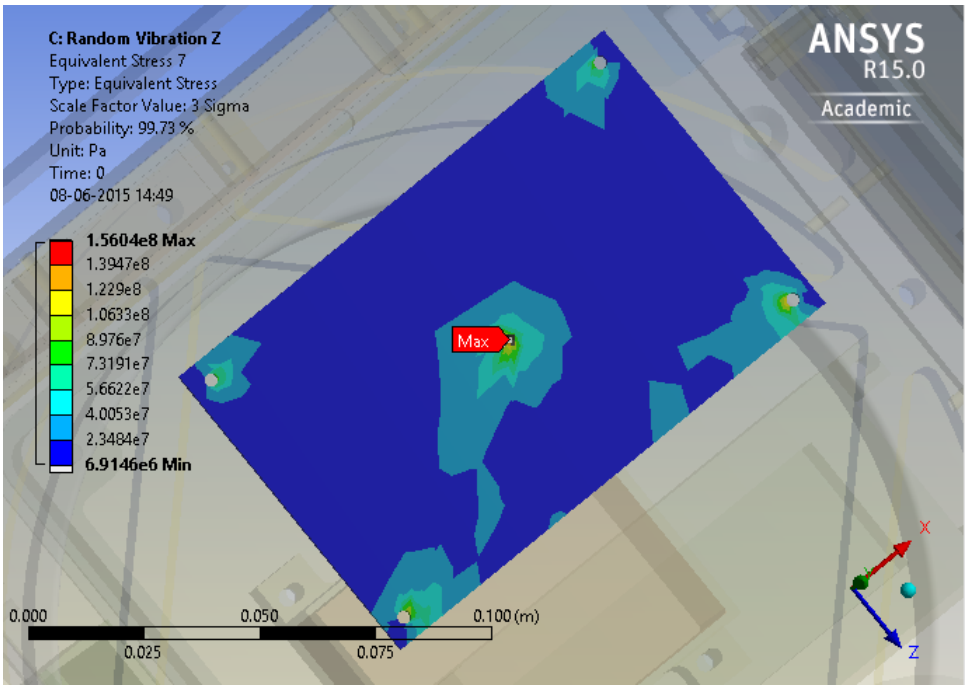

Figure 6.20: Max eq stress: Sunsensor PCB(Random Loading in Y)

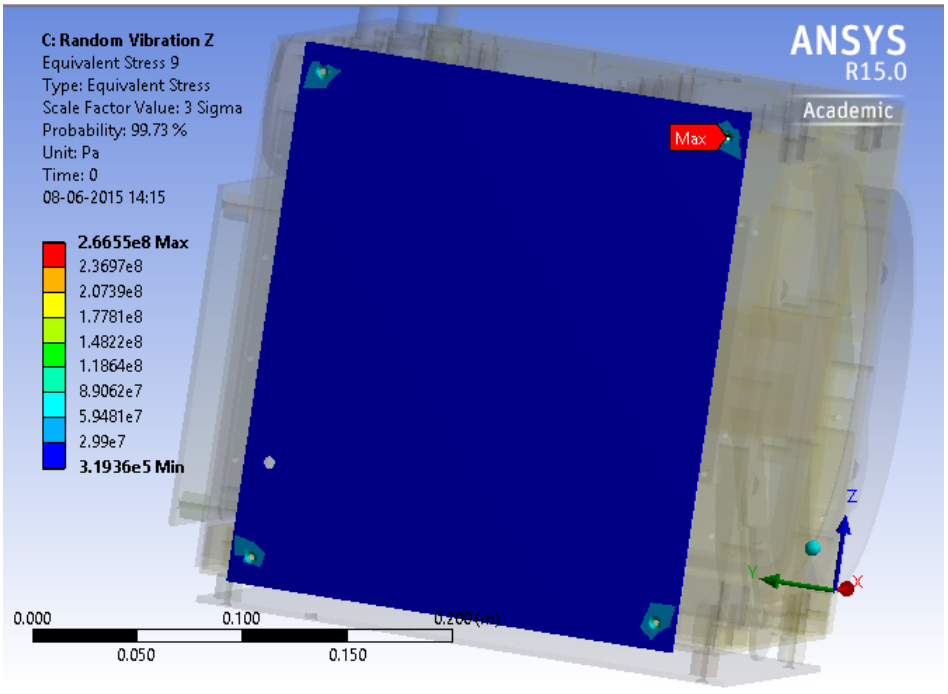

Figure 6.21: Max eq stress: Lagging Solar Panel (Random Loading in X)

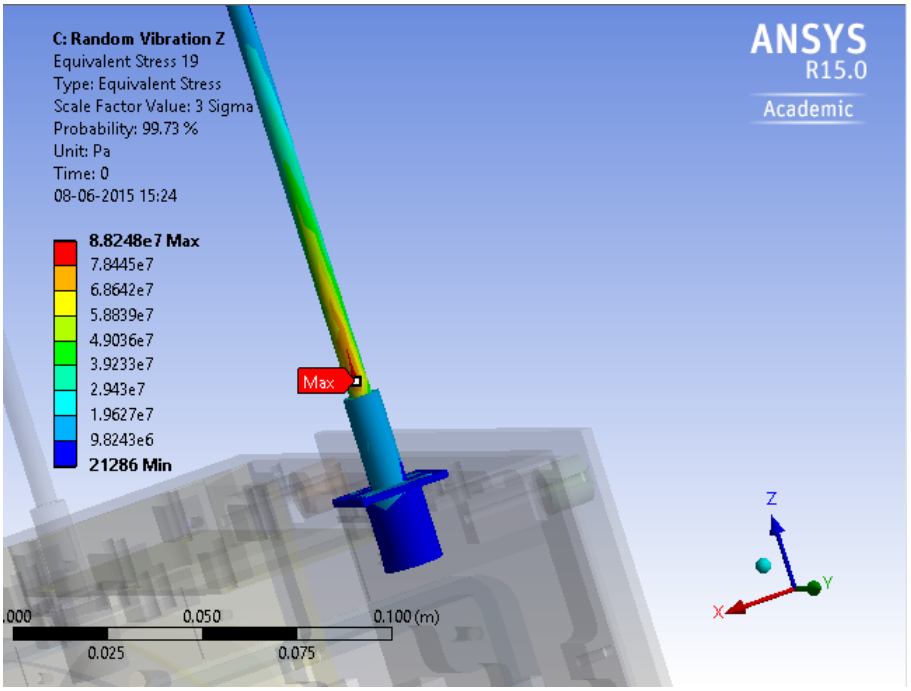

Figure 6.22: Max eq stress: Monopole+Holder (Random Loading in Z)

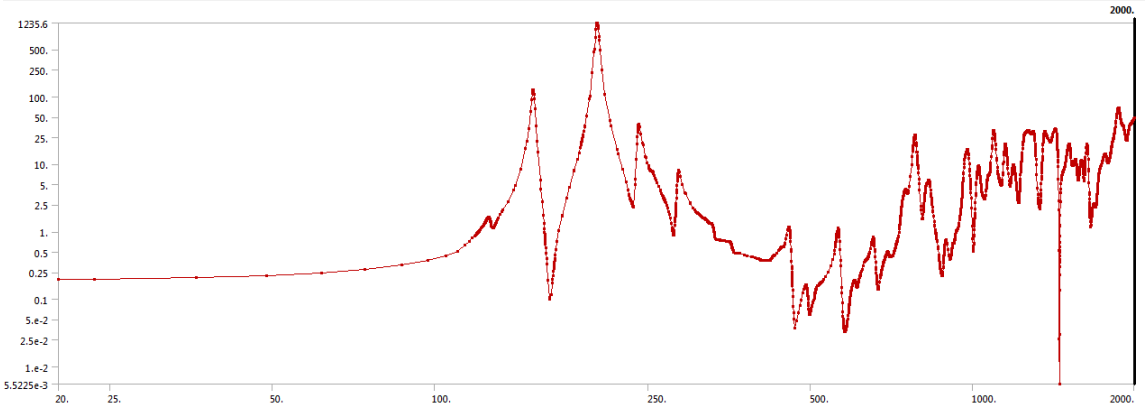

Figure 6.23: PSD Response Acceleration (X): Leading Side (Loading in X)

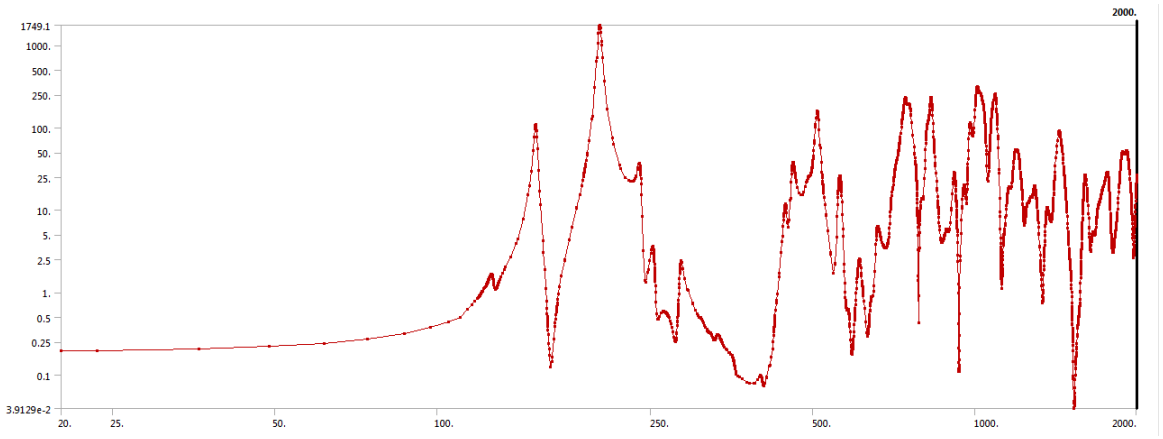

Figure 6.24: PSD Response Acceleration (X): OBC Board (Loading in X)

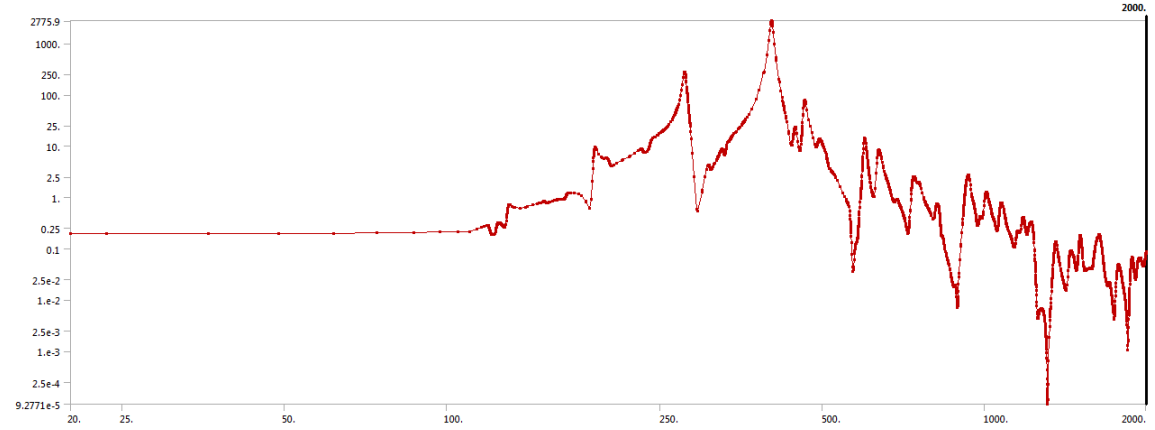

Figure 6.25: PSD Response Acceleration (Y): Power Board (Loading in Y)

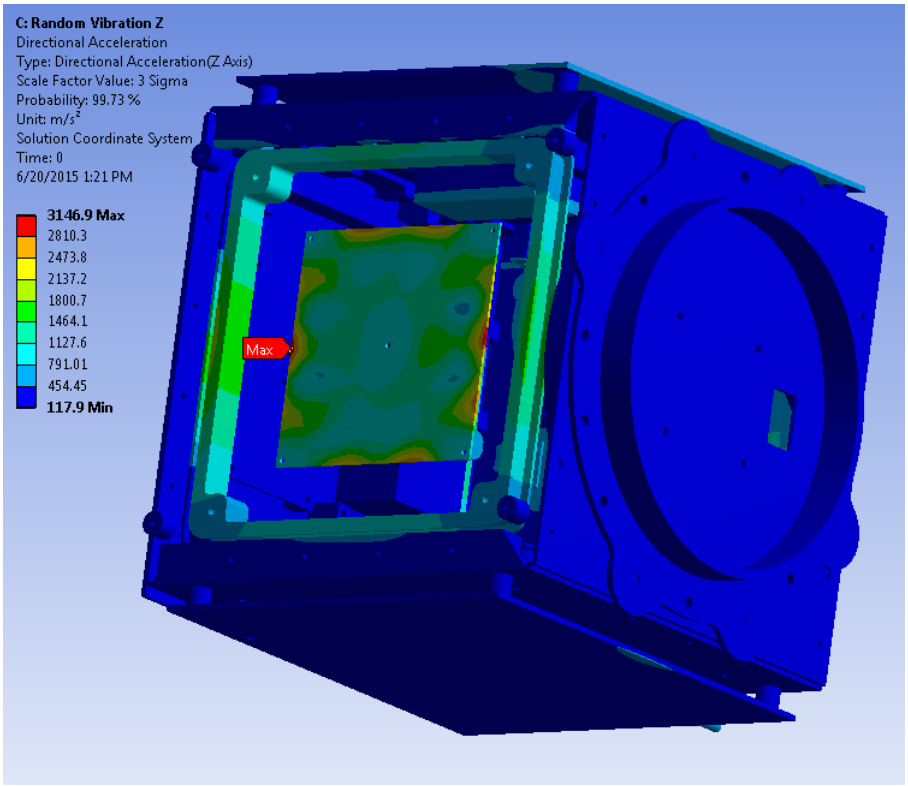

Figure 6.26: Directional Acceleration (Z) for Random Loading in Z

11. **Interpretation of results:** The maximum stress is obtained on a washer and is far less than the yield strength. Also, the total deformation is far too less for any contact between 2 surfaces to take place. Thus, the structure does not fail under random vibrations.
    The maximum stress-points observed in the simulation is located near the hole in majority of cases. Since washer is not taken into account in the simulation. Therefore we need to observe the stress outside the 6 mm diameter circle concentric to holes. Observed stress values in mentioned location is much less than the max stress value mentioned in the table.

12. **Conclusion:** For all the above simulations FOS values for different material is greater than 1.

Chapter 7

Integration Subsystem

7.1 Weights of Components

SubSystem	Weight (in gms.)
Structure	4316.100
PCB & Mounted	724.000
Other Elec & Hardware	3784.500
Integration	864.461
Miscellaneous	89.967
Total	9779.028

Table 7.1: Total Weight

S.No.	Components	Weight for Single Quantity (in gms)	Quantity	Total Weight (in gms)	Dimensions
1.1	Nadir	1122.31	1	1122.310	253 x 253 x 23.24
1.2	Sunside	559.49	1	559.490	254 x 253 (Flange) x 23.08
1.3	Anti-sunside	578.1	1	578.100	254 x 253 (Flange) x 23.16
1.4	Zenith	588.7	1	588.700	254 x 253 (Flange) x 23.14
1.5	Leading	576.87	1	576.870	254 x 253 (Flange) x 23.22
1.6	Lagging	610.26	1	610.260	254 x 253 (Flange) x 23.14
1.7	Monopole Antenna	45	3	135.000	
1.8	Antenna Holder	17.5	3	52.500	
1.9	Battery Box	92.87	1	92.870	74.35 x 60.4 x 42
Sub-Total		4316.100			

Table 7.2: Structure

S.No.	Components	Weight for Single Quantity (in gms)	Quantity	Total Weight (in gms)	Dimensions
2.1	ADC Board	54	1	54.000	125 x 81 x 13.65
2.2	Power Board	182	1	182.000	135 x 135 x 13.65
2.3	OBC Board	152	1	152.000	135 x 135 x 14.65
2.4	Downlink Board	114	1	114.000	165 x 55 x 30.65
2.5	Uplink Board	103	1	103.000	166 x 55 x 30.65
2.6	Beacon Board	119	1	119.000	166 x 55 x 29.65
Sub-Total		724.000			

Table 7.3: CB and PCB Mounted Devices

S.No.	Components	Weight for Single Quantity (in gms)	Quantity	Total Weight (in gms)	Dimensions
3.1	GPS Module	232.5	1	232.500	115.1 x 55.1 x 40.23
3.2	GPS Antenna	139	1	139.000	
3.3	Magnetometer	92	1	92.000	82.42 x 38.14 x 22.65
3.4	Magnetorquer	256	3	768.000	210 x 210 x 19 (mm3)
3.5	Solar Panels - Type 1	600	3	1800.000	22 x 26 (cm2)
3.6	Solar Panel - Type 2	475	1	475.000	26 x 16.5 (cm2)
3.7	Battery	278	1	278.000	65.9 x 55.98 x 37.86 mm3
Sub-Total		3784.500			

Table 7.4: Other Electronics Hardware

S.No.	Components	Weight for Single Quantity (in gms)	Quantity	Total Weight (in gms)
4.1	Screws & Washers	N/A	102	139.758
4.2	Connectors connecting boards and other electronic hardware.	N/A	20	159.775
4.3	Wires in Wire Routing	N/A	N/A	261.491
4.4	PCB - Connectors Mouted Screws	N/A	38	171.000
4.5	SMA Connectors for Monopole Antenna	28	3	84.000
4.6	Beta Clamps & Cable Tie	0.581	41	48.437
Sub-Total		864.461		

Table 7.5: Integration

7.2 Integration Sequence

Sr. No.	Steps	Comments	Reference	Precautions	Torque Value
1	Lay the side panels as per the routing plan				
2	Screw Beacon (Wires) Connectors to Beacon.				Male Screw Lock 0.34
3	Mount Beacon board on Antisunside				M3 X 10, 0.4
4	Tie Beacon-OBC Connecting wire to clamp A_C_1				
5	Tie Beacon Thermistor wire on A_C_7.				
6	ScrewDownlink (Wires) Connectors to Downlink				Male Screw Lock 0.34
7	Mount Downlink board on Antisunside				
8	Pass Beacon-OBC and Downlink-OBC Connecting wire on clamp A_C_2	Leave cable tie loose.	16,57,66		
9	Tie Downlink Thermistor wire & Beacon Thermistor wire on A_C_8.				
10	Mount Battery Box(Batttery pack inclusive) on Nadir from outside	integrate vertically, with washers inside (GFRP) and outside	Guidelines Sheet	Use Torque wrench of higher resolution	M4 X 16, 0.86
11	Screw all Power (Wires) Connectors to Power board.			Use Torque wrench of higher resolution	Male Screw Lock 0.34
12	Mount Power board to Sunside			Use Torque wrench of standard resolution.	M3 X 10, 0.4
13	Tie Power-Battery, Power-Battery Switch and Power-SNAP Connecting wires to N_C_1	The wire has to be tied on S_C_3 so leave the wire loose enough.			

Sr. No.	Steps	Comments	Reference	Precautions	Torque Value
14	Pass Power-SNAP, Power-Battery Switch and Battery-Battery Switch Connecting wires to N_C_2	Leave cable tie loose for Battery Box- Thermistor wire. Place the snap connector carefully inside the groove made in nadir fixture.(or LVI) such that it does not touches the table. Use Kapton tape if required to fasten the outgoing snap connector.	15		
15	Pass Battery Box-Thermistor wire to N_C_2.	Tighten the cable tie.	14		
16	Pass Battery-Battery Switch and Power-Battery Switch connecting wires to A_C_2.	Keep the cable tie still loose.	8,57,66		
17	Pass Battery-Battery Switch and Power-Battery Switch connecting wires to A_C_3.	Leave cable tie loose.	58,66		
18	Tie Power-Battery, Power-Battery Switch and Power-SNAP Connecting wires to S_C_3				
19	Tie Power-Battery and Power-Battery Switch Connecting wires to S_C_2				
20	Tie Power-Uplink wire on S_C_4				
21	Tie Power-OBC on S_C_1				
22	Tie Solar Panel (Sunside,Zenith) Connecting wires on S_C_5.		57	On the Power board, (Zenith, Sunside) clubbed together &(Lagging, Leading) clubbed together.	
23	Tie Solar Panel (Sunside,Lagging) Connecting wires on S_C_6.				
24	Tie Solar Panel (Sunside,Lagging) Connecting wires on S_C_7.				
25	Make Nadir vertical along the edge N_LD.	Pull Nadir little back so that the wires attached to Power board are not taut.		Avoid compression of Beacon-OBC & Downlink OBC wires.	
26	Make Antisunside vertical along the edge A_LD.				
27	Rotate Antisunside along the edge A_N.				
28	Mount Nadir to Antisunside	Avoid compression of Beacon-OBC & Downlink OBC wires. ** IMPORTANT		Use Torque wrench of standard resolution.	M3 X 10, 0.4
29	Make Sunside vertical along the edge S_LD.				
30	Rotate Sunside along the edge S_N.				
31	Mount Sunside To Nadir	Avoid compression of Snap,Battery wires. ** Important		Avoid compression of Snap,Battery wires CHECK CLAMP SHOULD NOT CLASH WITH TORQUERS ON OTHER SIDE(nadir frame and torquer sunside distance is 6mm only)	M3 X 10, 0.4
32	Rotate Nadir-Sunside -Antisunside Assembly along the edge N_LD to lie down Nadir	Make Nadir as base.			
33	Screw OBC-Downlink Connector to OBC			Use Torque wrench of higher resolution	Male Screw Lock 0.34
34	Screw OBC-Beacon Connector to OBC			Use Torque wrench of higher resolution	Male Screw Lock 0.34

Sr. No.	Steps	Comments	Reference	Precautions	Torque Value
35	Screw OBC- Magmeter Connector to OBC			Use Torque wrench of higher resolution	Male Screw Lock 0.34
36	Screw OBC-ADC Connector to OBC			Use Torque wrench of higher resolution	Male Screw Lock 0.34
37	Screw OBC-Power Connector on OBC			Use Torque wrench of higher resolution	Male Screw Lock 0.34
38	Screw OBC-GPS Connector to OBC			Use Torque wrench of higher resolution	Male Screw Lock 0.34
39	Screw OBC-Preflight Connector to OBC	small connector upto antisunside			
40	Mount OBC on Leading				
41	Tie Beacon-OBC and Downlink-OBC Conne- -cting wire on LD_C_1				
42	Tie Beacon-OBC Connecting wire on LD_C_2				
43	Screw ADC-Sunsensor Connector to ADC			Use Torque wrench of higher resolution	Male Screw Lock 0.34
44	Screw ADC-OBC Connector to ADC			Use Torque wrench of higher resolution	Male Screw Lock 0.34
45	Mount ADC on Zenith				M3 X 10, 0.4
46	Tie ADC-Sunsensor (all 6) Connecting wire on Z_C_1				
47	Tie ADC-Sunsensor (Nadir, Antisunside) Connecting wire on Z_C_2				
48	Tie ADC-Sunsensor (Nadir, Antisunside) Connecting wire on Z_C_7	ADC-Sunsensor(Nadir) and ADC-Sunsensor (Antisunside) wire should be beneath the ADC board(in the path made by ADC Board & GPS)			
49	Tie ADC-Sunsensor (Nadir, Antisunside) Connecting wire on Z_C_8				
50	Tie ADC-Sunsensor (Sunside,Zenith,Leading) Connecting wire on Z_C_3	LG_SS here diverges to LG before this clamp.			
51	Tie ADC-Sunsensor (Zenith,Leading) Connecting wire on Z_C_4	S_SS here diverges to S before this clamp.			
52	Tie ADC-Sunsensor (Zenith,Leading) Connecting wire on Z_C_5	Z_SS here diverges towards Z window after this clamp.			
53	Tie ADC-Sunsensor (Leading) Connecting wire on LD_C_8				
54	Tie OBC-Power Connecting Wire on LD_C_3.				
55	Tie Magmeter-OBC Connecting wire and ADC-Sunsensor(Nadir, Antisunside) on LD_C_6.	Include Nadir,Antisunside sunsensor and Uplink Thermostor wires in this clamp.		Both wires are running in opposite direction	
56	Tie ADC-Sunsensor (Nadir,Antisunside) on LD_C_7.	Include Thermistor wires (Beacon, Downlink, Battery Box) and Preflight connector in this clamp.			

Sr. No.	Steps	Comments	Reference	Precautions	Torque Value
57	Pass ADC-Sunsensor (Antisunside and nadir), Thermistor(Beacon, Downlink) and Preflight connecting wire on A_C_2.	Leave the cable tie still loose.	8,16,66		
58	Pass ADC-Sunsensor (Antisunside and Nadir) and Preflight connecting wire on A_C_3.	Leave the cable tie still loose.	17,66		
59	Rotate Nadir-Sunside-Antisunside Assembly along the edge- N_LD	Make Leading as the base.			
60	Rotate Nadir-Sunside-Antisunside Assembly along the edge- N_LD	Make Leading as the base.			
61	Mount Sunside to Leading	Tie the extra connecting wire between OBC/PC using cable tie.		Use Torque wrench of standard resolution.	M3 X 10, 0.4
62	Mount Antisunside to leading			Use Torque wrench of standard resolution.	M3 X 10, 0.4
63	Tie the extra connecting wire between OBC/PC using cable tie.				
64	Tie Solar Panel (Sunside, Lagging) Connecting wires on A_C_6		65		
65	Take both solar panels connectors from antisun window		17		
66	Slightly pull the ADC-Sunsensor (Antisunside, Nadir) wires from Antisunside window.	Tighten the cable tie of A_C_2 and A_C_3 respectively.	8,16,17,57,58		
67	Mount OBC- Preflight connector on antisunside window	Nuts to be outside, screws from inside			
68	Put Zenith on Outer Zenith Fixtutre and leading side on leading fixture almost simultaneously				
69	Mount GPS Puck Antenna on Zenith.				
70	Screw GPSA-GPS Coaxial cable on GPS Puck Antenna.			Use spanner	33.9
71	Screw OBC-GPS Connector to GPS			Use Torque wrench of higher resolution	Male Screw Lock 0.34
72	Screw GPS-GPSA Coaxial cable on GPS.			Use Torque wrench of higher resolution	0.96
73	Mount GPS to Zenith			Use Torque wrench o f higher resolution	M4 X 12, 0.86
74	Mount Uplink monopole assembly to Antisunside		Guideline Sheet		
75	Mount Downlink monopole assembly to Antisunside		Guideline Sheet		
76	Mount Beacon monopole assembly to Antisunside		Guideline Sheet		

Sr. No.	Steps	Comments	Reference	Precautions	Torque Value
77	Connect Uplink monopole to Uplink coaxial cable using L connector	Leave it hanging.		Use Torque wrench of higher resolution	0.96
78	Connect Downlink monopole to Downlink board using L connector			Connector details	
79	Connect Beacon monopole to Beacon board using L connector			Connector details	
80	Tie OBC-Magmeter Connecting wire on A_C_4		94		
81	Tie OBC-Magmeter Connecting wire on A_C_5		95		
82	Rotate zenith side about LD-Z to make vertical				
83	Screw zenith to sunside				
84	Screw zenith to anti sunside				
85	Rotate Sunside-Nadir-Antisunside-zenith assembly along the edge LD_Z to make zenith as base			All wires near that edge, All the cable mounts on torquer should not be outside the torquer, very less distance between the torquers	
86	Mount Leading to Nadir			Use Torque wrench of standard resolution.	M3 X 10, 0.4
87	Mount Leading to Zenith.			Use Torque wrench of standard resolution.	M3 X 10, 0.4
88	Screw Magnetometer-OBC wire to Magnetometer.			Use Torque wrench of higher resolution	Male Screw Lock 0.34
89	Screw Magnetometer to Lagging.			Use Torque wrench of higher resolution	M4 X 12, 0.86
90	Move all the sunsensors except zenith from all the respective windows				
91	Mount Magnetometer-OBC wire on LG_C_1.	Leave the cable tie loose.	92		
92	Tie Uplink Thermistor wire on LG_C_1.	Tighten the cable tie.	91		
93	Pass Uplink - Thermistor wire to Z_C_9.				
94	Mount Magnetometer-OBC wire on LG_C_2.				
95	Tie Lagging-Sunsensor wire on LG_C_3.				
96	Screw Uplink-Power Connector to Uplink			Use Torque wrench of higher resolution	Male Screw Lock 0.34
97	Screw Uplink board - Uplink Monopole coaxial cable to Uplink board.			Use Torque wrench of higher resolution	0.96
98	Mount Uplink board on Lagging.			Use Torque wrench of standard resolution.	M3 X 10, 0.4

Sr. No.	Steps	Comments	Reference	Precautions	Torque Value
99	Tie Uplink-Power wire on LG_C_4.				
100	Tie Uplink-Power wire on LG_C_5.				
101	Holding lagging rotate whole assembly to make leading as base			leading sunsensor should be inside the fixture cutout	
102	Take lagging sunsensor outside				
103	Mount Lagging onto the N-A-S-LD-Z assembly.			Use Torque wrench of standard resolution.	M3 X 10, 0.4
104	Rotate the satellite assembly so that Zenith is the base.	Put it on Fixture			
105	Mount the Mock LVI on Nadir.			Screw should be attached in diagonal mode. Mock LVI should be handled with care such that it doesn't slide over the side panels. The main aim in doing this is that there should be no scratch on the Mock LVI.	M6 X , 2.8
106	Mount Nadir SS on nadir sides corner which is coming out from ASS window				
107	Rotate assembly to nadir as base				
108	Integrate MLI onsides\ (Leading,Lagging, Sunside,Zenith)		Guideline sheet		
109	Rout Sunsensor wire outside the satellite side		wire routing sequence	Nadir SS taken out from Antisunside window	
110	Mount Solar Panel on Sunside		Guideline sheet	It is connected with Zenith Solar Panel	
111	Mount Sunside Sunsensor on Sunside Solar Panel				
112	Mount Zenith Solar Panel on Zenith side				
113	Mount Zenith Sunsensor on Zenith Solar Panel		Sunsensor Guideline		
114	Route Sunside and Zenith SolarPanel wire to Antisun side window	All rounting is instantaneous using Kapton tape			
115	Mount Leading Solarpanel on Leading side			Lagging Solar Panel is connected	
116	Mount Leading Sunsensor on Leading Solar Panel		Sunsensor Guideline		
117	Mount Lagging Solar Panel on Lagging side				
118	Mount Lagging Sunsensor on Lagging side				
119	Route Leading and Lagging SolarPanel wire to Antisun side window	All rounting is instantaneous using Kapton tape			
120	Tie All SolarPanels wires on outer clamp				
121	Screw Solar Panel connectors				
	Integration Completed				

Chapter 8

Operational Sequence

The Satellite passes through various stages of operation (modes). This chapter lists the tasks that the Satellite should do in each of these modes.

8.1 Modes of Operation of the Satellite

The different modes of operation of the Satellite are listed below. The flowchart (Fig. 8.1) describes the transfer from one mode to another. Mode -1: Pre-flight checks
Mode 0: Liftoff
Mode 1: Detumbling
Mode 2: Nominal operation without Downlink
Mode 3: Nominal operation with Downlink
Mode 4: Emergency Mode
Mode 5: Safe Mode

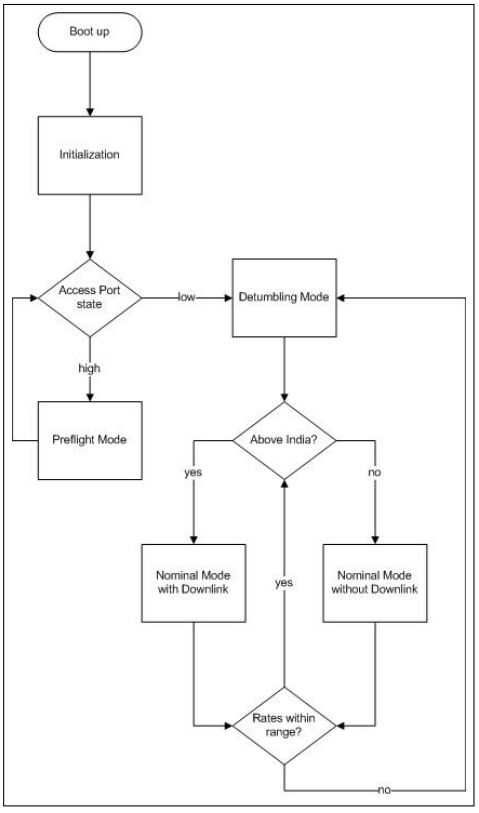

Figure 8.1: Flowchart for the Modes of Operation

Mode -1: Pre-flight checks

- Satellite shall be inside the Clean Room at the launch site.

- The access ports shall be used to check the Satellite's health.
- The batteries shall be charged to full capacity.
- The Satellite is ready for launch and mounted on the Launch Vehicle.
- Before launch, the battery connector should be plugged in.
- This mode starts about 6 days before launch. (T – 6 days)
- In the event of a delay, the batteries shall be recharged after 30 days on the launch vehicle.

Mode 0: Liftoff

- Satellite shall be inside the Launch Vehicle. This mode starts with liftoff and ends within 17-22 minutes after launch (T_0).
- All Sub-Systems shall be switched off.
- The Satellite shall be deployed into orbit by the Launch Vehicle, using the Launch Vehicle Interface.
- The SNAP circuit (Deployment Switch) shall detect the Satellite is deployed.

Mode 1: Detumbling

- The SNAP circuit shall switch on the Power circuit after 50 minutes of SNAP.
- The Power circuit shall switch on the other components in the following order:
  - Uplink circuit
  - OBC circuit
  - Beacon circuit
  - All control sensors and magnetorquer
- All processors, memory units, sensors and actuators shall be initialized by the OBC.
- Health Monitoring data should be sent by power to OBC board.
- When Satellite is deployed it has rotational rate about 5deg/sec on all 3 axis, this shall have to be reduced to 0.1deg/sec for nominal mode operation. This process is called Detumbling. It takes about 2-6 orbits, or a maximum of 9 hours to detumble completely.

Mode 2: Nominal operation without Downlink

- This shall be the normal mode of operation of the Satellite in orbit but when not over India.
- Beacon will remain switched on. It will on a 100% duty cycle.
- Health Monitoring data should be sent by power to OBC board.
- Health Monitoring data as per the Data Budget, shall be stored by the OBC.

Mode 3: Nominal operation with Downlink

- This shall be the normal mode of operation of the Satellite in orbit when it is over India.
- Beacon shall be switched on at 100% duty cycle.
- The Downlink shall be switched on such that:
  - When Satellite will be over India but not over IITB, Downlink monopole will transmit the instantaneous position and attitude data.
  - When Satellite will be over IITB, monopole will transmit health monitoring and temperature stored data of EEPROM.

8.2 Emergency Mode and Safe Mode

8.2.1 Emergency Mode

This mode shall be entered when the battery voltage drops below 6.6V.
All components except the Beacon and the Power board will be switched off by the power board in the following manner:

1. Downlink
2. All control sensors and magnetorquer
3. OBC circuit

8.2.2 Safe Mode

This mode shall be entered when the battery voltage drops below 6V.
The components will be switched off in the following manner, by the Power board:

1. Beacon
2. Power Circuit(other than Microcontroller)

Chapter 9

Power Subsystem

9.1 Introduction

9.1.1 Power Sources

The main sources of power for a space craft are

- Solar panels and
- Battery

9.1.2 Power Budget Summary

Power SubSupply	Supply Voltage (V)	Load Current (mA)	Load Power (W)
PBEACON	5.00	548.60	2.74
PDOWNLINK	5.00	460.82	2.30
PCONTROL /TORQ	3.60	865.70	3.12
POBC	3.30	24.77	0.08
PGPS	5.00	400.10	2.00
PMAG	8.40	35.00	0.29
VBAT	8.40	130.84	1.10
		Total Power Budget	11.64

Table 9.1: Power Budget Summary

9.1.3 Incident radiation

The satellite receives light from three sources:

- Direct solar radiation
- Sunlight reflected from Earth
- Earth's thermal radiation

Direct solar radiation is the major component of these. Power available from solar radiation is calculated analytically.

9.2 Power Requirements

9.2.1 Requirements from On Board Computer Sub-System imposed on Power Sub-System

- Power Sub-System should send Health Monitoring (HM) data received from loads,current sensors and battery when the OBC polls for data. Note that HM data does not include temperature data.
- Power Sub-System shall inform OBC Sub-System if some component misbehaves (over-current) and has to be shutdown. The decision to shut it down shall be taken by the On Board Computer (OBC) unless it is the OBC itself which misbehaves.
- For the case when the OBC itself experiences over-current, Power Board will shut it down and decide when to start it again.

9.2.2 Requirements from Integration Sub-System imposed on Power Sub-System

- The size of the circuit board should be 12cm X 12cm.
- 1cm border shall be left on all sides along with a central square of 1cm, and it must be grounded.
- In the region which is 0.7cm from the circuit bottom, and tall components should not be mounted.

9.2.3 Requirements from Power Sub-System imposed on On Board Computer Sub-System

- OBC Sub-system should poll for HM Data every two seconds.
- OBC Sub-System shall update Power Sub-System every two seconds, with the list of components that should be turned ON or OFF.

9.2.4 Requirements from Power Sub-System imposed on Integration Sub-System

- Integration Team should place solar panels on the 4 sides, namely sun-side, zenith, leading side and lagging side.
- Integration Team should feed the incoming power coming from the solar panels to the power board via two connectors
- Integration Team shall make sure that shadows due to other deployed parts shall not fall on the solar panels.

9.2.5 Requirements from Power Sub-System imposed on Attitude Determination and Controls Sub-System

- During Nominal Mode, Attitude Determination and Controls Sub-System should try to achieve an attitude such that maximum solar irradiation falls on the solar panels.

9.2.6 Requirements from Power Sub-System imposed on Thermals Sub-System

- Thermals Sub-System should protect the solar panels from heating above 70^oC.
- They should maintain the temperature range of the battery within 0^oC to 30^oC.
- They should maintain the temperature of the board within the operating temperature range of the components(industrial grade) i.e. -40^oC to $+85^oC$.

9.3 Charging/Discharging of Battery

9.3.1 Depth of Discharge

Table 9.1 shows the load values for calculation of power consumption. This does not include power requirement of magnetorquer as it is calculated in the matlab code which runs the attitude determination and controls simulations. The condition for battery charging depending on the cell voltage and the power from solar panels is as follows:

- Incoming solar power greater than power consumption AND
- Cell voltage less than 4.1 V if battery is in discharging mode in previous time step OR
- Cell voltage less than 4.2 V if battery is in charging mode in previous time step

9.3.2 Switching Condition

- Start the GPS when the average moment drops below a threshold (0.04 N-m/T) and remains there for some duration (0.4times Orbital period)
- GPS must be off in eclipse region because of power constraints.
- In light region, GPS is switched on periodically after every 10 minutes and kept on for 2 minutes.
- The switching from detumbling to nominal mode is decided by the estimated angular rates.

9.3.3 Simulation results for DOD for various altitudes

Detumbling mode is characterised by high angular rates and hence power generation through solar panels will take place with a lower efficiency in detumbling than in nominal mode. Accordingly, simulations are carried out for two cases for the altitude of 500 km with initial angular rates of [5,5,5] deg./s:

1. The battery does not get charged at all in detumbling mode (worst case scenario)
2. The power generation of solar panels in detumbling mode takes place with an efficiency lower than that in nominal mode. Since the exact efficiency is difficult to estimate, it is taken as half of nominal mode. Nominal mode efficiency is 16%. Therefore, for this case, the efficiency in detumbling mode is taken as 8%.

The initial DOD is determined by the current drawn by the electric switch SNAP circuit. Since electrical switch SNAP uses only 100 μA current, the battery will lose less than 0.036 % of its charge per day. Even in the case of delayed launch of one month or so, battery will drain approximately 1 % of its charge. Hence, corresponding to this worst case scenario, the initial DOD is taken to be 0.01.
Note: We are going to use battery switch for flight model. We will plug in the battery switch only after placing the satellite on Launch Vehicle Interface. Hence the battery will never drain so much before launch.
The following are the essential outputs obtained:

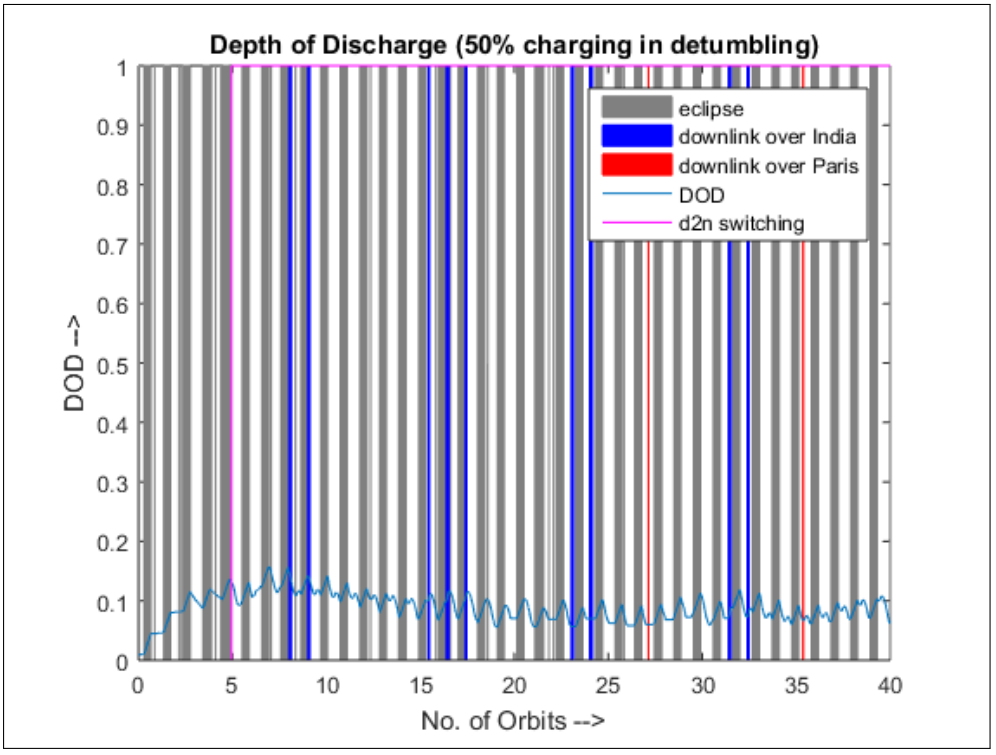

Figure 9.1: Solar power efficiency of 8% in detumbling

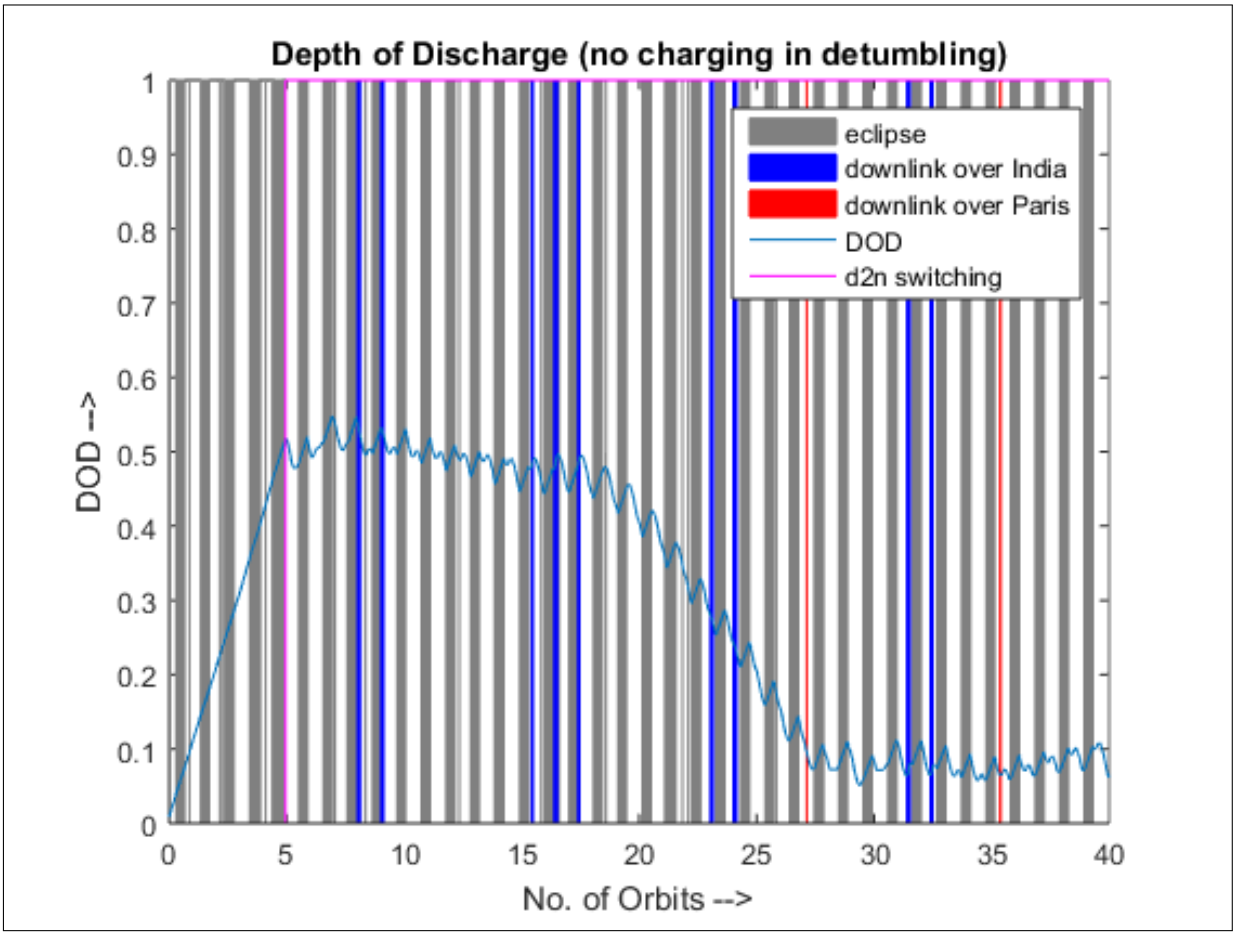

Figure 9.2: No Solar Power in Detumbling

Inference

- DOD value reaches to a maximum of 0.15 in the case of charging during detumbling (Fig. 9.1) and 0.55 in the absence of charging during detumbling (Fig. 9.2).
- In the case of no charging during detumbling, DOD reaches upto 0.55 after initial detumbling(Fig. 9.1 and Fig. 9.2). But after about 20 orbits, it starts to decrease and then remains within 0.15 for subsequent orbits.
- In the case of charging during detumbling, the DOD does not shoot up to a high value during initial detumbling
- The actual scenario will be somewhere between the two cases, since the efficiency of charging during detumbling will steadily increases as the angular rates continue to decreases. So, even for the worst case scenario, DOD is within 55 %.

9.4 Flight Hardware

Now we describe the hardware to be used on the satellite

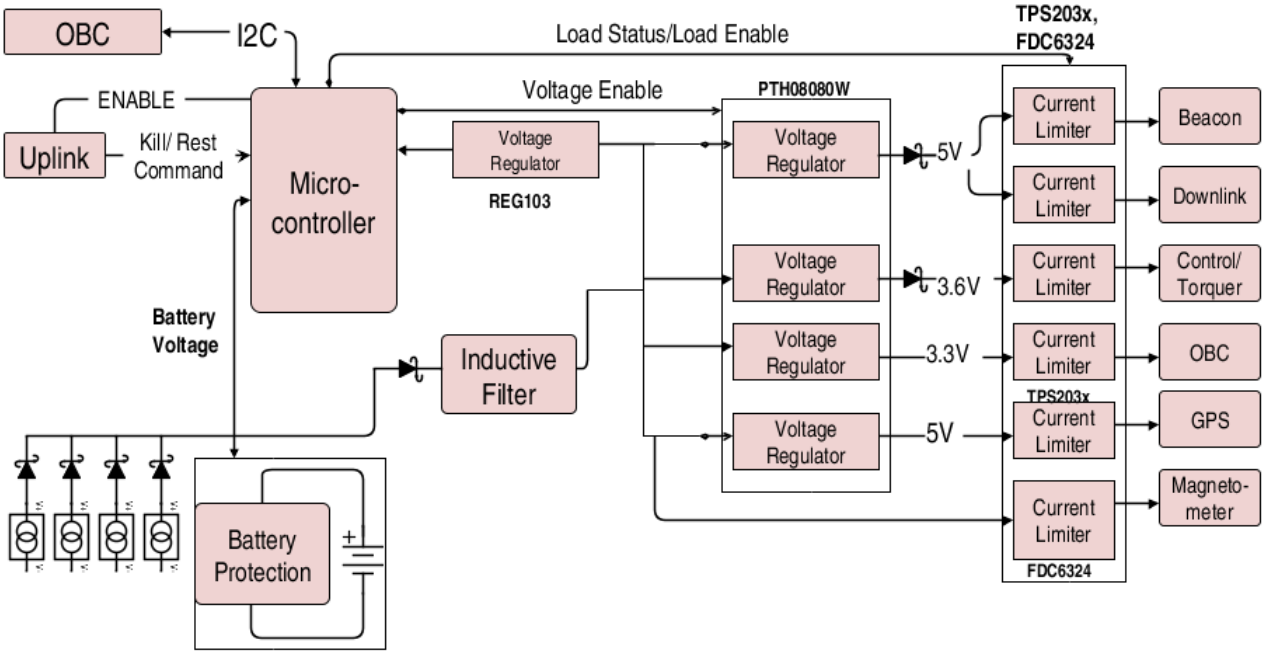

Figure 9.3: Schematic of the Power Board

Four solar panels with reverse blocking diodes are connected to the battery bus. The batteries are connected in a 2-series 3-parallel configuration for redundancy and have protection circuits on them. Voltage regulators step down the battery voltage to 5V, 3.6V and 3.3V. There are current limiting switches in series with each load to ensure shut-down in case of excessive power drawn by that particular load.

9.4.1 Solar Cells

The satellite is powered by solar panels on four faces. One of the side faces is reserved for the antennae and another for launch vehicle interface.

Rough values of characteristics of solar cells are as follows (all characteristics at intensity of 1353 W/m^2 and Temperature: 28^0C):

- Open Circuit Voltage (V_{OC}): 1010 mV
- Voltage at maximum power(V_{MP}): 870 mV
- Short Circuit Current(I_{SC}): 260 mA

- Current at maximum powerI_{MP}: 235 mA
- Maximum Efficiency: 18%
- Dimensions: 20.25 mm (± 0.05mm) x 40.25 mm (± 0.05 mm)

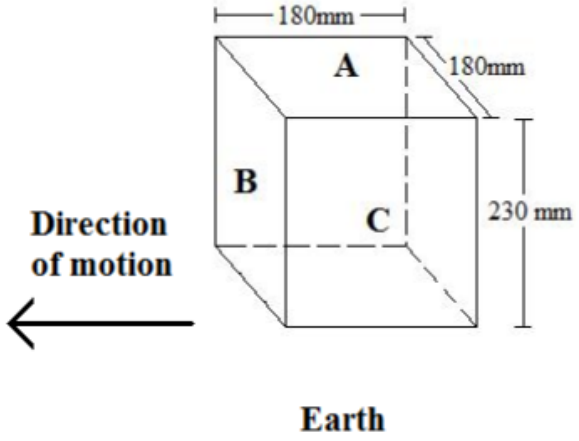

9.4.2 Solar Panel

The faces Leading, Lagging, Sun-side will have 44 cells each and face Zenith has 33 cells to make space for GPS antenna. All faces have the cells connected in strings of eleven cells in series. Hence, faces Leading, Lagging, Sun-side have 4 such strings while the Zenith face has 3 such strings. Since no sunlight ever falls on the face anti sun-side, that face has been used for the antennae, while the face nadir has been used for Launch Vehicle interface.

The voltage ratings of all the panels are the same: V_{OC} = 11.1V and V_{MP}= 9.57V. Panels are designed to have such high V_{MP} because at higher temperature this value falls. Since, MPPT is not used, if V_{MP} falls below battery voltage, very low power output is obtained.

9.4.3 Battery Pack

Rechargeable lithium-ion technology has been selected for the satellite considering their superior performance and characteristics over the other battery technologies. 18650 cylindrical Lithium Ion cells are chosen. The cells are provided by ISRO. Above mentioned cells have the following characteristics:

They will be assembled into a 2-series 3-parallel pack. Thus, the total rating of the battery is:

- Guaranteed Capacity: 6.6 Ah

- Maximum Voltage on Charge: 8.4 V
- Minimum Voltage on Discharge: 6.0V
- Depth of Discharge: 10% to 40%
- Mass: 317 gm
- Dimensions ($L * B * H$): $35mm * 40mm * 75mm$ (excluding harness)

9.4.4 Battery Charge Regulation and Protection

The ideal charging method for Li-ion batteries is a constant-current, constant voltage (CCCV) charging algorithm. In this method, the battery is charged with a constant current (1 A) until the voltage reaches the end-of-charge (EOC) voltage. Once the EOC voltage is reached, the charger switches to a constant voltage charging where the charging current automatically falls with time. The battery is declared "charged" when the charging current drops to a predetermined limit. The limit is determined by the charge management IC.

The varying sunlight intensity makes it impossible to maintain the CCCV algorithm always. Hence, it was decided not to use any dedicated battery charger IC but to use a combination of the microcontroller and the battery protection cum charge regulation IC for regulating the battery charging.

The IC BQ2057W from the Texas Instruments was selected to serve our purpose. The IC has overvoltage protection thresholds which are suitable for our Li-ion dual cells with an EOC voltage of 8.4V. The specifications of BQ2057W are:

- Better than $\pm 1\%$ Voltage regulation accuracy with preset voltages
- Provides three phases of charging: Conditioning, Constant Current and Constant Voltage
- Protects Sensitive Lithium-Ion and Lithium-Polymer battery from overcharging.
- Charge Recharge Threshold of V_{REG} - 0.2V
- Recommended Operating Supply Voltage Range of 4.5V to 15V. The solar panel voltage falls well within this range.
- Operating free-air temperature range of -20 to 70C.
- Total Power Dissipation: 300mW at 25C
- External pass-transistor (PNP) required for current and voltage regulation

To summarize, the battery protection cum charge regulation IC BQ2057 will provide the CCCV charging mode, overvoltage protection and charge recharge threshold. Undervoltage protection is provided by the microcontroller.

9.4.5 Battery Box

Battery box will be a simple rectangular casing for battery. It will be made of aluminium and insulated from the inside with kapton. Following figure gives an idea of the design.

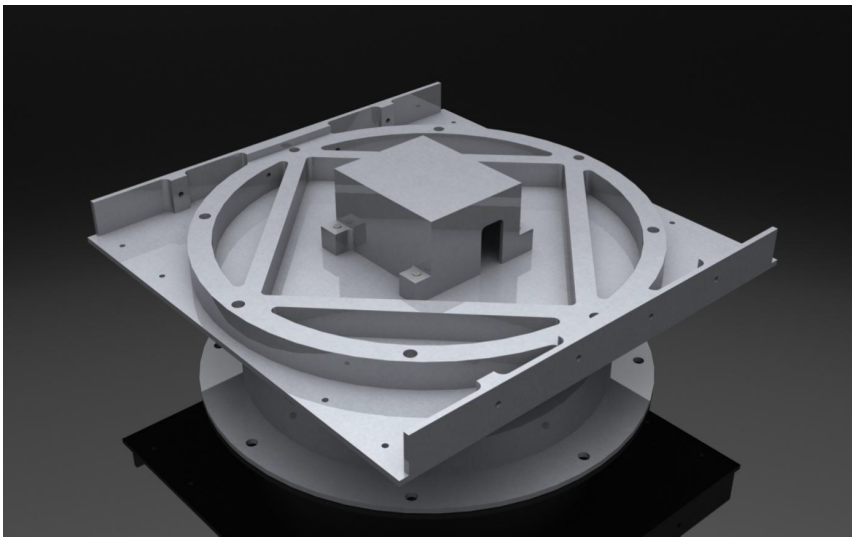

9.4.6 Voltage Regulators

The voltage regulator (also known as the power conditioning module) converts the raw battery or solar panel voltage into a regulated voltage for the loads. An industrial grade DC- DC converter will be used considering following factors:

- Output voltage(s) : 3.3V, 3.6V, 5V
- Input voltage range : 5-10 Volts

The PTH08080W step-down switching regulator and the family REG103 from the Texas Instruments have been selected for this purpose.

9.4.7 Hardware List

Sr. No.	Components	Description	Nos Used
1	Solar Cells	GaAs 18% eff. , 0.87V VMP	165
2	Battery	2S-3P arrangement of 18650 Li-ion cells	1
3	3.3 V Regulator	REG103UA-3.3	1
4	5 V Regulator	PTH08080W (3.3,3.6, 5V)	4
		REG103UA-5	1
5	Microcontroller	ATmega32	1
6	Power Distribution Switches	TPS203x	5
		FDC6324L	1
7	Battery Protection	BQ2057	1
8	Power-O Ring Diodes	MBRS320	7

Table 9.2: Hardware List

9.4.8 Testing of Hardware

Battery Overcharge Protection Testing

Initial Conditions: External Power source connected across Solar Panel connector
V_{BAT} = 7.5V (Before switching on power supply)
V_{CC} = 10.5V
I_{CC} = 1.18A

Observed Charging Curves:

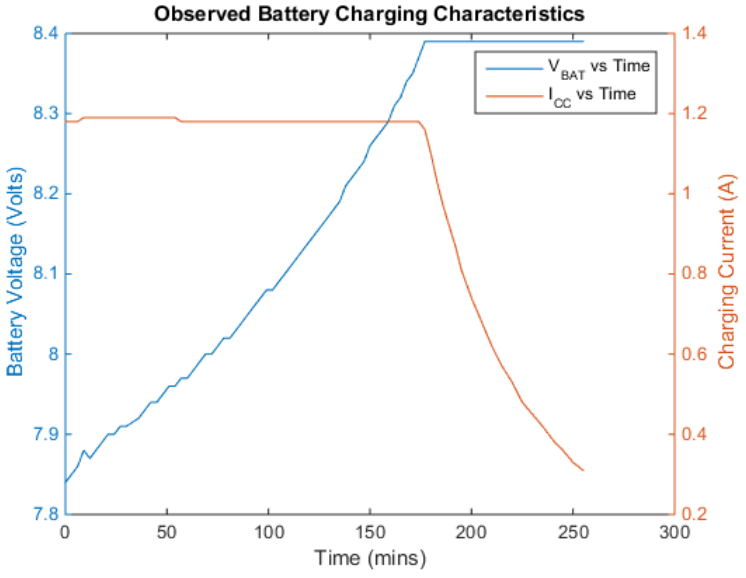

Figure 9.4: I_{CC} vs Time

Final Conditions:
$V_{BAT} = 8.39$V
$V_{CC} = 10.5$V
$I_{CC} = 0.08$A

As can be seen from the plots, the BQ2057 IC effectively prevents overcharging of the battery

Battery Undervoltage Protection Testing

Testing Environment: Fully Charged Battery is connected to the loads through the power board. Microcontroller is programmed to turn of the loads when battery voltage falls below a pre-determined threshold.
Thresholds Tested:
6.6V (Power Saving Mode), 6V (Safe Mode)

Observations:
Loads are turned off as expected.

PTH08080W Testing

Input to each PTH: V_{BAT} - 0.3V (diode drop)
where V_{BAT} is between 6V and 8.39V
Outputs:
5V regulator : 5.0V
3.3 V regulator: 3.28V
3.6V regulator: 3.59V

Inferences: The regulators are providing satisfactory output regulated voltage

TPS Testing

1. **Normal-mode testing:**

Input to TPS of:	**Output of TPS of:**
Beacon: 4.8V (diode drop)	Beacon: 4.8V
Downlink: 4.8V(diode drop)	Downlink: 4.8V
Magnetorquer: 3.3V(diode drop)	Magnetorquer: 3.3V
OBC: 3.29V	OBC: 3.29V
GPS: 5V	GPS: 5V

Inferences: The voltage drop across the TPS is negligible and hence its power consumption is negligible. Thus, the TPS works satisfactorily as a switch

2. **Over-current Testing:**
   Testing Environment:

   (a) A potentiometer was used as a load and its resistance was slowly reduced to zero to produce over-current

   (b) A short was connected across the load

   Observations:

   (a) In case (a), the TPS switched to a constant current mode and the voltage tapered off after the current rose above the rated threshold (0.2 A for OBC and 0.6 A for all other loads). After a short time, the Over Current pin of the TPS went low and this generated the signal of overcurrent for the microcontroller to take further action.

   (b) In case (b), the Over Current pin of the TPS went low immediately on turning on the load and this generated the signal of overcurrent for the microcontroller to take further action.

   Inferences: The behaviour of the TPS was expected as per its datasheet. Thus, the TPS works effectively as an over-current protection switch.

9.5 Software

Software for micro-controller is written in embedded C language. A basic framework for the final code has been written and tested. Micro-controller monitors seven loads and communicates with On Board Computer with I2C interface. Two critical currents and three critical voltages are read and saved. Currently, it can accept command through I2C. Accordingly, command is executed and critical quantities and load status data is sent back. The battery voltage is also continuously monitored and suitable actions are performed when it falls below pre-determined thresholds. All loads are also monitored for over-current and the information is sent to the OBC via I2C and the power board itself switches off the OBC in case of over current experienced by the OBC.

9.6 Health Monitoring

The following quantities are part of the health monitoring data:

1. Load Status - This byte indicates whether a particular load is ON or OFF. It has one bit corresponding to each of the seven loads, Beacon, Downlink, Magnetorquer, Magnetometer, OBC, GPS and Uplink. One bit is unused

2. Panel Current - This byte contains the digital voltage corresponding to the panel current. This digital voltage is provided by the current sense amplifier MAX4372
3. Consumption Current - This byte contains the digital voltage corresponding to the consumption current provided by MAX4372
4. Battery Voltage / 3 - This byte contains the battery voltage divided by three
5. Downlink Voltage / 2 - This byte contains the downlink voltage divided by two
6. OBC Voltage / 2 - This byte contains the OBC voltage divided by two
7. OC Status - This byte indicates whether a particular load is experiencing over-current. It has one bit corresponding to each of the five loads, Beacon, Downlink, OBC, Magnetorquer and GPS. Three bits are unused

Thus, the health monitoring data is seven bytes long and is transmitted to the OBC every two seconds

9.7 SNAP Overview

9.7.1 Introduction

SNAP is the event of the ejection of the satellite from the launch vehicle. The SNAP circuit is required to make sure that the satellite starts operation only after the ejection from the launch vehicle. The RF communication, sensors and actuators are completely off during launch. The micro-controller on only one of the circuit boards (power board) is in sleep mode and hence consumes only 3.26μA (Eq. 9.1). All other circuit boards are switched off.

9.7.2 Circuit Diagram

Fig. 9.5 shows the pin configuration of the SNAP connector on the Power Board. The micro-controller used on the power board is ATmega32.

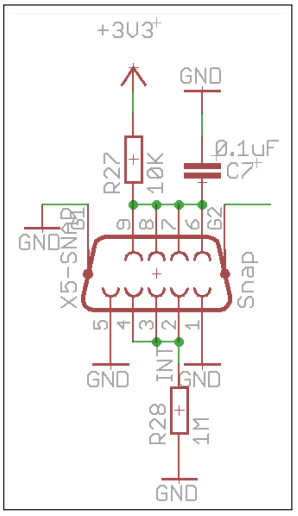

Figure 9.5: Pin Configuration of SNAP Connector on Power Board

An electrical SNAP is used. As can be seen from Fig. 9.6a, two connectors from the satellite side are connected to the corresponding connectors on the launch vehicle before launch. This establishes a connection between V_{CC} and GND. Since the ratio of the resistors used is 1:100, the voltage level at the interrupt pin is close to V_{CC} ($0.99V_{CC}$). After SNAP occurs, the interrupt pin is pulled down to 0V as can be seen in Fig. 9.6b. LOW at the INT pin for a specified amount of time (few hundreds of microseconds) causes the ATmega to wake up from sleep. Level Triggered Interrupt is used so that the ATmega doesn't wake up in case of any stray noises. Two connectors connected in parallel have been used for redundancy. Hence unless both the connectors are separated, the micro-controller will not wake up.

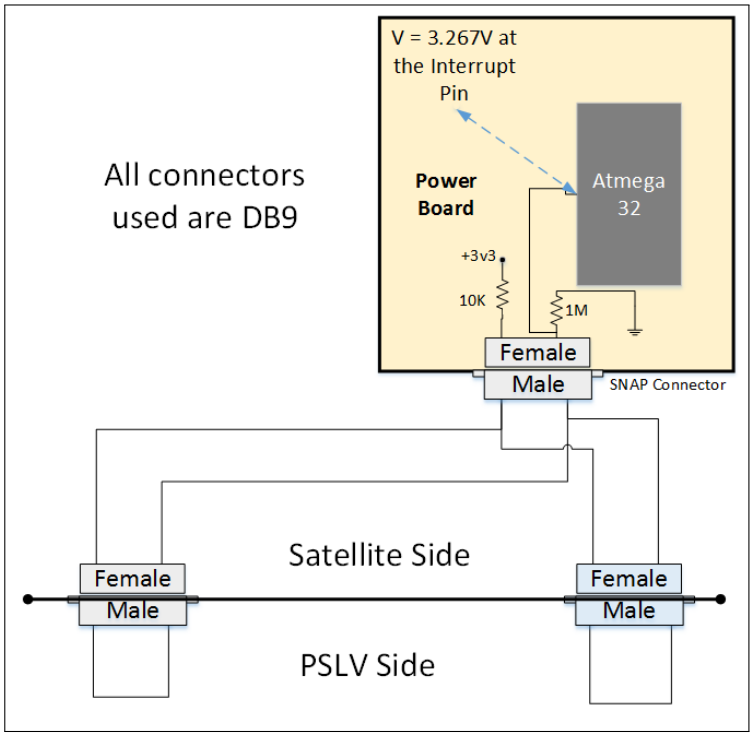

(a) Before SNAP

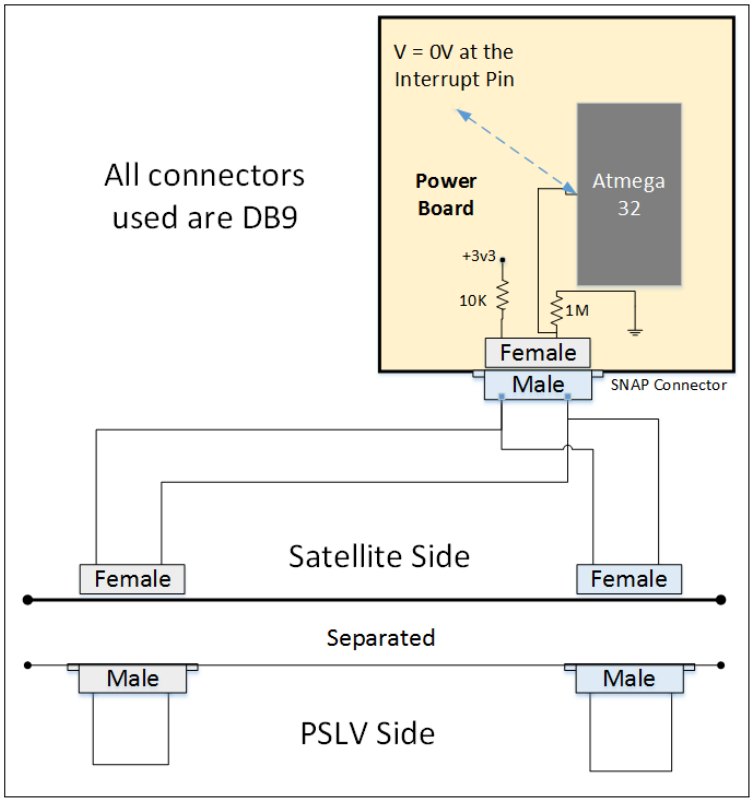

(b) After SNAP

Figure 9.6: SNAP Overview

9.7.3 Sequence of Operations after SNAP

Here is the sequence of operations after SNAP takes place:

- Micro-controller of the power board wakes up from sleep and timer is started.
- It waits for 50 minutes so that the satellite moves sufficiently away from the launch vehicle.
- It powers on On-Board Computer (OBC), Beacon and the sensors and actuators.
- Detumbling mode control law begins.

9.7.4 Power Consumption while in SNAP

The current consumed by the SNAP circuit:

$$I = \frac{V}{R} = \frac{3.3}{1010000} = 3.26\mu A \tag{9.1}$$

The power consumed:

$$P = \frac{V^2}{R} = \frac{3.3^2}{1010000} = 0.0107mW \tag{9.2}$$

Total charge drained in 30 days:

$$Q = I * t = 3.26 * 10^{-6} * 3600 * 24 * 30 = 8.44992C = 2.3472mAh \tag{9.3}$$

The total charge capacity of the battery (2S-3P Li-ion battery) is 6600 mAh. Thus, the charge drained before SNAP is negligible (0.036% in 30 days).

9.7.5 Placement of SNAP connectors on the Satellite

Two DB-9 SNAP connectors will come outside the Nadir window and properly routed on the inner side of the FE ring. They are placed oppositely to maintain symmetry. Similar another two DB-9 connectors are placed on AE ring inner side which will be connected to the above two connectors in parallel.

9.8 Provision for Battery Charging through Pre-flight board

For charging the battery in the integrated satellite, a provision has been provided on the preflight board. A connector has been provided on the anti-sun side which is connected to the preflight connector on the OBC board. The preflight board is connected to this connector externally. The OBC-Preflight connector has a PCHARGE pin through which charging voltage can be applied (Figure 9.7). On the OBC board, the PCHARGE line

goes to the OBC-Power connector (Figure 9.8). and on the power board, this line goes to the battery(Figure 9.10). On applying the desired voltage to the PCHARGE pin on the preflight board, we can charge the battery.

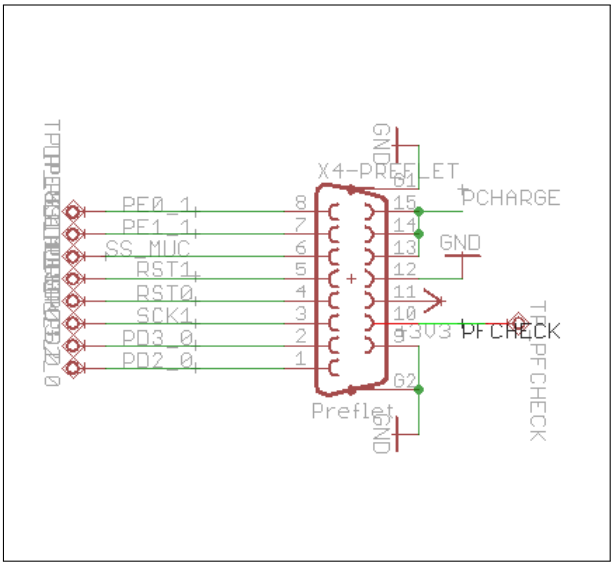

Figure 9.7: Pre-flight connector on OBC

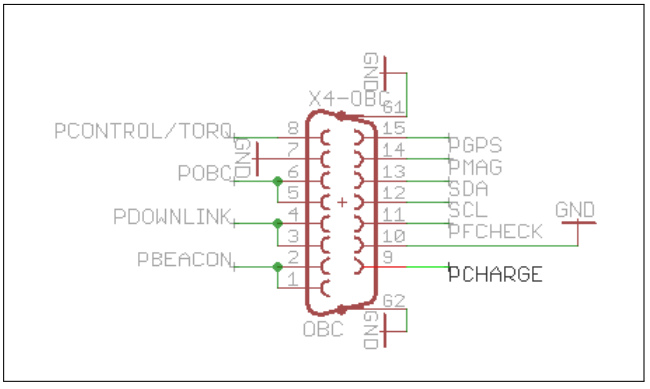

Figure 9.8: Power connector on OBC

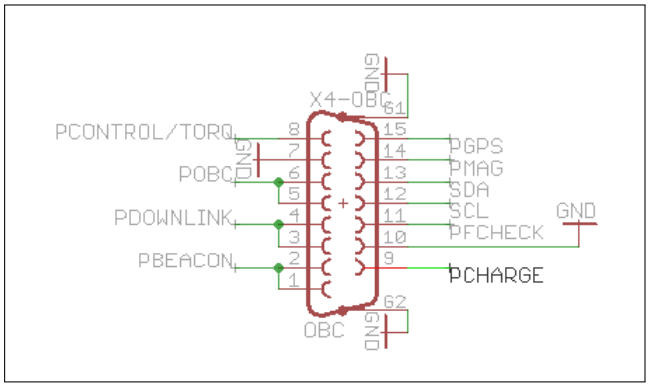

Figure 9.9: OBC connector on power board

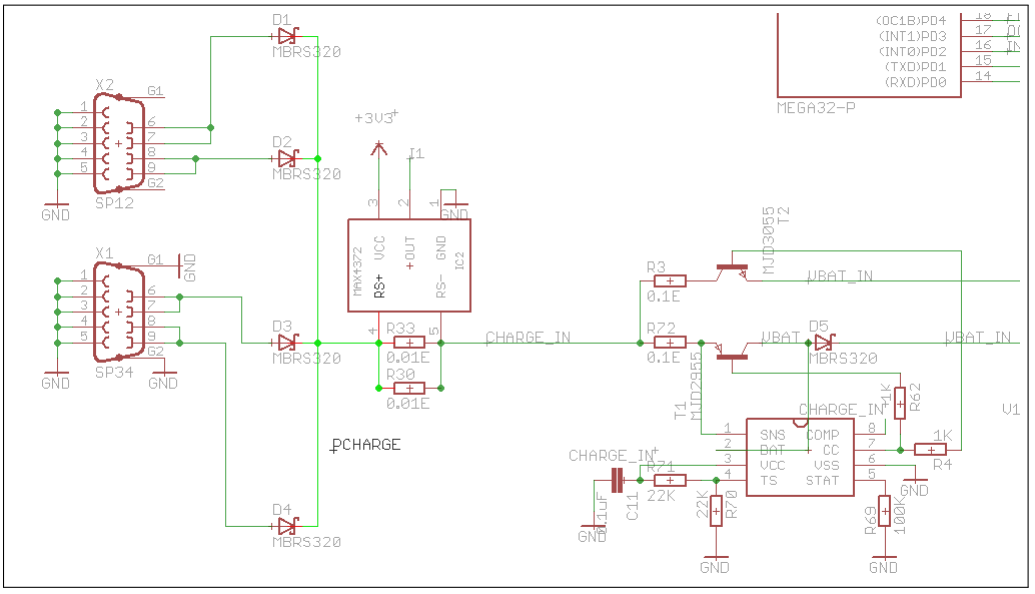

Figure 9.10: PCHARGE line on the power board going to the battery

9.9 Flowchart of the Software

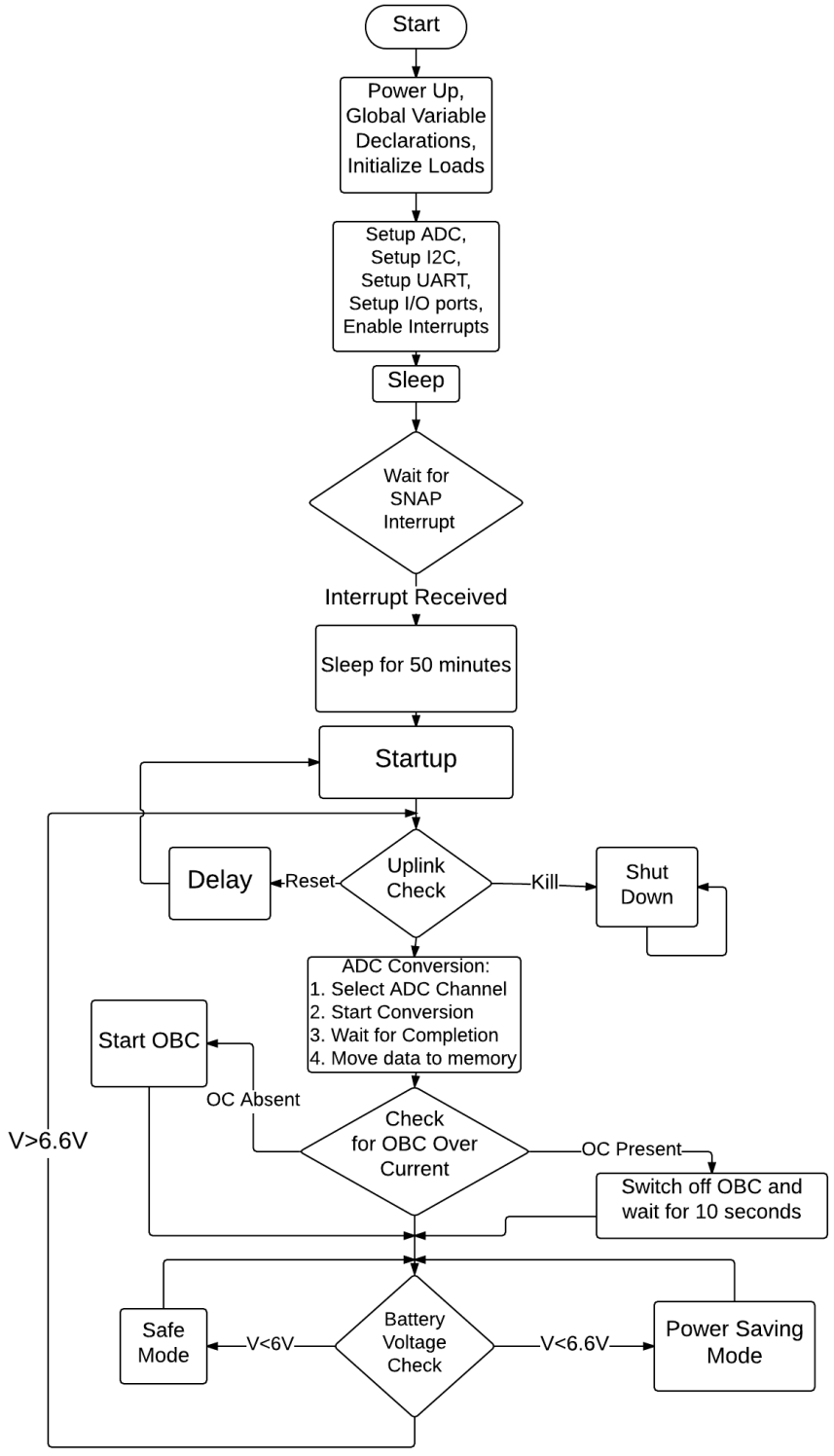

Figure 9.11: Main Code Flow Diagram

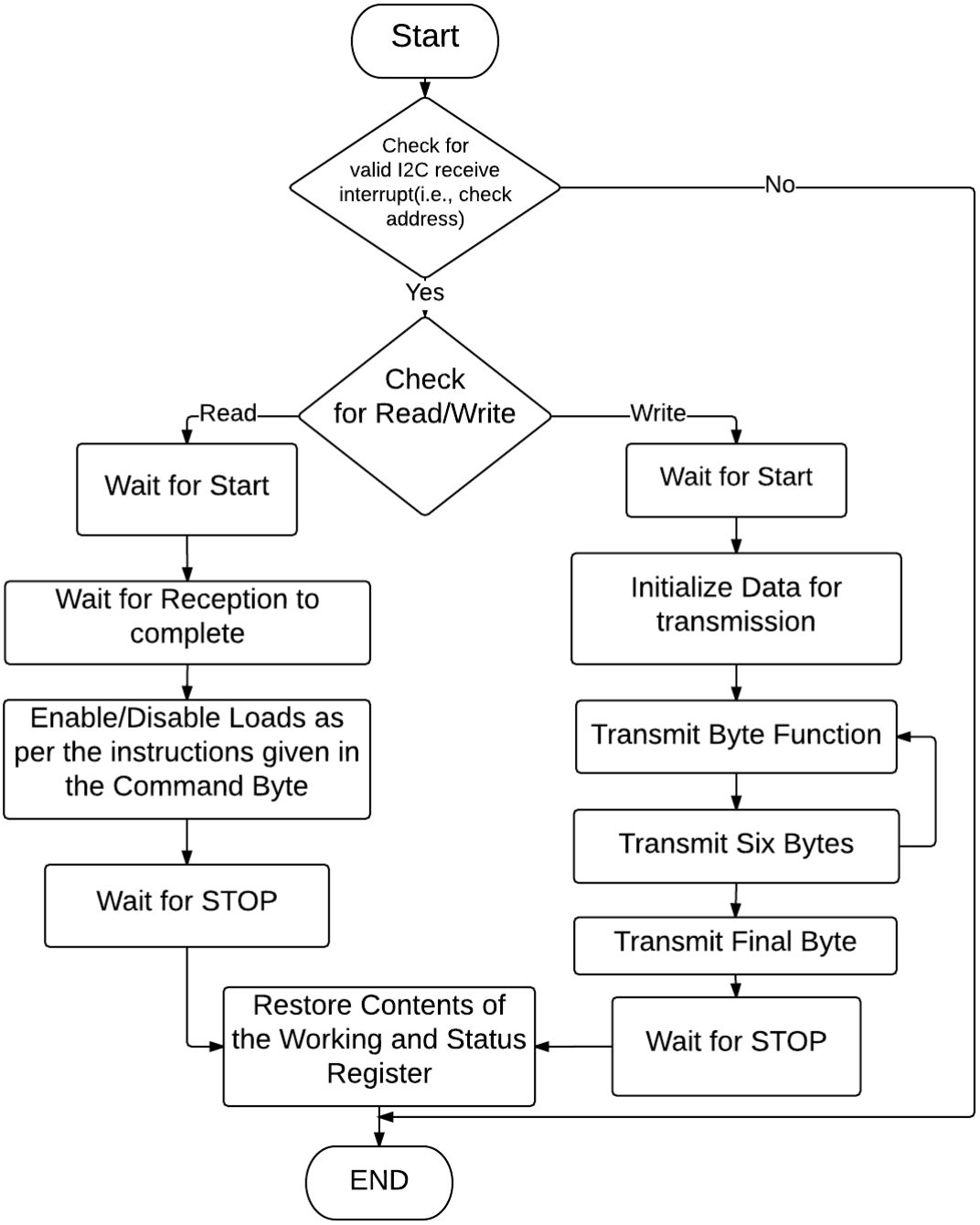

Figure 9.12: Power-OBC TWI(I2C) Interrupt Service Routine Flow Diagram

Chapter 10

Attitude Determination and Control Subsystem

10.1 Introduction to ADCS

10.1.1 Objectives:

- Position determination - To determine the position of the satellite in space, with respect to an inertial reference frame.
- Attitude Determination - To determine the attitude of the body frame of the satellite with respect to orbit frame.
- Attitude control - To bring the satellite into earth pointing orientation after ejection and to maintain this attitude within given bounds throughout the period of operation.

10.1.2 Requirements from other subsystems:

- Position requirements are required by the communication subsystem to know when to begin data transmission when over a ground station.
- Requirements of the ADCS subsystem arise due to need for obtaining the components of earth's magnetic field and the sun vector in the orbit frame. This is required for attitude determination.
- Requirements of the payload subsystem arise due to the need for correlating the position of satellite with the measured value of TEC. This data is required on ground for post processing of the TEC data. Hence, either position must be calculated on ground using an orbit estimator or must be transmitted to ground from the satellite.

Requirement	**Imposed by**
Roll	Payload & communication subsystem
Pitch	Payload & communication subsystem
Yaw	Power subsystem
Position	Payload & communication subsystem

Attitude determination:

On board		
ADCS	Roll pitch Yaw	5 degrees (not stringent as long as control is obtained within desired limits)

- This is required to achieve attitude control of the satellite.

Attitude control:

Power	10 deg (yaw)
Communication and Payload	10 deg (roll, pitch)

- Yaw stabilization is required by the payload.
- Roll and pitch stabilization is required by the communication subsystem to ensure proper signal reception from the satellite.

10.1.3 Requirements from ADCS subsystem to other subsystems:

Requirements from Attitude Determination and Controls Sub-System to On Board Computer Sub-System

- OBC Sub-System shall execute the Control Law as per the operational sequence.
- They shall interface with the following sensors:
  - Magnetometer (UART)
  - GPS (UART)
  - 6 Sun-Sensors (1 ADC board with multiplexer)
- They shall drive the 3 magnetorquers using PWM.

Requirements from Attitude Determination and Controls Sub-System to Integration Sub-System

- Integration Team shall make the principal axis of the Satellite coincide with the geometric axis.
- They shall make the Satellite meet the conditions for Static stability, namely
  - $I_x > I_y > I_z$
  - $I_x < I_y + I_z$
- 3 magnetorquers shall be placed on 3 sides along the 3 body axis, namely the zenith, the leading velocity and the sun-side.
- GPS shall be placed on zenith and expose the antenna to space.
- Magnetometer shall be placed at the position with least magnetic disturbances.
- 6 Sun-Sensors shall be placed on the 6 faces such that their field of view is not curtailed.

10.1.4 Reference frames and axis conventions

Reference Frames

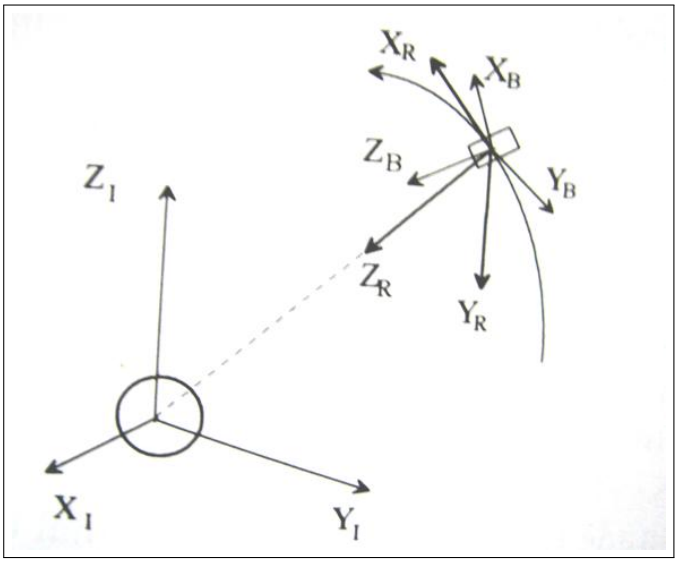

Figure 10.1: Reference Frame

1. Inertial Frame (I)
   $X_I \rightarrow$ First point of Aries
   $Z_I \rightarrow$ Axis of rotation of Earth
   $Y_I \rightarrow Z_I$ x X_I

2. Orbit Reference Frame (R)
   $Z_R \rightarrow$ Towards Earth
   $Y_R \rightarrow$ Opposite to angular momentum of satellite
   $X_R \rightarrow Y_R$ x Z_R

3. Body Frame
   Centered at the mass center and axis perpendicular to faces
   $X_B \rightarrow$ Perpendicular to leading side in the direction of velocity vector
   $Z_B \rightarrow$ Perpendicular to Nadir side towards the earth
   $Y_B \rightarrow Z_B$ x X_B (Perpendicular to antisun side)

4. Earth Centered Earth Fixed frame (ECEF)
   Centered at earth mass center; Fixed to Earth and rotates with it. Two of the axes point to the North Pole and Greenwich meridian.

   A vector is converted from ECI frame to Orbit frame as follows:

$$e_y = -\frac{r \times v}{|r \times v|}$$

$$e_z = -\frac{r}{|r|}$$
$$e_x = e_y \times e_z$$
$$T_{OI} = [e_y \; e_y \; e_y]^T$$
$$v_O = T_{OI} * v_I$$

where, r & v are position and velocity vectors respectively.

10.2 Sensors and Actuators

PRATHAM uses 3 sensors:

- Global Positioning System (GPS) receiver
- 3 axes magnetometer
- 6 Solar cells as Sun sensors

The actuator used is magnetorquer, it is a magnetic coil to produce a magnetic moment that will interact with Earth's magnetic field to produce torque.

10.2.1 GPS receiver

- The GPS receiver is used for position determination/navigation of the satellite.

Figure 10.2: GPS receiver

- Specifications of the receiver:
  The antenna for receiving signals from the GPS satellites is on the zenith face.

The GPS was tested out at place with a clear view of the sky. The terrace of the Aerospace Engineering Department was chosen for this purpose.

Phase 1

The GPS was connected to the primary microcontroller (Master) on the OBC and the output data was transmitted via UART to a PC where it was observed on the serial terminal. The following procedure was then followed:

1. The output of the GPS was first independently observed via UART on the GUI provided by the manufacturer, Accord.
2. On verifying that the GPS puck antenna was sending the correct data, the GPS was connected to the Master OBC and the output was observed on the terminal.

Observation: As expected from the datasheet, after about 80 seconds, the puck antenna started sending the correct data and the array was getting updated in every loop of the Master OBC. The change was observed on the terminal.

Phase 2

After establishing that the GPS is working, the next step was to check the effect of the view factor. The GPS puck antenna was mounted on the zenith side and the solar panel on the zenith reduces the view factor of the puck antenna. Hence, it was necessary to study the effect of the solar panel on the GPS performance.

Testing Environment: The GPS receiver was mounted on the zenith side with the mock solar panel placed appropriately. The satellite was placed on the Nadir side. Therefore, the zenith side was facing the sky.

Observations: The solar panel had negligible effect on the GPS performance and the correct data was sent by the puck antenna in the same time as in the case without the solar panel.

Phase 3

The satellite was turned so that the zenith was no longer on the top, i.e. the zenith was no longer sky-facing. This was done to simulate the worst case scenarios and find out that to what extent can we reduce the view factor. This test was performed in two steps

1. The satellite was placed on the sunside so that the zenith would be one of the lateral faces.
2. The satellite was inverted such that the zenith side was the bottom most side and the Nadir side was sky-facing.

Observations:

- In the first case, the time taken by the puck antenna to send the correct data increased to 120-140 seconds.
- In the second case, correct data was not received even after 180 seconds.

Sources of Error

In all the tests performed above, multiple things could further constrain the view factor. For instance, the presence of humans around the GPS puck antenna etc.

Use of the GPS receiver-

1. The GPS receiver gives the position and velocity of the satellite in Earth Centered Earth Fixed (ECEF) frame. They are then converted to the Earth Centered Inertial (ECI) coordinates.
2. Due to the high power consumption of the GPS, the GPS is not kept ON for the entire time. It is switched ON so that the position and velocity readings are obtained every 10 minutes. This figure is obtained via simulations done keeping in mind the permissible position error. Intermediate values are propagated using J4-gravity model. (see section on SGP4)

Figure 10.3: GPS Antenna

Testing of the GPS receiver and antenna-

1. The testing of the GPS was done on the terrace of the Aerospace engineering department.
2. The GPS device was powered on and the data was logged using a serial port for around 6 minutes.
3. The readings for the first 70 seconds were all NULL. After 70 seconds the data was valid and the PDOP value was around 5. Within 20 seconds the PDOP value reduced to around 200.
4. The uncertainty in the X, Y, and Z components was around 1 m. Position error could not be calculated as the true position was not known.

10.2.2 Three axis magnetometer

The testing of magnetometer majorly consists of calibration. Testing the working of the device is done by simply connecting it to a power source, sending a poll command, receiving the data and viewing it on a serial terminal.

Calibration

- Calibration was carried out using a Helmoltz coil setup. The magnetometer was placed on a platform with one of its axes aligned with the axis of the coils and a current was passed through the coils to generate a known magnetic field.
- The field was then recorded by the magnetometer and after the field value settled, a time averaged reading was recorded and compared to the known value.
- The field was varied from -1 to 1 Gauss.
- The calibration curve along all the axes was observed to be linear.

Results

- The result for X axis is as shown below (squared correlation coefficient (R^2) = 1; RMS error: 8.9×10^{-4})

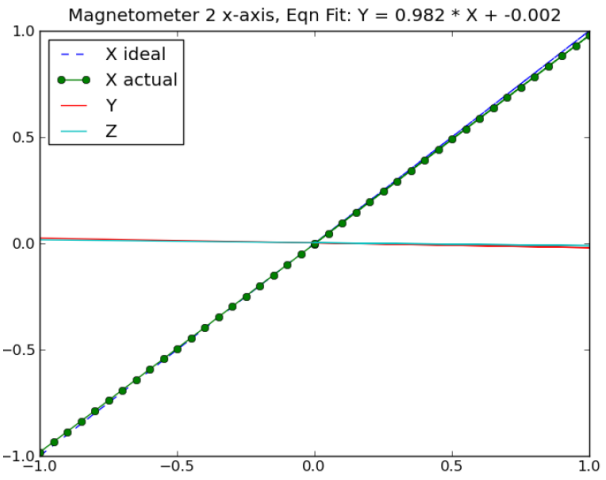

Figure 10.4: Calibration along X-axis

- The result for Y axis is as shown below ($R^2 = 1$; RMS error: 9.5×10^{-4})

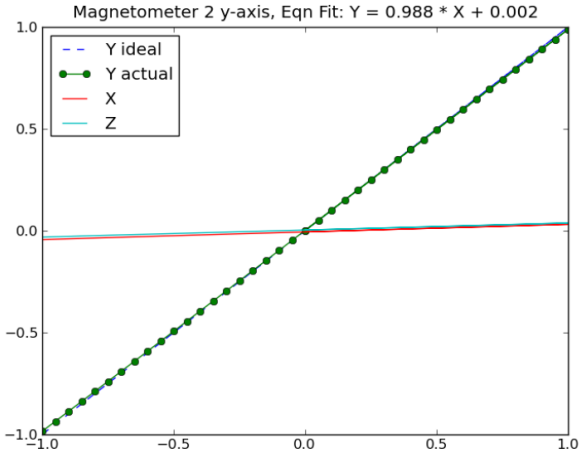

Figure 10.5: Calibration along Y-axis

- The result for Z axis is as shown below ($R^2 = 1$; RMS error: 3.6×10^{-4})

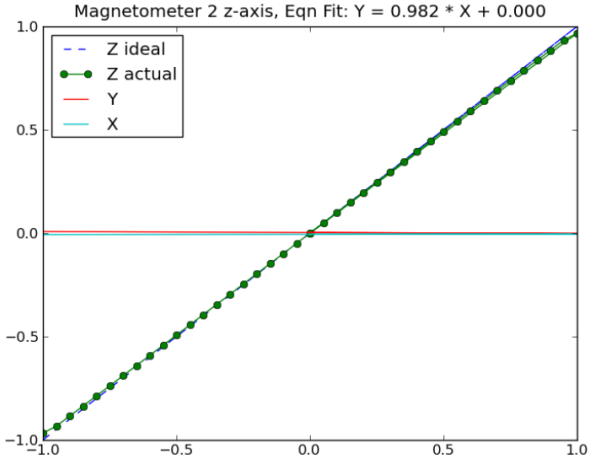

Figure 10.6: Calibration along Z-axis

The magnetometer is used for attitude determination. It is placed on the lagging face of the satellite.

- Specifications:
  - The 3 axes magnetometer used is the HMR2300. It is a magneto resistive, digital magnetometer.

Figure 10.7: HMR2300 Magnetometer

– The HMR2300 is chosen because of its favorable characteristics like space grade, space accuracy, space heritage, low weight and size, ease of data communication as seen in the specifications

Characteristic	Conditions	Min	Typ	Max	Unit
Supply Voltage	Pin 9 referenced to pin 5	6.5		15	Volts
Supply Current	Vsupply=15V, with S/R=ON		27	35	mA
Operating Temperature	Ambient	-40		85	°C
Storage Temperature	Ambient, unbiased	-55		125	°C
Field Range	Full scale (FS) - total applied field	-2		+2	Gauss
Linearity Error	Best fit straight line ±1 Gauss (at 25°C) ±2 Gauss		0.1 1	0.5 2	%FS
Hysteresis Error	3 sweeps across ±2 Gauss @ 25°C		0.01	0.02	%FS
Repeatability Error	3 sweeps across ±2 Gauss @ 25°C		0.05	0.10	%FS
Gain Error	Applied field for zero reading		0.05	0.10	%FS
Offset Error	Applied field for zero reading		0.01	0.03	%FS
Accuracy	RSS of all errors ±1 Gauss (at 25°C) ±2 Gauss		0.12 1	0.52 2	%FS
Resolution	Applied field to change output	67			µGauss
Temperature Effect	Coefficient of gain Coefficient of offset (with S/R ON)		-600 ±114		ppm/°C
Power Supply Effect	From 6 -15V with 1G applied field		150		ppm/V
Vibration (operating)	5 to 10Hz for 2 hours 10Hz to 2kHz for 30 min.		10 2.0		mm g force
Max. Exposed Field	No perming effect on zero reading			10	Gauss
Weight	Board only In Aluminum Enclosure - extended - flush base		28 98 94		grams

Figure 10.8: Magnetometer Specifications

Use of the magnetometer

- The magnetometer measures the magnetic field in body fixed coordinates.
- The magnetometer is on right from injection. Readings are used in the detumbling control (B-dot) law
- The communication of the readings to the microcontroller (μc) is done by the On Board Computer (OBC) team. Their function regarding the magnetometer is data sampling, set-reset and averaging of the data, subject to the constraints of 7 V voltage, 0.03 A current and 0.1 ms time to take the readings

Sources of error

- Error due to electronics of the satellite: The magnetometer is surrounded by other satellite electronics, which have a magnetic field of their own.
- Error due to the satellite body: Due to the metallic body of the satellite, there is magnetization error which can change the magnetic field.
- Mounting error: There will always be a misalignment between the magnetometer axes and the satellite body axes. Integration team will try to minimize the error.
- Error due to temperature variation: Temperature varies from -10 to 60 degree Celsius. This introduces a scaling error, the maximum value of which is 2.1
- Drift error: The magnetic field reading at the same point varies with time. This is known as drift. Experiments were performed, which put a value to the drift as $\sim$ 2.5 μ gauss/s.
- Bias and random error: The maximum bias is $3e^{-4}$ gauss. The maximum random error is $52e^{-4}$ gauss.
- Sudden changes in magnetic field (of the factors of 4 and 5) will be taken care of by putting checks on the OBC.

Calibration of the Magnetometer

- Calibration was carried out using a Helmoltz coil setup. The magnetometer was placed on a platform with one of its axes aligned with the axis of the coils and a current was passed through the coils to generate a known magnetic field.
- The field was then recorded by the magnetometer and after the field value settled, a time averaged reading was recorded and compared to the known value.
- The field was varied from -1 to 1 Gauss.
- The calibration curve along all the axes was observed to be linear.

Results

- The result for X axis is as shown below (squared correlation coefficient (R^2) = 1 RMS error: 8.9x10^{-4})

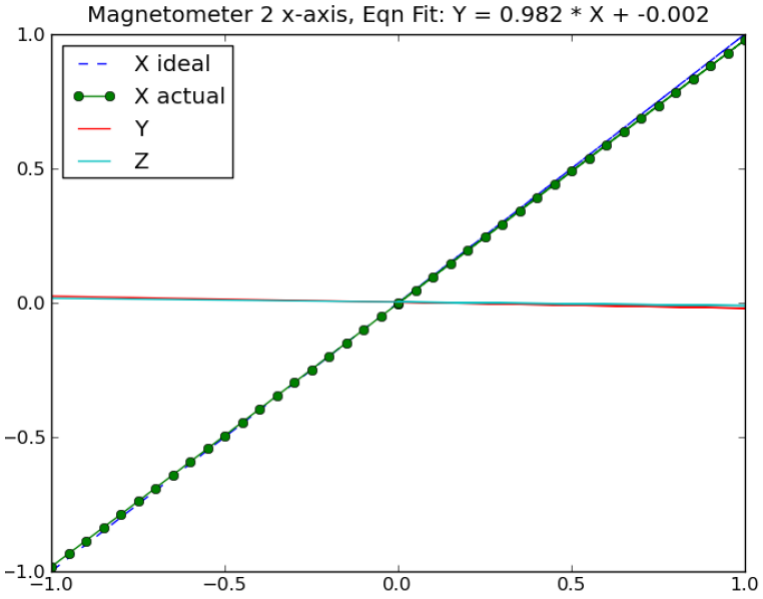

Figure 10.9: Calibration along x-axis

- The result for Y axis is as shown below (R^2 = 1 RMS error: 9.5x10^{-4})

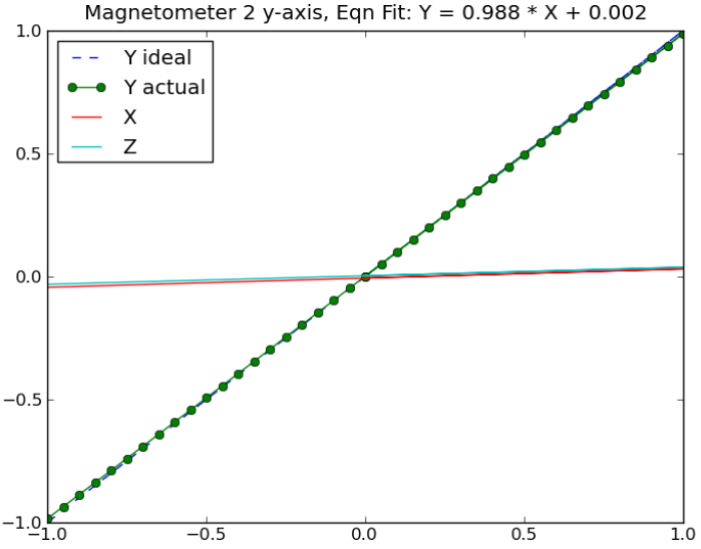

Figure 10.10: Calibration along y-axis

- The result for Z axis is as shown below ($R^2 = 1$ RMS error: $3.6\text{x}10^{-4}$)

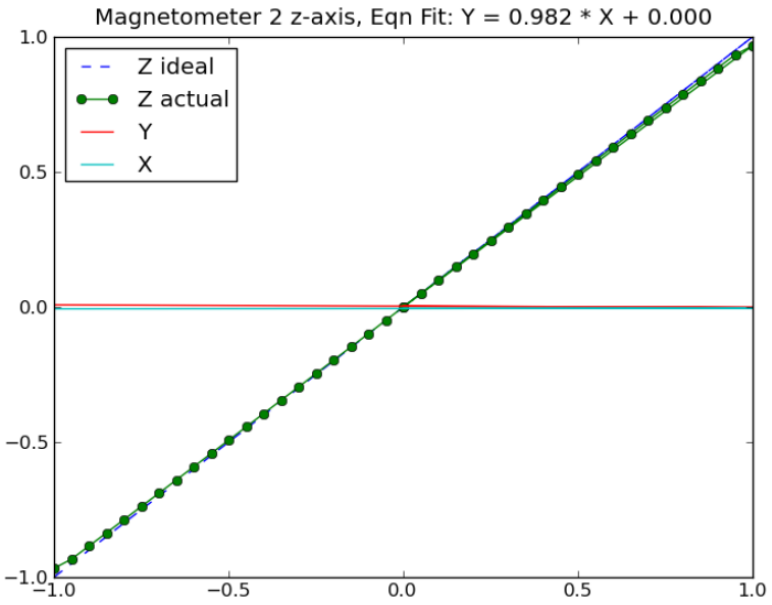

Figure 10.11: Calibration along z-axis

10.2.3 Magnetorquer

The torquer was tested using a helmontz coil setup. The Helmholtz coil has a radius of 20 cm. The axial distance between the Helmholtz coil used was 24 cm. The size of the torquer side is 21 cm.

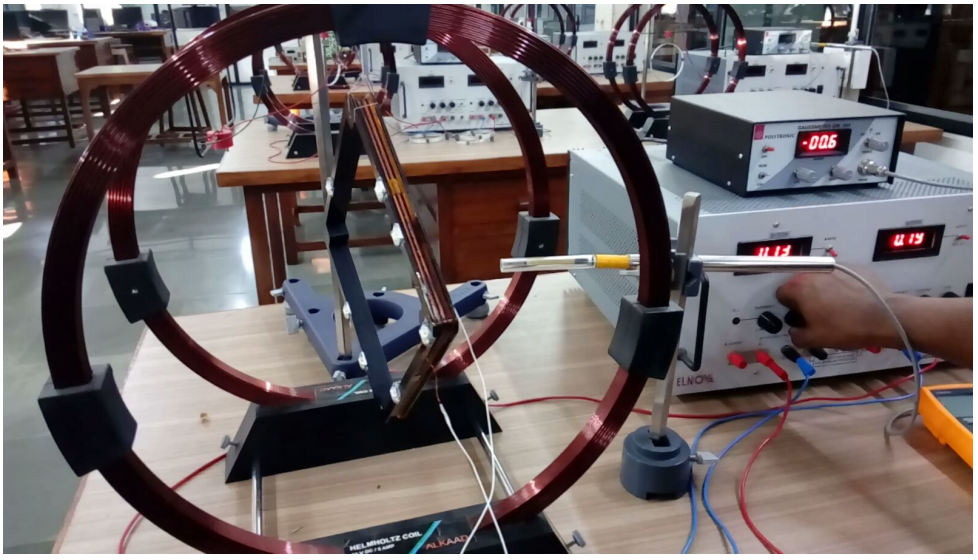

Figure 10.12: Torquer Testing Set-up

Process

1. The torquer was suspended between the helmholtz coil through a string ensuring single point of contact at the knot, perpendicular to the magnetic field generated to produce maximum torque.

2. A gauss meter as seen in Fig: 10.12 measures the magnetic field through a probe between the two coils.

3. When the torquers were OFF, the currents were changed in the helmholtz coil till the magnetic field reached between 0.7 and 0.8 gauss (as magnetic field of earth is of this order).

4. Then the torquer was supplied currents at various voltages.

5. On supplying current, angular deflections were observed in the torquer.

Observation

The amplitude of angular deflections were low initially when constant currents were provided but increased when the currents were changed dynamically by changing the input voltage.

10.2.4 Sun sensors (SS)

- Directional solar cells are used as sun sensors. 6 solar cells are placed on the face centers. The SS are used in attitude determination. The solar cells give an output depending on the angle made by the sensor normal to the sun vector. The lesser the angle, the more is the output.

- Specifications of the receiver:

SL. NO.	DEVICE PARAMETERS	SPECIFICATIONS
1.	Type of detector :	Silicon planar diffused 'n on p' junction
2.	Size:	5mm± 0.05mm x 5mm± 0.05mm
3.	Active region :	4mm±0.02mm x 4.5mm±0.02mm
4.	Responsivity:	Responsivity of the photosensor shall be a minimum of 35mA/cm^2 (AMO) at 25^{0}C
5.	Wafer Thickness:	0.35 to 0.40mm
6.	Resistivity:	10±3 ohm-cm
7.	Short circuit current, I_{sc}:	>35 mA/cm^2 at one solar constant
8.	Dark Current, I_d:	max. 50nA at V_R = 2V (at 23^0 C ± 3^{0}C)
9.	Reverse break down voltage:	5V minimum
10	Shunt resistance, R_{sh}:	>1MΩ in short circuit mode
11	Series resistance, R_s:	Less than 10Ω in short circuit mode
12	Junction capacitance, C_j:	< 8nf typical at V_R = 2V < 15 nf typical at V = 0V
13	Variation in the dark current w.r.t temperature:	Not more than double for every 5^{0}C temperature increase
14	Operating temperature:	-85^{0}C to +85^{0}C
15	Storage temperature :	-100^{0}C to +100^{0}C
16	Anti reflection coating:	Compatible to apply the adhesive 'DC 93500' and meet the responsivity requirement specified
17	Uniformity:	Variation in I_{sc} not more than ±5%
18	Radiation resistance:	% degradation of responsivity not more than 12.5% for an electron fluence of 7x10^{14}e/cm^2 of 1 MeV
19	UV degradation:	not more than 2% for radiation of 1250 equivalent sun hours at a minimum vaccum of 10^{-5} Torr

Figure 10.13: Sun Sensor Specifications

SS electronics

- A simple current to voltage convertor followed by a 10-bit ADC is used to obtain digital values of voltage readings from each SS.

Use of the SS

- The solar cells give an output depending on the angle made by the sensor normal to the sun vector. The lesser the angle, the more is the output. The relation is approximately

$$I = I_0 cos\theta \tag{10.1}$$

where I_0 is the intensity at 0 angle.

- The voltage output is controlled by the SS board circuitry.
- The reconstruction from the SS readings is explained in the simulations chapter.
- In the eclipse part, the readings from all SS are expected to be approximately 0.
- The SS aren't on all the time. Their readings are not used during the detumbling phase. They work in tandem with the magnetometer only in the nominal phase.

10.2.5 Magnetorquers

- 3 orthogonal magnetorquers form the actuator system of the satellite.
- Torquer specifications:

Sr. No.	**Parameter**	**Value**	**Unit**
1.	21x21	Cute 1.7	cm^2
2.	Resistance	$\sim$ 15.6 2	Ohm
3.	Inductance	$\sim \mu$	Henry
4.	Max moment	0.95	Am^2
5.	No. of turns	40	-
6.	PWM resolution	16	bits

Table 10.1: Magnetorquer Specifications

10.3 Simulations

10.3.1 Overview

- The simulations involve the satellite mechanics and dynamics, the satellite environment, the sensor models, the onboard computations (involving navigation and attitude determination), the control law and the torque actuation.
- Block diagram:

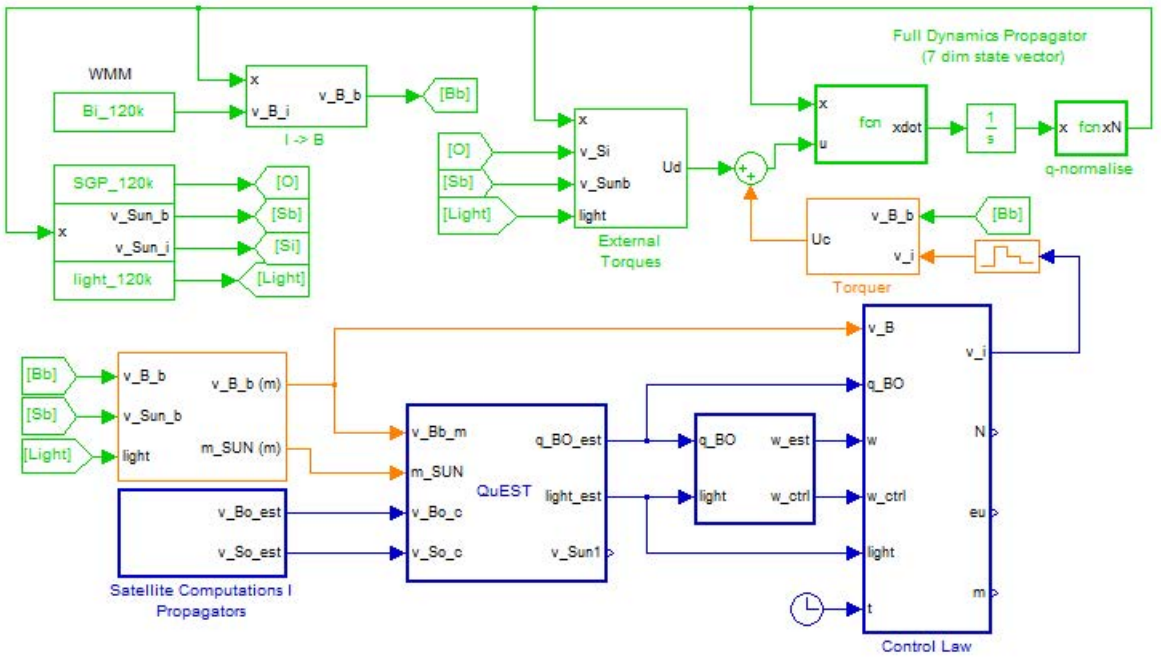

Figure 10.14: ADCS Simulation Block

The green blocks are the environment simulation blocks, which run at a time step of 0.1 sec.
The orange blocks are the hardware blocks, which simulate the noise of the sensors. The output of the hardware blocks is similar to what would be really obtained on board.
The blue blocks are the On Board Calculation (OBC) blocks which evaluate once every frame (2 sec), and hold that value until the next evaluation.

*In All block diagrams, WMM stands for World Magnetic Model 2005, which is now replaced with IGRF-11 13^{th} order for Environment and IGRF-11 8^{th} order for On-board.

Signal flow in a nutshell:

- The SGP4 orbit propagator is the 1st block to evaluate, and runs independently of other blocks. It gives the position vector in ECI frame (O). The Sun model is also independent of any other blocks and depends only on time. It outputs the sun vector (S). Magnetic field (B) in ECI frame is obtained from position vector using IGRF -11 13^{th} order model. All these environmental models run offline.
- Eclipse model is based on O and S and gives the light signal (a Boolean indicating light/dark).
- Disturbance torques are calculated from S, B, O, and the previous state vector (x). These, along with the control torque, are input to the attitude dynamics propagator

which outputs the next state (x). x is the attitude quaternion and rate (of body frame with respect to the ECI frame).

- Real S, B, body frame and O go to hardware blocks which output the measured vectors (position and velocity vector readings from the GPS receiver and the magnetic field vector readings (BB) from the magnetometer) and the 6 sun sensor readings. The SS algorithm extracts the sun vector in the body frame (SB). It also estimates whether the satellite is in the light or eclipse phase.

- The GPS gives the position and velocity vectors at only 10 min intervals. In between the position and velocity are propagated onboard using a simple J2 propagator, fed with initial conditions from the GPS receiver. The position readings are used to calculate the orbit frame magnetic field vector (using IGRF-11 8th order model) (B_O) and the orbit frame sun vector (S_O) on board using on board models.

- The Quaternion Estimation (QuEST) is used to estimate the orbit to body frame quaternion (q_{BO}) (desired to be kept as small as possible within $\pm$ 10 degrees) from $B_B, B_O, S_B, S_O, q_{BO}$ is differentiated to find the rate of the satellite with respect to the orbit frame, expressed in body frame (w_{BOB}).

- These are then used to calculate control torque via the control law.

- The required torque is then applied by the actuator (magnetotorquer). This torque along with the disturbance torques is applied to the real dynamics propagator for state propagation.

10.3.2 Frames of reference

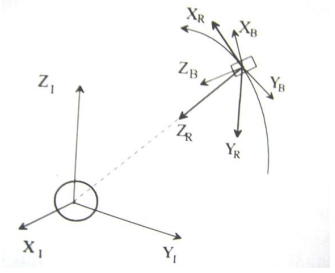

Figure 10.15: Reference Frames

- Inertial Frame (I)
  X $\rightarrow$ First point of Aries
  Z $\rightarrow$ Axis of rotation of Earth
  Y $\rightarrow$ Z $\times$ X

- Orbit Reference Frame (R)
  X → Y × Z
  Z → Towards Earth
  Y → Opposite to angular momentum of satellite

- Body Frame
  Along the geometric body axes

- Earth Centered Earth Fixed frame (ECEF)
  Fixed to Earth and rotates with it. Two of the axes point to the North Pole and Greenwich meridian.
  A vector is converted from ECI to Orbit as follows:

$$\begin{cases} e_y = -(r \times v)/|r \times v| \\ e_z = -r/|r| \\ e_x = e_y \times e_z \\ T_{OI} = [e_x e_y e_z]^T \\ v_O = T_O I * v_I \end{cases} \tag{10.2}$$

10.3.3 Environmental models and real propagators

- Real Dynamics propagator

$$\Omega = \begin{bmatrix} 0 & w(3) & -w(2) & w(1) \\ -w(3) & 0 & w(1) & w(2) \\ w(2) & -w(1) & 0 & w(3) \\ -w(1) & -w(2) & -w(3) & 0 \end{bmatrix} \tag{10.3}$$

$$\begin{cases} \dot{q} = 0.5\Omega q \\ \dot{w} = I^{-1}(u - w \times Iw) \end{cases} \tag{10.4}$$

- Real Orbit propagation: SGP4 model
  - The Small Gravitational Perturbation Model is a standard gravity model for the earth.
  - It is a sophisticated model which iteratively calculates the earth's gravity at any point by including effects like J2, J3, secular effects of gravitation, periodic effects of gravitation, short term perturbations.
  - The inputs are the orbital elements of the satellite orbit (sun synchronous, 500 to 800 km altitude) in the form of a Two Line Element (TLE).

- The output is the ECI position and velocity vector.

- Sun model
  - The sun model takes as input the time elapsed since the latest vernal equinox.
  - It gives as output the ECI sun vector. Calculation is shown below:

$$\text{t} = \text{days since the equinox}$$

$$\begin{cases} \lambda = 2\pi \frac{t}{365.256363} \\ \varepsilon = \frac{23.5\pi}{180} \\ sin(\delta) = sin(\varepsilon)sin(\lambda) \\ tan(\alpha) = \frac{cos(\varepsilon)sin(\lambda)}{cos(\delta)} \\ x = cos(\delta)cos(\alpha) \\ y = cos(\delta)sin(\alpha) \\ z = sin(\delta) \\ v_{Sun_i} = [x; y; z]; \end{cases} \tag{10.5}$$

    where r and v are the position and velocity vectors respectively.

- True Magnetic field model: IGRF-11 O-13
  - International Geomagnetic Reference Field 2011 (IGRF -11) model is used.
  - It calculates the geomagnetic field vector in the ECI frame. It models the earth's magnetism as a magnet with the desired order of polarity (dipole, quadrapole, octapole,etc.). Here a 13th order model is used.
  - The input is the position of the satellite in the ECI frame.

- Light model
  - It says whether the satellite is in light or eclipse region (shadow of the earth on the satellite).
  - The satellite is assumed to be a point mass. However the Sun and the earth are assumed to finite size spheres.
  - When in the umbra or penumbra of the earth, the satellite is in eclipse phase. The sun sensors give no readings. Otherwise the satellite is in light.

– The input is the position of the satellite. The equations for calculation are as follows:

$$\begin{cases} r_{umbra} = \frac{r_0 R_e}{(R_s - R_e)} \\ r_{penumbra} = \frac{r_0 R_e}{(R_s + R_e)} \\ \alpha = asin(\frac{R_e}{r_{umbra}}) \\ \beta = asin(\frac{R_e}{r_{penumbra}}) \\ \theta = acos(\frac{x.v_s}{|x|}) \\ p_u = acos(\frac{x + r_{umbra}.v_s}{|x + R_{umbra}|}) \\ p_p = acos(\frac{x - R_{penumbra}).v_s}{|x - R_{penumbra}|}) \\ if \theta \geq \frac{pi}{2} + \alpha \&\& p_u \leq \alpha \\ light = 0; \\ else \\ light = 1 \end{cases} \tag{10.6}$$

10.3.4 Disturbance torque models

- Gravity Gradient torque:

$$\tau_{GG} = \frac{3\mu}{|r_B|^5} r_B \times I r_B \tag{10.7}$$

where r_B = position vector in body frame,
I = inertia matrix

- Solar drag force:
Solar radiation exerts a drag force on satellite and thus a corresponding torque.

$$F_{Solar} = -A_P C_a P_{flux} \hat{v_{SB}} * light \tag{10.8}$$

- Aerodynamic drag force:

$$F_{aero} = -0.5 A_P C_D \rho |v_B|^2 v_B \tag{10.9}$$

Torque exerted = force crossed with vector from center of mass to center of pressure.
where A_p = projection area,
C_D = drag coefficients,
v_B = position vector in body frame,
ρ = atmospheric density.

10.3.5 Sensor modeling

- GPS modeling
  - The inputs are the position and velocity vectors from the SGP4 model.
  - Random errors in the range as specified in the datasheet are added to the input to give the sensor readings.

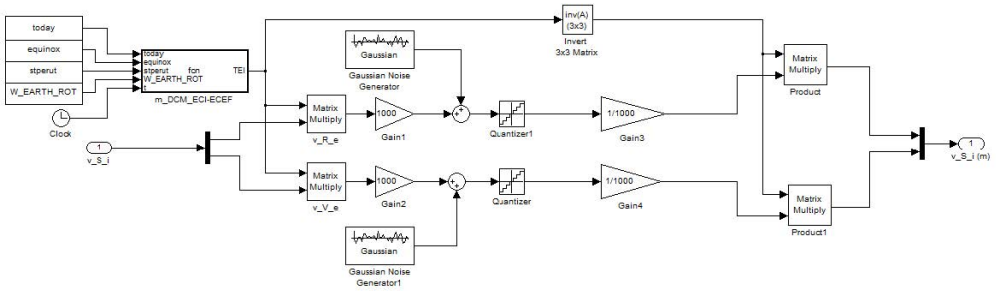

Figure 10.16: GPS modeling

- Magnetometer modeling
  - The input is the geomagnetic field vector from the IGRF environmental model.
  - The RSS error is simply added to the above. Additional bias is also included for robustness.

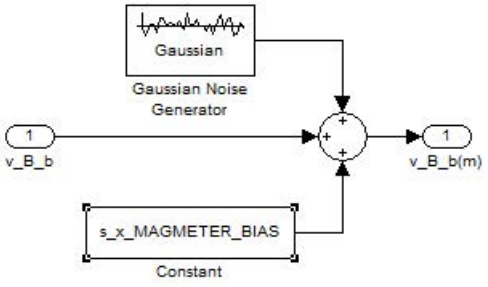

Figure 10.17: Magnetometer Modeling

- SS modeling
  - The input to the SS model is the sun vector in the body frame.

– The model involves adding random error, saturation, ADC gains to the sensor output (a measure of the angle between the sensor normal and the sun vector) to give the SS readings.

– The output of all the 6 SS is theoretically 0 in the eclipse region. But in the sensor block, noise does not allow it to be exactly zero.

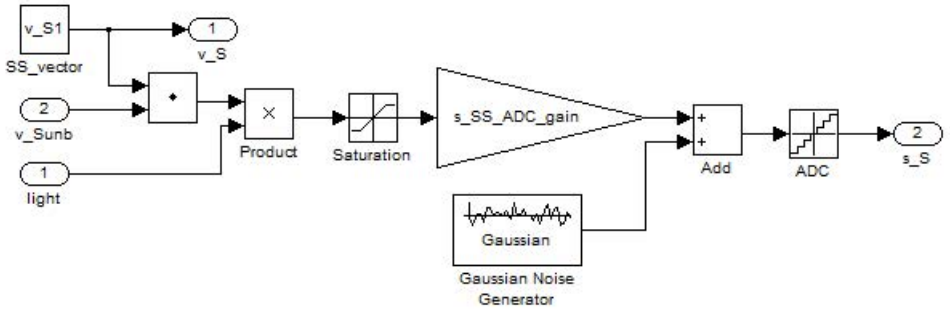

Figure 10.18: Sun Sensor Modeling

10.3.6 Onboard computations

- Orbit propagation/Navigation

  – This model propagates the ECI position and velocity (i.e. the orbit basically) of the satellite between two successive GPS readings. The GPS readings serve as the initial conditions every 10 minutes. (The resetting of the initial conditions is done by the pulse generator in the simulations).

  – The main calculation is that of the earth's acceleration due to gravity at any point. It is integrated successively to get velocity and the position.

  – The acceleration due to gravity g is calculated by employing a J2 model of the earth's gravity. It is important to incorporate J2 because this is the effect responsible for sun synchronous orbits.

  – The model equations are:

$$\begin{cases} V = \frac{\mu}{r}[1 - \sum_{n=1}^{\infty} \frac{a}{r}^{2n} J_{2n} P_{2n}(cos\theta)] \\ V_{J2} = -\frac{\mu}{r}[1 - \frac{J_2}{2}(\frac{a^2}{r^2})^2(3cos^2\theta - 1)] \\ g = -\nabla V_{J2} \\ g_x = -\frac{\mu x}{r^3}(1 + \frac{3}{2}J_2\frac{a^2}{r^2} - \frac{15}{2}J_2\frac{a^2z^2}{r^4}) \\ g_y = -\frac{\mu y}{r^3}(1 + \frac{3}{2}J_2\frac{a^2}{r^2} - \frac{15}{2}J_2\frac{a^2z^2}{r^4}) \\ g_z = -\frac{\mu z}{r^3}(1 + \frac{9}{2}J_2\frac{a^2}{r^2} - \frac{15}{2}J_2\frac{a^2z^2}{r^4}) \end{cases} \tag{10.10}$$

- Calculation of sun vector and magnetic field vector in the orbit frame
  - The position vector obtained from the orbit propagator is used as input to calculate the sun vector and magnetic field vector in the orbit frame.
  - The sun model described above is used for calculating the sun vector onboard too. The time elapsed from vernal equinox is required as the input
  - The magnetic field vector is calculated using the IGRF-11 model of order 8.
- Estimation of light/eclipse, reconstruction of the sun vector and QuEst
  - The first step is to estimate if the satellite is in light or eclipse. This is done by the 6 SS measurements. If all the SS readings are less than some threshold (i.e. cos(half FOV)*max. SS gain), the satellite is in eclipse. Otherwise it is in light. If the satellite is in light, we use the 6 SS readings to reconstruct the sun vector in the body frame and then use the 4 vectors (measured and propagated magnetic filed vector and sun vector) to obtain quaternion using QuEST.
    Sun vector reconstruction: let a1, a2, a3 be three SS normal vectors that see the sun. Their corresponding outputs be V1, V2, V3 and angles with the sun vector v be $\theta_1, \theta_2, \theta_3$,
    then

$$\begin{cases} a_1^T v = cos(\theta_1) = V_1/V_0 = kV_1 \\ thus, \\ Av = kV \\ v = kA^{-1}V \end{cases} \tag{10.11}$$

    Now normalize v to eliminate k: $\hat{v} = (A^{-1}V/|A^{-1}V|)$ For choosing the 3 SS, sort them according to their outputs and choose the top three, while keeping a check to not include anti-parallel sunsensors.

– The Quaternion Estimation (QuEST) algorithm is used to estimate the attitude. The attitude is estimated by the orbit frame to body frame quaternion, qBO. The QuEST algorithm requires two non parallel reference vectors in the orbit frame and two non parallel measurement vectors in the body frame. The sun vector and magnetic field vectors in the respective frame are used for the QuEST.
If the satellite is in eclipse, the quaternion cannot be estimated. It is simply output as [0;0;0;1].

– Calculation of wBO from qBO:

$$\omega_{BOB} = 2(\eta I_{3\times3} - \eta\varepsilon^{x} + \varepsilon\varepsilon^{T})\dot{\varepsilon}/\eta \tag{10.12}$$

Since just after eclipse, the filtered w readings are incorrect for a few seconds, we multiply it by a ω_{ctrl} pulse, which is 1 everywhere except 300 seconds after light region is entered.

* filter w using 1st order low pass filter with time constant = 60 s
* generate ω_{ctrl} pulse to delay control by w (reason discussed in control strategy later)

By this logic, ω_{ctrl} is is 0 for 300 s after light region begins, and 1 else.

- Control law

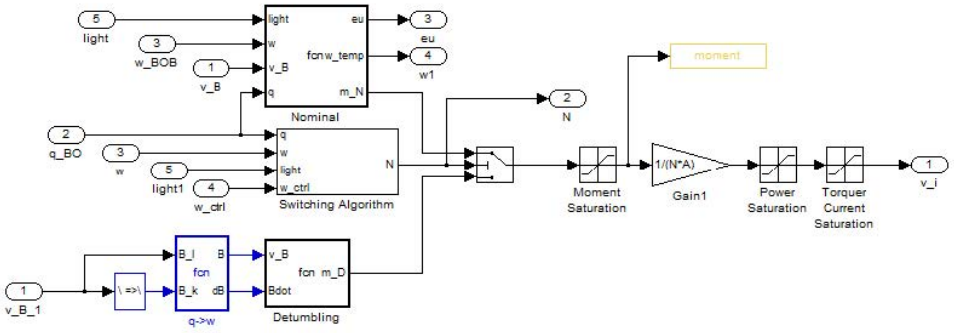

Figure 10.19: Control Law simulation block

– Nominal Controller :

$$m = K_p\frac{\theta}{|B|^2} + K_d\frac{\omega_{BO}}{|B|^2} \tag{10.13}$$

where $\theta = 2q_v q_0$
m_n = m × B
Also,
$K_p = 1/(T^2\zeta^2)$
$K_d = 2I/T$
$K_i = where\zeta$ and T are chosen to be 1.15 and 0.125* T_{orbit} respectively
and m_n = control moment,
q_v=quaternion vector part,
q_0 = scalar part,
B = magnetic field in body frame.

- Detumbling Controller :
  B dot controller is used. Magnetic moment in detumbling is calculated as:

$$m_d = -KB_0\Big(\frac{\dot{B}}{|B|}\Big) \tag{10.14}$$

  where K = 4×10^4, is a constant gain.

- Switching:

  Switching strategy is defined as follows:

  1. For the first 2000 s, run detumbling mode.

  2. After initial detumbling (and also in general), switching to nominal will occur if
     a) The angular rates drop below a certain threshold (4e-8 rad/s). But since the rates are estimated from the quaternions, there can be sudden peaks and drops in the rates due to noise. Therefore, a window of 60 seconds has been defined such that if the rates are consecutively low for this duration, then switch to nominal.
     b) The satellite is in light region.
     c) The satellite was in light 300 seconds before. This is done, so that the switching does not occur in the penumbra region of eclipse.

  3. Switching to detumbling mode will occur if
     a) The angular rates increase over a threshold (8e-8 rad/s) for a window of 60 seconds as with the case of nominal. There is no switching between 4e-8 and 8e-8. The threshold for the rates have been decided by observing the angular rates as they stabilize from detumbling to nominal.
     b) A check time of 10,000 seconds is kept for switching from nominal to detumbling.

4. In order for the switching to take place from detumbling to nominal, estimated angular rates are needed. The angular rates are estimated using the QuEst algorithm which requires the position and velocity of the satellite. Hence, GPS has to be on for the switching to take place. GPS is switched on when
   a) The average of norm of magnetic moment decreases below 0.04 N/m. For initial switching, if the magnetic moment does not fall below the threshold, switching will still take place if time elapsed is more than 6 complete orbits. The time has been decided by observing the initial switching for worst case scenario of initial rates of 6-7 deg/s along the three axes.
   b) GPS is kept switched off in eclipse region and is switched on 150 seconds before light region. The time of eclipse is estimated beforehand from the altitude and the orbit geometry.

10.4 OILS

In order to verify the C-code of the control algorithm which will be part of the overall flight code, the sensor data are simulated from the environment data without noise and given as an input to the OBC C code at a time step of 2 seconds. Noise is not added since it is in open loop. All the switching conditions of GPS starting and detumbing to nominal are verified. The outputs of current and quaternion are also verified from the data of the closed loop matlab model. The currents are seen to stabilize hence verifying the C code. The setup for OILS is described pictorially as follows

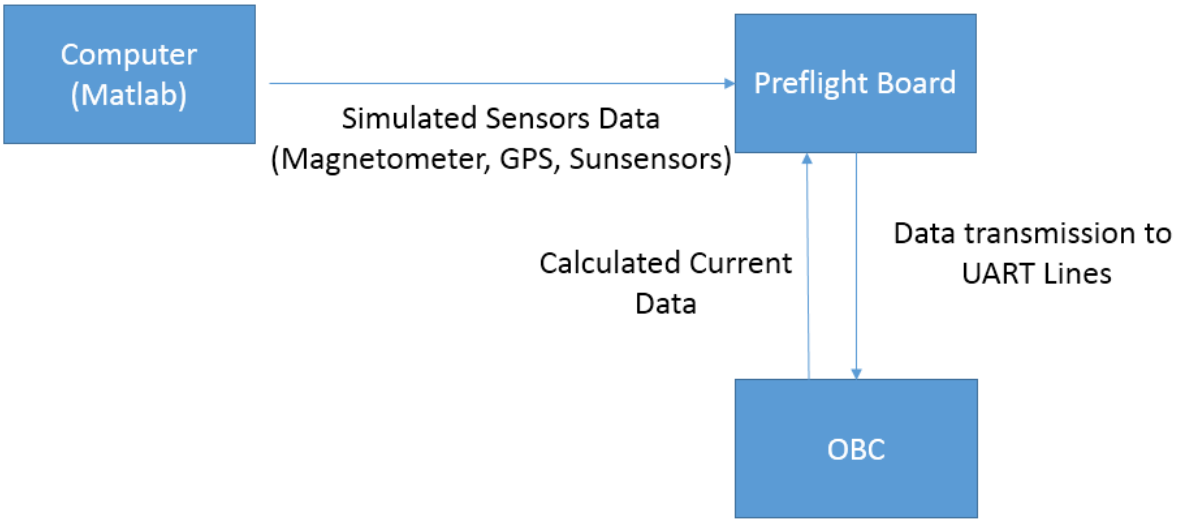

Figure 10.20: Detumbling current from C code

The currents from the C code are plotted below

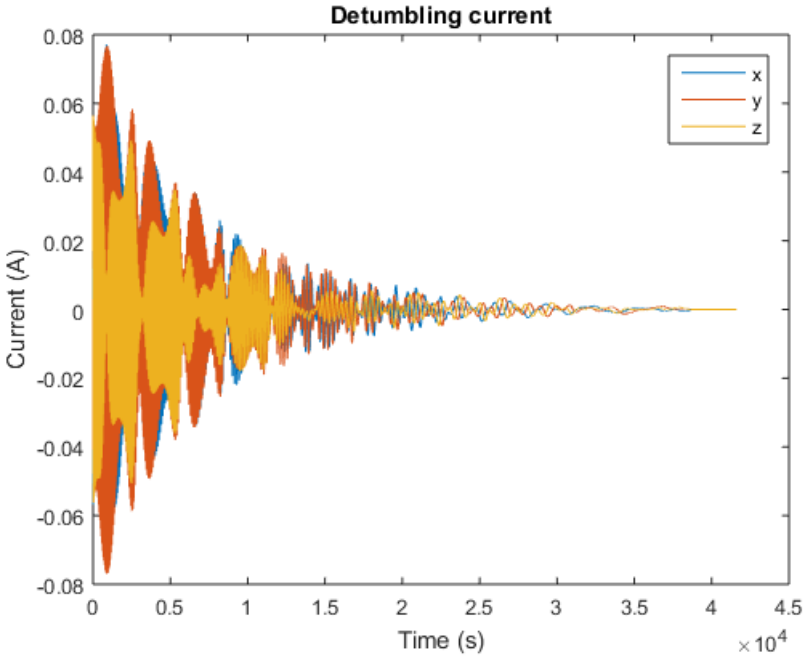

Figure 10.21: Detumbling current from C code

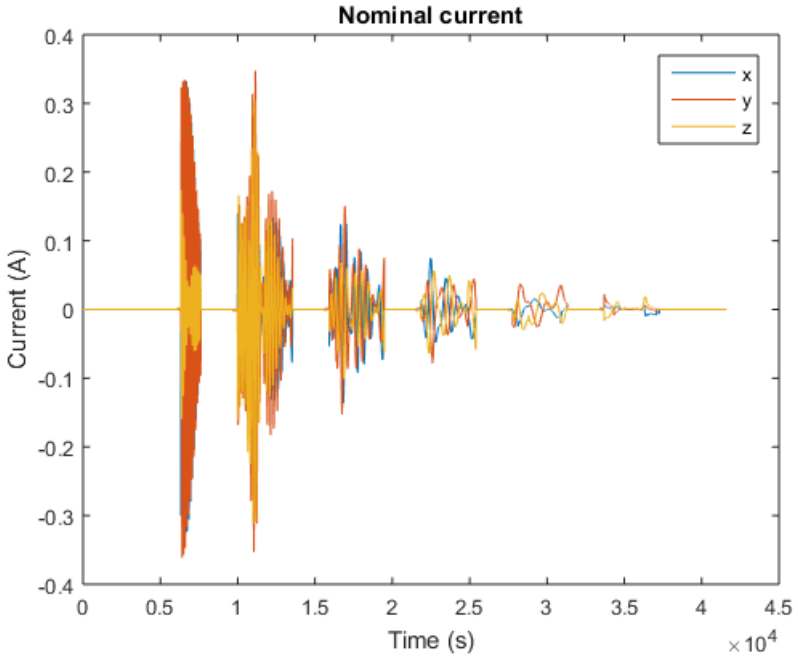

Figure 10.22: Nominal current from C code

10.5 Simulation Results

Latest results show that satellite attitude is controlled well within the bounds imposed by the payload and communication teams, even if initial conditions are large for all the four altitudes that the simulations were carried out-500 km, 600 km, 700 km, 800 km. Unless stated otherwise, the results are for 500 km.

10.5.1 Case 1: Nominal launch conditions:

Initial Angular rates: [5,5,5] deg/s along the X,Y,Z body axes respectively
Initial Euler angles: 20^0 roll, 140^0 pitch, 80^0 yaw

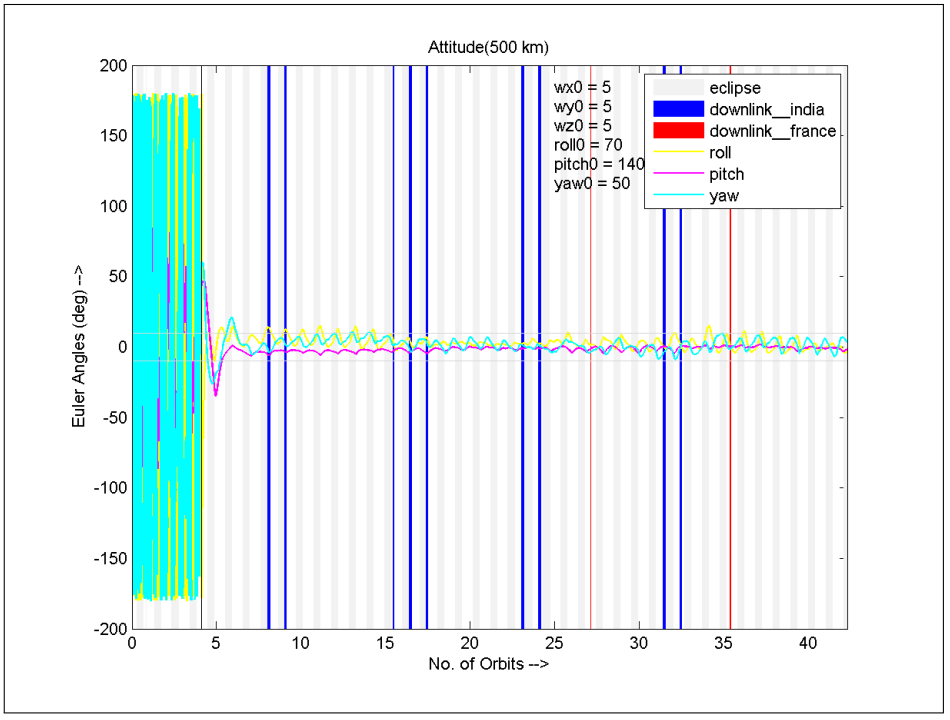

Figure 10.23: Euler angles

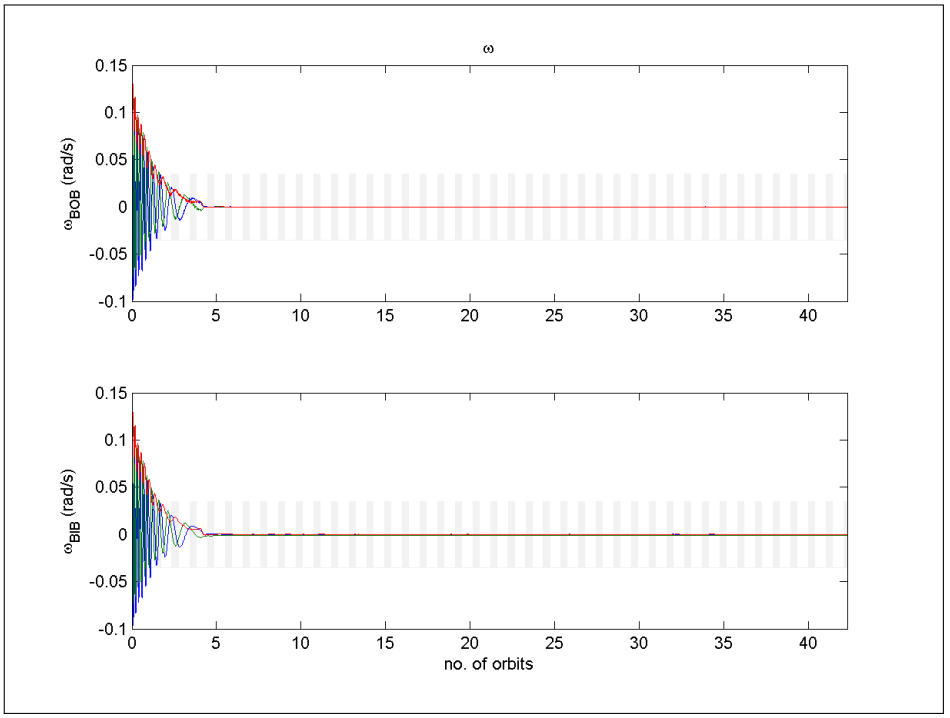

Figure 10.24: Rate of orbital frame/inertial frame w.r.t body frame expressed in body frame

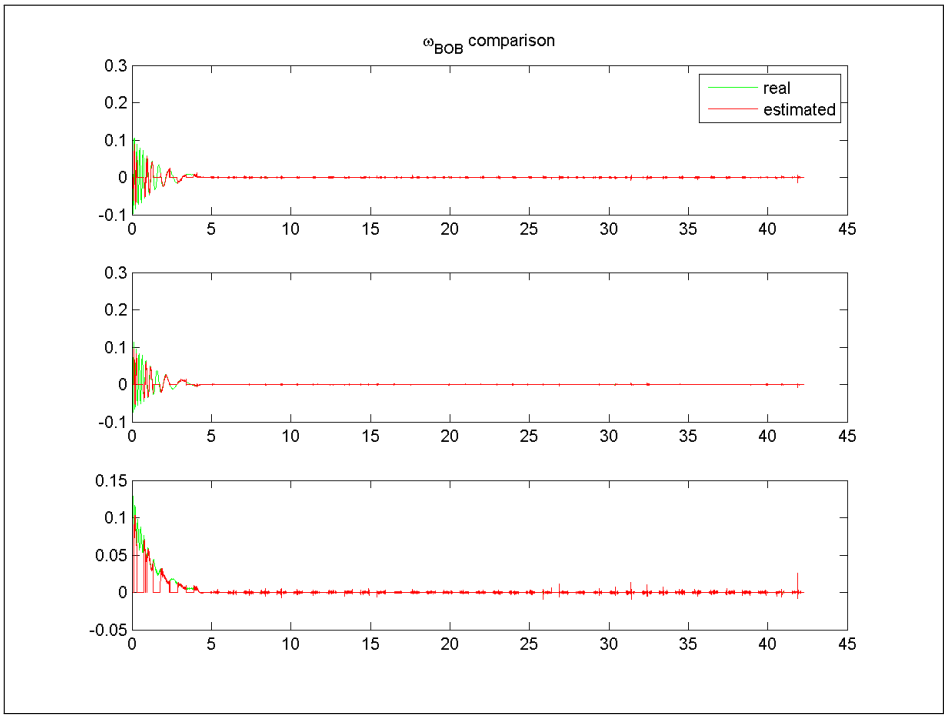

Figure 10.25: Rate of orbital frame w.r.t body frame expressed in body frame, estimated v/s real

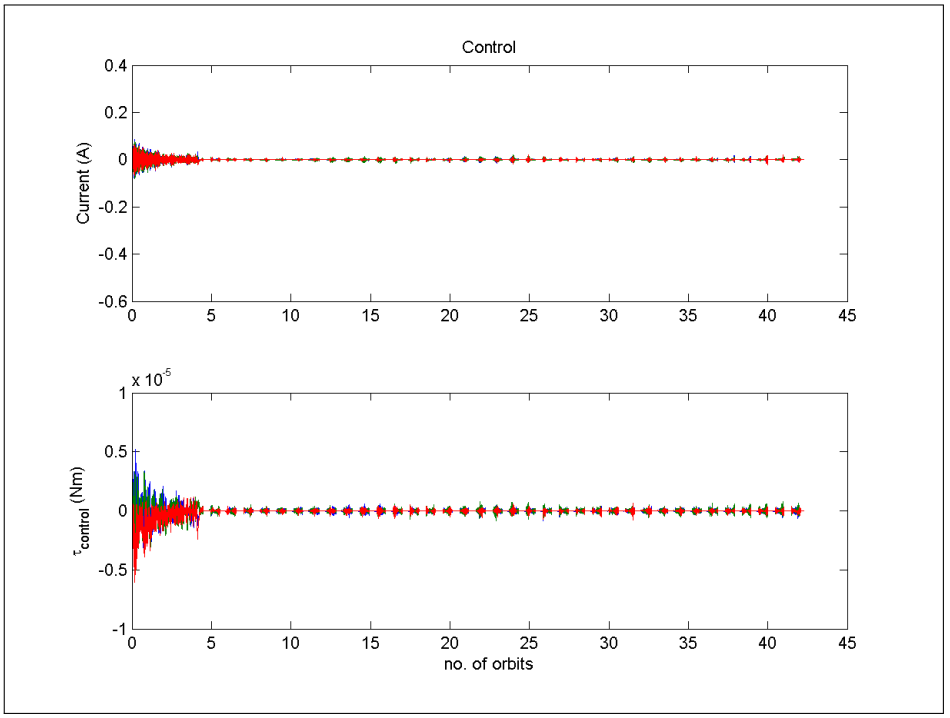

Figure 10.26: Control current and torque

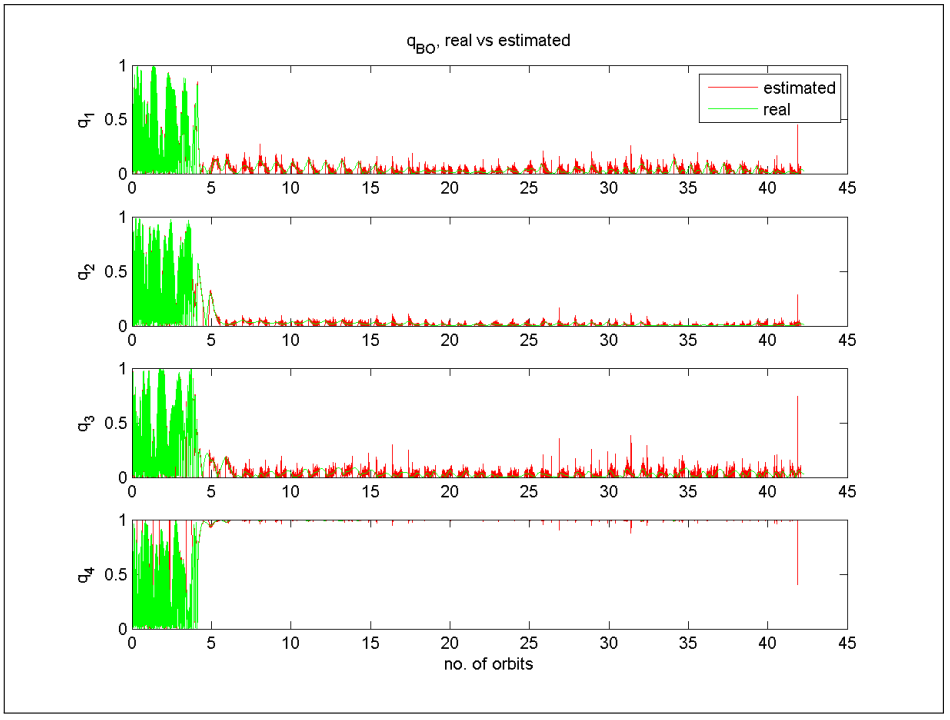

Figure 10.27: Quaternion of orbital frame w.r.t body frame

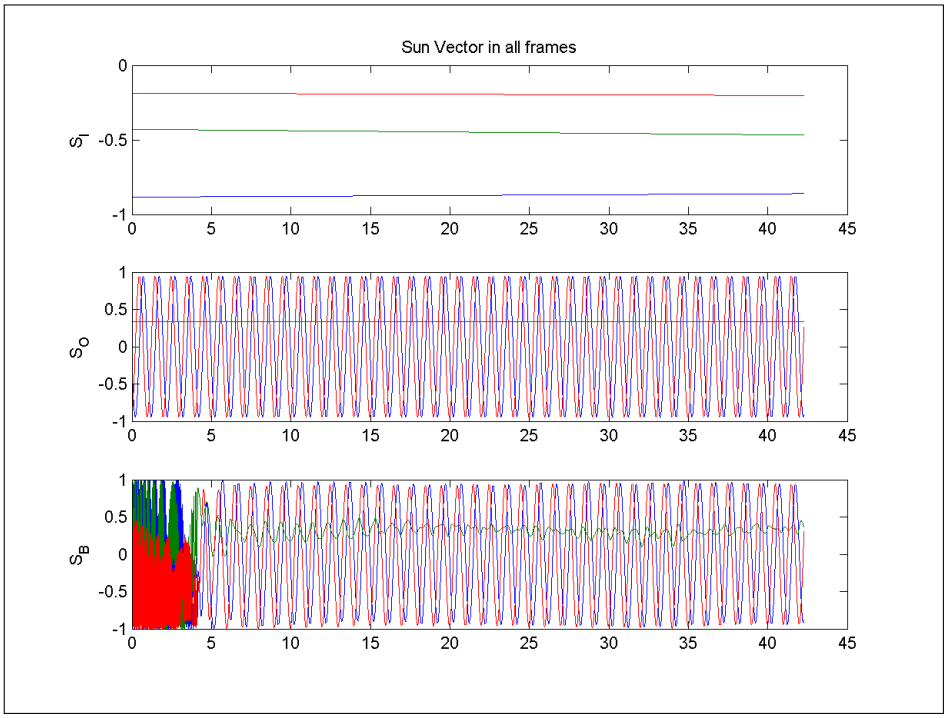

Figure 10.28: Sun vector expressed in different frames

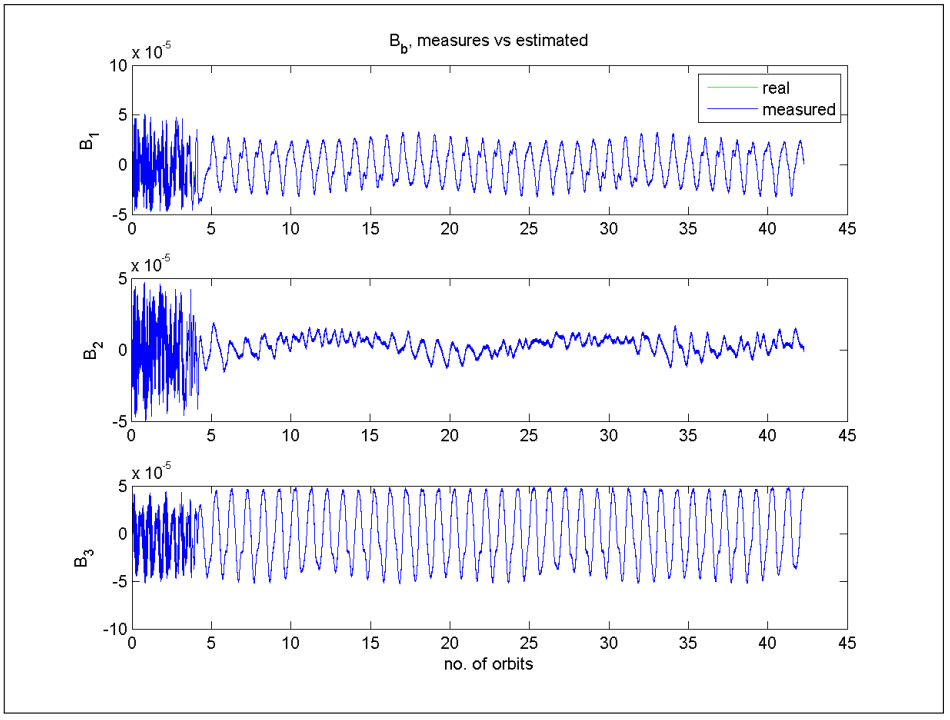

Figure 10.29: Magnetic field measured v/s estimated

10.6 Monte Carlo Simulations

Monte Carlo simulations were carried out to verify that the nominal mode controller can stabilize the Euler angles within the required limits for any starting combination of Euler angles with rates within the limits required for end of detumbling.
The 1st test run was conducted with a set of 100 Euler angles which were generated using the random number generator. The control law simulation was run with only the nominal mode controller active for 20 orbits. The checking criterion was the maximum value of any Euler angle in the last 3 orbits.
The results were then plotted on a 3D domain representing the 3 Euler angles and the points were color coded as per maximum value of checking criterion.
The scatter plot of the cases run is shown below

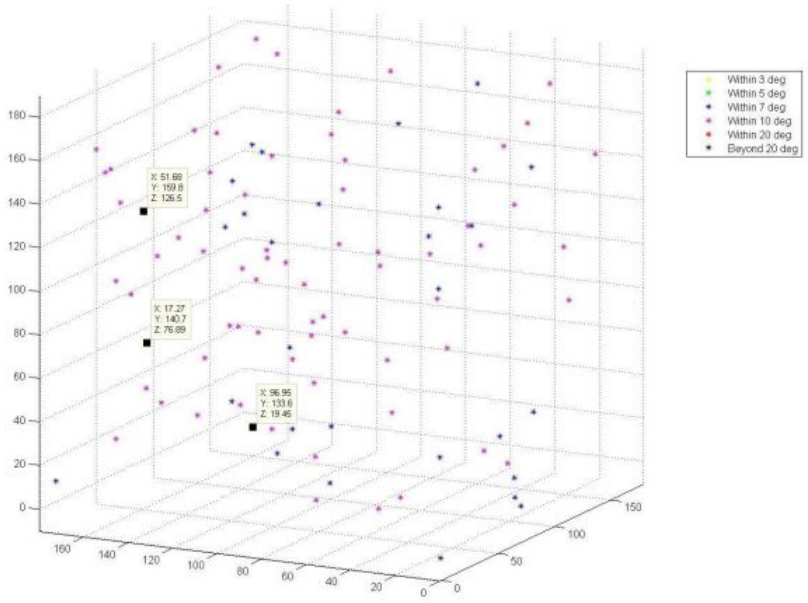

Figure 10.30: Euler angles from Monte Carlo simulations

The points marked on the plot indicate the points where one of the Euler angle was greater than 10. In the worst case the maximum value of the angle was 14 for the initial case corresponding to the Euler angle set [17.27 140.7 76.69] deg according to [Roll Pitch Yaw]. Further when the simulation was rerun, the angles were shown to be within 10 by the 20^{th}orbit.
A typical result for one of the cases in the simulation is shown below

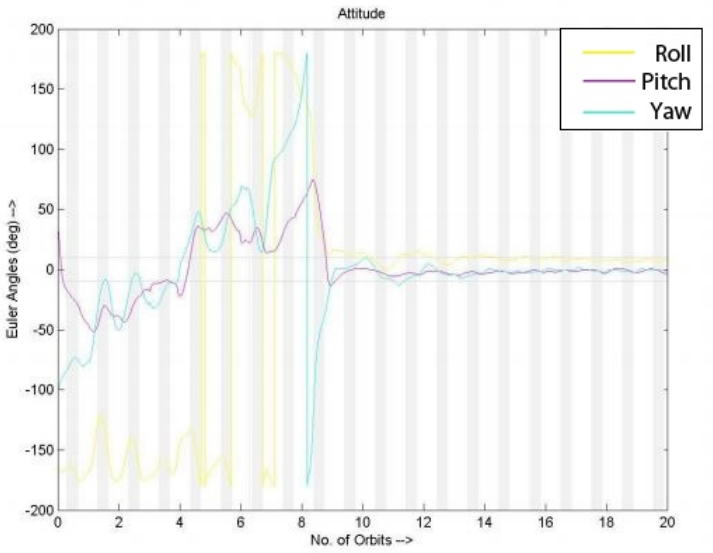

Figure 10.31: Euler angles from Monte Carlo simulations

The following are the results obtained from 500 cases

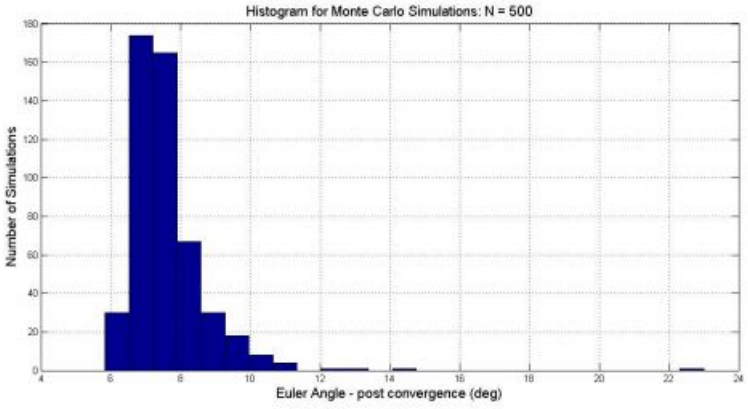

1

Figure 10.32: Histogram for Monte Carlo simulations, N = 500

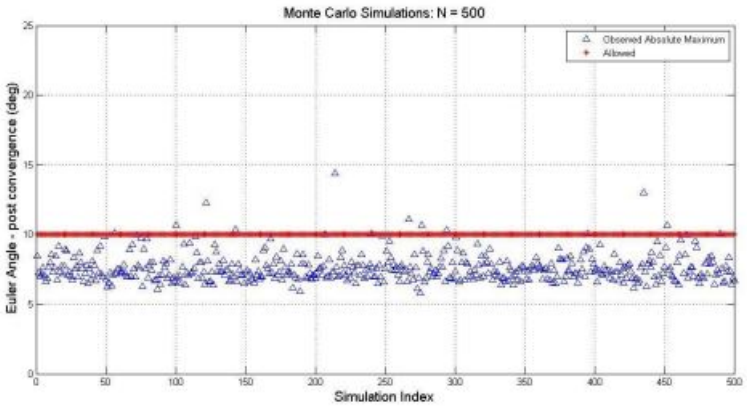

Figure 10.33: Post convergence Monte Carlo, N = 500

The following were the observations from the simulation

1. 15 cases of 500 were giving Euler angles post 20 orbits > 10 deg
2. Out of this 15 cases ONLY 5 were > 11 deg
3. Out of this 05 cases ONLY 1 was > 15 deg [Initial angles : -9.54 -136.73 -178.35]

The 2nd test run was conducted with a set of 100 initial Euler rates between 5 deg/s and 12 deg/s which were generated using the random number generator. The control law simulation was run with only the nominal mode controller active for 40 orbits. The checking criterion was the maximum value of any Euler angle in the last 3 orbits.
The scatter plot of the cases run is shown below.

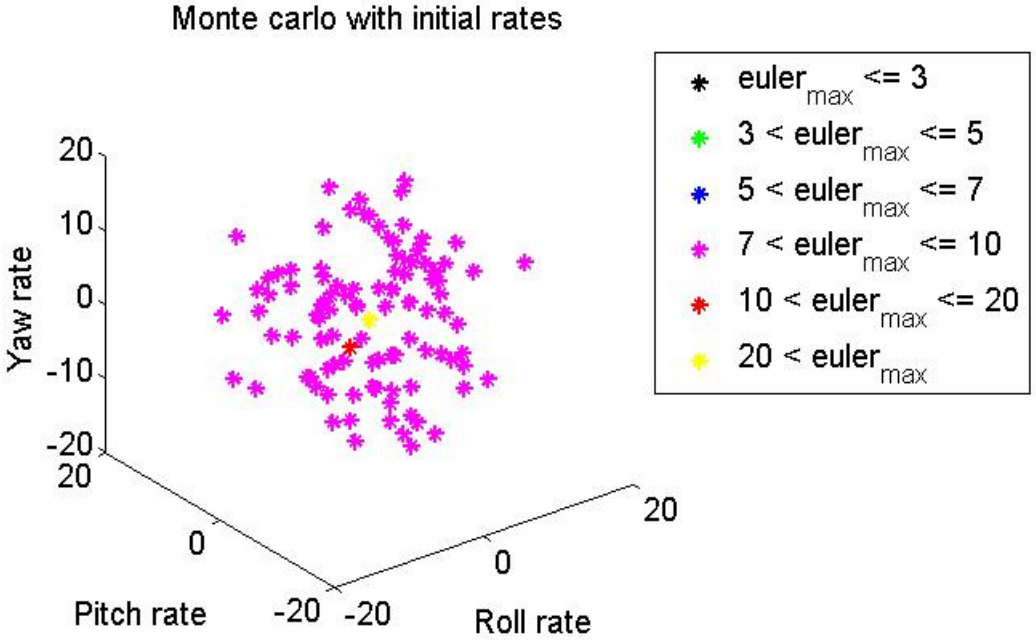

Figure 10.34: Monte Carlo with initial rates, 100 cases and 40 orbits

The following were the observations from the simulation

1. 98 cases out of 100 had Euler angles between 7 and 10 degrees
2. Only 1 case had Euler angles between 10 and 20 degrees (15.3 degrees) [Initial rates :[-7.58,-6.62,2.07]]
3. Only 1 case had Euler angles greater than 20 degrees [Initial rates :[0,0,0]]

10.7 Battery Simulations

10.7.1 Introduction

The battery power simulink model essentially incorporates the modeling of power consumption from battery by the various loads and the power generation through solar panels with the attitude determination and controls model. The conditions for charging and discharging are determined by the voltage level of the battery and the differential power available or consumed.

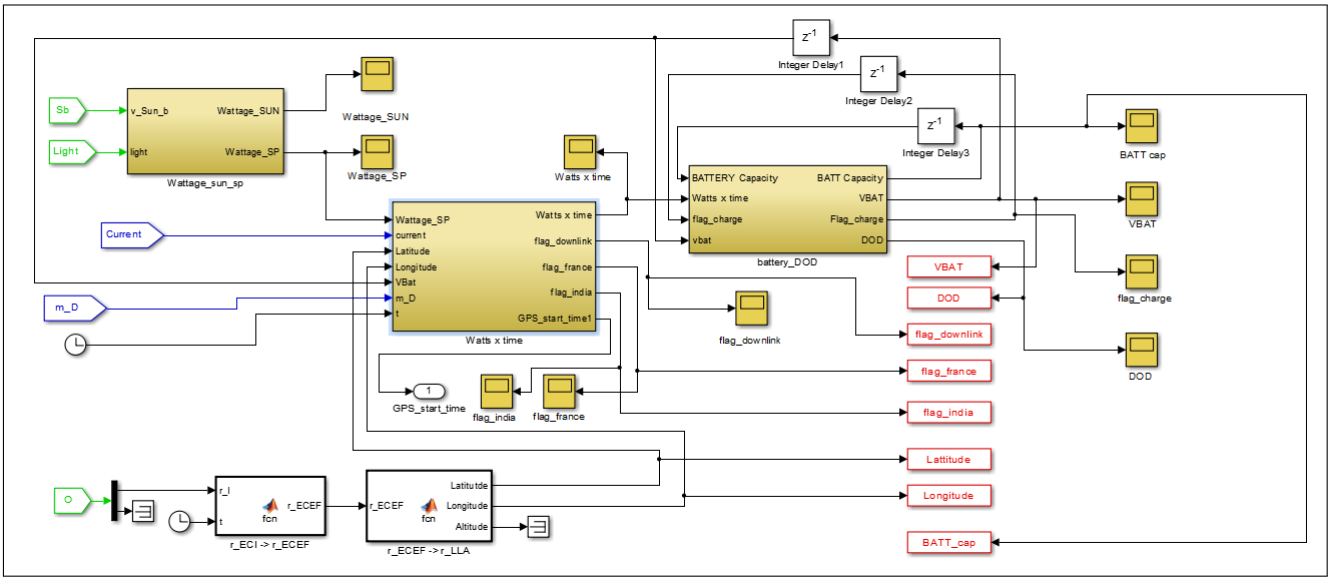

Figure 10.35: Battery simulation block

10.7.2 Power from solar panels

The simulink model for power generation through solar panels is as follows

- The angle between the sun vector and the area vector of the solar panel face is determined by taking their dot product. The light flag determines whether the satellite is in light or eclipse phase.

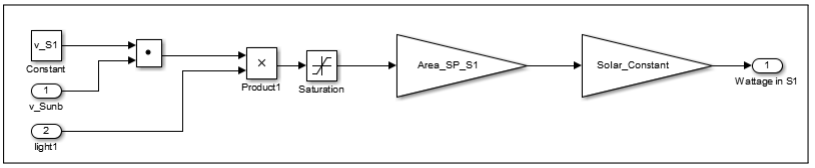

Figure 10.36: Simulation of power through solar panel

- The solar intensity on the panel face can be determined using Lambert's cosine law $I = I_0 \cos(\theta)$
  where I_0 denotes the normal intensity

- The total solar power is the sum of the solar power available from all the faces multiplied by the efficiency of the solar panel (0.16).

Chapter 11

OBC Subsystem

11.1 Introduction

On-board Computer (OBC) Overview

- The OBC Subsystem comprises of almost all the computing power employed by Pratham.
- The mission statement of Pratham requires the satellite to stay in a stable orbit for a reasonably long period of time and transmit data to the ground-station in order to facilitate measurement of the Total Electron Count (TEC) in the atmosphere.
- The design of Pratham has the various sub-systems like the Communication sub-system and Controls sub-system providing the equipment for communication and controls respectively while the OBC subsystem interfaces with these elements and executes the algorithms to keep the satellite stable and transmit data to earth.

11.2 Sub-System Requirements

11.2.1 Requirements from other sub-systems on OBC

Attitude Determination and Control

The Controls subsystem is primarily concerned with determining the satellite's position and maintaining a stable orbit. The On-board Computer is required to interface with sensors and actuators and execute the control-law calculations that determine the required actuation from the current position.

Sensor Interfacing

The On-board Computer is required to interface with the following sensors:

1. Global Positioning System (GPS) Unit
2. Magnetometer
3. Sun-Sensors

Control Law Execution

The On-board Computer shall execute the control law as designed by the Controls sub-system. This includes performing the requisite numerical calculations with the desired accuracy as well as according to the predefined sequence and timings.

Actuation

The On-board Computer will interface with and actuate the magnetorquers according to the control law. This implies provision of suitable pulse-width-modulated signals for suitable time intervals.

Power

The power subsystem is concerned with acquiring, regulating and distributing power to the various components of the satellite. The Power and On-board Computer subsystem must interact to exchange data about satellite health (HM data).

Response to low-power situations:
The Power subsystem will generate a signal indicating a predicted inability to supply adequate power to the On-board Computer subsystem. The data exchanged regularly between the Power and On-board Computer subsystem will indicate any misbehaviour (over-current) on the part of any component. The Power board itself will respond to situations where the OBC malfunctions or low power situations which might arise, and take suitable measures to shut down various components. In all other situations of malfunction the OBC directs the Power board to shutdown components in a defined sequence.

Communication and Ground-Station

For the purposes of monitoring the status of the mission, the satellite will transmit the health of the various components during downlink. In this regard, the OBC sub-system is required to send the health, temperature, latitude, longitude and altitude data in packets encoded using the AX-25 communication protocol, at a maximum rate of 1.2 kbps whenever the satellite is over the Ground- Station.

Integration

To ease the integration of the On-board Computer sub-system with the rest of the satellite, the final Printed Circuit Board (PCB) of the On-board Computer must be 12 cm x 12 cm in dimensions, with a natural frequency above 120 Hz. The final PCB must confirm to the requirements of the harness to be designed by the integration team

Quality

The Quality sub-system requires the On-board Computer hardware to be tested extensively to reduce chances of infant mortality. While the exact testing procedures have not yet been fixed, they must provide an estimate of the probability of failure. For the satellite to have a life of 4 months, the estimate of the probability of failure should be below some threshold. The quality of the software plays a big role in the success of the satellite as a whole. The quality will be ensured by keeping proper coding conventions in mind including naming conventions and extensive in-line comments. The software will be tested by a code walk through to ensure that the software performs the requisite functions

in the correct manner. A formal verification of the software seems unnecessary due to the deterministic nature of the system. Finally, the complete electrical subsystem including the OBC will be tested using OILS (On board computer In-Loop Simulations) to ensure that the probability of failure is low.

11.2.2 Requirements from OBC on other subsystems

In order to execute the above functions, the On-board Computer sub-system places several constraints on other sub-systems:

Power

The Power sub-system is required to supply continuous power of up to 1 Watt at all times. The Power sub-system will also respond to the On-board Computer's requests to turn ON/OFF certain components depending on their need. This information will be communicated to the Power sub-system in the form of one byte every cycle (2 seconds). The Power sub-system will also send HM data regarding the status of each of the major loads on the satellite to the On-board Computer when polled for this data. Also the OBC also tells the power board to turn off the loads in case of over-current situations and also decides when to turn them ON. In case of over-current in the OBC the power board decides to switch off the OBC.

Thermals

The Thermals sub-system will be required to remove excess heat from the On-board Computer PCB, in order to maintain the temperatures of all the components between -40^0 C and 85^0 C (the operating range of the components).

11.3 Software Design

11.3.1 Hardware Control

In order to execute various tasks, it is necessary to use a number of the ATmega128's peripherals. One part of software design is to write the C code required to drive these peripherals. This effort was further sub-divided into two portions:

Sensor interfacing

The On-board computer interfaces with the GPS unit, the magnetometer, and the sun-sensors. The GPS and Magnetometer are both compatible with the RS232 communication standard. As the ATmega 128 has 2 fully independent UART peripherals, both the magnetometer and the GPS have a dedicated UART peripheral interfaced with them.The sun-sensors uses the analog-to-digital convertor (ADC) peripheral of an atmega 8 which communicates with On-board computer using SPI.

- In order to interface with these components, the UART (Universal Asynchronous Receiver Transmitter) peripheral needed to be configured. This peripheral allows for complete duplex reception and transmission. The configuration of this peripheral for asynchronous use involves the specification of the required baud rate, and the frame format (number of stop bits and the presence/absence of parity bits). Transmission is initiated by simply writing the byte to be transferred to a specific hardware register. The end of transmission or reception is indicated by the corresponding flag in a dedicated status register. The setting of these flags can also be used to trigger appropriate interrupts.
  - The magnetometer will be operated in polling mode. Every time a reading is required, the primary micro-controller will send a 5 byte command to the magnetometer via the UART peripheral. The micro-controller will then enable receive-complete interrupts and wait for a response (wait for the UART receive complete flag to be set and the interrupt to be triggered). The magnetometer will send a 7 byte string of the magnetic field values (2 bytes each for x, y and z directions and one 'end of message' byte, i.e., carriage return (0x0D)). As soon as a byte is received, the setting of the receive-complete flag will trigger an interrupt. The received byte will be buffered in each interrupt. Once 7 bytes are received, they will be processed. Note that interrupts do not process the received data but only buffer it for processing in the main code.
  - GPS will be run in interrupt mode. It takes around 85 seconds for the first valid reading to arrive. This validity is based on the PDOP value being sent by the GPS. During this period, the receive-complete interrupt of that UART peripheral will be enabled. The GPS unit will send one packet of GPS data every second. Each data packet consists of 8 messages conveying position, velocity, time-date and other information. Each message consists of a number of bytes. All the received bytes will be buffered in the receive-complete interrupt for future processing. The buffered message will be processed for a specific messages like position and velocity using the start and end flags and the relevant information will be used for further processing. The GPS UART interface will be operated at 9600 baud.
- The sun-sensors are similar in operation to photo-diodes. They provide an analog current as output. These currents are converted to analog voltages using an op-amp. The analog voltages are then routed to the Analog-to-Digital convertor peripheral of an atmega8 chip which converts it to digital voltage. The micro-controller (ATmega 128) will use the SPI interface to obtain the data from the atmega 8 chip.

Data Communication

The Onboard Computer design involves the exchange of data between the micro-controllers and several other devices on board the satellite. These data transfers are handled by several on-chip peripherals and codes must be written to drive these peripherals. The data pathways on board the satellite are:

- Power ⇔ On-board computer
  Health monitoring data and load on-off decision (I^2C)
- Primary Microcontroller ⇔ Secondary Microcontroller
  Health monitoring and attitude data, commands for downlink (SPI)
- Secondary Microcontroller → Downlink
  AX.25 packeted data (UART)
- Secondary Microcontroller ⇔ EEPROM
  Data storage before downlink (I2C)
- Primary microcontroller ⇔ ADC
  Sun-sensor Readings (SPI)

Task Execution

List of Tasks

1. Control Law Implementation
2. Communication Routines
3. Health Monitoring

Control Law Implementation
Data Acquisition
Read from GPS

1. Read GPS – receive data via UART, store sentence in array (This buffering takes place in the UART receive-complete interrupts). Since the GPS has a warm start-up time of around 80 seconds, the GPS must be turned on about 80 seconds before readings are to be taken. (Once every 10 minutes)
2. Parse array and store Latitude, Longitude, Altitude and Time in separate arrays/-variables. (Once every 10 minutes)

Read from Magnetometer

1. Read Magnetometer – receive data via UART, directly receive Bx, By, Bz readings in binary. Store in array/variables (This buffering takes place in the UART receive-complete interrupts). (Polled for readings once every 2 seconds)
2. Convert the stored binary values to decimal values for use in the control law. (Once every 2 seconds)

Read from Sun-Sensor

1. Using the ADC peripheral of the atmega8 on ADC board the analog voltage values of the 6 sun-sensors are converted to digital voltages and stored in an array.(Once every 2 seconds)

Data Processing

Data processing involves the following steps:

1. Use GPS/Orbit propagator and sun-sensor readings along with solar model to get the sun vector.

2. Use the sun-vector along with the magnetic field readings to estimated the attitude quaternions using a quaternion estimation (QuEST) algorithm. The GPS will be used only once every 10 minutes – to correct the orbit estimator. At other times, the orbit estimator itself will be used to determine the satellite's position.

3. Calculate the moment of the satellite.

4. Use the moment to determine which control law to use (De-tumbling / Nominal)

Actuation

The 2 second time frame for actuation comprises of:

1. While reading magnetometer, no PWM (first 1 ms of frame) is executed to remove interference due to magnetic field of torquers.

2. For rest of cycle previously calculated values of current are provided to the torquers using PWM.

3. PWM duty cycles for next cycle are updated in the micro-controller registers after control law is executed. Attitude quaternions/moment are used to calculate necessary PWM signals to magnetorquers using control law.

NOTE: Entire sequence of Data Processing and Actuation steps is done once every 2 seconds. All these routines occur on the primary micro-controller. Thus 2 seconds is our primary frame time, while the GPS read routine occurs once every 10 minutes. Downlink is the only asynchronous event in the system.

Communication Routines

Check Position Use GPS readings/Orbit Propagator to determine if we are over India or over ground-station or neither; and act accordingly (executed every 2 second cycle):

1. If we are over Ground Station over India, switch on second monopole and switch on CC1101 chip (via downlink board) else put CC1101 to power-down mode.

2. If we are over ground-station – transmit Health montoring and Position (Latitude, Longitude and Altitude) data.

3. If we are over India but not over ground station – transmit Position data.

Transmission

1. Primary micro-controller detects position and sends commands to the secondary micro-controller and the power micro-controller. The Power micro-controller switches on the downlink micro-controller.
2. The downlink micro-controller configures the CC chip.
3. Once successful configuration of the CC1101 chip is done, the secondary micro-controller takes data from the EEPROM flash memory and primary micro-controller then packages it into AX.25 format and sends it to the downlink microcontroller, which sends it over to the CC1101 chip.
4. Data transmission happens continuously while the satellite is over India/ground-station.

Health Monitoring

Data Acquisition

1. Primary microcontroller requests and receives (stores in temporary buffer) load data packet from Power microcontroller (via I2C). (Once every 2 seconds).
2. Primary microcontroller creates a data packet containing the HM data. (Once every 2 seconds)

Data Analysis

1. Loads currently switched on are monitored.
2. If necessary, loads are turned on/off, as in the case when second monopole must be turned on when over ground-station.

Data Storage and Retrieval

1. Primary microcontroller sends packets to secondary microcontroller (via SPI bus) as follows:
   (a) In nominal operation: HM packet (load + temperature data) – once every 2 seconds.
   (b) When over India (and not over Ground-Station): packets containing both position and HM data once is sent every 2 seconds.
   (c) Over Ground Station: packets containing both position and HM data once is sent every 2 seconds.
2. Secondary microcontroller processes the data as follows:

(a) Packets containing HM data are stored in the EEPROM without packaging.

(b) After the power-on of the CC chip for downlink, the secondary microcontroller reads the EEPROM and transmits the data to the downlink microcontroller after packaging it into AX.25 format.

3. When downlink is in progress, the position and HM data packets are received by the downlink microcontroller from the secondary microcontroller.

11.3.2 Integration and Scheduler Design

The final portion of software design consists of putting together all the individual blocks to form the execution sequence. The determination of the execution sequence itself depends only on the list of tasks, their nature and the requirements on onboard computer.

Issues in design of execution sequence

- The presence of asynchronous events – interrupts from various interfaces, the downlink process – complicates the scheduling of blocks into a neat sequence. However, it must be noted that that the presence of interrupts allows for the delays associated with communication and sensor interfacing tasks to be bypassed – removing idle periods.
- The requirement for a fixed frame time necessitates the implementation of a system timer. This timer must be used to trigger execution of tasks at the appropriate times.
- For every task in the task list, worst case execution times must be calculated. It is imperative that the sum of the execution times of all tasks in a frame be smaller than the frame time itself.

Implementation The features greatly simplify the integration:
The separation of communication tasks and control tasks allows us to write separate schedulers for the primary and secondary microcontrollers. The scheduler for the primary microcontroller comprises of the control and health monitoring tasks; the scheduler for the secondary microcontroller consists of the routines necessary for communication with downlink microcontroller and memory management.

A simple round-robin scheduler is proposed for both microcontrollers – tasks are placed in a predetermined sequence in a cycle and in every frame time (2 seconds for the primary microcontroller) all the tasks in the cycle are executed one by one. This simple design is thought to be sufficient for our purposes due to the existence of very few event driven / hard-real-time tasks. Downlink is the only "real-time" task – and the handling of this event (the event: entering the field of vision of the ground-station; the handling: downlink initialization) is taken care of by the primary, secondary and downlink microcontroller col- lectively. The start of each cycle of the primary microcontroller is triggered by the system clock (implemented using one of the 3 timers). This is the same timer that is used to trigger the switching on the GPS unit. The start of downlink will depend on the

satellite's position. This is re-evaluated every frame (2 seconds – either by the GPS or by the orbit estimator). The primary microcon- troller will decide when to initiate/terminate downlink. The secondary microcontroller's cycle is triggered by commands/data received from the primary microcontroller. If health monitoring data is received, a cycle consisting of the following is triggered:

1. Receive and buffer all the data sent.
2. Once all the data has been received, store it in the EEPROM

If the command for downlink is received, a different cycle consisting of the following is triggered:

1. Command the power microcontroller to switch-on the downlink microcontroller which automatically configures the CC1101 chip.
2. The secondary microcontroller reads the data from EEPROM and transmits it to the downlink microcontroller until a "Stop Downlink" command is received.

11.4 Hardware Design

11.4.1 Requirements of the Hardware Design

Basic Design and Interfaces

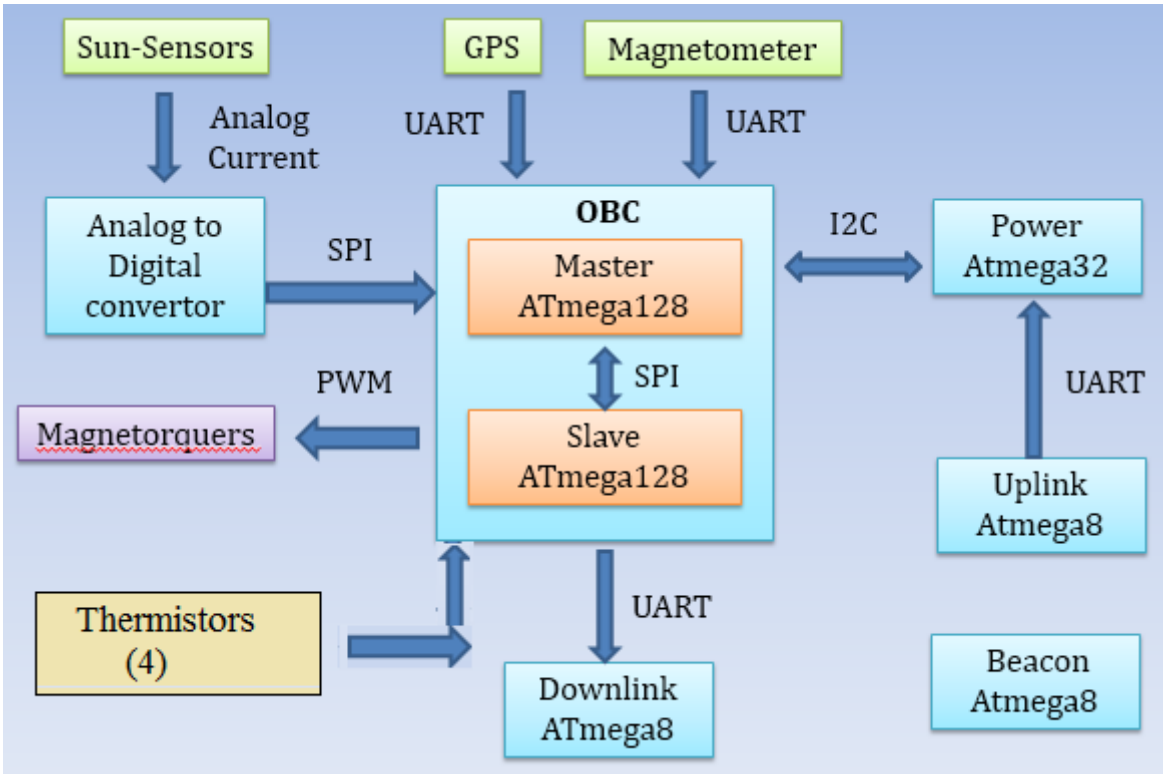

The specific microcontroller chosen was the Atmel ATmega 128. This micro-controller had been used for various other embedded systems projects in our institute. It also boasts of an incredible set of peripherals that would greatly simplify the rest of the design. Some of its features are:

1. 8 MIPS throughput at 8 MHz operating frequency
2. Low Power Consumption (3mW/MHz)
3. 4 KB on-chip SRAM, 128 KB on-chip Flash, 4 KB on-chip EEPROM

Some of the peripherals that are essential to the hardware design:

1. 3 timers (two 8-bit and one 16-bit) for PWM generation and system clock
2. Two-Wire Serial Interface (TWI or I2C) to interface with power micro-controller and external memory bank
3. Two independent UART lines to interface primary microcontroller with magnetometer and GPS; one UART line to interface the secondary micro-controller with downlink micro-controller.
4. On-chip Watchdog timer to restart micro-controller in case of system lock-up.

The micro-controller will be operated at the rated clock frequency of 8 MHz at 3.3 V.

The on-chip Flash memory will be used to store the program memory. While it is realized that the use of Flash increases the susceptibility of the system to radiation induced failures, it is felt that the use of an external PROM to store the program memory would overly complicate the design. Precautions against radiation have been taken by coating the PCB's. The execution of the control law in a speed optimized manner necessitates the use of several tables for computational purposes. These tables will be stored in the on-chip EEPROM and the on-chip Flash memories.To provide an accurate record of any failures or shut-downs and to keep a record of what the satellite was doing prior to these failures; a concise history will be maintained in the on-chip EEPROM. This will consist of flags signaling the state of the system before the most recent failure/shut-down. Sample computations, of a similar complexity as that of the final control law, have been executed on these microcontrollers and it has been determined that the amount of on-chip SRAM is sufficient for these purposes.

Need for 2 separate microcontrollers Introducing 2 separate microcontrollers into the hardware design was necessary for a number of reasons:

1. Logical separation of the ADCS and the Communication portions of the Onboard Computer. The Primary microcontroller handles the interfaces with the sensors and actuators of the ADCS and also runs the control law. The secondary microcontroller interfaces with the CC1101 chip provided by the communications subsystem through the Downlink Microcontroller and handles the various subroutines involved in the downlink of data to earth.

2. Separation of data acquisition and data handling: The primary microcontroller is responsible for the collection of data from the sensors as well as receiving health monitoring data from the Power subsystem. The secondary microcontroller stores this data in the external memory bank and sends the data directly through the UART when indicated by the primary microcontroller

3. Simplification of the Operational sequence: When the satellite is over the ground-station, it must simultaneously execute 2 main functions – attitude determination and control, and downlink of accumulated data. In order to execute these tasks concurrently without the need for multi-threading or context-switching, these tasks are executed on two different microcontrollers.

Inter-Microcontroller Communication Interface

The two microcontrollers will be interfaced using the on-chip SPI peripheral communication interfaces. The primary microcontroller will always initialize any communication (act as a Master) and the secondary microcontroller will be hardcoded to act as the Slave. The SPI interface is a byte-oriented serial interface that is essentially two shift registers (one on each microcontroller) connected together. The transfer of bytes between this shift register is synchronized by a clock generated by the Master. The data carried by this channel will be described later.

Downlink Data

The mission statement requires the onboard computer to transmit two types of data.

1. **Attitude data**: In order to carry out atmospheric tomography, the satellite's position and attitude must be known to reasonable accuracy. The position of the satellite can be accurately tracked by ground-stations and with the aid of agencies such as NORAD. However, the attitude of the satellite can be best determined using the sensor readings transmitted from the satellite.

2. **Health Status**: As Pratham is the first student-satellite initiative at IIT Bombay, data regarding the progress of the mission will be immensely useful to subsequent missions. This data will consist mainly of the health of various components onboard, and the history of any component failures and will be stored on an external flash memory. This data will help us diagnose design faults and determine the gap, if any, between design conditions and operating conditions. This

Features of External EEPROM In order to store HM data, an external EEPROM, 24FC1025 from Microchip, has been chosen as the third component of the onboard computer hardware. The main features of the EEPROM are:

1. 128 KB serial EEPROM

2. Two-Wire Interface (I2C) interface (100 kHz or 400 kHz clock compatible)

3. Low Power Consumption (2.25 mW max)
4. High speed operation – 3ms page write.
5. 128 byte page (buffered write)

Memory Read/Write Interface

The memory is read from or written to using the on-chip I2C interface of the secondary microcontroller. The interface consists of one line for the clock (generated by the secondary microcontroller) and one bi-directional line for the data. The EEPROM allows for sequential and random reads, and page or byte writes.

INTER MICROCONTROLLER SPI BUS

- Bidirectional (uses SPI protocol)
- A permanent master (Microcontroller 1) and a Slave (Microcontroller 2) is used to transmit HM data to Microcontroller 2.
- Also, the access port can be used to program each of the microcontrollers by pulling low the appropriate RESET pin.

POWER STATUS COMMUNICATION BUS

- Bidirectional I2C bus
- Micro-controller 1 is always the master with the power micro-controller always the slave
  - Current status (ON/OFF) of various loads, battery voltage etc. on power bus, sent from power micro-controller
  - Required/desired status (on/off) of various loads sent from Micro-controller 1

UART BUSES

1. 3 independent bi-directional UART lines. Two of them on the primary microcontroller and the third on the secondary micro-controller.
2. GPS line
   - Used to receive GPS data at regular intervals
3. Magnetometer line
   - Used to configure magnetometer after launch
   - Used to poll for and receive magnetic field data at regular intervals

4. Downlink line

    - Used to send data for Downlink from EEPROM when above groundstation

EEPROM R/W BUS

1. Bidirectional I2C bus
2. Used to store/retrieve HM data from EEPROM

Auxiliary components

The Onboard Computer main board will also host a few other circuits.

1. **H-Bridges**: The GPIO pins of the micro-controllers will not be able to drive the magnetorquers themselves. They will serve as the logic inputs to a H-Bridge which will then drive the torquers with the required currents. The micro-controller output pins will provide the PWM signal which will act as inputs to the enables of the magnetorquers.
2. **Thermistors**: 4 thermistors of industrial grade are used to monitor temperature of Battery box, Uplink LNA, Downlink's and Beacon's power amplifier, which are thermally critical positions in the satellite. This data is converted to digital format and then combined in the Health monitoring data by secondary micro-controller.

Chapter 12

Communication Subsystem

12.1 Introduction

The Communication and GroundStation Subsystem has the major goal of providing a robust link between the satellite and the Groundstation for the purpose of achieving Health monitoring data and Telemetry.

12.1.1 Objectives

The objectives of the subsystem are as follows

- To design an onboard system comprising of a Beacon, a telemetry Downlink and an Uplink
- To design a receiving segment at the Groundstation for the purpose of telemetry and beacon
- To design an uplink segment at the Groundstation to operate the telecommand
- To design a polarization measurement system for Payload subsystem for TEC measurements
- To develop low cost Groundstation for other Universities which are part of the Social Goal
- To design an automated system to track satellites at the GroundStation

12.1.2 Subsystem Requirements

Power Subsystem

- Telemetry: 1.75 watt when operational. This includes the power consumed by the transmitter circuit as well as the amplifiers and other transmission line losses. The power required will drop to about 0.06 watts when the monopole is in power down mode.
- Beacon: 1.75 watt when operational. This includes the power consumed by the amplifier and the modulator circuit. The duty cycle of the beacon is 100 % throughout the orbit.
- Uplink: The power consumption of the Uplink module is negligible. However, the uplink module is always switched on as there should be a provision of shutting down the satellite from any groundstation incase it strays from the allocated frequency.

On Board Computer

The On Board Computer has 2 separate microcontrollers on its Printed circuit board, a master and a slave. The Master microcontroller signals the start of communication by giving an interrupt to the Slave microcontroller after entering in the region of transmission. The region is determined by the GPS readings. Apart from these, the OBC should also perform the following tasks:

- The OBC team should provide AX.25 data packets to the CC1101 transmitter chip.
- The OBC team will also control the power modes of the transmitter.
- The data provided to the chip should be in the NRZ format.
- The Slave microcontroller should implement CRC on the data packets

Controls

The controls subsystem is responsible for the following tasks:

- Position determination - To determine the position of the satellite in space
- Attitude Determination - To determine the attitude of the body frame of the satellite with respect to orbit frame
- Attitude control - To bring the satellite into earth pointing orientation after ejection and to maintain this attitude throughout the period of operation

The following are the requirements on the ADCS subsystem:

Requirement on	To achieve	Purpose
Position determination	1 km	Start of Communication with the Ground station. The value, however, comes from Payload resolution requirements.
Attitude determination	Yaw – 5 degrees Roll – 5 degrees Pitch -5 degrees	This is required to achieve attitude control of the satellite. This will also be essential in case of an emergency due to antenna failure
Attitude Control	10 degrees	To minimize pointing error. The value, however, comes from Payload requirements.

Integration

The Integration team is responsible for Integration of the entire structure, both mechanically and electrically. Thus, the integration of the PCB on the satellite and the connections between different modules of the communication system shall be done by the Integration Subsystem. The requirements on the Subsystem from communication point of view are:

- The monopole holder should be rigid mechanically and should withstand Vibration loads
- The monopole should be insulated from the satellite body using an epoxy and heat shrinkable tube.
- The onboard antennae should be parallel to each other and any error in parallelism should be measured beforehand and should be quoted as bias error. This value should not change during the mission life of the satellite.
- The PCB's should be mounted in a way to transfer all the vibration loads to the structure.
- The PCB's should be potted before mounting on the flight model
- The CC and PA daughter boards should be fixed to their mounts using an epoxy based glue which shall withstand the launch loads.

Thermals

The thermals subsystem is responsible for maintaining the operating temperature of the satellite between 10 and 30 degree Celsius. The requirements from the thermal subsystem are:

- To maintain the temperature of the modules within their operating range.
- The dissipation of heat from the amplifiers during communication with the Ground station is an essential requirement from the thermals subsystem.
- The temperature of the monopole should not exceed 100 degree Celsius.

12.2 Onboard Communication System

The onboard segment consists of a telemetry unit, an uplink and a beacon. There are 2 monopole antenna onboard for the purpose of transmission. The beacon and uplink are independent units and the telemetry is controlled by the On board computer. The following is a block diagram of the 3 modules- the uplink, telemetry and beacon.

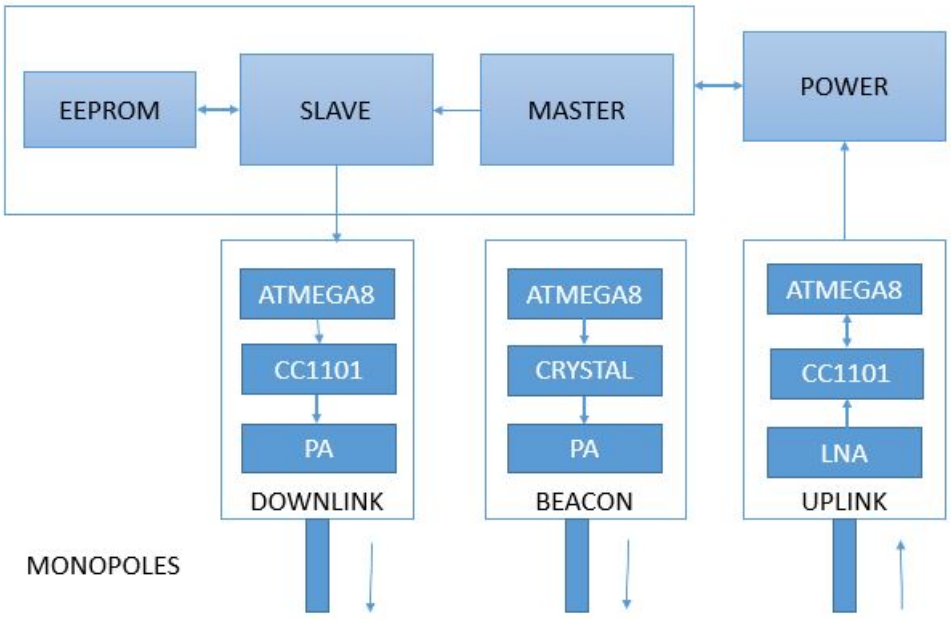

Figure 12.1: Telemetry Unit

Parameter	**Downlink**	**Beacon**	**Uplink**
Frequency	437.45 MHz	145.98 MHz	437.45 MHz
Modulation	FSK	CW	FSK
Telemetry EIRP	20 dBm	10 dBm	-
Command receiver G/T	-	-	-24 dB/K
Antenna type	Monopole	Monopole	Monopole

Table 12.1: Overview of On-Board Communication system

12.2.1 Telemetry

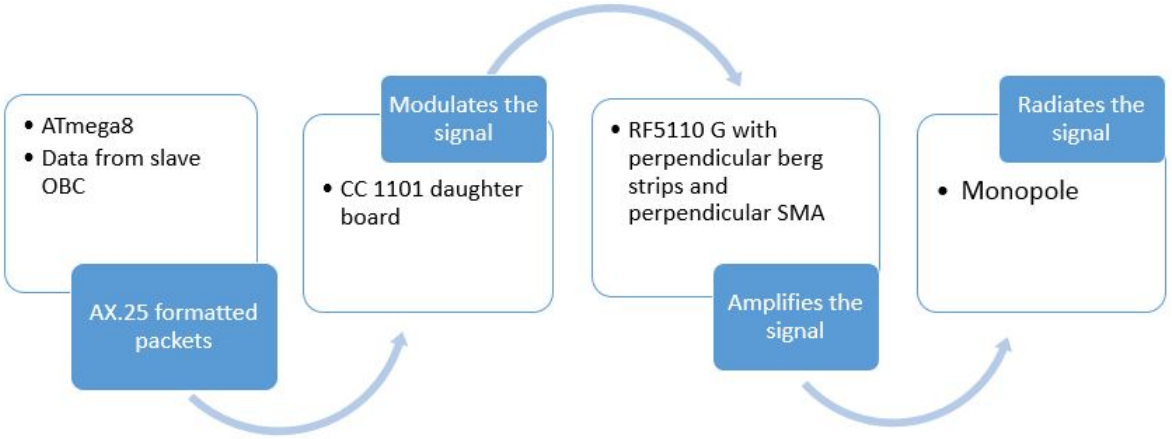

Figure 12.2: Telemetry Unit

The telemetry unit is activated by the Slave mcu when the GS is above India and France. The position is detected by the Master mcu and the start of the communication is communicated to the Slave mcu. The Slave mcu transmits data to the downlink mcu using UART communication. The downlink mcu codes the telemetry transmitter using SPI. The Power sub-system will send "Health Monitoring" data (HM Data) regarding the status of each of the major loads on the satellite to the On-Board Computer when polled for this data. The OBC is required to send this data in packets encoded using the AX.25 communication protocol, at a rate of 1.2 kbps. The Slave will receive temperature data from its ADC pins and will include it in the HM data.

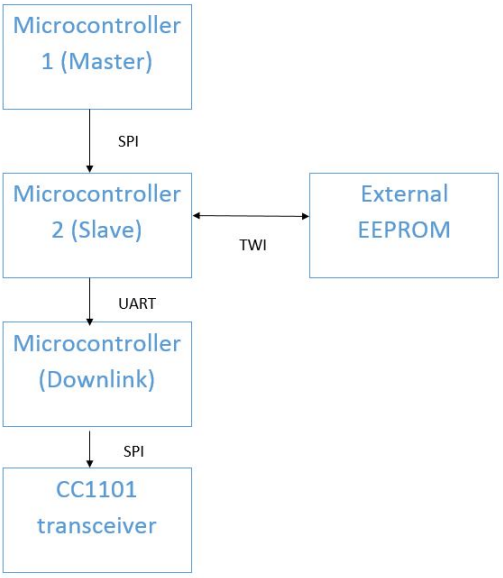

Figure 12.3: Schematic of OBC

CC1101 daughter board

The downlink microcontroller provides the benefit of encoding the CC1101 using SPI instead of GPIO bit banging. The CC1101 goes into the sleep mode after each data packet is transmitted. After every packet, the CC is checked for PLL lock, for register values and CRC is implemented on the data packets.

The data related to the operating parameters of the CC1101 are the following

Parameter	Operating Range	Operating value
Frequency	402 – 470 MHz	437.45 MHz
Voltage	2.3 V – 3.6 V	3.3 V
Current	15 mA	15 mA
Bit rate	0.45 - 156.2 kbps	1.2 kbps
Modulation	NA	FSK
Transmission time frame	NA	Off for 15 seconds in every 120 seconds
Input power	Max 10 dBm	10 dBm
Output power	Max 10 dBm	10 dBm
Temperature	-40 to 85 degree Celsius	10 to 30 degree Celsius

The schematic for programming interfacing with the CC1101 using the downlink microcontroller is shown below

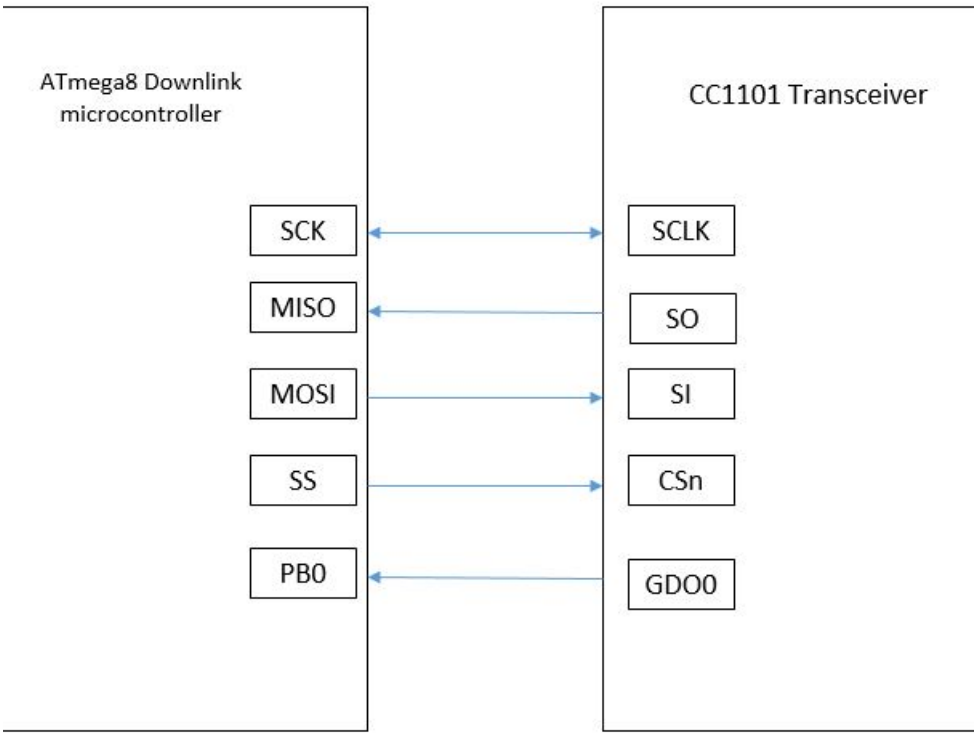

Figure 12.4: CC1101

AX.25 protocol

The AX.25 protocol is of the following format:

Flag	Address	Control	PID	Info	FCS	Flag
1111110	112/224 Bits	8/16 Bits	8 Bits	N*8 Bits	16 Bits	1111110

The flag field is 8 bit. Flag is used to delimit frames, it occurs at both the beginning and end of each frame. Two frames may share one flag, which would denote the end of the first frame, and the start of the next frame. A flag consists of a zero followed by six ones followed by another zero, or 01111110 (7E hex). As a result of bit stuffing, this sequence is not allowed to occur anywhere else inside a complete frame.

The Address bits identify both the source of the frame and its destination. It can also contain command/response information facilities for level 2 repeater operation. The control field is used to identify the type of frame being passed and control attributes of the level 2 connection.

The General types of AX.25 frames are

- Information frame (I frame)
- Supervisory frame (S frame)
- Unnumbered frame (U frame).

The Protocol Identifier (PID) field shall appear in information frames (I and UI) only. It identifies what kind of layer 3 protocol, if any, is in use. If 0x0F is used then it indicates that No level 3 protocol implemented. The information field is used to convey user data from one end of the link to the other. Range is from 32 bits to 1024 bits.

Frame check sequence (CRC)

The frame-check sequence (FCS) is a sixteen-bit number calculated by both the sender and receiver of a frame. It is used to ensure that the frame was not corrupted by the medium used to get the frame from the sender to the receiver. To assure that the flag bit sequence doesn't appear accidentally anywhere else in a frame. The sending station monitors the bit sequence for a group of five or more contiguous one bit. Any time five contiguous one bits are sent the sending station shall insert a zero bit after the fifth one bit. During frame reception, any time five contiguous one bits are received, a zero bit immediately following five one bits shall be discarded. With the exception of the FCS field, all fields of an AX.25 frame shall be sent with each octet's leastsignificant bit first. The FCS shall be sent most-significant bit first.

CC1101 Testing

- The CC1101 chips in transmitter and receiver mode were tested by connecting one microcontroller to the transmitter and one to the receiver.
- The receiver was coded to check the received data and give visual LED signals to indicate progress and errors. Data was also observed on computer terminal.
- AX.25 was implemented. Succesfull decoding at receiver confirmed validity of data.
- Finally, it was tested in a closed loop while connected with the OBC and the power boards.

Telemetry Link budget

Parameter	Value	Units
Spacecraft Transmitter Power Output:	0.4	W
In dBW:	-4.0	dBW
In dBm:	26.0	dBm
Spacecraft Total Transmission Line Losses:	0.4	dB
Spacecraft Antenna Gain:	-3.0	dBi
Spacecraft EIRP:	-7.4	dBW
Downlink Path:		
Spacecraft Antenna Pointing Loss:	0.3	dB
S/C-to-Ground Antenna Polarization Loss:	0.2	dB
Path Loss:	151.0	dB
Atmospheric Loss:	1.1	dB
Ionospheric Loss:	0.3	dB
Rain Loss:	0.0	dB
Isotropic Signal Level at Ground Station:	-160.3	dBW
Ground Station (EbNo Method):		
——- Eb/No Method ——-		
Ground Station Antenna Pointing Loss:	0.3	dB
Ground Station Antenna Gain:	12.0	dBi
Ground Station Total Transmission Line Losses:	0.2	dB
Ground Station Effective Noise Temperature:	307	K
Ground Station Figure of Merrit (G/T):	-13.1	dB/K
G.S. Signal-to-Noise Power Density (S/No):	54.9	dBHz
System Desired Data Rate:	1200	bps
In dBHz:	30.8	dBHz
Telemetry System Eb/No for the Downlink:	24.1	dB
Demodulation Method Seleted:	G3RUH FSK	
Forward Error Correction Coding Used:	None	
System Allowed or Specified Bit-Error-Rate:	1.0E-04	
Demodulator Implementation Loss:	0	dB
Telemetry System Required Eb/No:	16.7	dB
Eb/No Threshold:	16.7	dB
System Link Margin:	7.4	dB
Ground Station Alternative Signal Analysis Method		
———- SNR Method ———		
Ground Station Antenna Pointing Loss:	0.3	dB
Ground Station Antenna Gain:	12.0	dBi
Ground Station Total Transmission Line Losses:	0.2	dB
Ground Station Effective Noise Temperature:	307	K
Ground Station Figure of Merrit (G/T):	-13.1	dB/K
Signal Power at Ground Station LNA Input:	-148.6	dBW
Ground Station Receiver Bandwidth (B):	2000	Hz
G.S. Receiver Noise Power (Pn = kTB)	-170.7	dBW
Signal-to-Noise Power Ratio at G.S. Rcvr:	22.1	dB
Analog or Digital System Required S/N:	10.0	dB
System Link Margin	12.1	dB

Table 12.2: Telemetry Link Budget

12.2.2 Beacon unit

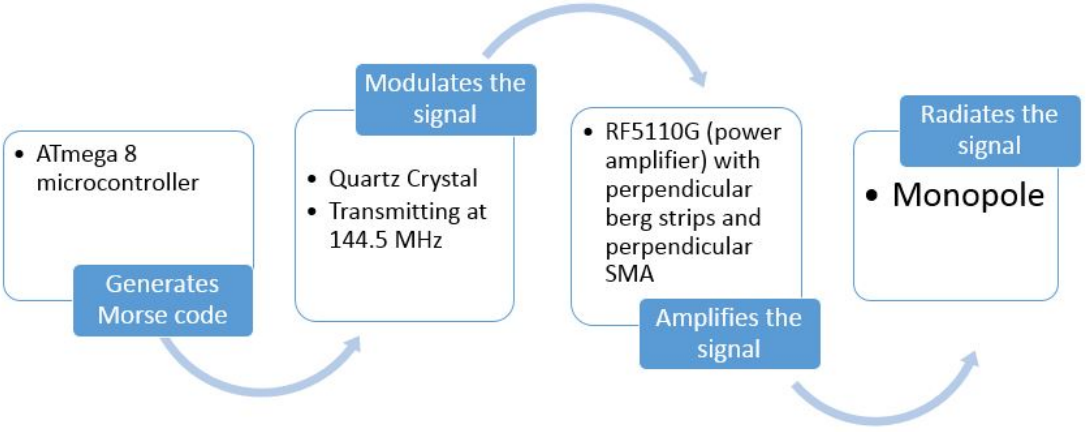

Figure 12.5: Beacon Unit

Beacon data format

Mode of communication is Simplex as per ANSI definition. The data transmitted from the beacon shall have the following components:

- Callsign: VU2MDQ
- IIT Bombay Student Satellite, Pratham

This has to be transmitted using Morse code. The Morse code would follow the International Standards.
Each part would have the following format: Part no./header – "partname" – Information.
Part 1:
Header = 0 Morse equivalent: ——
Part name: Call sign Morse equivalent: -.-. .- .-.. .-.. ... .. –. -.
Information: VU2MDQ Morse equivalent: ...- ..- ..— – -.. –.-
Part 2:
Header: 1 Morse equivalent: .—-
Part name: Identification Morse equivalent: .. -.. . -. - .. ..-. .. -.-. .- - .. — -.
Information: IIT Bombay Student Satellite, Pratham Morse equivalent: .. .. - -... — – -... .- -.– ... - ..- -.. . -. - ... .- - . .-.. .-.. .. - . –..– .–. .-. .- - .....- –

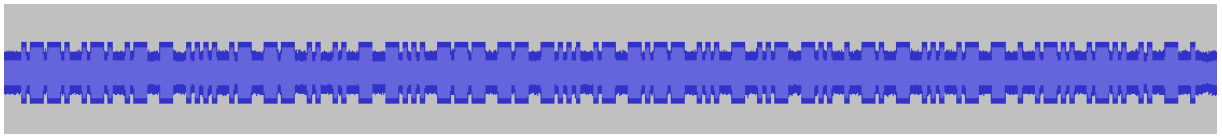

Figure 12.6: Beacon morse code recorded

Beacon Link Budget

Parameter	Value	Units
Spacecraft Transmitter Power Output:	0.03	W
In dBW:	-15.2	dBW
In dBm:	14.8	dBm
Spacecraft Total Transmission Line Losses:	0.4	dB
Spacecraft Antenna Gain:	-3.0	dBi
Spacecraft EIRP:	-18.7	dBW
Downlink Path:		
Spacecraft Antenna Pointing Loss:	0.3	dB
S/C-to-Ground Antenna Polarization Loss:	0.2	dB
Path Loss:	141.0	dB
Atmospheric Loss:	1.1	dB
Ionospheric Loss:	0.3	dB
Rain Loss:	0.0	dB
Isotropic Signal Level at Ground Station:	-161.6	dBW
Ground Station (EbNo Method):		
——- Eb/No Method ——-		
Ground Station Antenna Pointing Loss:	0.3	dB
Ground Station Antenna Gain:	12.0	dBi
Ground Station Total Transmission Line Losses:	0.2	dB
Ground Station Effective Noise Temperature:	1065	K
Ground Station Figure of Merrit (G/T):	-18.5	dB/K
G.S. Signal-to-Noise Power Density (S/No):	48.2	dBHz
System Desired Data Rate:	1200	bps
In dBHz:	30.8	dBHz
Telemetry System Eb/No for the Downlink:	17.4	dB
Demodulation Method Seleted:	User Defined	
Forward Error Correction Coding Used:	None	
System Allowed or Specified Bit-Error-Rate:	1.0E-05	
Demodulator Implementation Loss:	0	dB
Telemetry System Required Eb/No:	9.6	dB
Eb/No Threshold:	9.6	dB
System Link Margin:	7.8	dB
Ground Station Alternative Signal Analysis Method		
———- SNR Method ————		
Ground Station Antenna Pointing Loss:	0.3	dB
Ground Station Antenna Gain:	12.0	dBi
Ground Station Total Transmission Line Losses:	0.2	dB
Ground Station Effective Noise Temperature:	1065	K
Ground Station Figure of Merrit (G/T):	-18.5	dB/K
Signal Power at Ground Station LNA Input:	-149.8	dBW
Ground Station Receiver Bandwidth (B):	2000	Hz
G.S. Receiver Noise Power (Pn = kTB)	-165.3	dBW
Signal-to-Noise Power Ratio at G.S. Rcvr:	15.5	dB
Analog or Digital System Required S/N:	10.0	dB
System Link Margin	5.5	dB

Table 12.3: Beacon Link Budget

12.2.3 Uplink unit

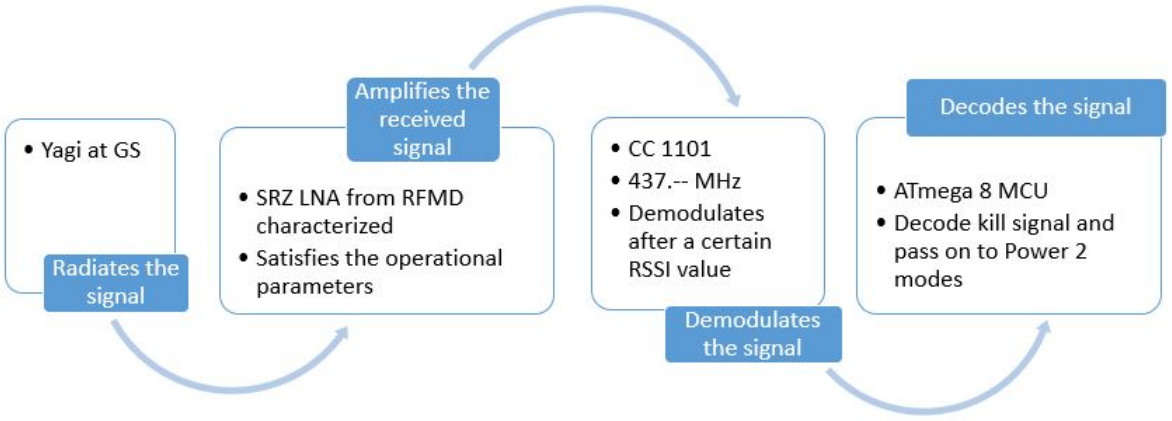

Figure 12.7: Uplink Unit

Uplink is used to reset the satellite or switch it off if required. Only these two functions are controlled by command. All other functions of the satellite are autonomously performed.

Allocation of frequency by IARU

The operation of a transmitter or a receiver in an amateur band requires the authorization of the International Amateur Radio Union. The union has a charter and a bandplan of its own for various regions of the world. The bandplan allocates certain bandwidth in the amateur band for amateur satellite operation. However, the frequency allocation is subject to fulfillment of certain prerequisites. The agency needs to be informed about the entire onboard as well as groundstation system. The following requirements need to be fulfilled:

- Amateur Ham License or a Custodian
- Detailed link budget analysis
- Telemetry sequence
- Details about the GS and Onboard circuity and their functionalities
- Uplink or telecommand to control the satellite.

The telemetry sequence is yet to be worked upon alongwith the encryption of the telecommand. The daughter board that we are using for Uplink is CC1101. Hence, the programming and coding aspects are similar to the one for the telemetry unit.

Uplink Link Budget

Parameter	Value	Units
Ground Station(GS) Transmitter Power Output:	1.0	W
In dBW:	0.0	dBW
In dBm:	30.0	dBm
GS Total Transmission Line Losses:	3.6	dB
GS Antenna Gain:	9.0	dBi
GS EIRP:	5.4	dBW
Downlink Path:		
Spacecraft Antenna Pointing Loss:	0.5	dB
S/C-to-Ground Antenna Polarization Loss:	0.2	dB
Path Loss:	141.9	dB
Atmospheric Loss:	1.1	dB
Ionospheric Loss:	0.7	dB
Rain Loss:	0.0	dB
Isotropic Signal Level at Ground Station:	-139.0	dBW
Spacecraft (EbNo Method):		
——- **Eb/No Method** ——-		
Spacecraft Antenna Pointing Loss:	4.7	dB
Spacecraft Antenna Gain:	2.2	dBi
Spacecraft Total Transmission Line Losses:	2.0	dB
Spacecraft Effective Noise Temperature:	261	K
Spacecraft Figure of Merrit (G/T):	-24	dB/K
S/C Signal-to-Noise Power Density (S/No):	60.9	dBHz
System Desired Data Rate:	1200	bps
In dBHz:	30.8	dBHz
Command System Eb/No :	30.1	dB
Demodulation Method Seleted:	Non-coherent FSK	
Forward Error Correction Coding Used:	None	
System Allowed or Specified Bit-Error-Rate:	1.0E-04	
Demodulator Implementation Loss:	1.0	dB
Telemetry System Required Eb/No:	13.4	dB
Eb/No Threshold:	14.4	dB
System Link Margin:	15.7	dB
Spacecraft Alternative Signal Analysis Method		
——- SNR Method ——-		
Spacecraft Antenna Pointing Loss:	4.7	dB
Spacecraft Antenna Gain:	2.2	dBi
Spacecraft Total Transmission Line Losses:	2.0	dB
Spacecraft Effective Noise Temperature:	261	K
Spacecraft Figure of Merrit (G/T):	-24	dB/K
Signal Power at Spacecraft LNA Input:	-143.5	dBW
Spacecraft Receiver Bandwidth (B):	15,000	Hz
Spacecraft Receiver Noise Power (Pn = kTB)	-162.7	dBW
Signal-to-Noise Power Ratio at S/C Rcvr:	19.2	dB
Analog or Digital System Required S/N:	14.4	dB
System Link Margin	4.8	dB

Table 12.4: Uplink Link Budget

12.2.4 Onboard Antenna System

The onboard antenna system can be broadly divided into 2 subsections based on the purpose it is to accomplish:

- Downlink RF antenna
- Uplink RF antenna

The downlink antenna needed a robust mounting mechanism which would be feasible to fabricate. The uplink RF antenna had to be simulated using 4NEC2 with the given design constraints.

Polarization purity

The simulations showed that a monopole designed from aluminium and having radius 1mm will have an axial ratio of more than 30 dB. The experimental verifications showed an axial ratio of close to 20dB.

Directivity towards earth: Simulation Results

The simulations were done using IE3D and the following was the pattern observed towards the earth when both the monopoles are radiating:

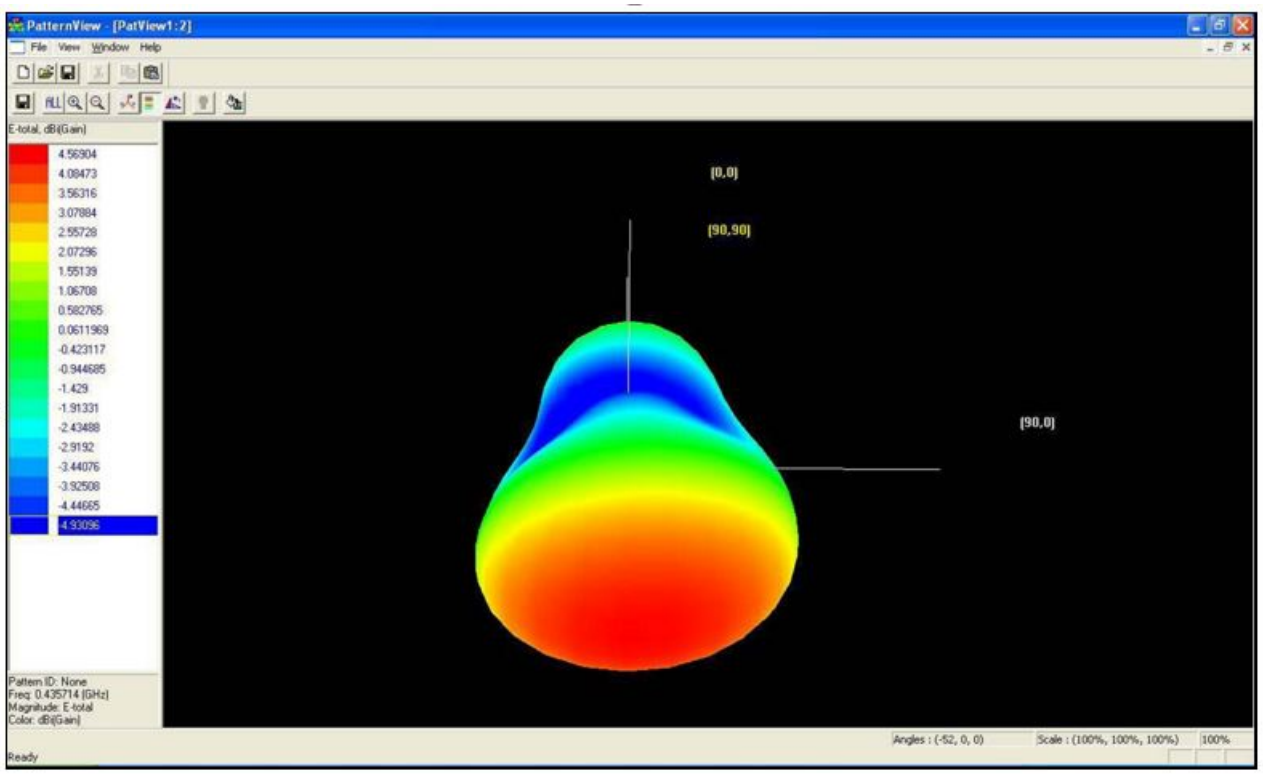

Figure 12.8: Directivity towards earth: Simulation Result

The red portion is towards the earth. The maximum gain is in the direction of earth and the value observed is 4.5 dB.

Effect of coating monopoles with dielectric: Simulation results

The gain of the antenna decreased by about 2-3 dB on being coated with a dielectric with a dielectric value of 6. The reduction was more or less uniform throughout the pattern and the directionality of the pattern remained constant. Thus the only effect this had was to reduce the efficiency of the antenna drastically.

Effect of change of Satellite size on the monopole simulations

There was hardly any change (0.1 dB) due to change in the satellite dimensions. The reasons for the same can be sighted as the wavelength of two monopoles are 70 cm and 200 cm respectively and hence the critical distance at which electrical properties change significantly is the lambda by 4 wavelength which in either case is high compared to a change of 3 cm. We tried to verify this claim by making our satellite dimension of the order of 17 cm and we did observe a sharp change in the pattern and after that the results did not vary much even after changing the satellite body dimension from 20 to 30 cm.

Monopole Holder

It is a fixture that holds a monopole in place on the satellite in the correct specified orientation

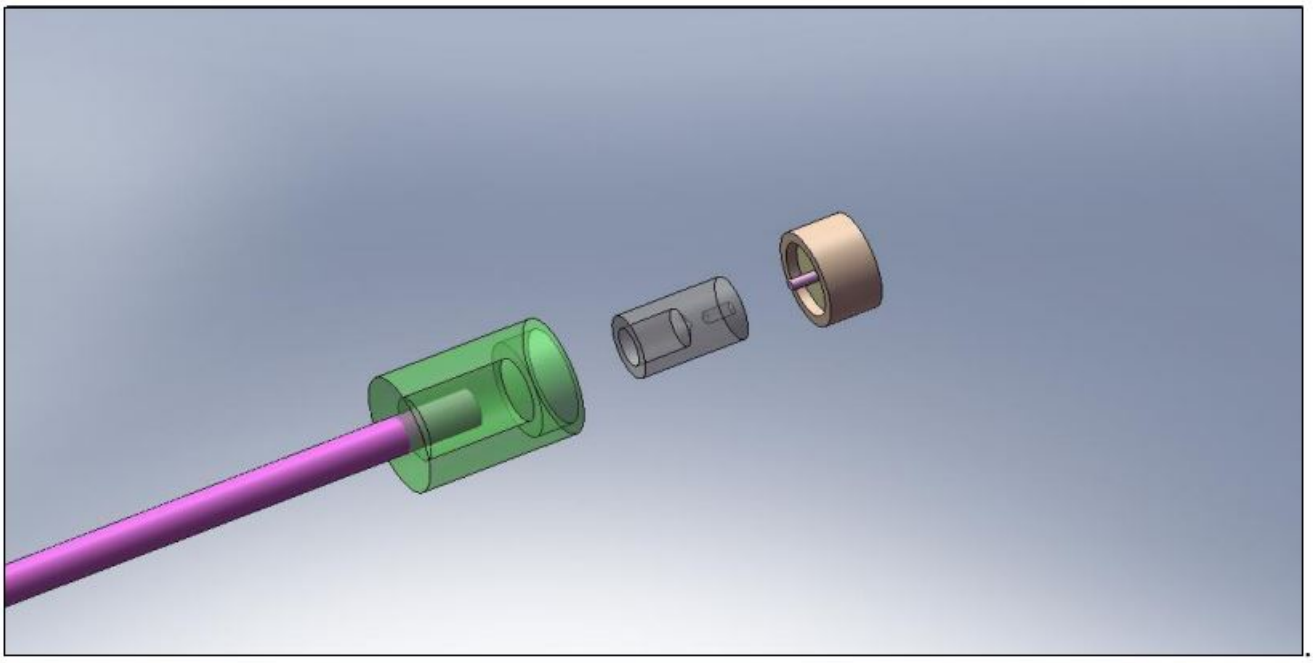

Figure 12.9: Monopole Holder

- Materials: Al-6061
- Dimensions of monopole holder:
  - outer diameter = 20mm
  - inner diameter = 8mm (see pic)
  - length = 29 mm + 2mm (thickness of square base)
  - length of square base = 25 mm

Antenna Configuration

The antenna configuration was simulated in NEC software and various configurations of the 3 antennae were tried before adopting a linear configuration of 3 monopoles on the anti sun side. The decision was taken keeping in mind the communication and integration constraints. The length of all the three monopoles is 17 cm. Two monopoles are fixed at the vertex of the edge joining Anti-sunside panel and zenith side panel. The third monopole is placed at various locations. The maximum gain is observed when the antennae are arranged in one single line on the edge of the cube. The results are as shown below:

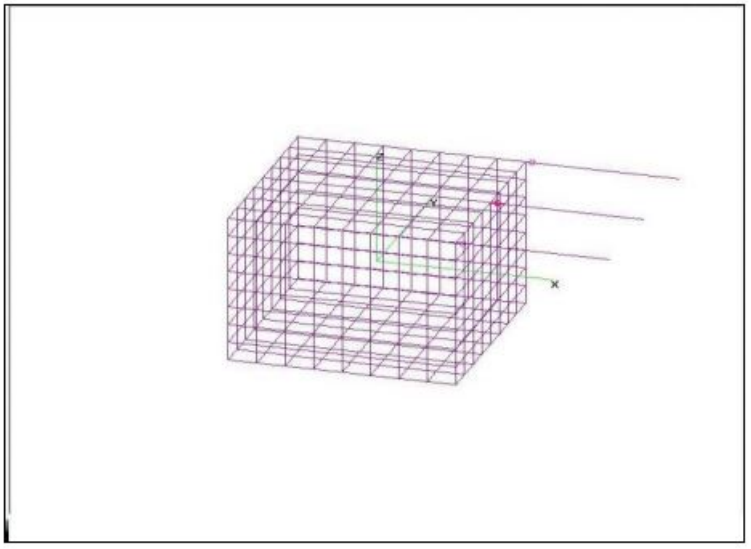

Figure 12.10: Satellite modelled in NEC

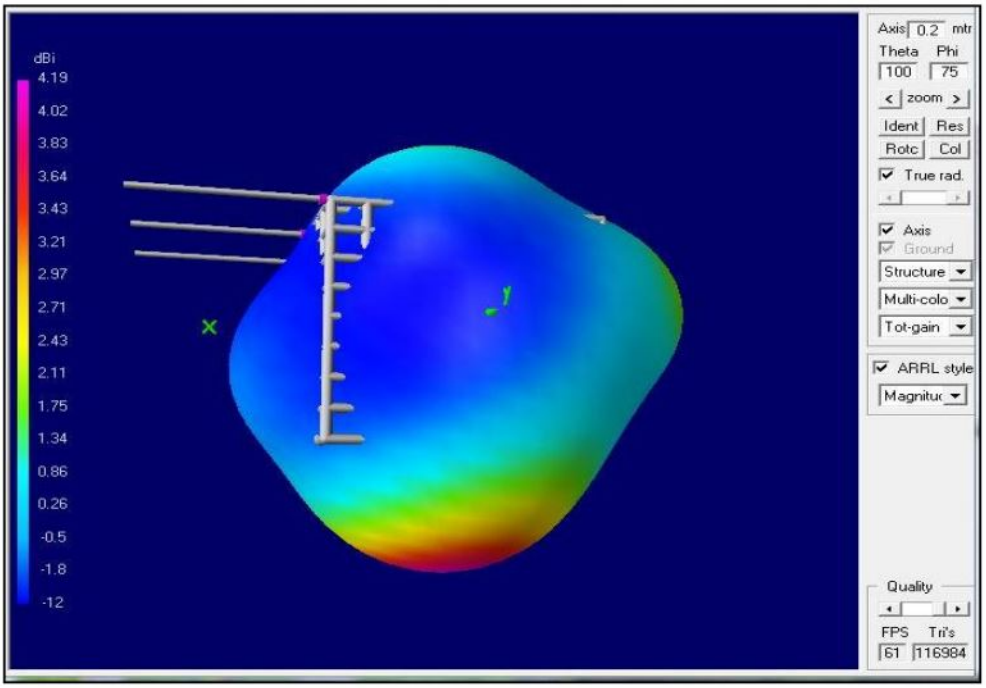

Figure 12.11: Radiation pattern with all antennae aligned in one line

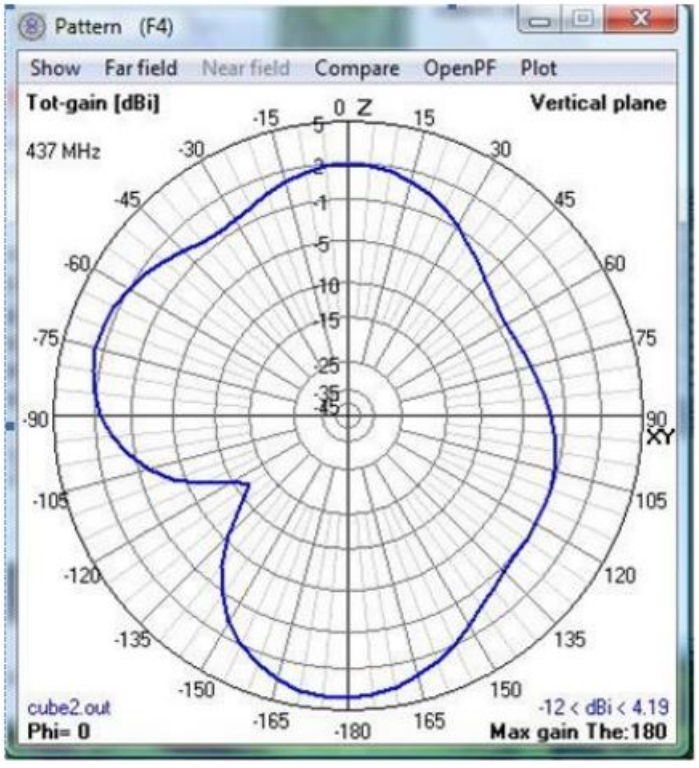

Figure 12.12: Vertical plane radiation pattern

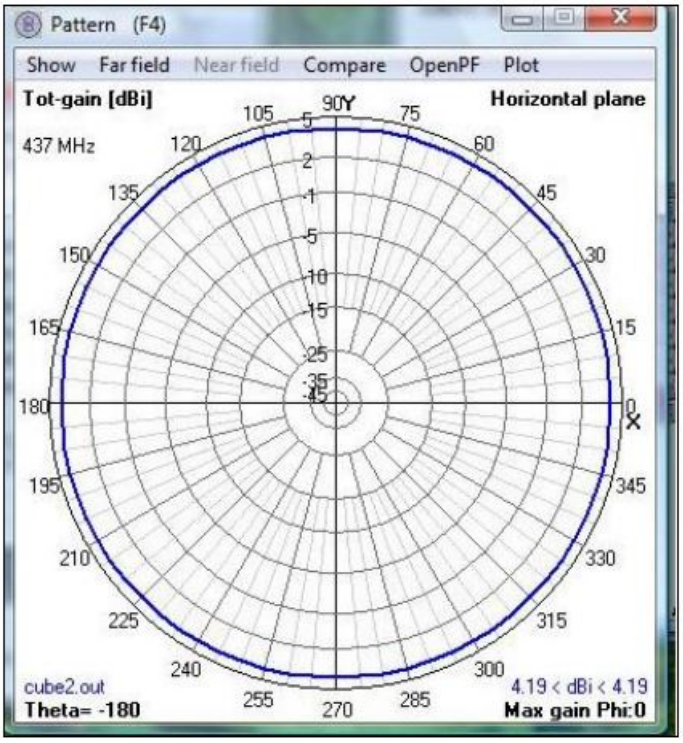

Figure 12.13: Horizontal plane Radiation pattern

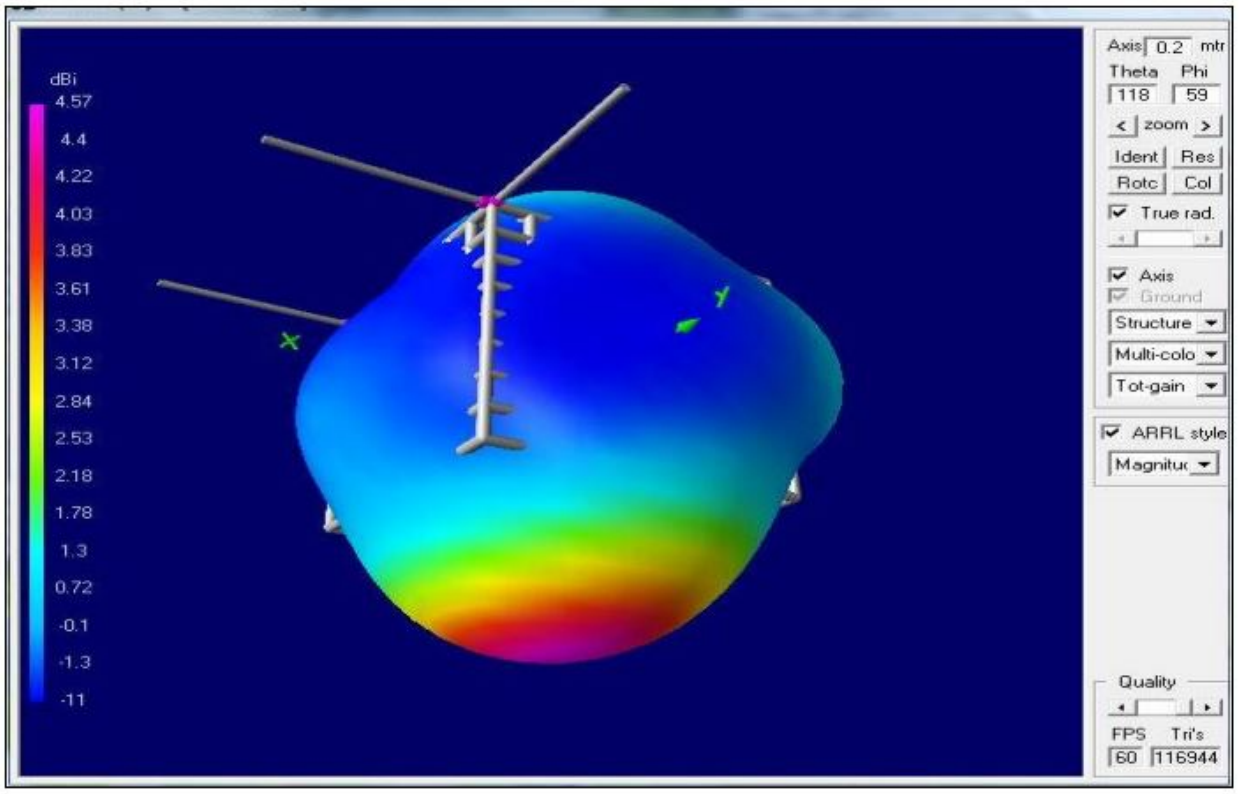

Figure 12.14: Radiation pattern with one antenna on a perpendicular edge

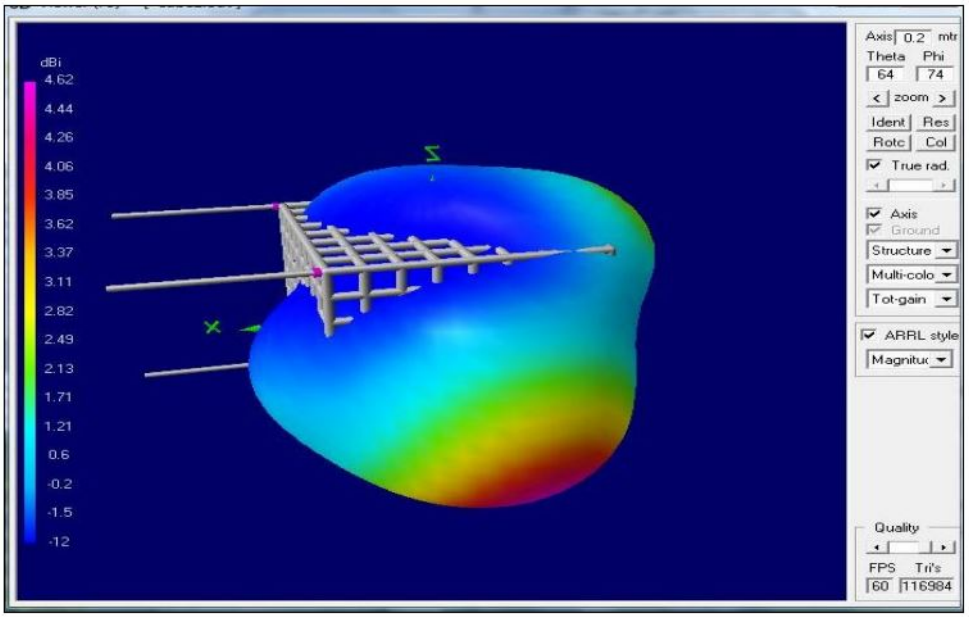

Figure 12.15: Radiation pattern when one monopole is on the corner of the opposite edge

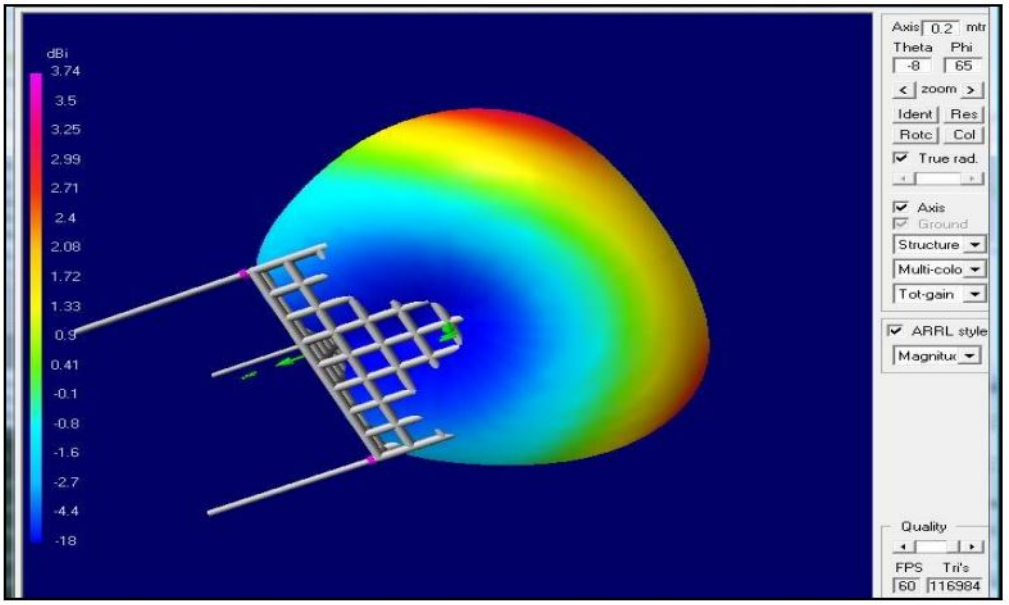

Figure 12.16: Radiation pattern when one of the monopoles is at the face centre

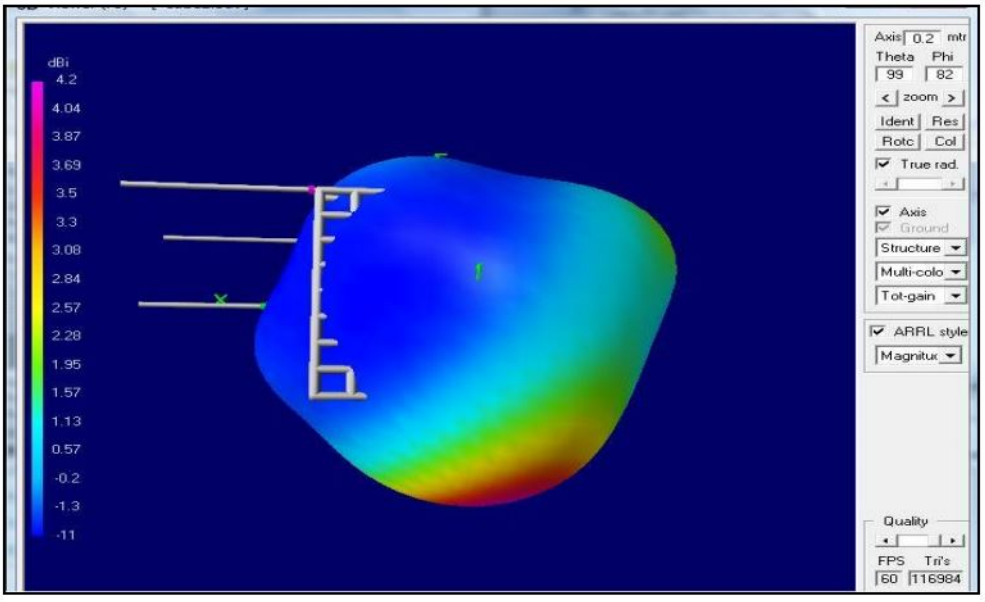

Figure 12.17: Radiation pattern when one monopole is at the centre of the opposite edge

Impedance matching

The impedance matching of the telemetry and uplink monopole was carried out before the anechoic chamber testing. The minimum return loss that was required for the satisfactory testing of the radiation pattern without damaging the equipments was -10 dB. The analysis of S11 parameter of the antenna using a network analyser showed that the antenna was matched to a lower frequency. Thus, it had to be trimmed in order to increase its resonant frequency to 437.5 MHz. The following table shows the variation of the resonant frequency with the length of the monopole and the conditions of testing the impedance.

Length(mm)	Resonant f(MHz)	Return loss at resonance	Return loss at 437.5 MHz	Conditions
170	412	-19 dB	-5 dB	Outside Anechoic chamber
164	421	-20 dB	-7 dB	Outside Anechoic chamber
160	426	-15 dB	-9 dB	Outside Anechoic chamber
155	429	-20 dB	-11 dB	Outside Anechoic chamber
150	433.04	-17 dB	-12 dB	Inside Anechoic chamber

Table 12.5: SWR of monopole for various lengths

12.2.5 Amplifier testing

The amplifier was tested at VHF frequency in order to characterise the following properties

- Gain of the amplifier
- VSWR of the amplifier
- Frequency response of the amplifier
- Voltage and current consuming characteristics of the amplifier
- Heat dissipation of the amplifier

The following are the results of testing:

Parameter	Observed value	Datasheet value
Gain	26 dB	30 dB
VSWR	-5.9	-20
Current consumption	0.4 A	0.4 A

Table 12.6: Power Amplifier test results

The following can be the sources of errors:

- The coaxial cables and the connectors can be sources of noise for the amplifier
- On chip connectors may not be matched to 50 ohms
- The chip can operate in ISM bands along with VHF and that maybe a reason for the spurious emissions
- The thickness of the PCB was not according to design thus affecting its RF properties.
- The heat dissipation can be controlled by controlling the Vapc voltage level. The thermal grounding for the PCB might be faulty as only local heating was observed.

12.2.6 Hot and Cold testing of RF cards at ISAC

Hot and cold testing of RF communication boards of Pratham was conducted at Indian Space Research Center (ISAC), Bangalore on 20^{th} and 21^{st} of May 2015. The following RF components were tested in Hot and Cold temperature cycles:

- Crystal 145.988 MHz
- Power Amplifier
- CC1101 evaluation board
- Low noise amplifier

Components Required

The following components were taken to ISAC:

1. PCBs:-

   a. Beacon board (with crystal of 145 MHz)- Quantity: 2

   b. Downlink board (with CC1101)- Quantity: 2

   c. Uplink board(with one LNA)- Quantity:1

2. Power board V4 : Quantity 1
3. Preflight board
4. Working LNAs- Quantity: 2

5. Working Power amplifiers- Quantity:2
6. Laptop and charger (containing codes for hot and cold, schematics of all the boards, datasheets of LNA, power amplifier, CC1101 and crystal 145 MHz)
7. Co-axial cables- Quantity:4
8. Connecting wires
9. SMA connectors box
10. SMA plug to plug cables
11. USB cable, Quantity:2
12. AVR ISP Programmer
13. Multi-meter
14. Antistatic wrist straps
15. NI-DAQ
16. Wire stripper
17. Solder iron and solder metal

List of components provided by ISAC:

1. Thermistor
2. Spectrum Analyzer
3. RF generator
4. 50 Ω loads
5. Thin co-axial RF cables

Execution Plan

The following temperature profile is set for testing.

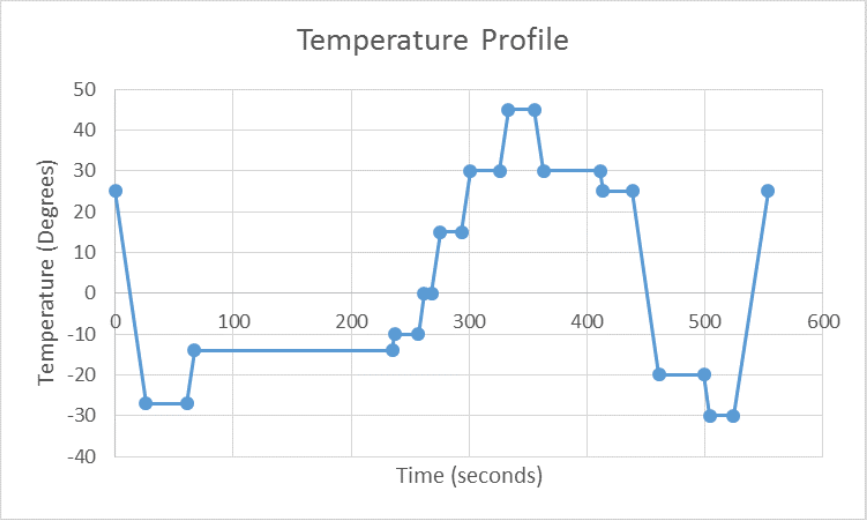

Figure 12.18: Temperature profile for the test

The soak time is kept 20 minutes.

Testing of Crystal

Provide 5 V and Ground externally to the power board. Connect co-axial cable at the output of Crystal and connect the co-axial cable to spectrum analyzer or oscilloscope to monitor frequency and gain variation.

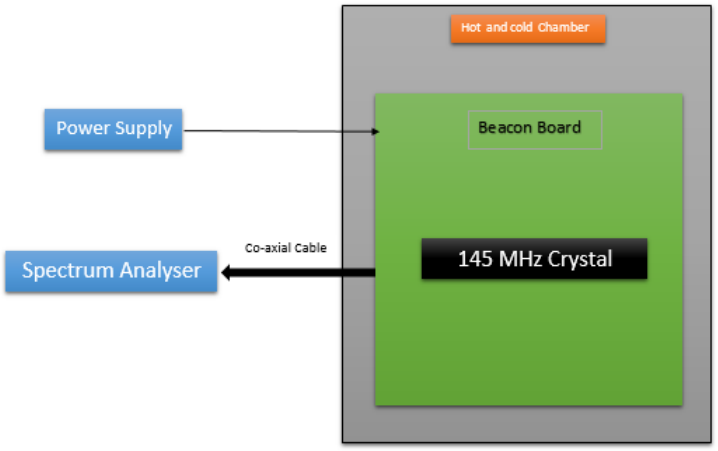

Figure 12.19: Crystal Testing schematic

Testing of Power Amplifier

Provide 5 V and Ground to the power amplifier. Also connect 3.3 V to enable pin of the Power amplifier. Connect input terminal of power amplifier to signal generator and output terminal to spectrum analyzer/ oscilloscope using co-axial cable. Monitor gain variation for the whole duration.

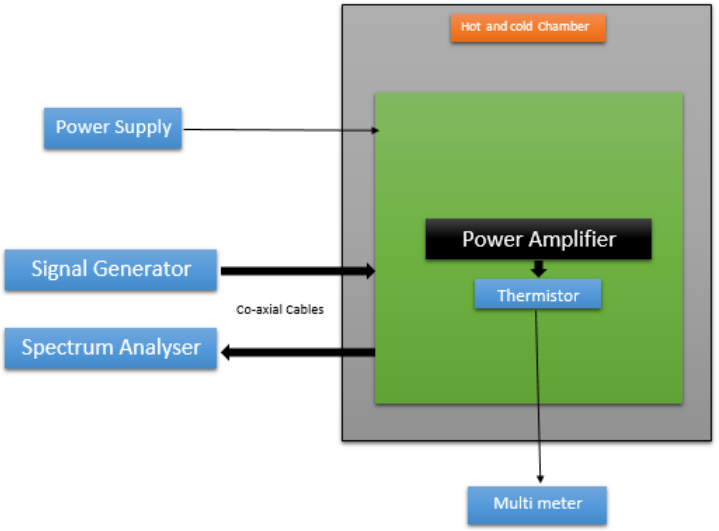

Figure 12.20: Power Amplifier Testing schematic

Testing of CC-1101

Provide 5V and connect ground to downlink board externally. Connect co-axial cable at the end of CC1101 to Spectrum analyzer/ oscilloscope outside the chamber. We will monitor the central frequency and gain.

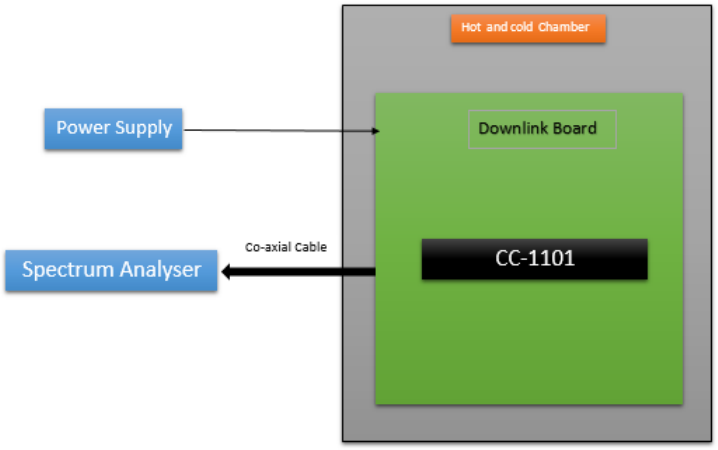

Figure 12.21: Power Amplifier Testing schematic

Testing of LNA

Power up the LNA from external power source. Connect input terminal of LNA to signal generator and output terminal to spectrum analyzer/ oscilloscope via co-axial cable.

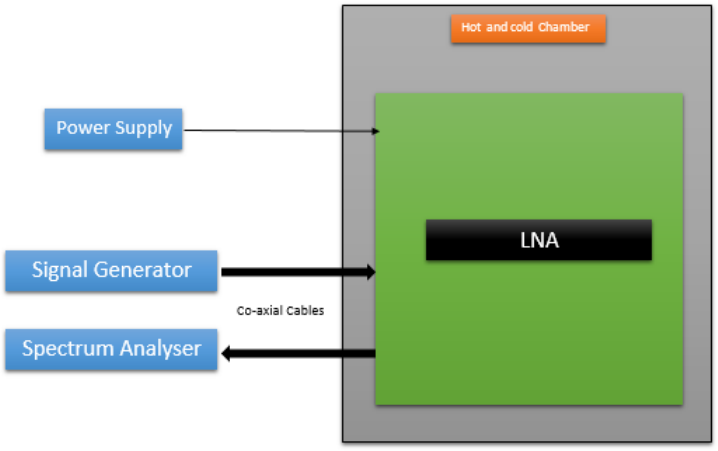

Figure 12.22: Low noise Amplifier Testing schematic

Results for CC1101

1. Power Output Variation

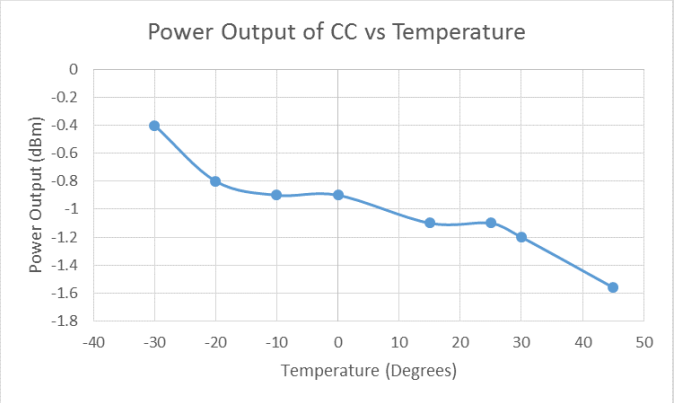

Figure 12.23: Power output variation of CC1101 with temperature

Power output varied by about 1 dBm with increase in temperature. According the program power output should be 0 dBm. Smaller power output is due to SWR and power loss of cable.

2. Power Consumption Variation

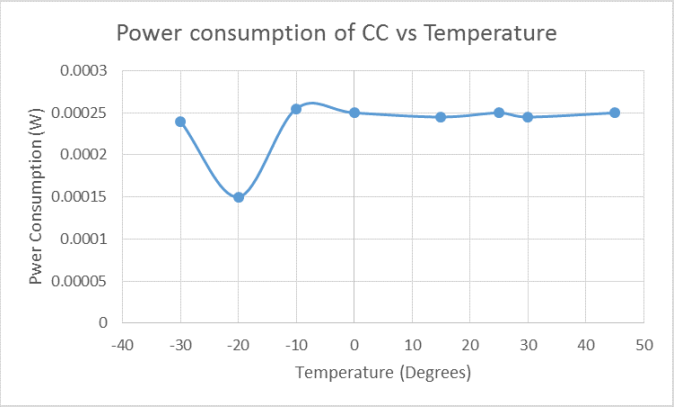

Figure 12.24: Power consumption variation of CC1101 with temperature

Power comsumption by CC1101 was very less. There was no significant variation in it with temperature. It matched with the specification given in datasheet.

Results for low noise amplifier

1. Power Consumption Variation

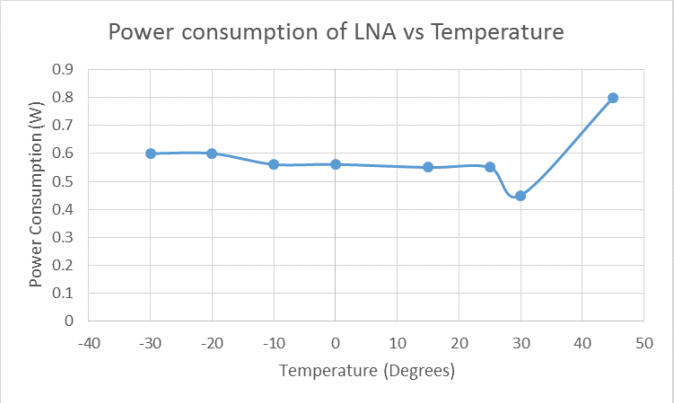

Figure 12.25: Power consumption variation of LNA with temperature

Power consumption is almost constant throught the cycle . There is an abrupt increase in power consumption at the hot peak. We think it is an anomaly in data recording.

2. Gain Variation

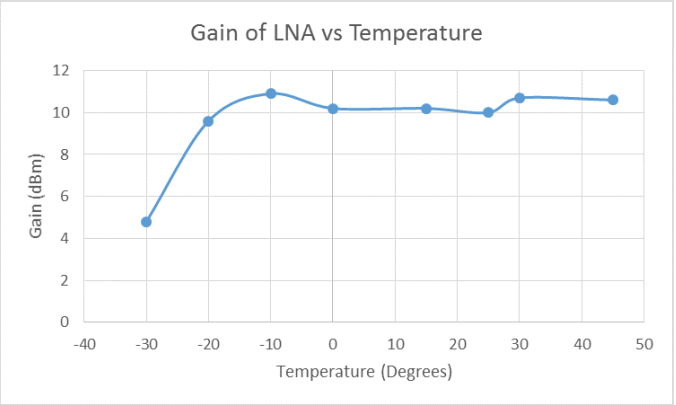

Figure 12.26: Gain variation of LNA with temperature

Gain is less at lower temperature. Above -20deg C gain is almost constant. It is less than the value specified in datasheet. This may be due to SWR of cable.

Results for power amplifier

1. Power amplifier temperature variation with chamber temperature

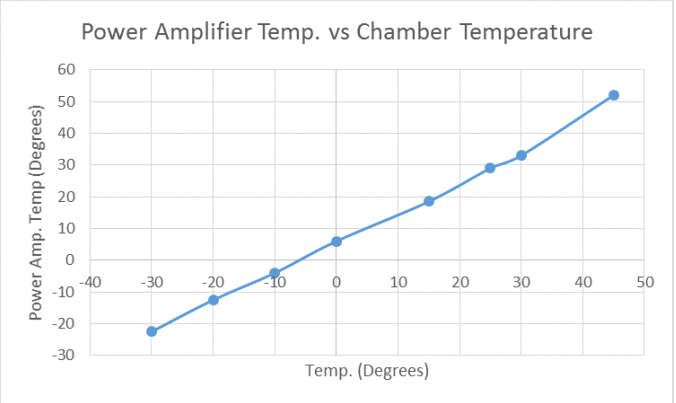

Figure 12.27: Power amplifier temperature variation with chamber temperature

Temperature of PA increases with increasing temperatue as expected. It did not exceed the operational temperature range (+80degC) at the hot peak.

2. Resistance of power amplifier thermistor variation with temperature

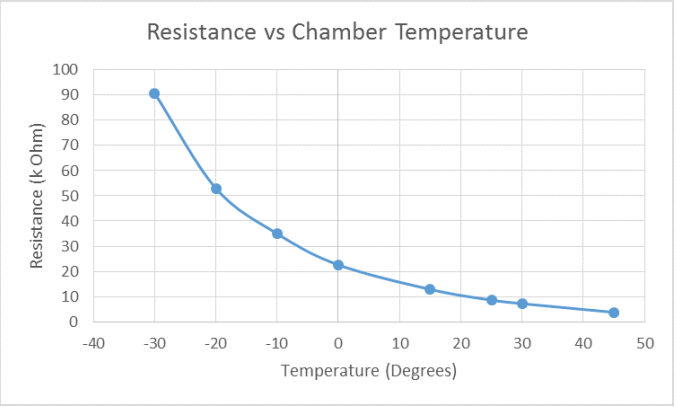

Figure 12.28: Resistance of power amplifier thermistor variation with temperature

Resistance of thermistor decreases which is because temperature increases.

3. Power output variation with different frequencies

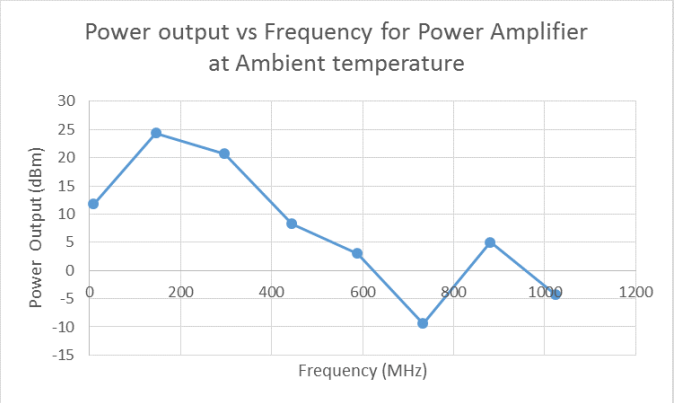

Figure 12.29: Power output variation with different frequencies

Power output is maximum at 145.98 MHz as expected. Second harmonic is at 5 dBm than the central frequency. All other harmonics are less than 20 dBm from the central frequency.

4. Power output variation with temperature

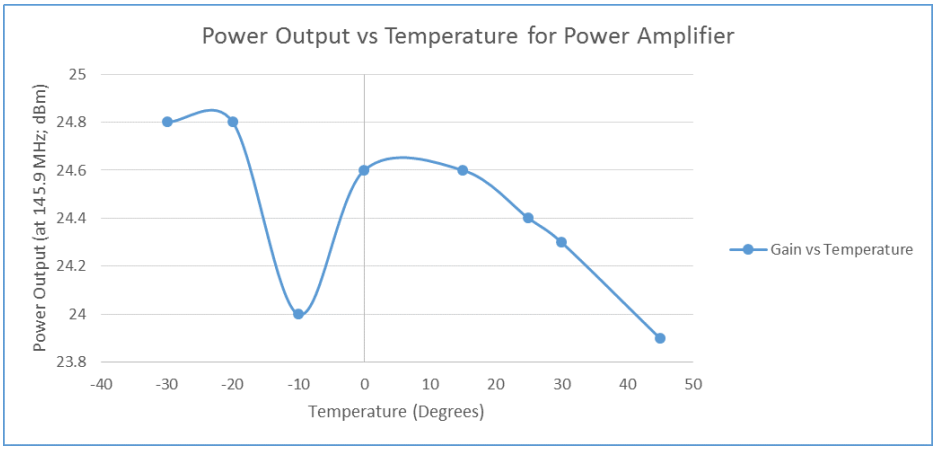

Figure 12.30: Power output variation with temperature

Power output varies within 1 dBm. Output is less than the value specified in datasheet. This is due to SWR and power loss of cable. Also there will be impedance mismatch between crystal output and PA input. So the input mighth be less than 0 dBm.

Results for Crystal

1. Power Consumption of crystal

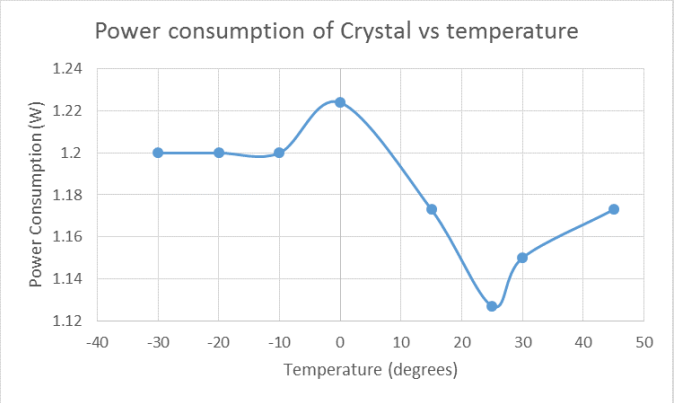

Figure 12.31: Variation of power consumption of crystal with temperature

Power consumption is more than the value specified in the datasheet. This may be because we were measuring the current consumed by the whole beacon board. The extra power might be consumed by other components, importantly Atmega8 and TPS voltage regulator.

2. Power output of crystal

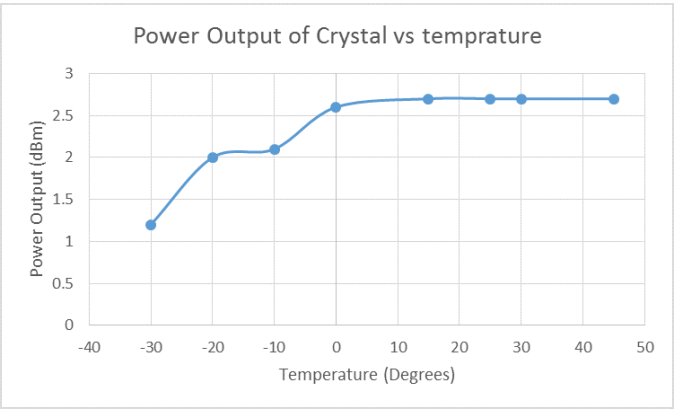

Figure 12.32: Variation of power output of crystal with temperature

Power output does not vary much which is good for estimating link budget.

Actions taken after testing

It was pointed out during testing that the power amplifier was operated at 3V which is the maximum allowed voltage. This can lead to damage to the PA. It was decided that voltage should be 2.8V. A different voltage regulator of the same series (TPS) was chosen - TPS76928. Beacon board and Downlink board was redesigned accordingly and new board was tested.

12.3 Groundstation segment

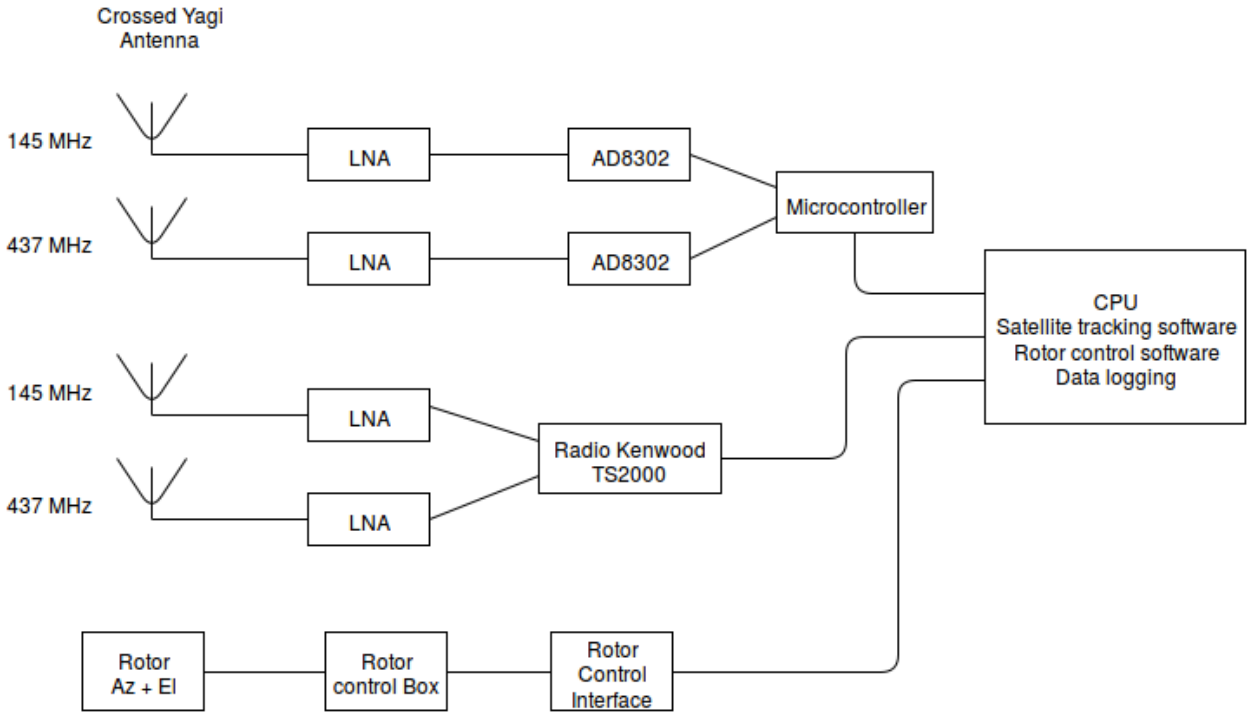

Figure 12.33: Ground station flow diagram

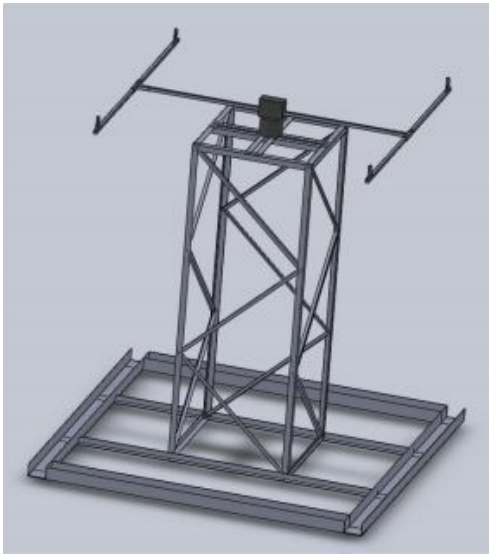

Figure 12.34: Ground station antenna mount

The ground segment for Pratham at IITB has following major functions

- Satellite tracking and receiving segment
- Uplink transmission segment
- Payload data logging

Towards these ends various off the shelf as well as self-fabricated components are used. These are:

- Antennas: Two pairs of crossed yagi antennas, one pair for each frequency band i.e. central frequency 145.8 Mhz, 437.5Mhz)
- Transceiver base station: Kenwood TS2000 radio demodulates the FSK signal and stores the data in the mainframe.
- A pair of AD8302 modules measures RF gain and phase value between the two inputs it takes Uses Log amplifiers to calculate the value of log (InpA/ InpB)
- Low Noise Amplifiers: 4 low noise amps are being used on the distinct feeds from antennas
- Rotor arrangement with an Interface circuit to integrate the device with software architecture. Rotor (Yeasu G-5500) is being used to orient the antenna structure to the required inclination with respect to reference level. The rotor interacts with the mainframe via Rotor Controller Interface (RCIUSB by EA4TX)

Figure 12.35: Ground station equipments

12.3.1 Antennas

As per the requirement set forth by the payload subsystem, the antenna should be able to capture the component of the plane of polarisation along both the X and Y planes. For this purpose crossed-yagi antennae are used at GS. These consist of a couple of dipole

antennae perpendicular to each other mounted on a boom along with a few other elements. The elements placed in front of the dipole are termed as directors. These help in increasing the antenna gain in the forward direction thus adding to the directivity of the antenna. Similarly the elements placed behind the dipole adds to the power collected/transmitted by the dipole, affecting the front to back ratio.

Simulations were done in the antenna design software NEC and the results were optimized giving maximum weight age to the Impedance of the antenna being as close to 200 as possible to give perfect matching.

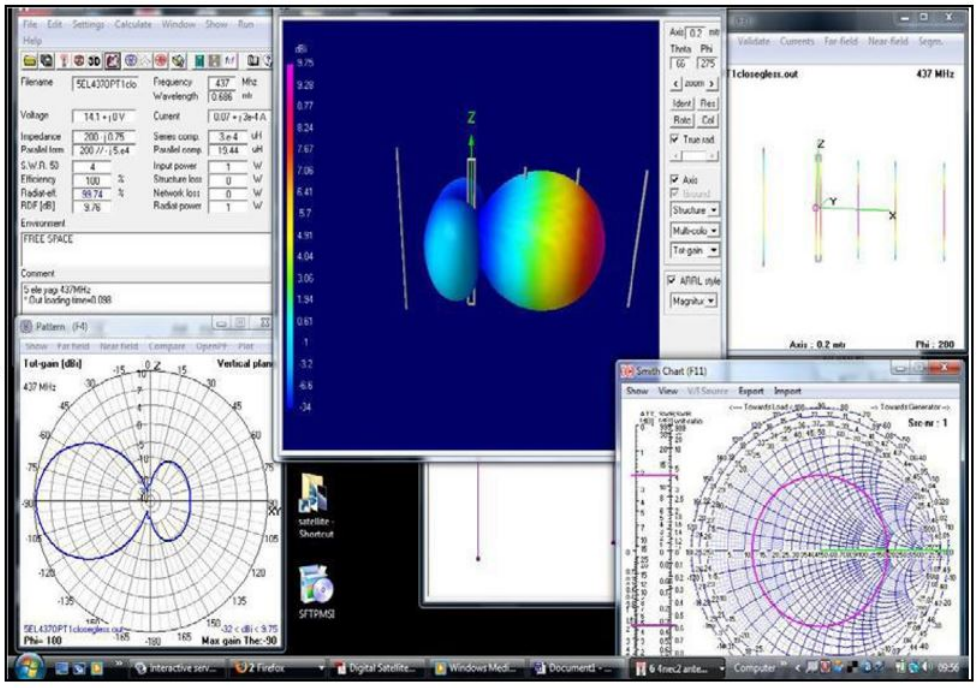

Figure 12.36: NEC2 Antenna simulations results

The simulation results were the following

- Gain : 9.75 dB
- Beam width : 50 degrees
- VSWR : 1
- F/B ratio 19.6

Experimental characterization

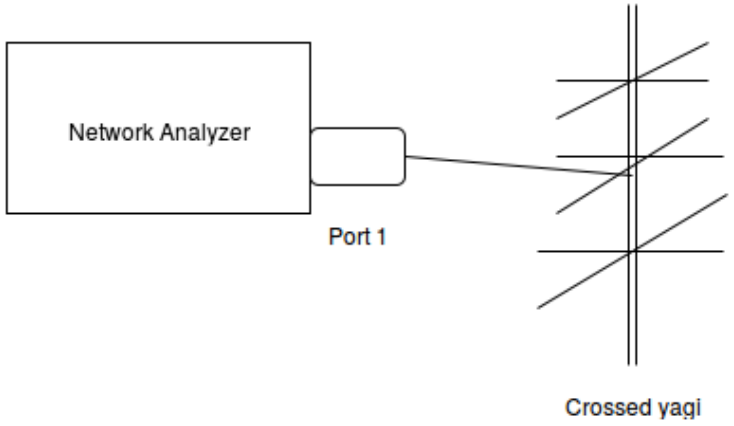

Figure 12.37: Yagi test setup

The impedance of the antenna was designed to be 200 ohms +- 10 ohms. Testing of balun was done with the help of Simple resistances and Surface mount resistances. The performance of the yagi was tested with the help of a network analyzer and the following results were obtained.
SWR vs. frequency 437MHz - 1: 1.1667 24
S11 vs. frequency 436.95MHz -1: -25.047 dB
Smith chart 46.9 ohms

For a perfectly working antenna, the S11 value below -10dB represents a 90 percent efficient antenna, so the value of -19dB is a good enough for sound reception.

Design and Production

We decided to design the Crossed yagis to be used at our Ground station ourselves after receiving encouraging results from the Yagi that we had designed earlier. We decided to use an Aluminium boom instead just to make the yagi more rigid and robust. We verified that the electrical characteristics of aluminium would not affect the characteristics of the yagi by a great deal using simulations and by consulting with Professor K.P. Ray of SAMEER. We designed couplers to be used with the help of professionals. The designs for the couplers were made in Solidworks and the same were forwarded to professionals. The Couplers too were of aluminium and their design was approved by Professor K.P. Ray.

12.3.2 Payload Data

The main agenda of the GS is to measure the TEC in the atmosphere from the signal received from the point where it stands. This is obtained by measuring the change in the plane of the plane polarised waves which are transmitted from the monopoles on the satellite. As we are unaware of the initial angle of the plane, we use two separate waves of

considerable different frequencies (145.98 MHz and 437.5 MHz) and then subtracting the angle to get rid of the initial component. This angle is then substituted in the equation given below as $\Delta\phi$

$$\Delta\phi = 4.87x10^{-4}xf^{-2}\int_{h_1}^{h_2} NBcos\theta dl \tag{12.1}$$

N:electron density; B:Magnetic field; θ:angle between magnetic field and direction of propagation

The measurement of the intensities are done by a Polarization measuring unit, namely AD8302 connected at the lines of the feed. The data obtained from the IC is automatically logged into a text file using a microcontroller.

12.3.3 AD8302 Polarisation Measurement Unit

The AD8302 is a fully integrated system for measuring gain/loss and phase in numerous receive, transmit, and instrumentation applications. The major blocks consist of two demodulating log amps, a phase detector, output amplifiers, a biasing cell, and an output reference voltage buffer. The log amps and phase detector process the high frequency signals and deliver the gain and phase information in current form to the output amplifiers. The output amplifiers determine the final gain and phase scaling. The reference buffer provides a 1.80 V reference voltage that tracks the internal scaling constants.

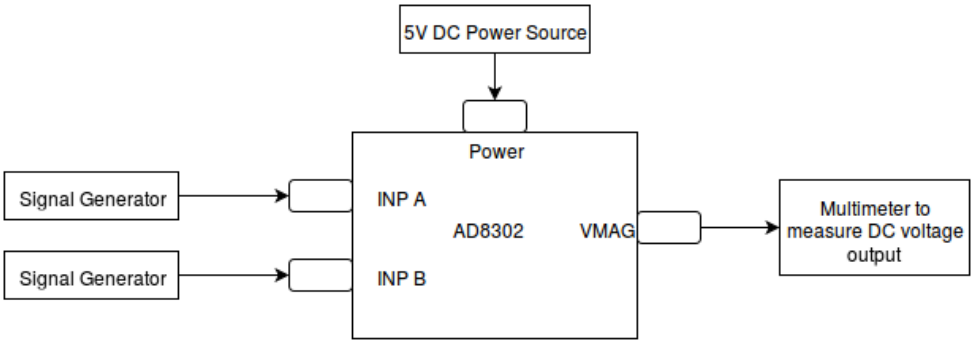

Figure 12.38: A8302 test setup

- We provided same input power to the pins INPA and INPB and obtained the output voltage from the pin VMAG
- Further we provided INPA and INPB with power having difference of -5 and increasing that difference up to -30 with a difference of 5 units and similarly for difference from 5 to 30 dB
- Plotted INPA-INPB vs. VMAG. The average of the VMAG values is taken plotting the graph

The results of the characterization can be seen below:

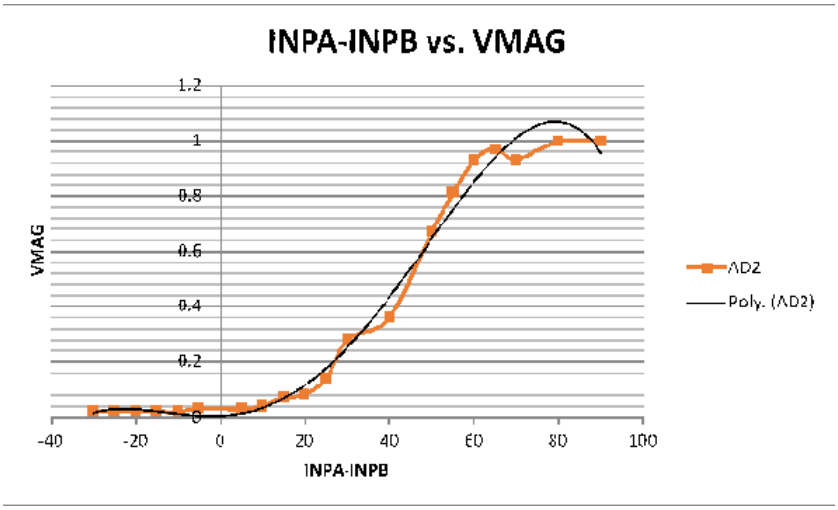

Figure 12.39: A8302 test data

12.3.4 Kenwood Transceiver

TS 2000 is used for receiving beacon and telemetry signal. The transceiver is being tested for operation in the VHF and UHF bands. The transceiver requires a high power source of 13.8V and 20 A current. The power source currently being used is from Yaesu. We switched on the receiver to the satellite mode and checked the squelch from the transceiver. We performed the Kenwood transceiver characterisation for Bandwidth, least signal strength detected, Demodulation of signal
The setup was as follows:

- A simple monopole served as a transmitter antenna.
- It was connected to the 145 MHz crystal on the beacon board without the power amplifier. Power output of crystal is 0 dBm. The power output from monopole is -10 dBm.
- The receiving antenna was a crossed yagi connected to the VHF input.

The cable loss for one cable was 2 dB. We used 2 cables and hence cable loss 4 dB. Considering the following parameters:
Cable loss = 2 dB
Transmitting antenna gain 3 dB
Receiving Antenna Gain 9 dB
Transmitted power = -10 dBm
Distance between the transmitting and receiving yagi = 10 cm - 0.5 m
Path loss = 5.25 dB - 19.32 dB
The transceiver S-meter (signal stregth) showed a received power of -105 dBm. The bandpass region is less than 50 KHz which is good enough for our purpose. Infact , the response is so sharp that the signal strength falls to zero from a good enough value by

changing the central frequency by 25 kHz on either side. Thus, the floor noise level for the device is absolutely low from kTB formula.

12.3.5 Rotor and Tracking Software

Rotor and controller

We are using Yaesu G5500 Azimuth Elevation rotor. It comes with a Rotor Control Box which can be used manually as well as through computer.

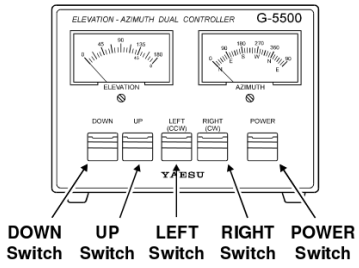

Figure 12.40: Rotor control box front

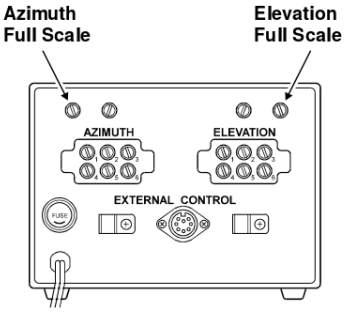

Figure 12.41: Rotor control box back

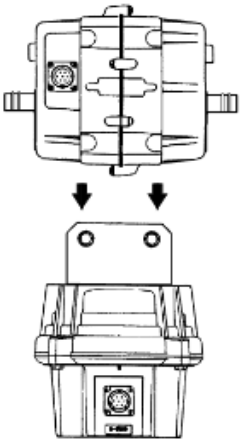

Figure 12.42: Rotor Azimuth(bottom) and Elevation(top)

For controlling by software EA4TX RCI-USB Rotor control Interface is used. This board serves as the interface between the mainframe computer and the rotor controller box, orienting the antenna. The RCI-USB circuit fulfils the two following objectives:

- It reads the current antenna position by means of an incorporated A/D converter.
- It controls the movement of the rotor. For an azimuth rotor, this would be right or CW and left or CCW. This is accomplished through relays using the data obtained from the A/D converter.

The following is the RCI-USB circuit schematic

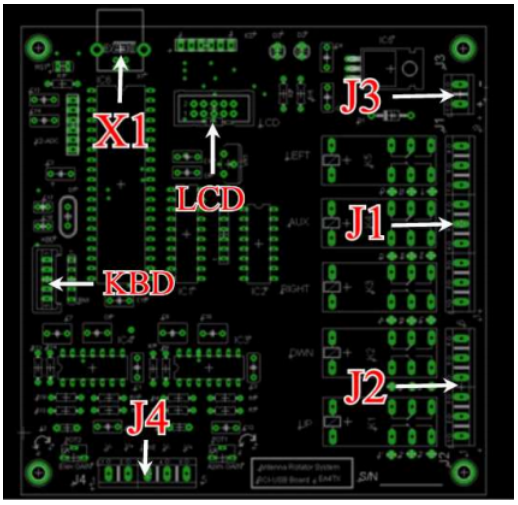

Figure 12.43: RCI-USB schematic

Here J1 is used for control of the azimuth of the rotor, J2 is for the elevation control and J3 is the Power input, J4 is for the ADC operation. Also, the RCI-USB has a potentiometer for each input providing all of these adjustments:

- Azimuth input: Pot1 adjusts the Gain/Attenuation between 3-24V.
- Elevation input: Pot2 adjusts the Gain/Attenuation between 3-24V.

Software

- Satellite Tracking Software
  The satellite orbital elements are available on the internet and keep updating. There are softwares available that take these two line elements and predict the satellite path. The G-predict software on Ubuntu systems has a library package named "Predict" for the same environment to calculate and predict the positions for the satellite. These satellite positions are then written into a file.

- Rotor controlling software
  The file written above is checked regularly by another program. Once it finds a visible pass for the marked satellite, it activates the rotor and passes on the respective azimuth and elevation angles to the RCI interface. This is been done with the help of the rotctl package in the hamlib library for Ubuntu.

- Rig Control The TS2000 rig is being controlled to sync its functionalities with the passes of satellite. This can be done using the rigctl package of hamlib library for Ubuntu.

Chapter 13

Thermal Subsystem

13.1 Introduction

The environment up to a height of around 500 km above the Earth is strongly affected by the presence of the denser layers of the atmosphere and by interaction with the hydrosphere, and thus experience relatively mild conditions of temperature. However, above 500 km, the atmosphere becomes too thin to moderate the ambient thermal conditions and consequently, the environment above such a height is prone to extremes of temperature, being directly exposed to solar radiation and deep space.

13.2 Requirements Constraint Analysis

In this part we will discuss the requirements of other sub-systems which need to be addressed by the thermals subsystem.

13.2.1 Requirements from Power Sub-System to Thermals Sub-System

- The optimal operating range of the battery is from 5^0 C to 20^0 C. The acceptable operating range is 0^0 C to 35^0 C. The thermals sub system shall try and maintain the battery within its optimal operating range. If that is not possible the battery must be maintained in the acceptable operating range.
- They shall remove the excessive heat from Power Circuits, since the temperature range of the components (industrial grade) is given in 13.1

13.3 Requirements from Communication and Ground Station Sub-System to Thermal subsystem

- Thermal sub-system will protect the monopoles from heating above 100^0 C
- They shall remove the excessive heat from the 2 monopole circuits, since the temperature range of the components (industrial grade) is given in 13.1

13.4 Requirements from On Board Computer Sub-System to Thermals Sub-System

- They shall remove the excessive heat from the OBC circuits, so that its temperature is inside the temperature range of the components(industrial grade) is given in 13.1

The aim of the thermal subsystem is to satisfy all these requirements. The most stringent requirement is maintaining the temperature of the battery. In the next chapter we will look into the design procedure and performing the thermal analysis of the satellite

	Operating Range		**Storage Range**	
Components/ Temperature (^{0} C)	**Min**	**Max**	**Min**	**Max**
Power Board	0	70	-40	125
OBC Board	0	70	-65	150
Sunsensor Board	-40	50	-40	85
RF Boards	0	70	-55	125
Magnetometer	-40	70	-55	125
GPS Receiver	-25	65		
Battery	0	35		

Table 13.1: Operating Temperature

13.5 Thermal Modeling

This chapter deals with the thermal modeling and simulation of the satellite, which would help us in determining the temperature of the various parts of the satellite. The thermal modeling and analysis has been done using the Siemens PLM Software NX Nastran 9.0. This software makes it easy to model nonlinear and transient heat transfer processes including conduction and radiation. Nastran uses finite element models (FEM) and highly accurate numerical methods for solving the element based thermal models. The thermals' scientist in ISAC associated with small satellites, Mr.Nagaraju helped us in the thermal modeling. The modeling involves specifying the geometric model of the various parts of the satellite, couplings and boundary conditions associated with it and the solution parameters required for solving the problem. The whole modeling process is explained in this chapter.

13.5.1 Modeling approach

For thermal modeling mid surface of all the components was created as most of the components - solar panel, satellite sides, pcbs, battery box have very small thickness which can be approximated as a surface. Then, thin shell property was defined for all the components for calculation of volume, mass and heat capacity. Few components like

- magnetometer and GPS are of significant thickness, but these components are defined in similar way, because we need a rough idea of temperature of such components. So, for the sake of simplicity and reduce computational time these were modeled similar to other components.

13.6 Grid

The model has been meshed using a structured grid. Quad4 elements are used for meshing. Total 9359 elements are created after meshing the model.

13.7 Boundary conditions and Couplings

Boundary Conditions defines known thermal conditions in the model. The Thermal Boundary condition consist of a variety of heat loads and fluxes, fixed temperatures, and joule heating. Thermal coupling are applied to specify conductance between two dissimilar meshes or to specify conductance between two surfaces that are connected through screws or stubs.

13.7.1 Solar Fluxes

Orbital heating option is used to determine heat flux as function of time that will fall on each face of satellite. Satellite has a 22.30 sun synchronous orbit. After giving input parameters like altitude, eccentricity etc. heat flux can be received for all the faces of the satellite. Solar flux was applied on respective faces and solar absorptivity of respective surfaces are defined.

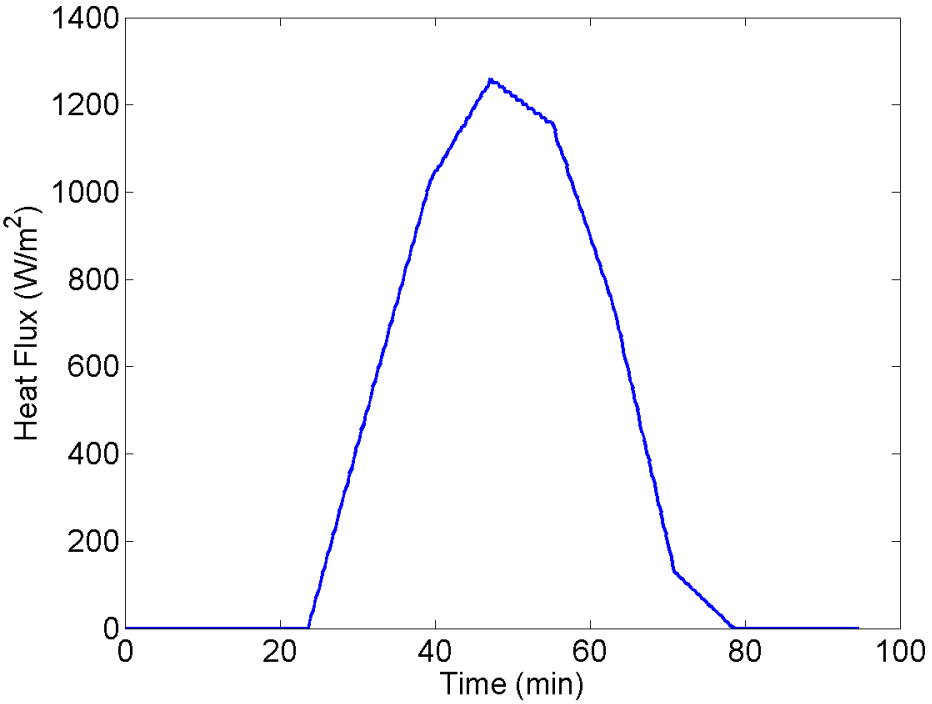

Figure 13.1: Solar Flux: Zenith

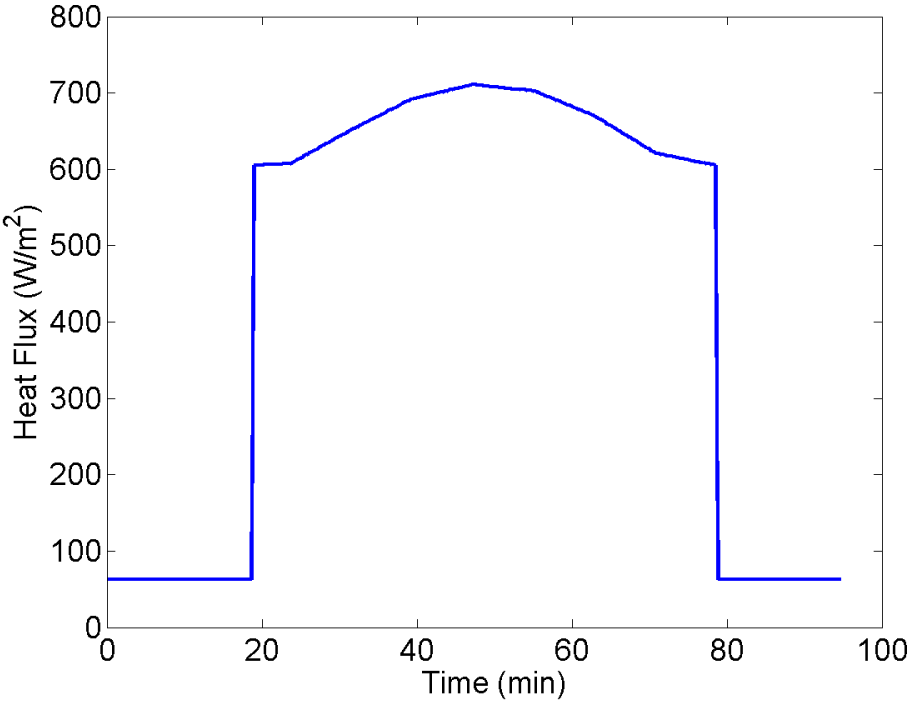

Figure 13.2: Solar Flux: Sunside

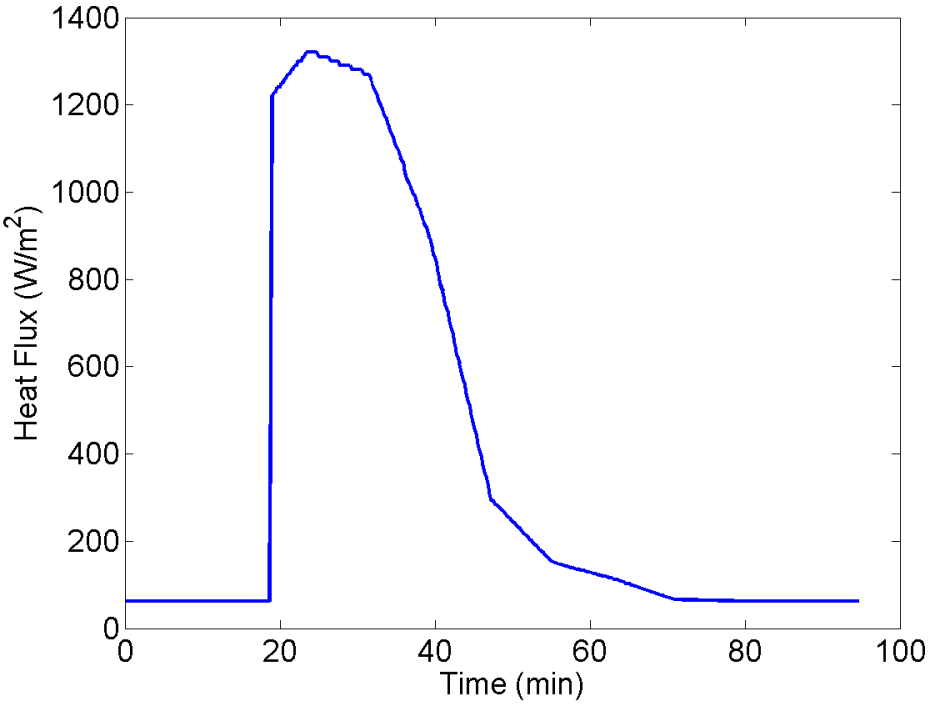

Figure 13.3: Solar Flux: Leading

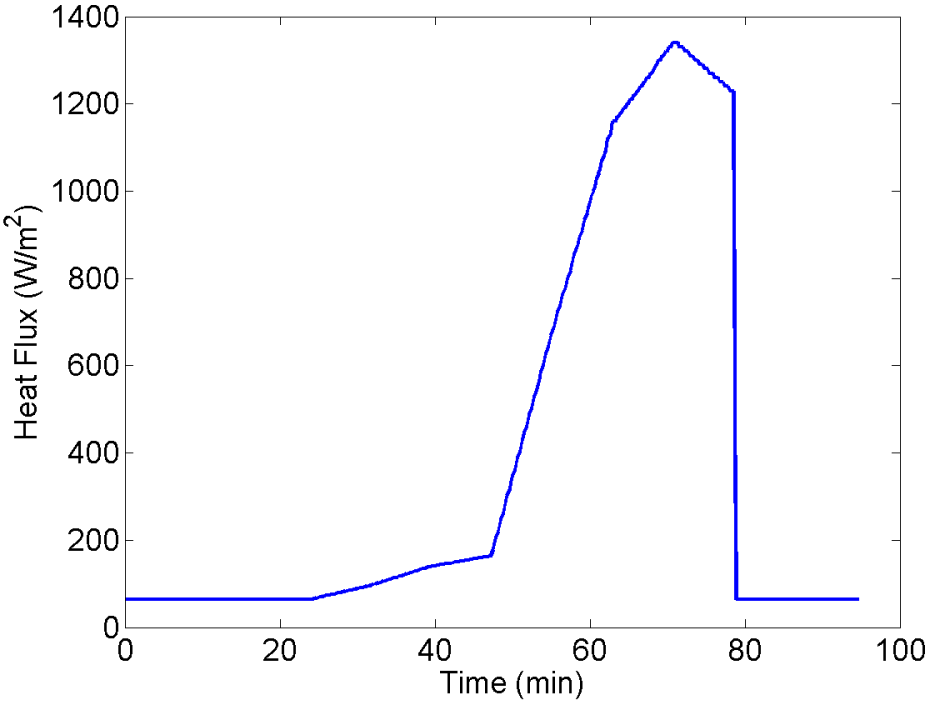

Figure 13.4: Solar Flux: Lagging

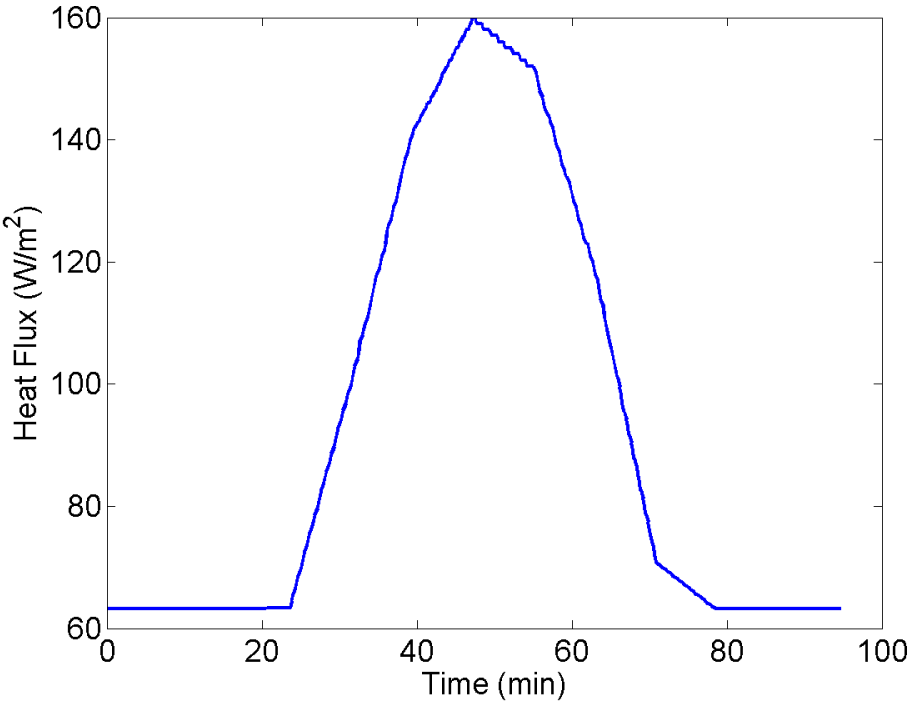

Figure 13.5: Solar Flux: Anti-Sunside

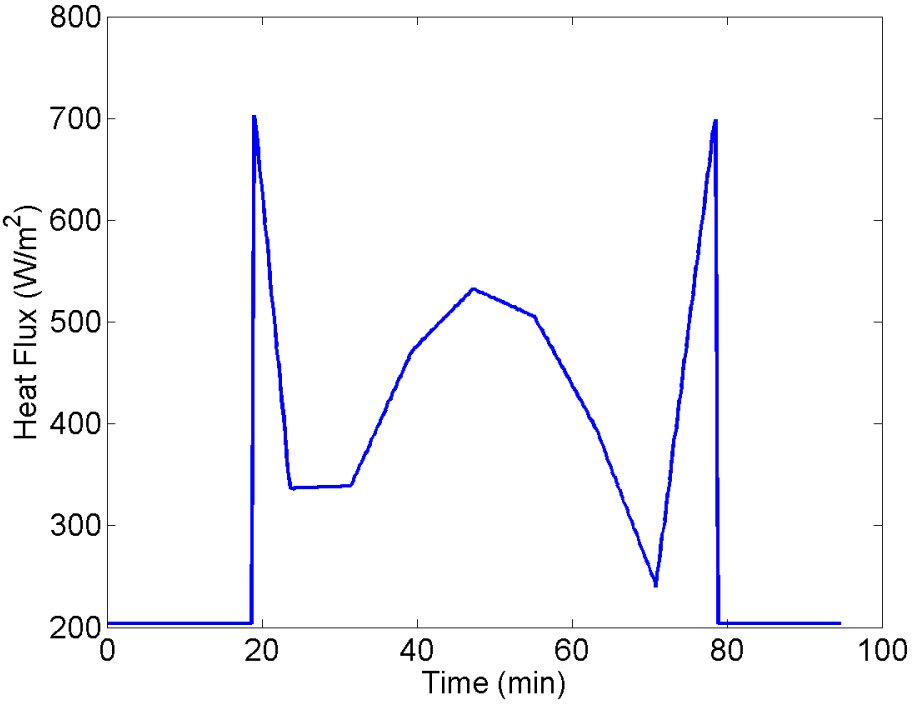

Figure 13.6: Solar Flux: Nadir

Source: NASTRAN Simulation

13.7.2 Heat dissipation from PCBs

Electrical components on the PCBs are major source of heat dissipation in the satellite. The electrical components on the PCB generate heat. We have heat dissipation data for all the PCBs which was applied as heat load on respective PCBs. Heat sinks are used on Downlink and Beacon boards for power amplifier and LNA on Uplink board as their heat dissipation is relatively more. heat table-:

PCB	**Heat dissipated(W)**
OBC	0.1425
Beacon	0.0425
Beacon Power Amplifier	1.7
Downlink	0.0836
Sun Board	0.025295
Uplink	0.14917
LNA	0.055
Magnetorquer	0.2924
GPS	2
Magnetometer	1.28
Battery Box	0.08

Table 13.2: Heat Loads: In-Orbit

Variable Heat Loads:

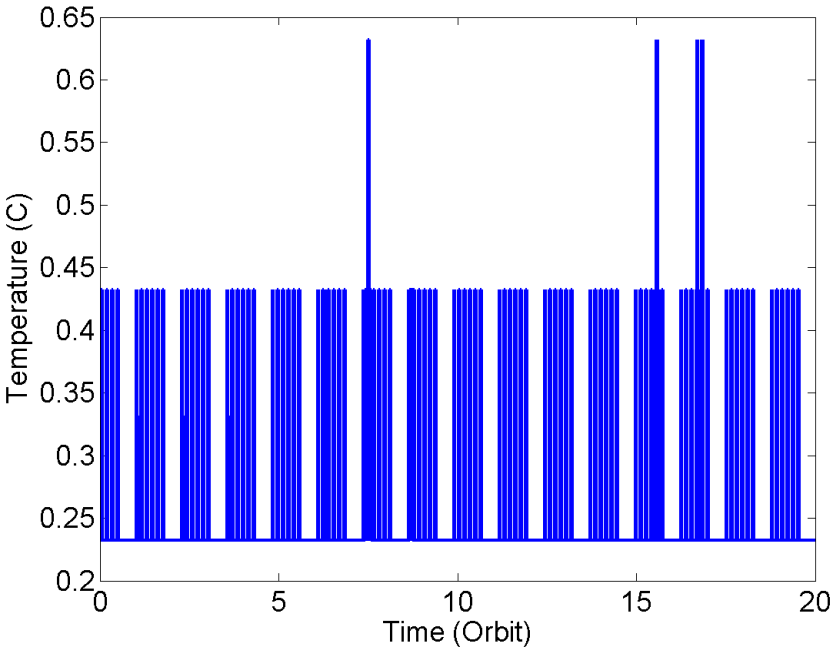

Figure 13.7: In-Orbit Heat Load: Power Board

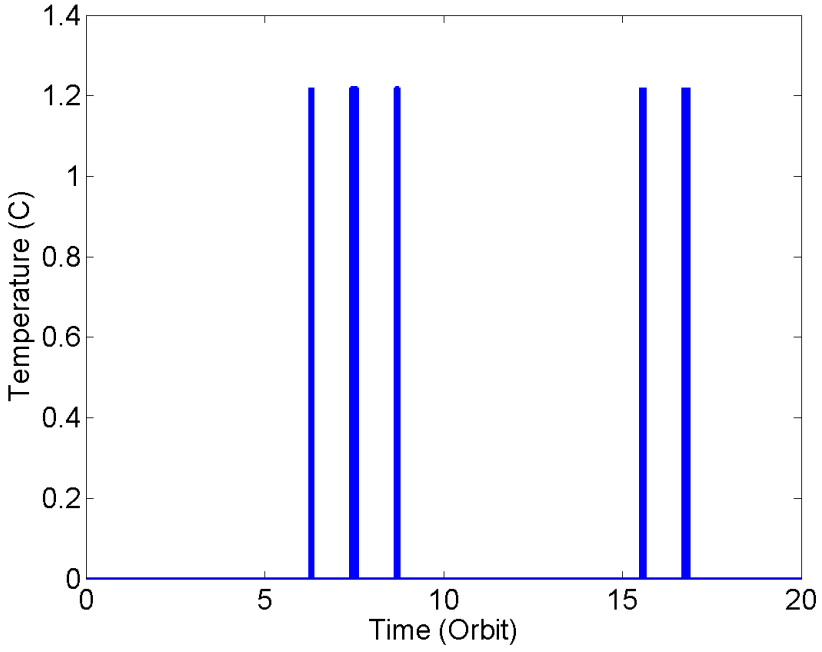

Figure 13.8: In-Orbit Heat Load: Power Amplifier on Downlink

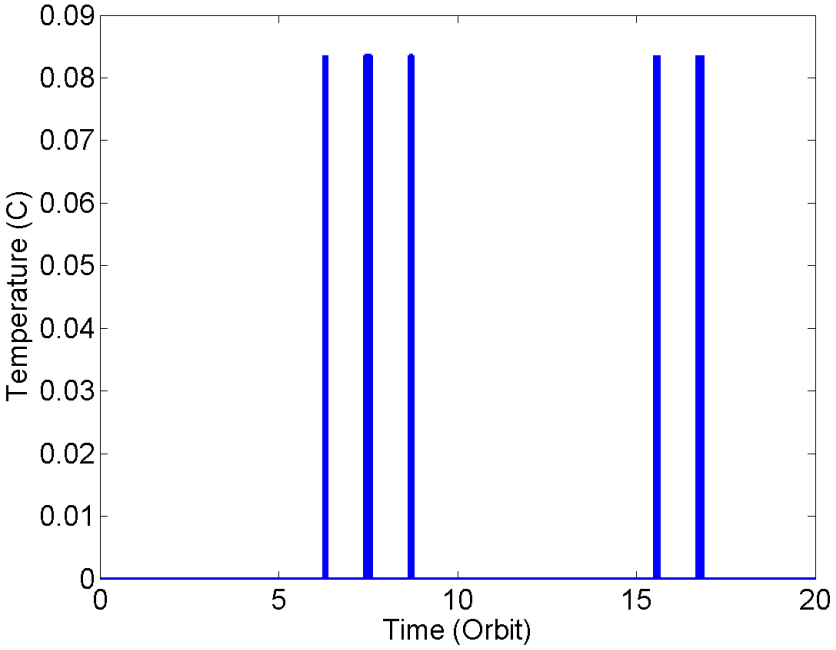

Figure 13.9: In-Orbit Heat Load: Downlink Board

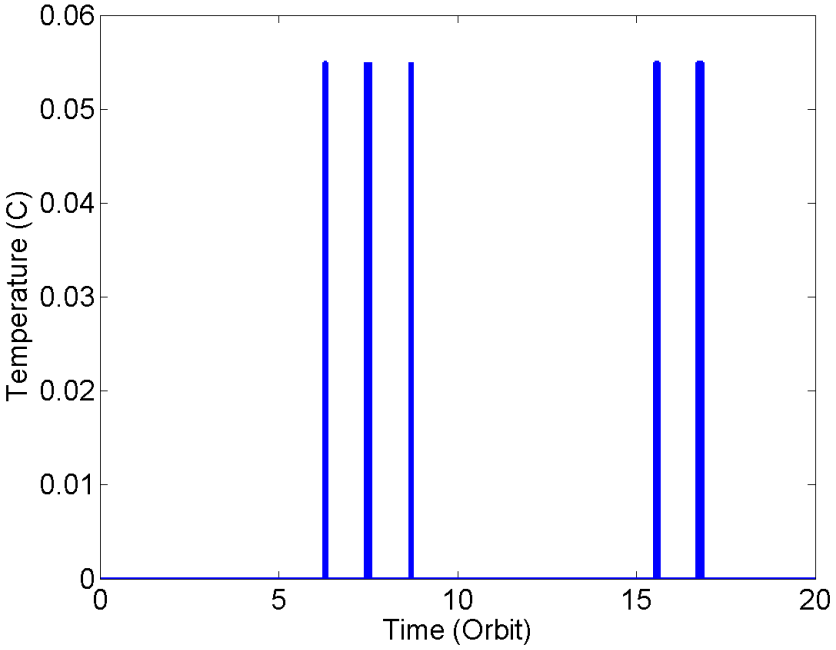

Figure 13.10: In-Orbit Heat Load: LNA on Uplink

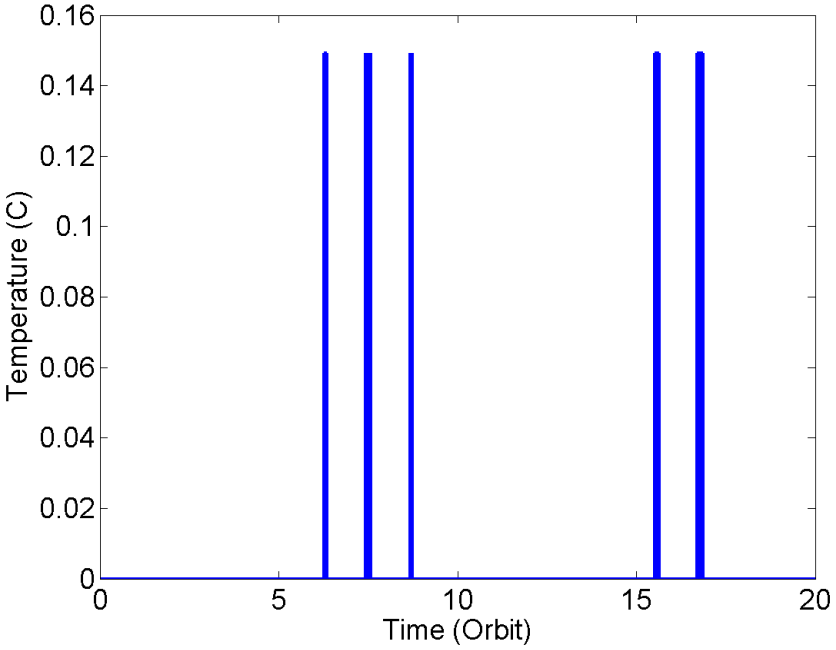

Figure 13.11: In-Orbit Heat Load: Uplink

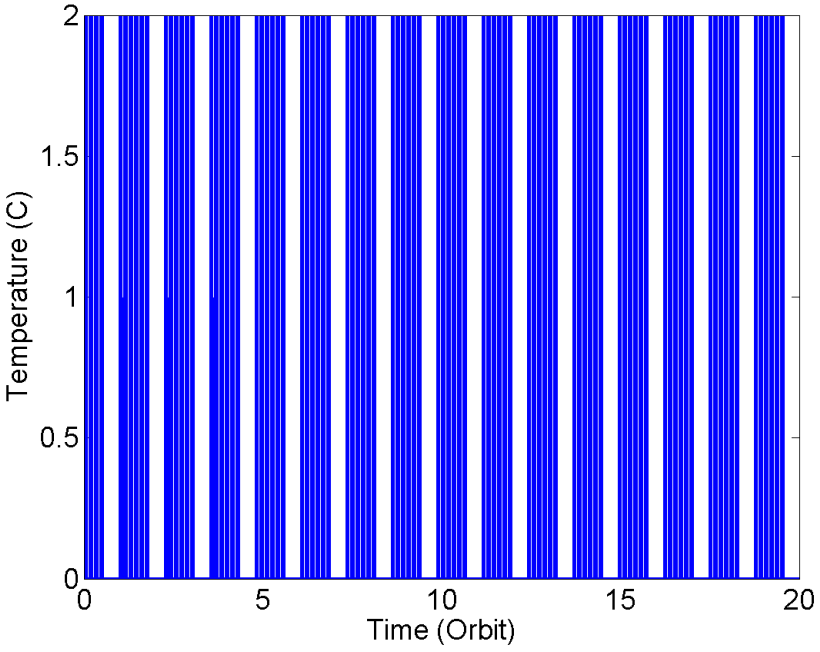

Figure 13.12: In-Orbit Heat Load:GPS Box

13.8 Internal radiation

All the surfaces inside the satellite radiate among each other due to the virtue of its temperature. Internal radiation is modeled by defining 'Enclosure Radiation' in NASTRAN. It calculates view factor and takes all the internal radiation into account.

13.9 OSR

OSR has been modeled as radiation to environment with emissivity of 0.78 on antisunside. It has been applied on entire Anti-sunside face of the satellite.

13.10 Transient Analysis

Thermal analysis has been done using NX space system thermal solver. Total 9220 elements were created after 2-D meshing of entire model. For any transient simulation, we must define the time span for the solution. In addition, we should also specify the Time Step, which is the time mesh for the solution. A smaller time step will give more accurate results at a cost of increased computation time. A time span of 20 orbits was specified for simulation. Time step of 30 second was used.

13.11 Results

The simulations are carried out based on the modeling described above. After the first round of simulations, temperatures on the various parts of the satellites were observed. After analyzing the temperature of the various parts, which parts require thermal treatment was decided. Thus, on the basis of the temperatures, we decided the thermal design that will be applied on the flight model. All the decisions related to thermal design have been stated below

- All the packages (including battery) which are mounted inside the spacecraft will be covered with black paint.
- All spacecraft panels will be black anodized from inside and covered with MLI blanket (8 layers) from outside on four sides which have solar panels on it.
- High dissipated chips (which dissipate 1W) will be placed on the Telemetry and Beacon PCB using thermal filler materials along with heat sink.
- All solar panels will be isolated from the spacecraft panels conductively and radiatively.
- All solar panels back side will be covered with low emittance tape (e = 0.05).

- GFRP Washer of thickness 3 mm is used between nadir side and battery box to reduce swirling of battery box temperature.
- OSR has been applied on entire Anti-sunside face of the satellite.
- Payload antenna consists of one holder and one monopole. Total three antennas are mounted on the spacecraft anti sun side panel.

13.12 Max and Min temperatures of different components

Following are the results of simulation done for 20 orbits for altitude of 500 km. Temperature has been given after initial fluctuation in temperature has stabilized, starting from initial temperature of 20^0C.

SI. No.	Components	Min (^{0}C)	Max (^{0}C)
1	Zenith Solar Panel	-49.9	65.3
2	Sunside Solar Panel	-43.0	32.5
3	Leading Solar Panel	-95.7	-18.6
4	Lagging Solar Panel	-92.8	-8.6
5	Zenith MLI	-47.0	64.7
6	Sunside MLI	-40.8	32.3
7	Leading MLI	-88.5	-46.8
8	Lagging MLI	-86.6	-40.0
9	Zenith Side Panel	16.9	18.6
10	Sunside Side Panel	19.7	21.9
11	Leading Side Panel	18.2	20.2
12	Lagging Side Panel	19.0	21.1
13	Nadir Side Panel	23.8	29.3
14	Anti-Sunside Side Panel	13.4	15.3
15	Power Board	20.6	23.2
16	OBC Board	19.2	20.9
17	ADC Board	18.8	20.4
18	Uplink Board	19.4	21.7
19	Downlink Board	17.4	19.9
20	Beacon Board	18.0	19.8
21	LNA on Uplink Board	17.6	19.7
22	Power Amplifier on Downlink Board	13.8	19.4
23	Power Amplifier on Beacon Board	22.5	24.2
24	Uplink Board below LNA	17.6	19.7
25	Beacon Board below Heat Sink	22.3	24.0
26	downlink Board below Heat Sink	13.8	19.3
27	Battery Box	22.4	24.2
28	GPS	16.6	18.3
29	Magnetometer	20.2	22.3
30	Magnetorquer on Zenith	17.7	19.6
31	Magnetorquer on Sunside	18.8	20.9
32	Magnetorquer on Leading	18.9	21.1
33	Monopoles	12.3	13.8

Table 13.3: In-Orbit Temperature: 500 km

13.13 Inferences

- Solar panels have high temperature fluctuations due to presence of the highly fluctuating solar flux incident on them.
- Exposed part of MLI on zenith side has higher temperature than MLI on other sides

because it faces direct solar radiation.

- Exposed part of MLI on zenith side has its maximum temperature greater than solar panel on the same side because solar panel is connected with side panel through screws (conductivity=16.2 W/m-K) for conduction purpose. Whereas, though MLI is in contact with side panel, its conductivity (0.05 W/m-K) is negligible. Also, emissivity of MLI (e = 0.45) is less than that of solar panel (e = 0.85).
- Solar panels have been isolated from the satellite sides both conductively and radiatively, so that the fluctuation in solar panels does not get reflected in the satellite body.
- Very less temperature variation ($\sim 6\ ^0$C) for internal components including PCBs is observed.
- Satellite body temperature has less variation over the orbit.
- Temperature of electrical components and battery box is within the range of operating temperature.

So, it has been concluded that all components are within their required temperature range.

Screenshot from simulations:

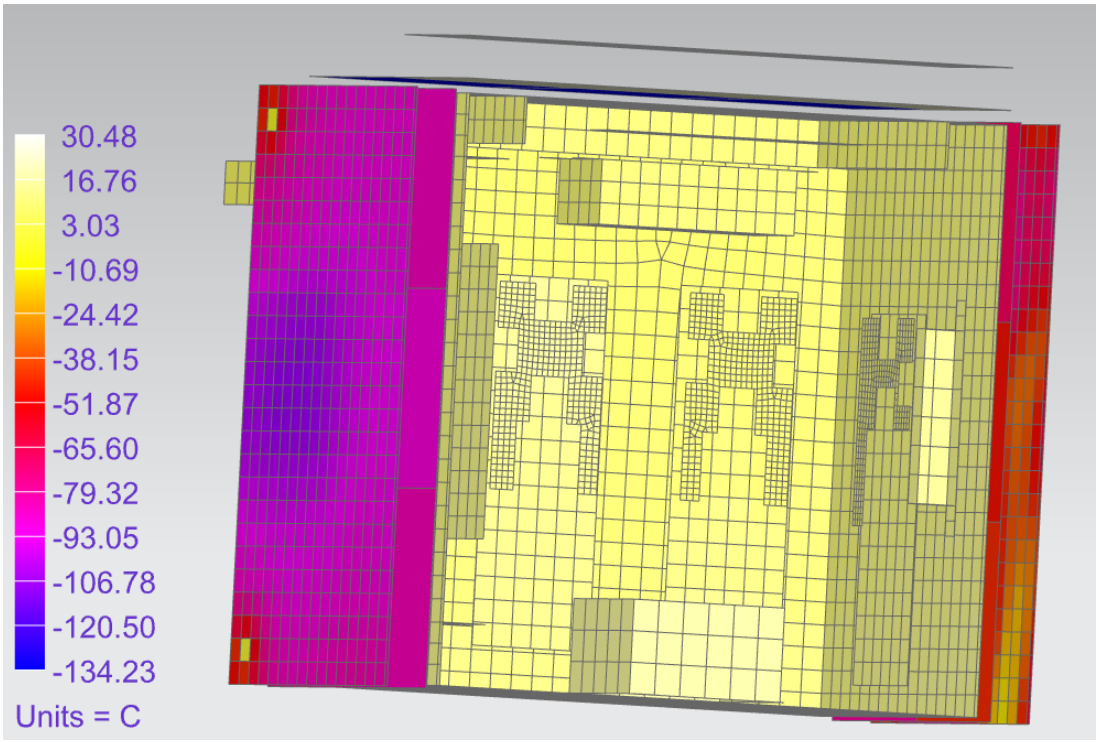

Figure 13.13: Solar panel and monopole temperature after 20 orbits for altitude: 500km

13.14 Temperature Plots for important components

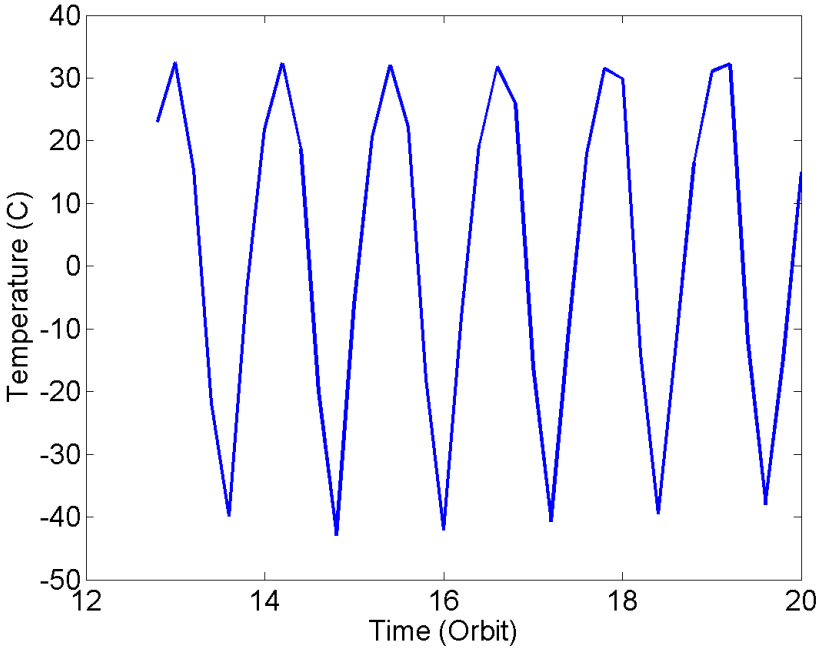

Figure 13.14: Temperature variation: Sunside solar Panel

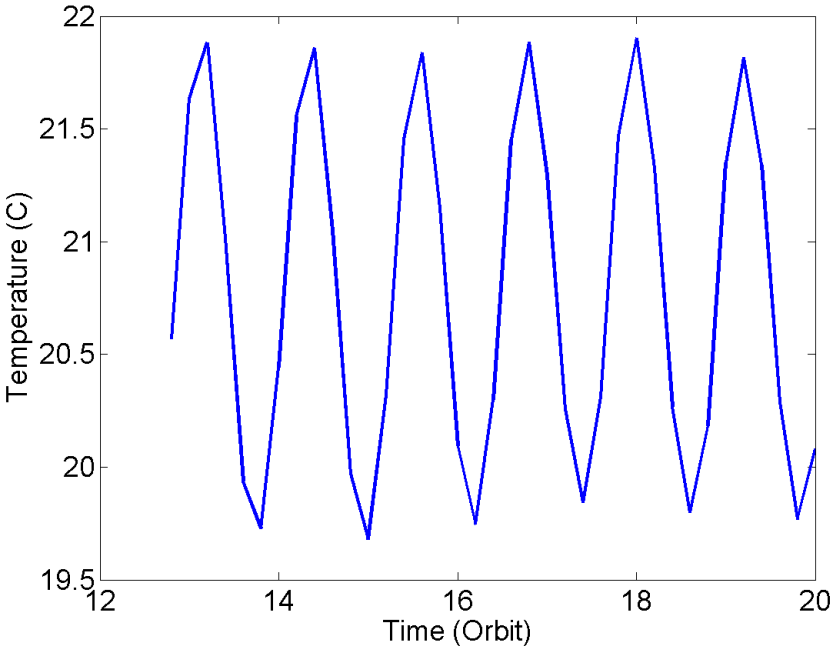

Figure 13.15: Temperature variation: Sunside Side Panel

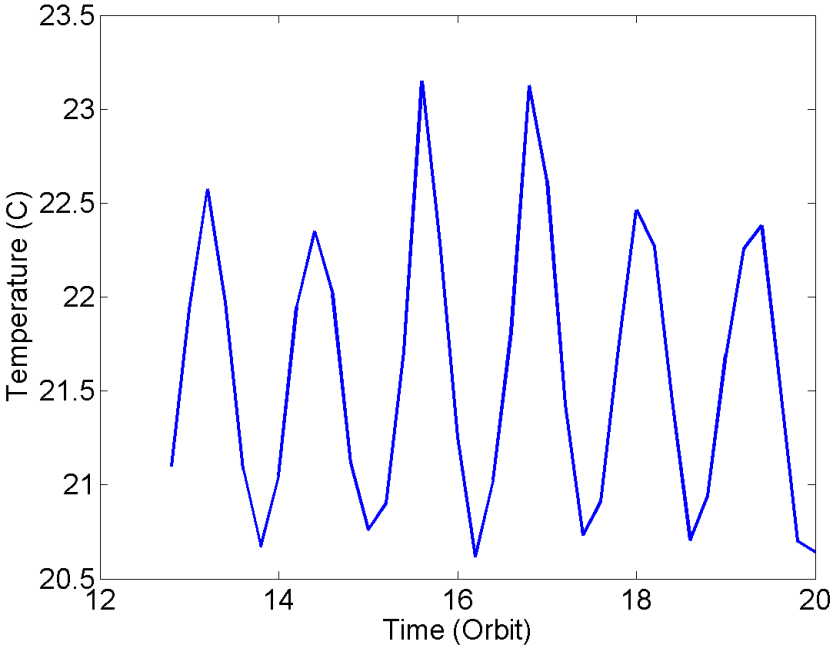

Figure 13.16: Temperature variation: Power Board

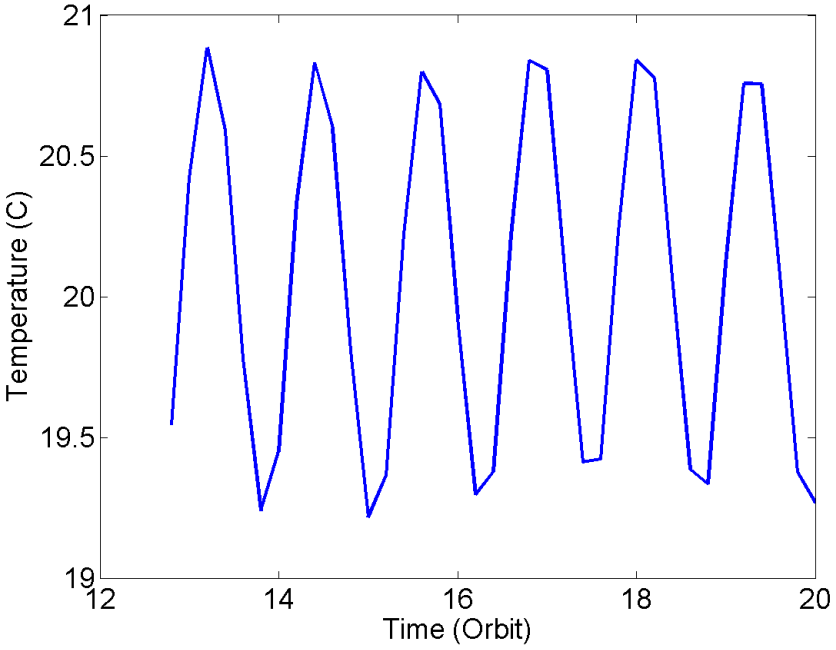

Figure 13.17: Temperature variation: OBC Board

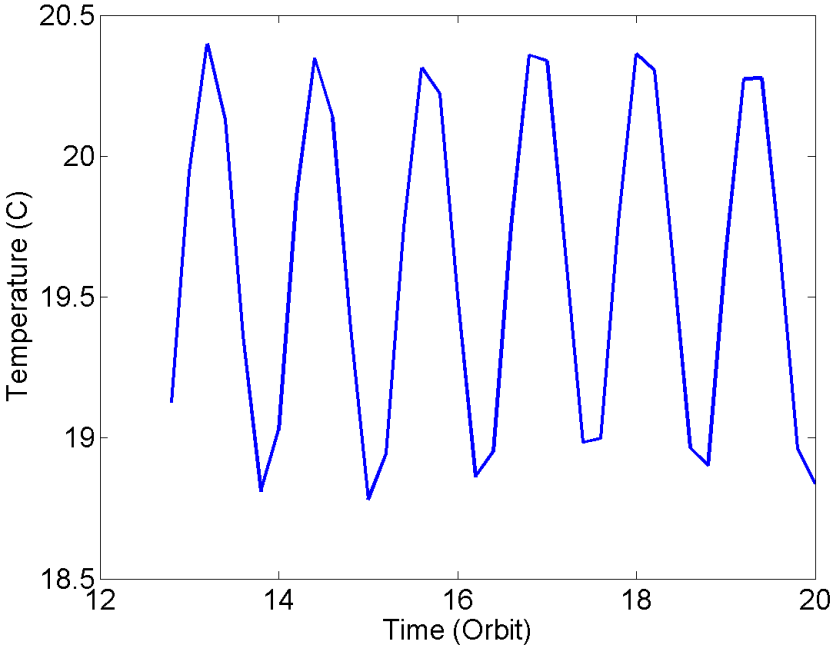

Figure 13.18: Temperature variation: Sunsensor Board

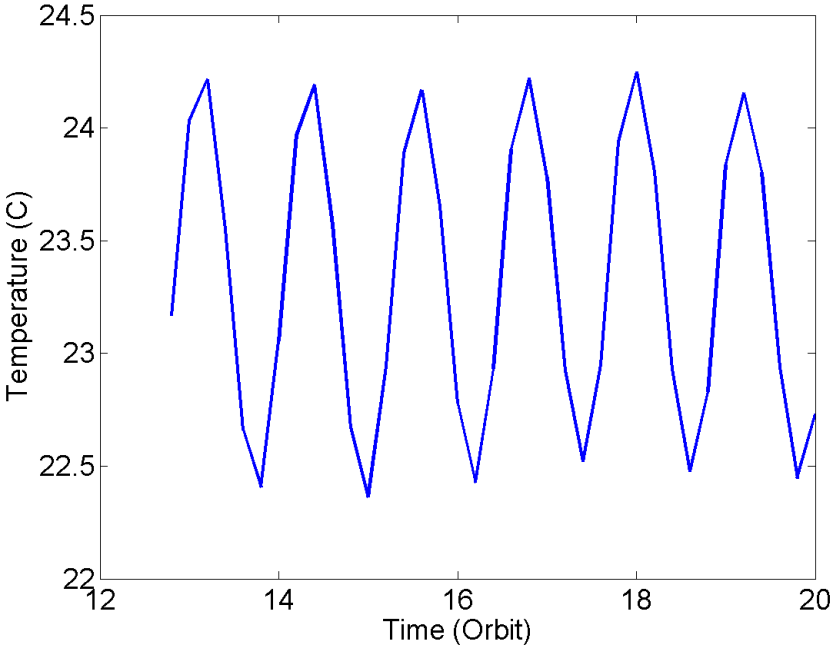

Figure 13.19: Temperature variation: Battery Box

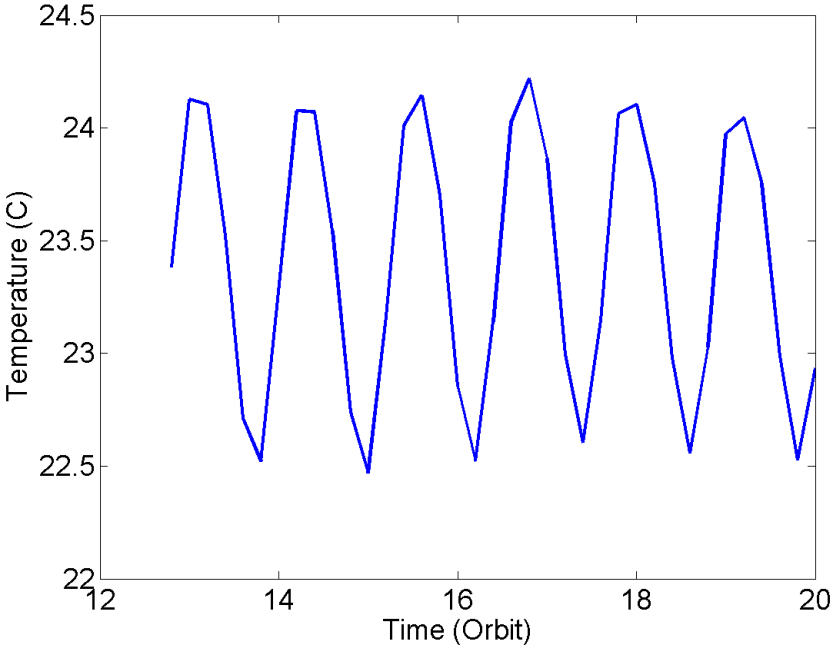

Figure 13.20: Temperature variation: Power Amplifier on Beacon Board

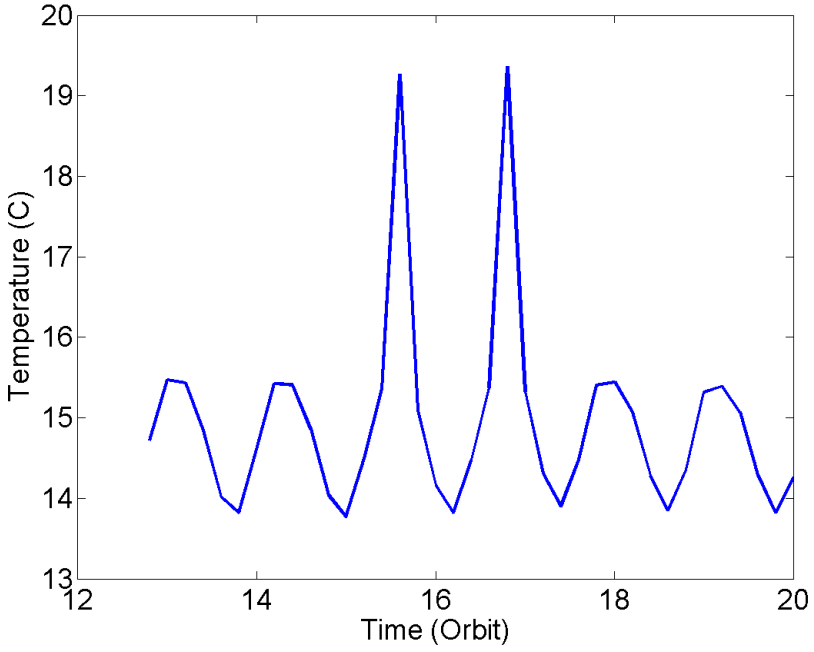

Figure 13.21: Temperature variation: Power Amplifier on Downlink Board

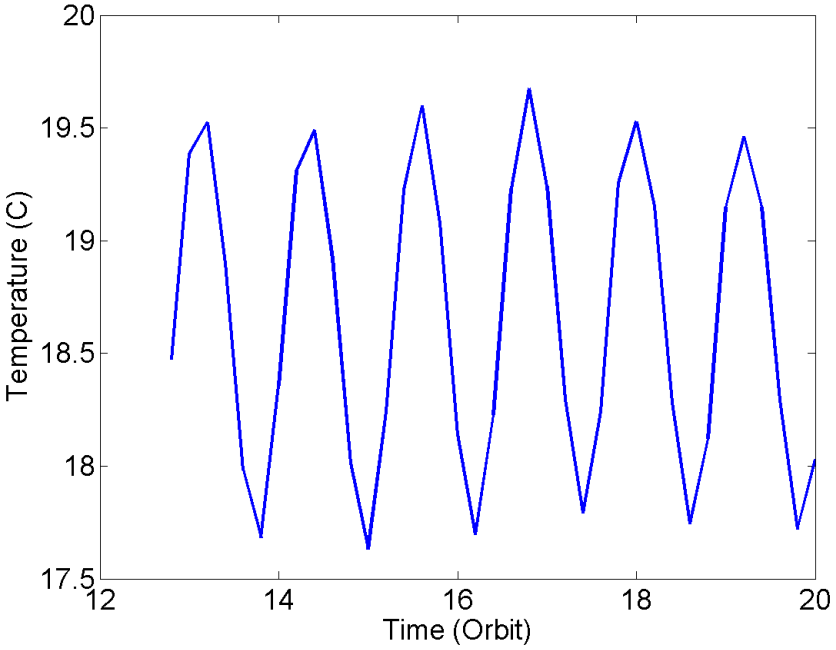

Figure 13.22: Temperature variation: LNA on Uplink Board

Chapter 14

Vibration Testing

14.1 Introduction

The Vibration testing for Qualification model of Pratham was done at ISAC from 5th to 6th November, 2015 under the guidance of scientists Ram Kumar Sir and Kulkarni Sir. The satellite had undergone a sequence of testing for all 3 directions with qualification level loads. Vibration testing aims to test and validate the satellite structural design against PSLV loads. We started preparation for the vibration testing setup from 28th October. We did the satellite integration on 1st and 2nd November. The fixture was fabricated for the interface between the satellite and shaker table. The fixture testing was done separately on 28th October to get the fixture response.

14.2 PSLV Load Requirements

The following section details the requirements imposed on the Structural Subsystem by the other subsystems of the satellite and the constraints under which the Structural Subsystem needs to design the satellite. It gives a broad look at the various tasks handled by the subsystem and their significance in the overall scheme of the satellite.

14.3 Launch Vehicle Placement Requirements

The satellite is launched into Low Earth Orbit by the Polar Satellite Launch Vehicle. The launch vehicle interface to be used is the IBL230V2, to be provided by VSSC.

1. Launch vehicle interface requires 8 no's M6x1, 9mm long helicoil inserts at 230mm PCD on bottom deck of the satellite.

2. There should not be any interference in the joint from the satellite to the launch vehicle body.

14.4 Launch Loading Requirements

The satellite is carried to its orbit by a launch vehicle in a flight lasting about 17 minutes. During this period, the vehicle experiences high levels of acceleration, vibrations and shocks which are transmitted to the payloads attached to the flight decks of the vehicle. Launch loads experienced include static loads, vibration loads, acoustic loads and shocks and impose certain strict requirements on the structure of the satellite. Satellite structure should be able to withstand these loads during launch. All the components should be safe and working after the launch. The loading specification for which the launch vehicle interface is tested is assumed to be the loading data for the satellite during launch.

14.4.1 Static Loading

Static loading occurs on the satellite during launch as a result of the accelerations experienced during flight. The static loads that are used for testing verify the design and ensure that structure meets the safety margins are as listed in Table 14.1.

Direction	**Loading**
Longitudinal	3.5g Tensile, 7g Compressive
Lateral	6g Tensile/ Compressive

Table 14.1: Static Loading

Lateral loads are considered to act simultaneously with longitudinal loads. All loads apply at every element of the satellite as body forces.

14.4.2 Harmonic Loading

The levels defined for qualification and acceptance in the sinusoidal vibration sweep test are as given in table 14.2. The satellite is tested in conjunction with its launch interface on the shaker table. Here, the 'Qualification level' is used to prove that the structure can withstand loads, which are a factor greater than the expected flight limit loads (qualification loads), while the 'Acceptance level' is used to discover production deviations, not discovered during inspection. The applied loads are equivalent to the flight limit loads.

	Frequency range(Hz)	**Qualification level**	**Acceptance level**
Longitudinal axis	(i)5-8	34.5 mm(DA)	23 mm (DA)
	(ii) 10-100	4.5g	3g
Lateral axis	(i)5-8	34.5 mm(DA)	23 mm(DA)
	(ii) 8-100	3g	2g
Sweep rate		2 oct/min	4 oct/min

Table 14.2: Sine sweep tests for qualification

These levels are defined at the interface of the satellite with the deployer. The test is to be carried out along all three axes of the satellite, on the flight model.

14.4.3 Random Loading

The conditions for testing for random and acoustic vibrations are the same as that of sinusoidal vibration testing.

	Qualification	Acceptance
Frequency(Hz)	**PSD(g^2/Hz)**	**PSD (g^2/Hz)**
20	0.002	0.001
110	0.002	0.001
250	0.034	0.015
1000	0.034	0.015
2000	0.009	0.004
g RMS	6.7	4.47
Duration	2 min/axis	1 min/axis

Table 14.3: Random vibration test levels

14.5 Vibration Testing of Fixture

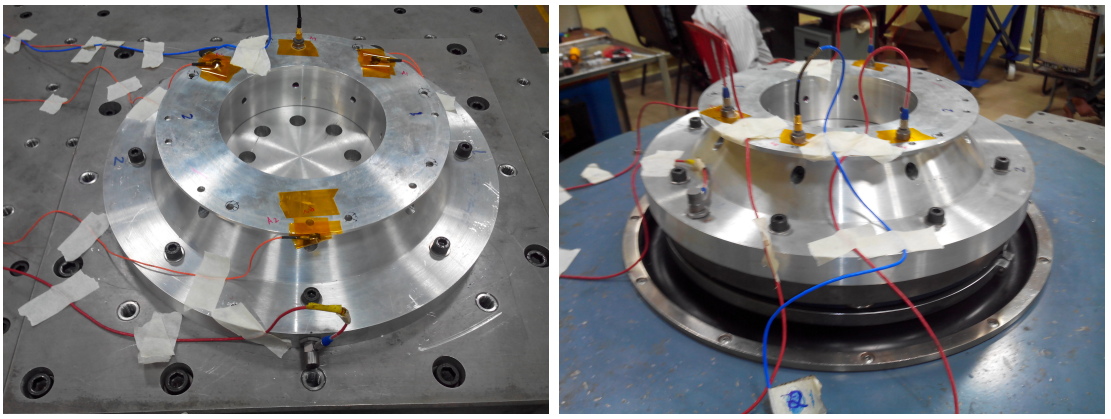

Figure 14.1: Vibration Testing of Fixture

Fixture with two rings one which will be attached to satellite nadir side and other which will be attached to shaker table is designed keeping in the point of integration difficulty during testing. Therefore the two rings will attached separately at its location and after that satellite is kept over the bottom fixture ring and screwed from sideways through M6 screws. The top ring weighs 1.08 kg and the bottom ring weighs 9.16 kg. This fixture is designed to be used only for vibration testing. The final LVI IBL230V2 will be provided by VSSC for flight model.
Note: The initial fixture drawing had some hole alignment errors which were corrected in ISRO with the help of ISRO scientists.

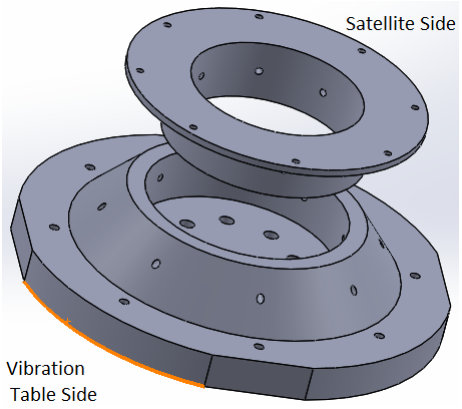

Figure 14.2: Z-direction set up

14.5.1 Testing Setup

The fixture is separately tested without satellite for low level random and sine test for two axis one for longitudinal and one for lateral. Since the fixture is symmetric only one lateral direction testing was sufficient. Four accelerometers were mounted on the top ring of the fixture and a controller mounted on the bottom bigger ring.

Testing for Z axis (longitudinal):

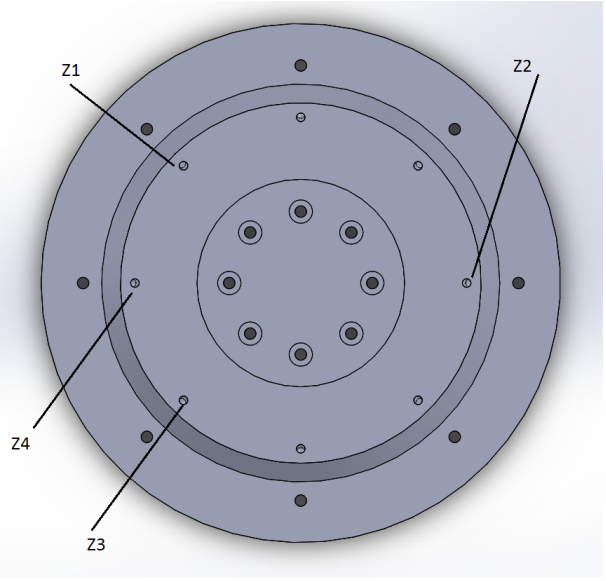

Figure 14.3: Z-direction set up

Location	Accelerometer No.	Sensitivity (mv/g(rms))	PB No.
Z1	173080	10.02	1
Z2	71672	10.12	2
Z3	169418	9.85	3
Z4	169432	9.81	4
Control on Fixture	71815	103.3	5

Table 14.4: Location of accelerometer for Z-direction Testing

Testing for Y axis (lateral):

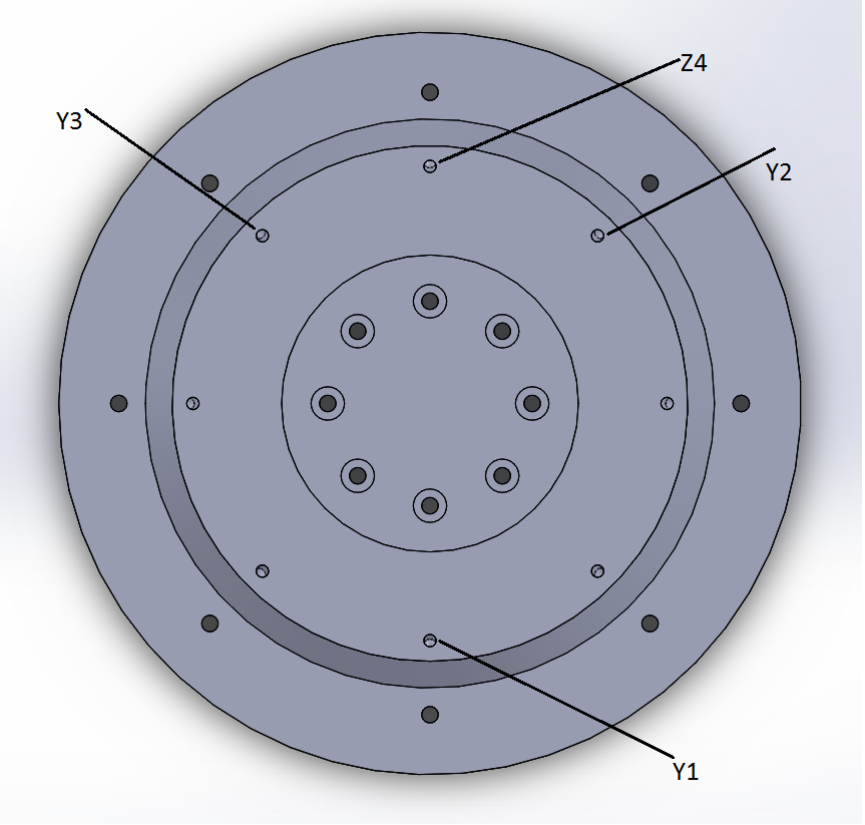

Figure 14.4: Y-direction set up

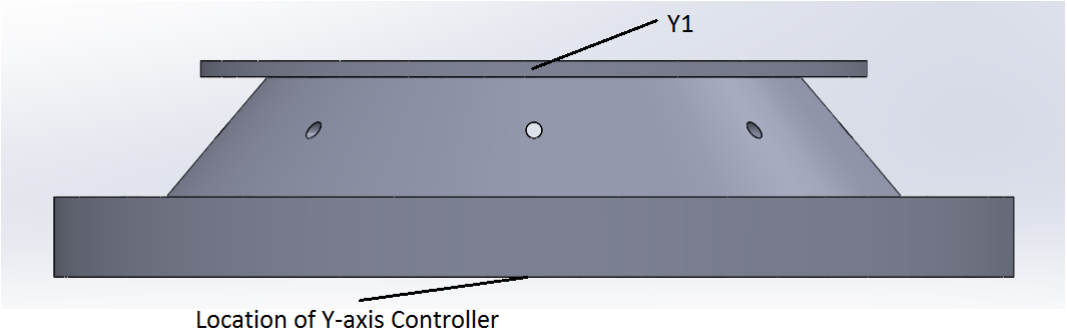

Figure 14.5: Y-direction set up

Location	Accelerometer No.	Sensitivity (mv/g(rms))	PB No.
Y1	50457	2.038	1
Y2	55398	1.867	2
Y3	55402	1.87	3
Z4	169432	9.81	4

Table 14.5: Location of accelerometer for Y-direction Testing

14.5.2 Results

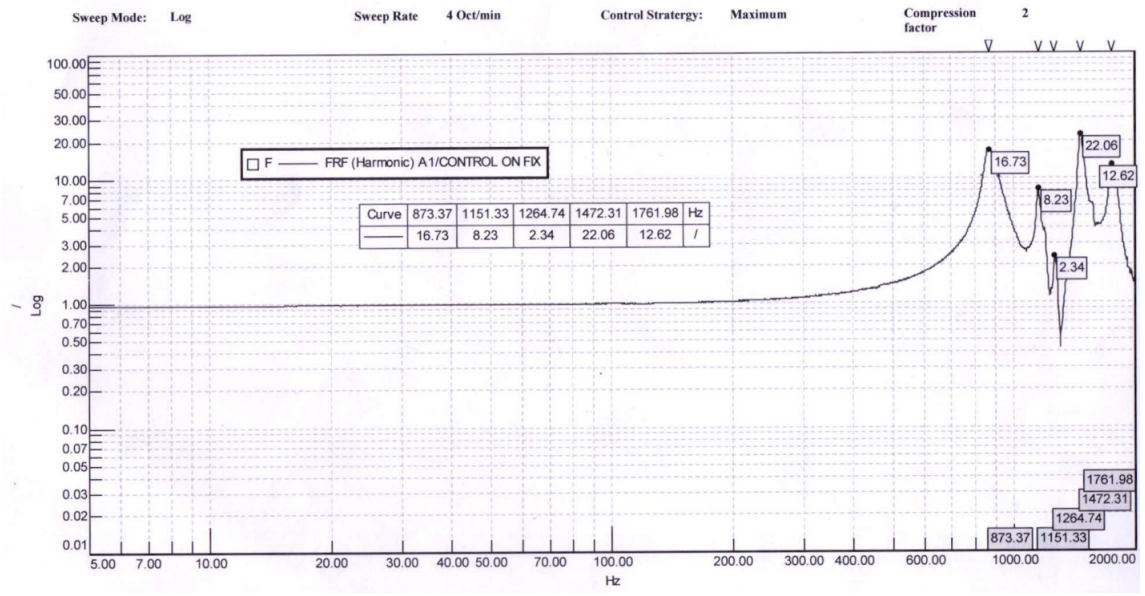

Figure 14.6: Frequency Response of Fixture during ZLLS on A1

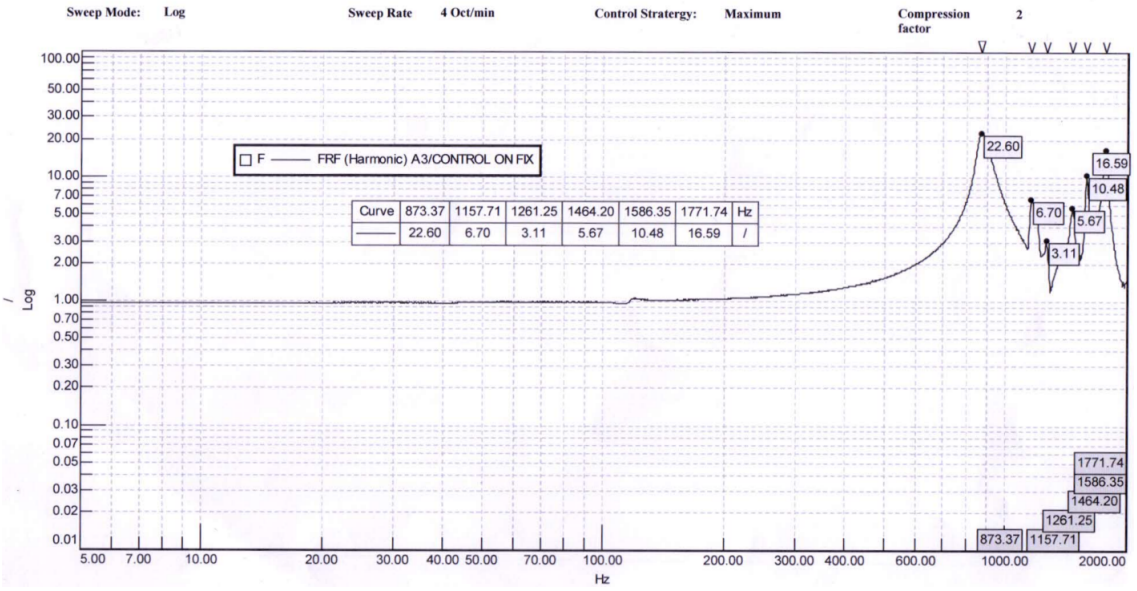

Figure 14.7: Frequency Response on Fixture during ZLLS on A3

14.5.3 Interpretation

Peak observed from both the above frequency response plot show the peak at frequency of around 873Hz. Which show the fundamental frequency corresponding to the fixture. The aim of the fixture was to transfer the load to the satellite properly. The constraints which was set to have a fundamental frequency of fixture around and above 5 times the satellite frequency which is coming around 150 Hz(satellite frequency) * 5= 750 Hz. The frequency observed is 873 Hz which shows that no frequency of fixture will resonate during the testing for the satellite.

14.6 Vibration Testing of Satellite

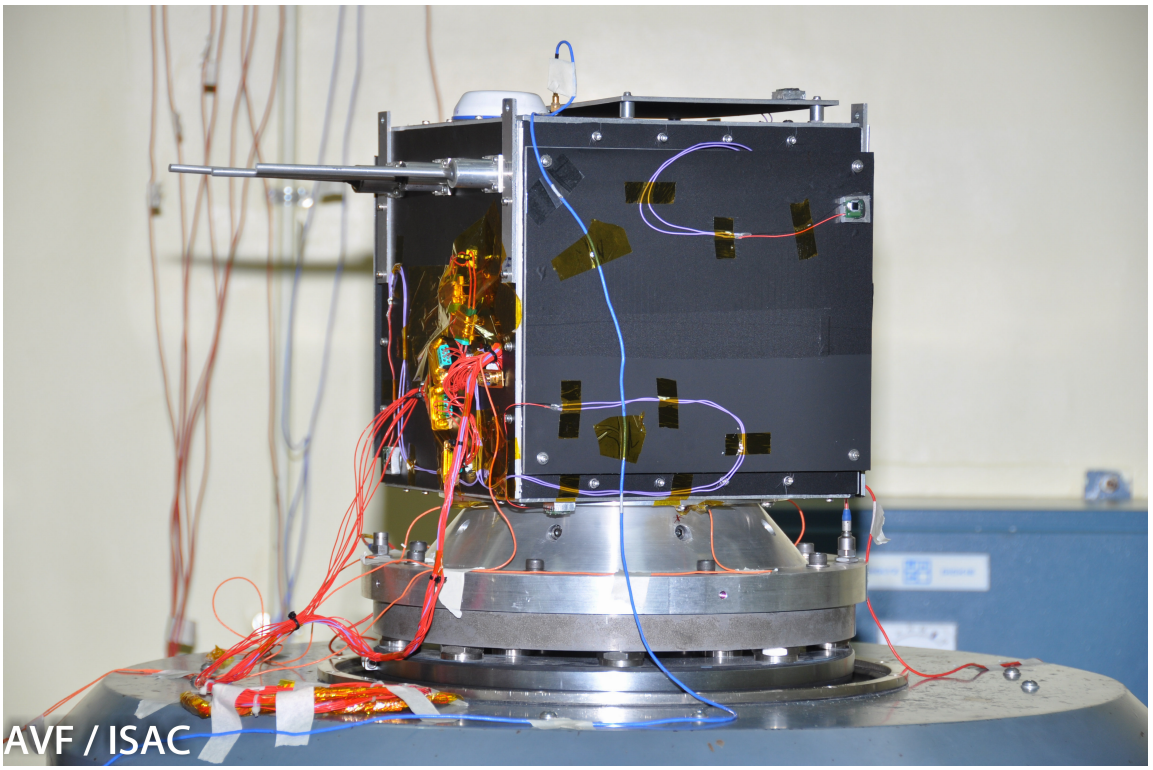

Figure 14.8: Vibration Testing of Satellite

14.6.1 Pre Vibration Functionality Check

1. Checked for torque values of all external M3, M4, M6 screws
2. Complete functionality check
3. Observations-:
   (a) Sun-side Sun-sensor was not working
   (b) Beacon signal not audible after closing with high tightening of SMA connector

14.6.2 Testing Setup

The bigger fixture ring is mounted on the shaker table. Complete integrated satellite along with the smaller LVI ring attached to the Nadir side of the satellite is mounted on it. The two rings are attached through sideways 8 M6 screws. In this way satellite is interfaced through the shaker table using fixture. Satellite is then separately tested for all three axis, one longitudinal and two lateral.
Sequence of testing:

1. Low Level Random
2. Low Level Sine
3. Qualification Level Sine
4. Low Level Sine (Post QLS)
5. Low Level Random (Post QLS)
6. Qualification Level Random
7. Low Level Random (Post QLR)

Similar sequence of testing is performed for all three axis. Applied loads are Qualification level loads according to the PSLV manual.

14.6.3 Location of Accelerometers

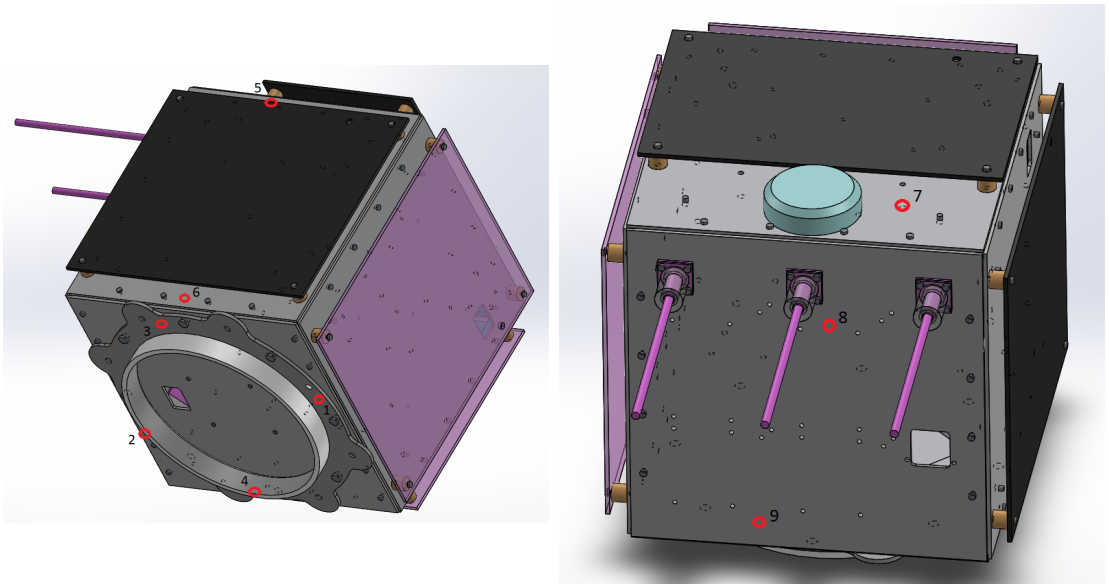

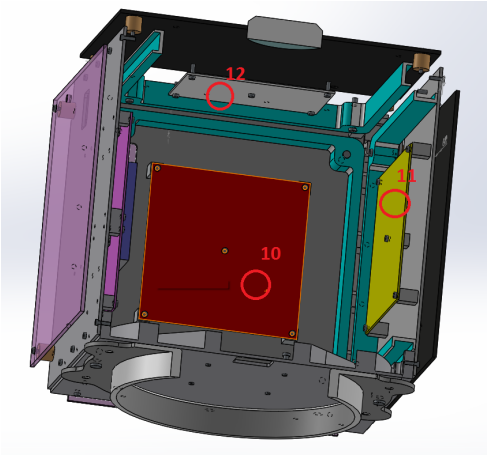

Figure 14.10: Location of accelerometer

Note: Red circles represents location of accelerometers

SI. No.	External Location	Side Name	Testing Axis
1	FE Ring (towards Sunside)	Nadir	X,Y and Z
2	FE Ring (towards Anti-sunside)	Nadir	X,Y and Z
3	FE Ring (towards Leading)	Nadir	X,Y and Z
4	FE Ring (towards Lagging)	Nadir	X,Y and Z
5	Towards Zenith Side	Leading	X
6	Towards Nadir Side	Leading	X
7	Near GPS Antenna	Zenith	Y
8	Below Monopoles	Anti-sunside	Z
9	Towards Nadir side	Anti-sunside	Z
	Internal Location		
10	Power Board	Sunside	X,Y and Z
11	OBC Board	Leading	X,Y and Z
12	ADC Board	Zenith	X,Y and Z

Location of Accelerometer	Accelerometer No.	Model No.	Sensitivity	P.B. No.	Direction of testing
ADC Board	61246	4517002	10.25mv/gm	6	X,Y,Z
Power Board	61239	4517002	10.2mv/gm	7	X,Y,Z
OBC Board	61229	4517002	10.21mv/gm	8	X,Y,Z
On fixture near leading side	55402	4517C003	1.87pc/gm	1	X,Y,Z
On fixture near anti-sunside	61248	4517002	10.51mv/gm	2	X,Y,Z
On fixture near lagging side	50457	4517C003	2.038pc/gm	3	X,Y,Z
On fixture near sunside	61269	4517002	10.05mv/gm	4	X,Z
Zenith side	71672	352C43	10.12mv/gm	9	Z
Control on fixture	71805	352C33	102.3mv/gm	5	Z
Control on fixture (sunside)	2015821	8704B500	9.838mv/gm	10	Z
Control on fixture (lagging)	2014938	8704B500	10.28mv/gm	5	Y
Leading side top	139248	352C43	9.894mv/gm	New PB	Y
Leading side bottom	71672	352C43	10.12mv/gm	9	Y
Anti-sunside bottom	139248	352C43	9.894mv/gm	New PB	X
anti-sunside top	71672	352C43	10.12mv/gm	9	X
control on fixture (sunside)	2014938	8704B500	10.28mv/gm	5	X
control on fixture (anti-sunside)	2015821	8704B500	9.83mv/gm	10	X
On fixture near sunside	50457	4517C003	2.038pc/gm	3	X

Table 14.6: Details of Accelerometer Used during Vibration Testing

The accelerometer mounted at 7-8 different locations during the vibration testing. When testing is in Longitudinal direction accelerometer mounted on Zenith side and when in lateral direction 2 accelerometer mounted on the corresponding side panel (Leading in X direction and anti-sunside in Y direction). 3 accelerometer mounted inside the satellite on 3 PCB cards OBC,ADC,Power on three mutually perpendicular directions. Controller is also mounted on the bottom bigger fixture ring. Accelerometer mounted on the power card was not working during the testing done for Y axis. Therefore the results interpreted for Y direction testing is only through accelerometer response which are mounted on anti-sunside.

14.6.4 Post Vibration Functionality Check

1. Checked for torque values of all external M3, M4 screws
2. For torque value of 0.6 0.8 N-m: Slight rotation in Solar Panel Screw
3. Completed functionality check : Sensors, Actuators, Telemetry, Uplink reset, Beacon
4. Observations: Sun-side Sun-sensor was not working
5. Visual inspection done after opening Lagging side panel to remove accelerometers mounted inside

14.6.5 Results

Note: All the vibration testing results are documented in environmental testing report.

Interpretation

Sr. No.	Test	Input	Observations
1	LLR	0.5 g rms	1st global mode 170 Hz
2	LLS	0.5 g	1st global mode 136 Hz
3	QLS	4.5 g (Z) & 3.5g (X,Y)	Sustained load 4.5 g, notching done near 87 Hz
4	LLS	0.5 g rms	No Signature difference from previous LLS
5	LLR	0.5 g rms	No Signature difference from previous LLR
6	QLR	Profile acc. to PSLV loads	High amplitude peak at ADC tray and Zenith side around 170 Hz
7	LLR	0.5 g rms	No Signature difference from previous LLR

Table 14.7: Observations in Longitudinal Axis (**Z**)

Sr. No.	Test	Input	Observations
1	LLR	0.5 g rms	1st mode 97 Hz(X), 82 Hz(Y)
2	LLS	0.5 g	1st mode 92 Hz (X), 76 Hz(Y)
3	QLS	3.5g	Sustained load at 3.5g
5	LLS	0.5g	No Signature difference from previous LLS
4	LLR	0.5 g rms	No Signature difference from previous LLR
5	QLR	Profile acc. to PSLV loads	Peak around 178 Hz
6	LLR	0.5 g rms	No Signature difference from previous LLR

Table 14.8: Observations in Lateral Axis (**X and Y**)

Conclusion

Direction of Testing	Modal Frequency from Testing	Modal Frequency from Simulation
X (leading to Lagging)	84	122
Y (Antisun to Sunside)	95	150
Z (Nadir to Zenith)	172	187

Table 14.9: Frequency Comparison between Testing and Simulation

Integrity is established by-:

1. Signature comparison done for all response
2. External mechanical inspection done
3. Performance test successfully checked

Chapter 15

Thermo-vacuum Testing

15.1 Introduction

Thermovac testing for Qualification model of Pratham was done at ISAC from 9th November to 11th November under the guidance of scientists Khened Sir, Ramachandran Sir, Ram kumar Sir and Harish Sir. Thermovac testing aims to test and validate the thermal deign and components sustainability for thermal loads during orbiting of satellite. The satellite has undergone three transient thermal cycles followed by cold soak and hot soak of 3 hrs. The complete testing runs for 37 hours. Battery (for lower side temperature) and the Power amplifier on beacon (for higher side temperature) were the critical components for deciding the thermovac profile.

15.1.1 Testing Environment

- Pressure of the chamber: $< 10^{-5}$ mbar
- Lower temperature limit: -5C on the battery
- Upper temperature limit: +55C on the Power Amplifier of the beacon board
- Rate of change of temperature: 1C/minute

During thermovac testing 16 thermistors and 6 thermocouples were used. Thermocouples were provided by ISAC while thermistors were brought by PRATHAM team. Out of 16 thermistors, 12 thermistors are mentioned in the table 15.1. Rest of the 4 thermistors were placed at the location of thermistors: T1, T2, T3 and T4. The data coming out of these thermistors was received at house-keeping telemetry.

SI. No.	Thermistor	Thermistor Location
1	T1	Battery
2	T2	Downlink
3	T3	Beacon
4	T4	Uplink
5	T5	PTH-1
6	T6	PTH-2
7	T7	PTH-3
8	T8	PTH-4
9	T9	Solar Panel (Sunside)
10	T10	Solar Panel (Lagging)
11	T11	Solar Panel (Zenith)
12	T12	Solar Panel (Leading)

Table 15.1: Location of Thermistors

SI. No.	Channels No.	Location
1	1	FE Ring (Lagging Side)
2	2	Anti-sunside Panel
3	3	Chamber Base Plate
4	4	Chamber Base Plate
5	9	Shroud Temperature
6	10	Shroud Temperature

Table 15.2: Thermocouple Location

15.1.2 Testing Sequence

- Functionality check was performed
  - Before closing the chamber
  - After closing the chamber and before de-pressurizing
- After de-pressurizing, the satellite was in OFF state till the battery temperature first reached -5C in the first thermal cycle
- After that, SNAP was done and the satellite went in sleep for further 5 minutes before turning ON
- House-keeping telemetry was kept on for most of the time till the cold soak began
- Once in the cold soak, the satellite was turned off for 2 hours till the temperature stabilized.
- After that, SNAP was done and functionality check was subsequently performed.
- After the functionality check, the satellite was again turned OFF and the temperature was increased to reach the beginning of the hot soak
- While in hot soak, the satellite was kept OFF for 2 hours for the temperature to stabilize
- After that, SNAP was done and functionality check was subsequently performed.
- After the functionality check, the satellite was again turned OFF and the chamber was allowed to reach room-temperature and was slowly pressurized
- After opening the chamber, the functionality check was performed again.

15.1.3 Functionality Check - Details

All the sensors, actuators and peripherals were monitored throughout the test. House-keeping telemetry was almost continuously ON and payload telemetry was also tested during Hot and Cold soaks (see figure 15.3). The temperature of the critical components were monitored throughout the test. We now present a brief overview of the methodology used to test the critical components/parameters:

- **Battery:**
  - Battery Voltage was continuously monitored via house-keeping telemetry
  - The Solar Panel Incoming current and the Load Consumption current were measured via house-keeping telemetry. Their difference gave the Battery charging current. Thus, in effect, the battery charging current was also continuously monitored.
  - The temperature of the battery was observed using two thermistors. The output of one thermistor was a part of the house-keeping telemetry. The output of the other thermistor was measured separately and continuously using the Data Acquisition System of National Instruments (NI-DAQ).

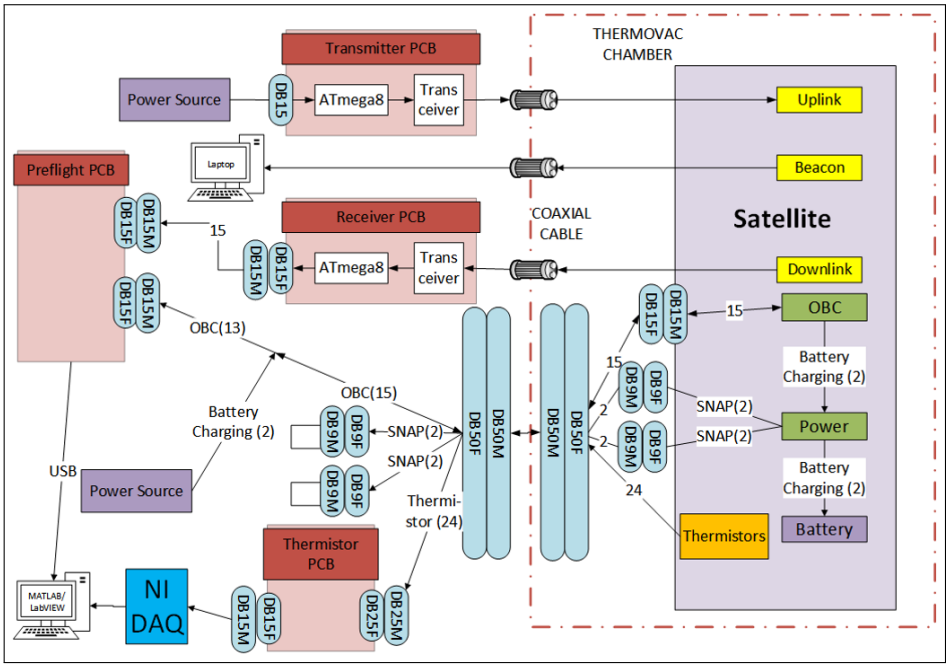

Figure 15.1: Functionality Check Schematic

- **Beacon:**
  - The gain was observed using a spectrum analyzer whenever house-keeping telemetry was kept ON.

  - The temperature of the beacon Power Amplifier (PA) was observed using two thermistors. The output of one thermistor was a part of the house-keeping telemetry. The output of the other thermistor was measured separately and continuously using NI-DAQ.

- **Downlink:**

  - The data stored in the EEPROM was transmitted via the downlink to the uplink on the receiving side. The accuracy of the data was determined by comparing it with the corresponding house-keeping telemetry.

  - The gain of the downlink was measured using a spectrum analyzer during the functionality checks in the hot and cold soaks.

  - The temperature of the downlink Power Amplifier (PA) was observed using two thermistors. The output of one thermistor was a part of the house-keeping telemetry. The output of the other thermistor was measured separately and continuously using NI-DAQ.

- **Uplink:**

  - Reset Command was sent to the satellite when the Uplink was ON and the subsequent reset of the satellite was verified using house-keeping telemetry.

  - The temperature of the uplink Low Noise Amplifier (LNA) was observed using two thermistors. The output of one thermistor was a part of the house-keeping telemetry. The output of the other thermistor was measured separately and continuously using NI-DAQ.

- **Sun-sensors:**

  - The Analog current was converted to Digital voltage and transmitted as a part of the house-keeping telemetry. The change in value on the application of a torch-light was observed both before and after the tests.

- **GPS:**

  - Transmission of data by the GPS was verified via house-keeping telemetry. The verification of data was not possible as the puck antenna of the GPS does not get give correct data indoors.

- **Magnetorquers:**

  - Command to start each magnetorquer successively for 30 seconds was given and the corresponding changes in the values of the magnetic field indicated by the magnetometer were observed

15.2 Temperature Profiles

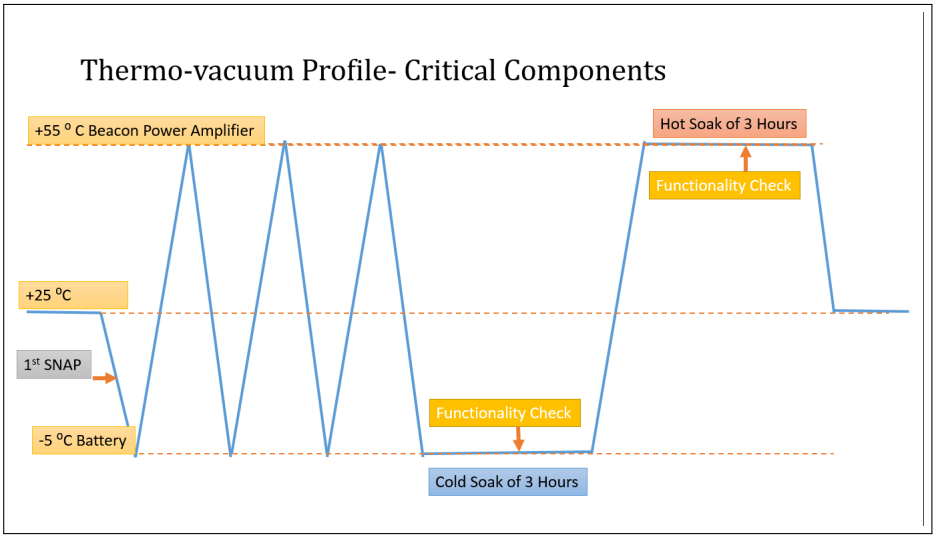

Figure 15.2: Expected Thermo-vacuum Profile

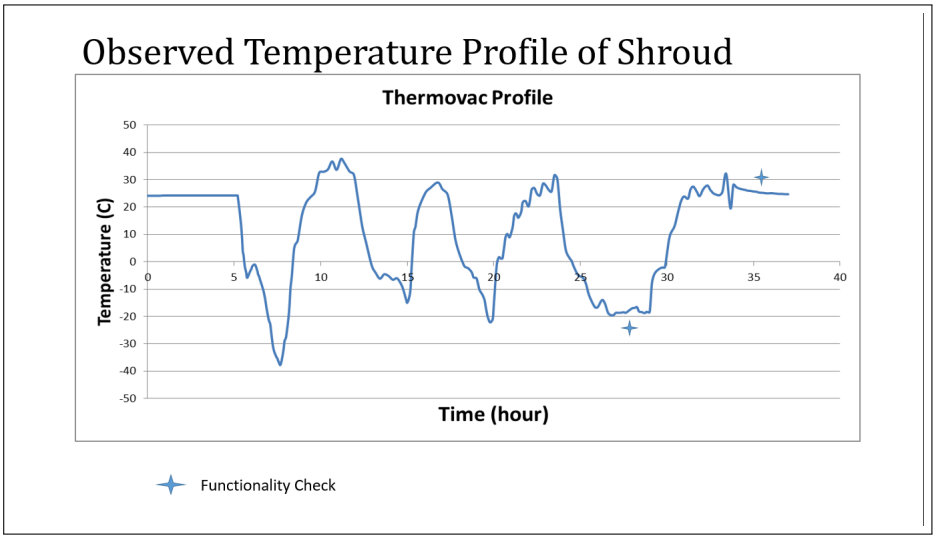

Figure 15.3: Observed Shroud Temperature Profile

15.3 Thermovac Testing Results

During thermovac testing of the satellite temperature of different components were monitored and stored. All the results are documented in environmental testing report and critical components are documented below in corresponding section.

Inference:

1. Qualification level temperatures were set having $+10/-10^0$ C to the in-orbit temperature observed.

2. All the components were tested for qualification level temperature with positive safety margin.

To compare simulation with testing, thermovac simulations were done after thermovac testing. In which, thermovac chamber along with base plate on which satellite is placed were modeled. Heat exchange between satellite, thermovac chamber and base plate has been taken into account. Thermovac profile for simulation is same as temperature profile used for testing.

Model used for Thermovac Simulation:

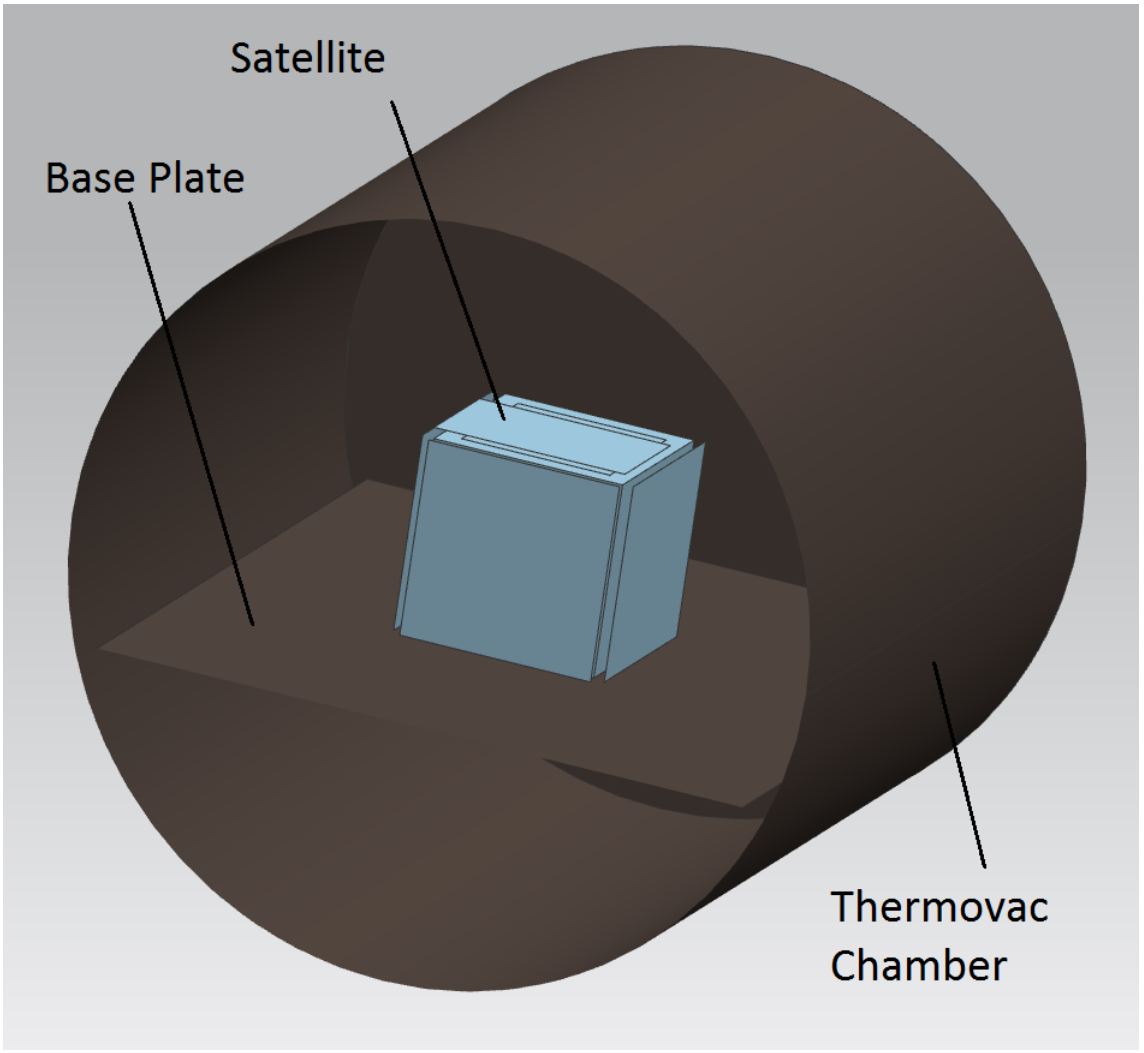

Figure 15.4: Section View: Satellite inside Thermovac Chamber

Dimension of Chamber: length = 1.2 m and Inner diameter = 1 m.

Using new model, two new thermovac simulations were done:

1. First simulation has been done for 7.38 hours. It starts from the time when testing was started and then calculated temperature for next 7.38 hours. Heat dissipation for electrical components has been applied according to actual testing. Temperature profile used for this simulation:

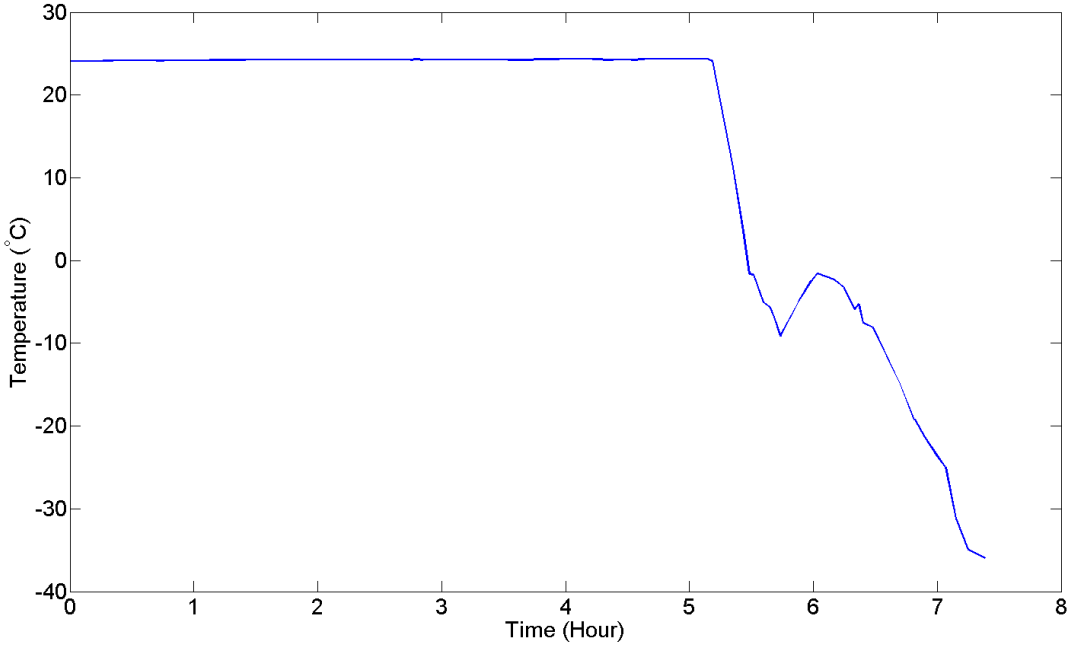

Figure 15.5: Temperature Profile used for simulation: first 7.38 hours of testing

Comparison of Plots Obtained from Thermovac Simulation and Testing:

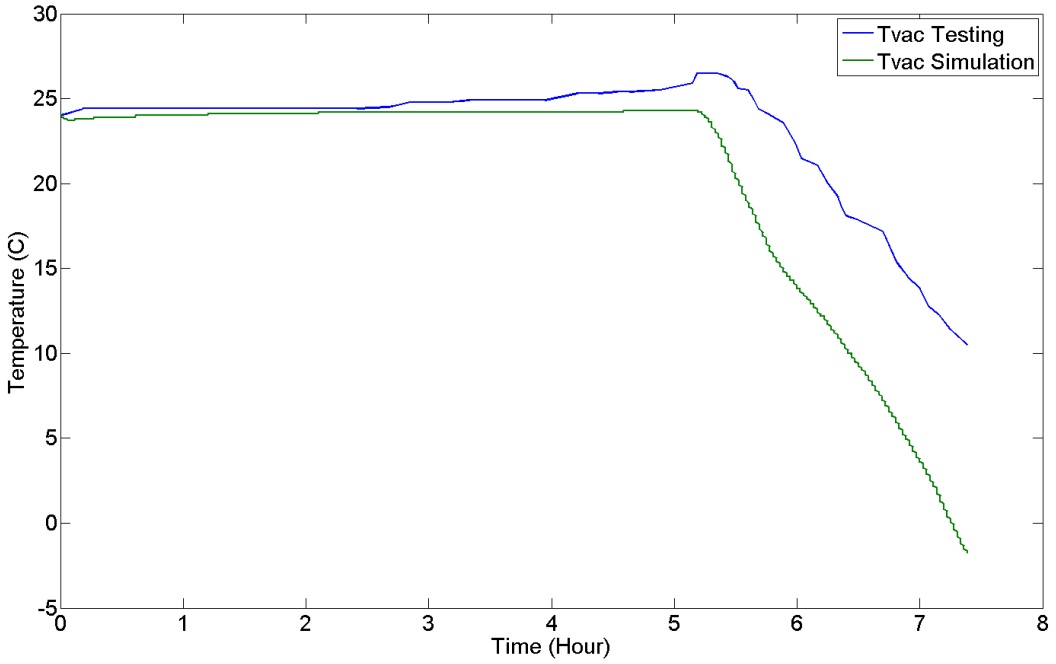

Figure 15.6: Temperature Plot: FE Ring

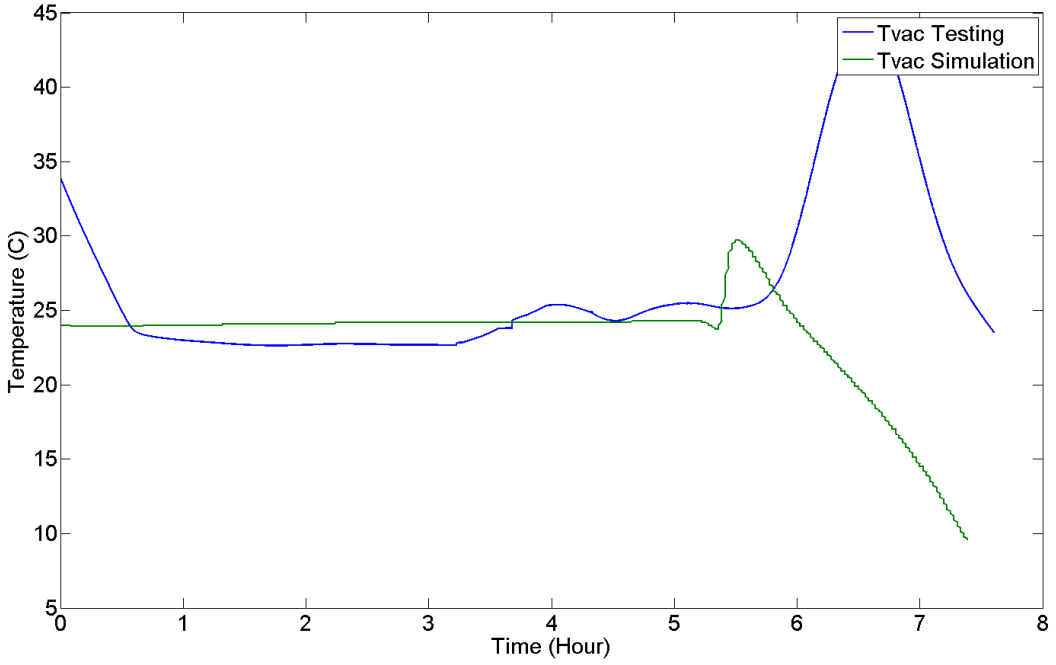

Figure 15.7: Temperature Plot: Power Amplifier on Beacon Board

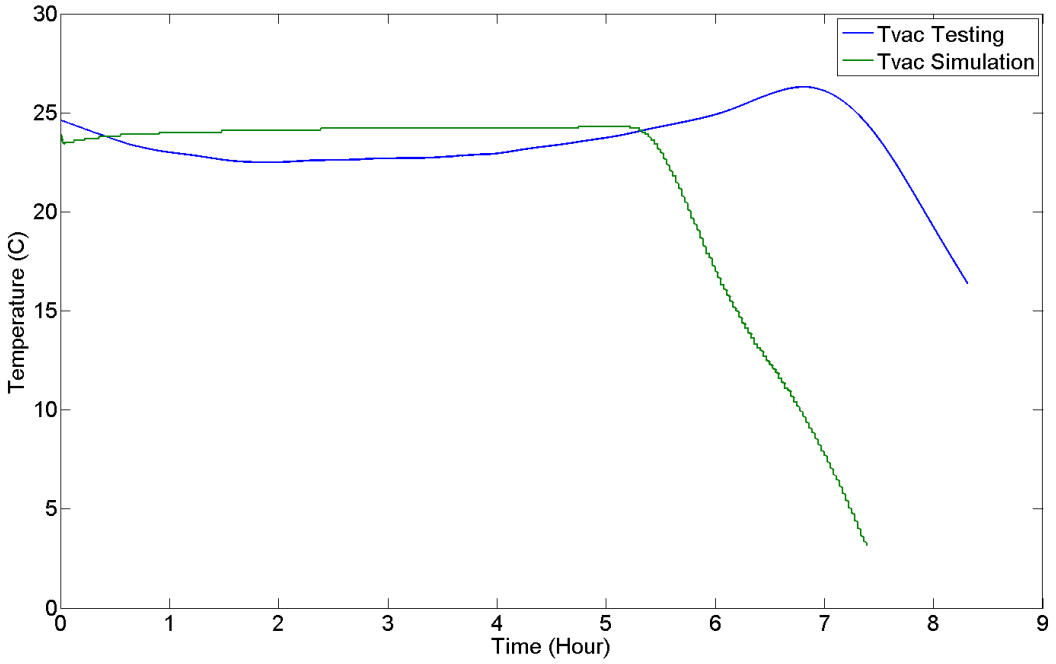

Figure 15.8: Temperature Plot: Battery

2. Hot Soak simulation: This simulation has been done for 2.6 hours, during which hot soak was performed. Heat dissipation for electrical components has been applied according to actual testing. Temperarature profile used for this simulation:

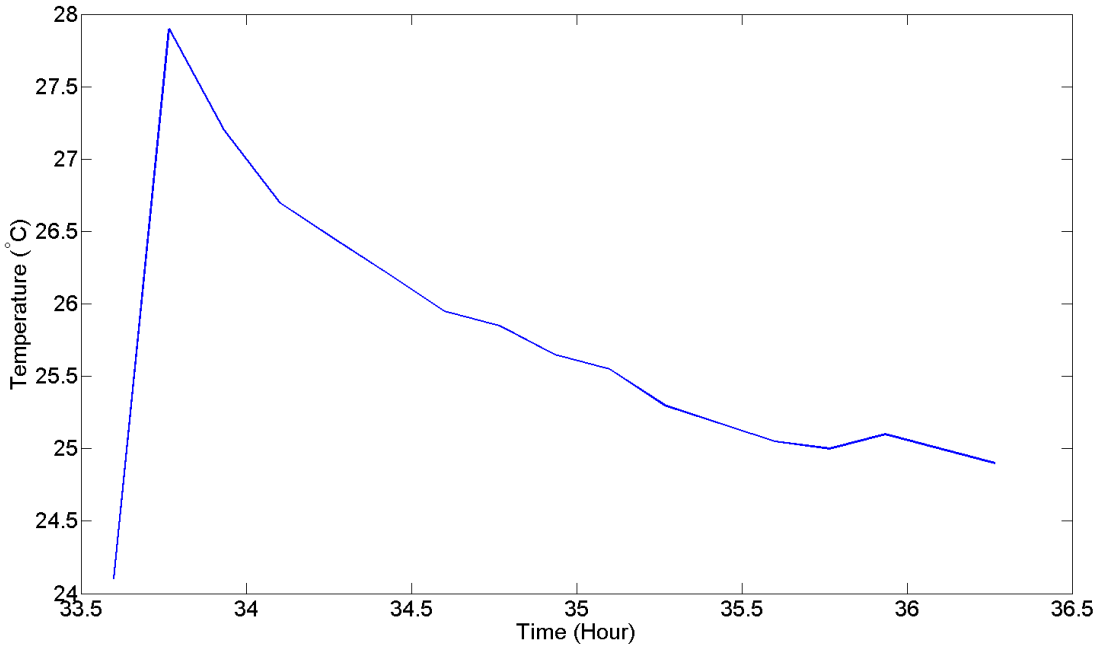

Figure 15.9: Temperature Profile used for simulation: During Hot Soak

Comparison of Plots Obtained from Thermovac Simulation and Testing:

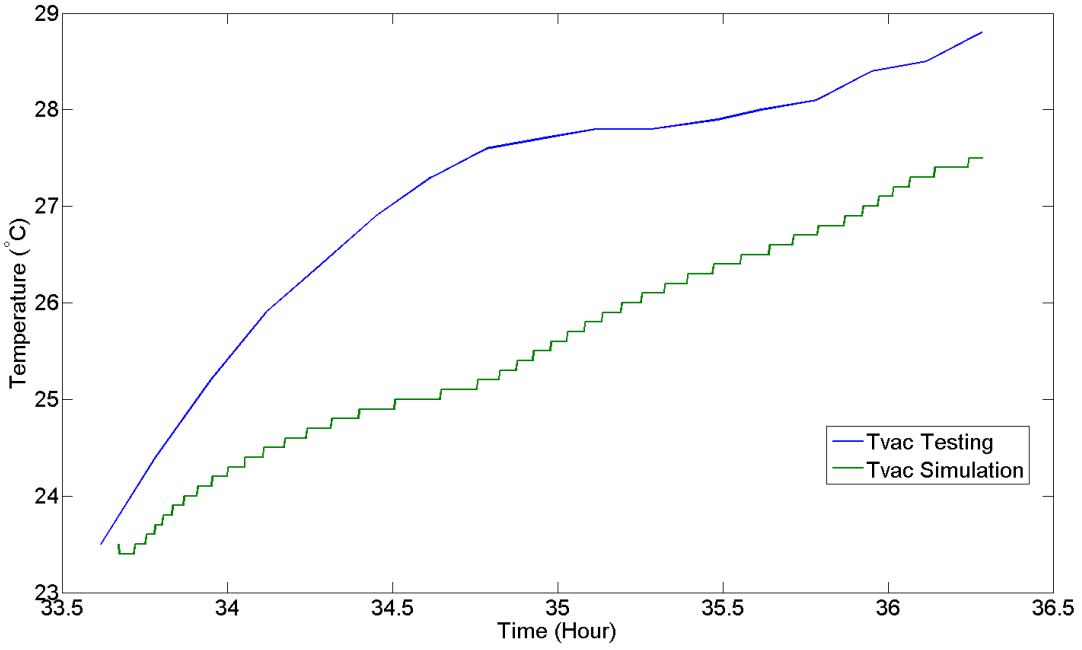

Figure 15.10: Temperature Plot: FE Ring

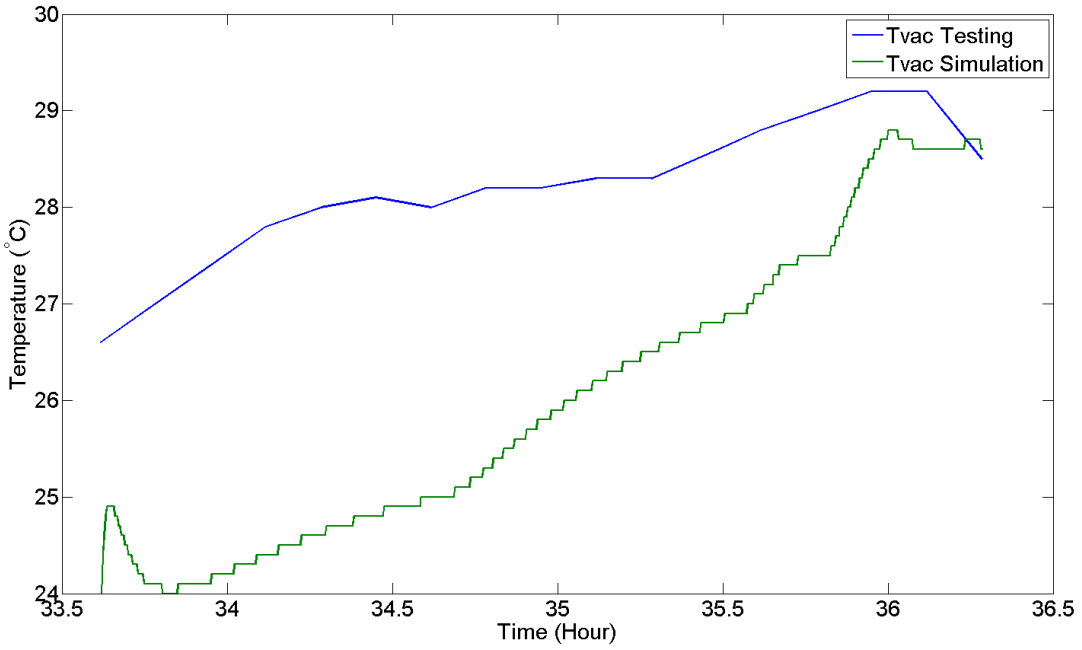

Figure 15.11: Temperature Plot: Anti-sunside

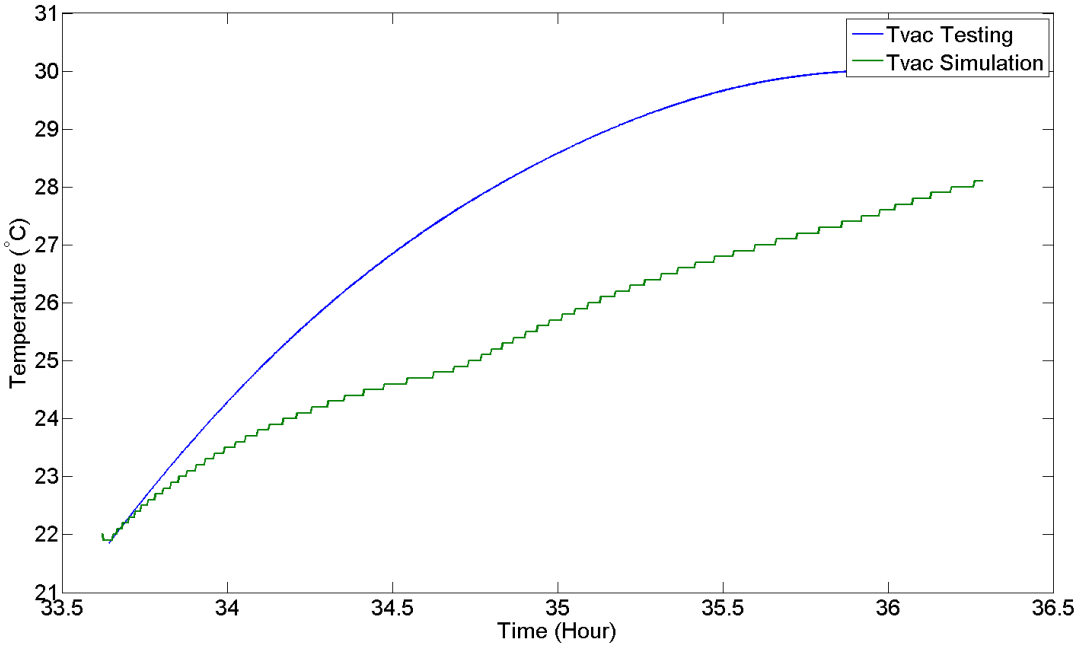

Figure 15.12: Temperature Plot: Battery

Inferences: Inferences:

1. Initial Temperature of a particular component in testing is not same as in simulation, because during testing, initially all the components were at different temperature while in simulation initial temperature of components was set to 24 ^{0}C.

2. Shape of temperature profiles are similar, but time lag can be seen. Time lag is relatively more for inner components (Communication boards) than outer components (Solar Panels).

3. Time lag mentioned above can be explained due to following reasons:

   (a) Wires used for temperature measurement by thermistors caries analog signals. And in our case length of wires used were longer than it should be for analog signal transfer causing time lag in data storage.

   (b) Thermistors were not mounted properly on the components which can cause time lag too.

   (c) Screws, Stubs and surface contacts have been modeled by total conductance which were calculated assuming, contacts are thermally ideal. But, in reality it never happens. So, in simulation, total conductance was more than that in testing. Which can explain pots of internal components. When snap was done after 5 hours beacon board experienced a temperature-kick before cooling down. This temperature-kick can be observed in case of simulation too, but of less magnitude. Because total conductivity defined between Power amplifier and Anti-sunside is more in the simulation thus heat is getting out very quickly which is not the case in testing. The same can be applied for other internal components. Due to this reason peak temperature achieved is more in testing and that is why it is taking a little extra time for cooling and thus generating a time lag.

   (d) Above argument supports the observation that time lag should be more in case of inner components than in case of outer components.

15.4 Functionality Check - Results

15.4.1 Test Results: Power Subsystem Perspective

SNAP

1. Two SNAP connectors were used in parallel for redundancy and the micro-controller woke up from sleep ONLY after both the connectors were removed.

2. The micro-controller on the Power board went for a further sleep of 5 minutes after SNAP and the loads were started only after waking up from this sleep. In the flight code, this period will be increased to 50 minutes so that the satellite is sufficiently away from the launch vehicle before starting the loads. This feature was satisfactorily tested.

Battery Charging and power sharing between Battery and Solar Panels **Testing Environment:** An external power source was used to charge the battery. Two wires from the DB 50 connector coming out of the chamber were used for charging purposes. The external power source acted as a solar panel, i.e. it was directly connected to the output of the solar panels in the Power Board. Therefore, the Power Board could not distinguish between solar panel and the external power source.

Observations: The following observations were made during the **second thermal cycle**

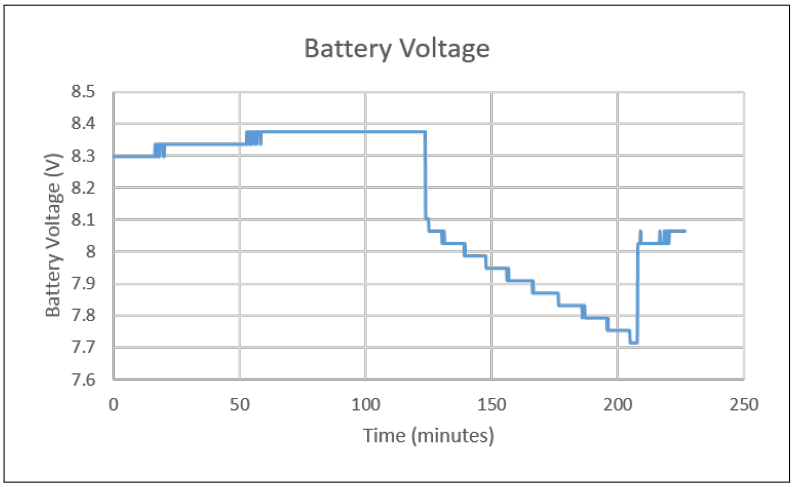

Figure 15.13: Battery Voltage

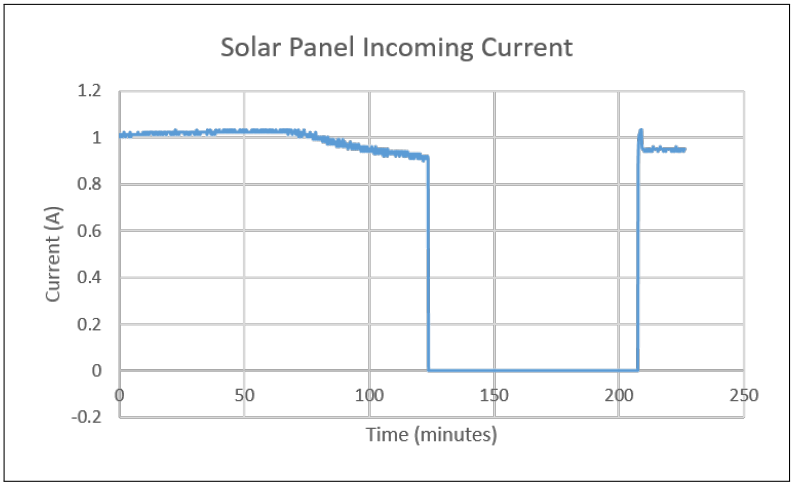

Figure 15.14: Current coming in from the Power Source

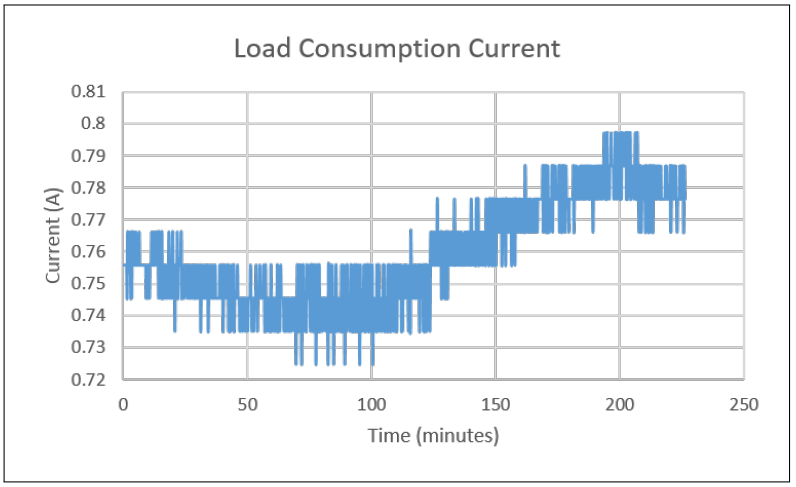

Figure 15.15: Current fed to the loads

Results and Inferences:

1. As can be seen from Fig. 15.15, the load consumption current is almost a constant with a difference of 0.7 A between minimum and maximum values. Thus the load current requirements can be assumed to be constant.

2. As can be seen from Fig. 15.13 and Fig. 15.14, the battery is charged via the Constant Current Constant Voltage mode CC-CV mode, which is essential for charging the Li-ion battery. Initially the charging charge is constant and the battery voltage is increasing and once it reaches the threshold (8.37 V in this case), the battery voltage remains constant, while the charging current gradually tapers off. Thus, the charging of the battery was satisfactorily tested.

3. Figures 15.13 and 15.14 also show that in the absence of solar power, the battery provides all the power required to drive the loads while if sufficient solar power is present, then all the power required to drive the loads is provided by the solar panels while the surplus is used to charge the battery.

Power-OBC Communication:
The communication between Power and OBC was verified both ways during the functionality check as follows:

1. On externally sending the signal to the OBC to start the downlink, the OBC would command the Power Board to turn ON the downlink board in the immediately next loop. The start of the Downlink transmission indicate that the communication from the OBC to the Power Board was successful and the Power Board faithfully followed the commands.

2. On turning ON the downlink, the load consumption current would increase and also the bit corresponding to the Downlink in the LoadStatus byte of the HM data

would change from 0 to 1. The increase in load consumption current on turning ON the downlink is shown in Fig. 15.16. The observations of these changes on the house-keeping telemetry GUI indicate the successful transmission of HM data from Power to OBC.

Power-Uplink communication and Reset of the Satellite

1. The Power Board checked for the Reset signal in each loop and on receiving the reset signal from the uplink, the micro-controller on the Power Board turned off all the loads for five seconds and then started the required loads again.

2. For testing this feature during the thermo-vacuum test, the software of the micro-controller of the Power board was designed such that the board would send all the HM data bytes as '0' on receiving the uplink signal and then reset the satellite.

3. Observing '0's on the house-keeping telemetry in the immediately next loop after sending the reset command to the uplink proved and the subsequent delay of 5 seconds in getting the next set of data on the GUI proved that the Power-Uplink communication was working well and that the power board was effectively resetting the satellite on receiving the signal. Also, the returning of the load consumption current after reset to the value when both Downlink and Uplink were OFF (see Fig. 15.16) further proves that the Power-Uplink communication and the subsequent reset were successful.

The following profile of the load consumption current was observed during the functionality check in the hot soak:

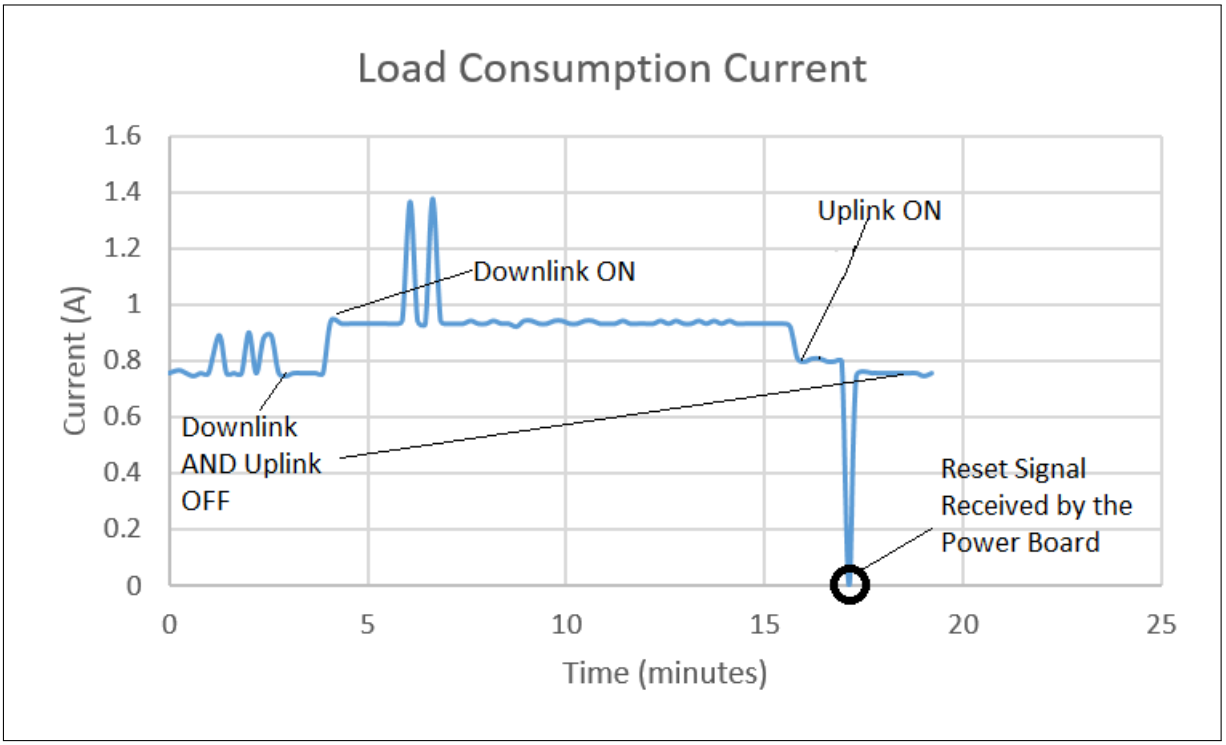

Figure 15.16: Load Consumption Current during Hot Soak

Notes:

1. The couple of peaks that are observed in the above profile are due to erroneous data.
2. This is not the load consumption current profile for the entire period of the hot soak, but a snippet of the profile.

15.4.2 Health Monitoring Data Results:

Data	**Unit**	**Expected Value**	**Observed Value**
Total Solar Panel Incoming Current	Ampere	0 - 1.2	0 - 1
Battery Voltage	Volts	6-8.4	7.5-8.3
Downlink Voltage	Volts	5	5
OBC Voltage	Volts	3.3	3.28
Over current Byte Status	No over current	1	1
	over current	0	
Load Status	Beacon	0: Off/ 1: On	1
	Torquer	0: Off/ 1: On	1
	GPS	0: Off/ 1: On	1
	Downlink	0: Off/ 1: On	Value switching as expected
	OBC	0: Off/ 1: On	1
	Magnetometer	0: Off/ 1: On	1
Load Consumption Current (Ampere)	OBC+Magnetometer +Beacon	approx 0.75*	Case not observed
	OBC+Magnetometer +Beacon+GPS	approx 1.17*	0.75
	OBC+Magnetometer +Beacon +GPS+Downlink	approx 1.77*	1.1
	OBC+Magnetometer +Beacon +GPS+Uplink	approx 1.77*	0.88

Table 15.3: Health Monitoring Data - Expected and Observed Values

* : Absolute maximum values

Inferences:

1. All the critical voltages and currents are within the expected range
2. Over-current was not observed anywhere
3. The Load consumption currents are much lower than expected as the expected values are the absolute maximum values. Beyond these values, overcurrent signal would have been be generated.

15.4.3 Sensor Results

Data	Condition	Expected	Observed
Sunsensors	During the Test	300-600 (for each sunsensor)	All values within range
	Before and after the test, on the application of torchlight	>600	All values above 600 except sun-side sunsensor
GPS	During the test	-	Transmission by GPS was verified by data in house-keeping telemetry
Magnetometers	During the test	-	Constant values, which changed when magnetorquers were turned ON

Table 15.4: Sensors - Expected and Observed Values

Inferences:

1. No problems were observed with any sensors
2. The change in magnetic field values when the magnetorquer was turned ON indicate that the magnetometer is working well
3. The increase in the values of the sunsensors on the application of a torch-light both before and after the tests indicate that the sunsensors were not damaged during the test. (Note: The sunsensor on the sun-side was not working before Vibration Test itself)

15.4.4 Actuator Results

Condition	Magnetic Field - x component	Magnetic Field - y component	Magnetic field - z component
All torquers OFF	2023	3731	2917
Torquer X turned ON	1944	3594	3592
Torquer X turned OFF and Torquer Y turned ON	2543	1876	640
Torquer Y turned OFF and Torquer Z turned ON	2960	4024	2274

Table 15.5: Changes in Magnetic Field values on Turning ON Torquers

Inferences:

1. As can be seen from table 15.5, the change in magnetic field values on turning ON the actuators was satisfactorily observed

Notes:

1. The magnetorquers were successively turned ON for **30 seconds** duration
2. The values were taken after more than 20 seconds of switching to each condition. The magnetometer values had become constant by then.
3. X axis: Lagging to Leading
4. Y axis: Sun-side to Anti sun-side
5. Z axis: Zenith to Nadir

15.4.5 Beacon Gain:

Following parameters were monitored on Beacon board:

1. Temperature of Power Amplifier RF5110
   Two thermistors were placed on the PA board to monitor temperature. One reading was obtained in HM data by Master via Slave microcontroller on the OBC board and other was through NI-DAQ.
2. Output of the Power Amplifier on a Multi Domain Oscilloscope
   The gain at desired output frequency, the corresponding harmonics and bandwidth was observed whenever the satellite was active.

Observations and inferences

1. The beacon board was not working properly for a certain range of temperature. This problem was later solved after extensive tests. The details can be found in the "Beacon Debugging" report

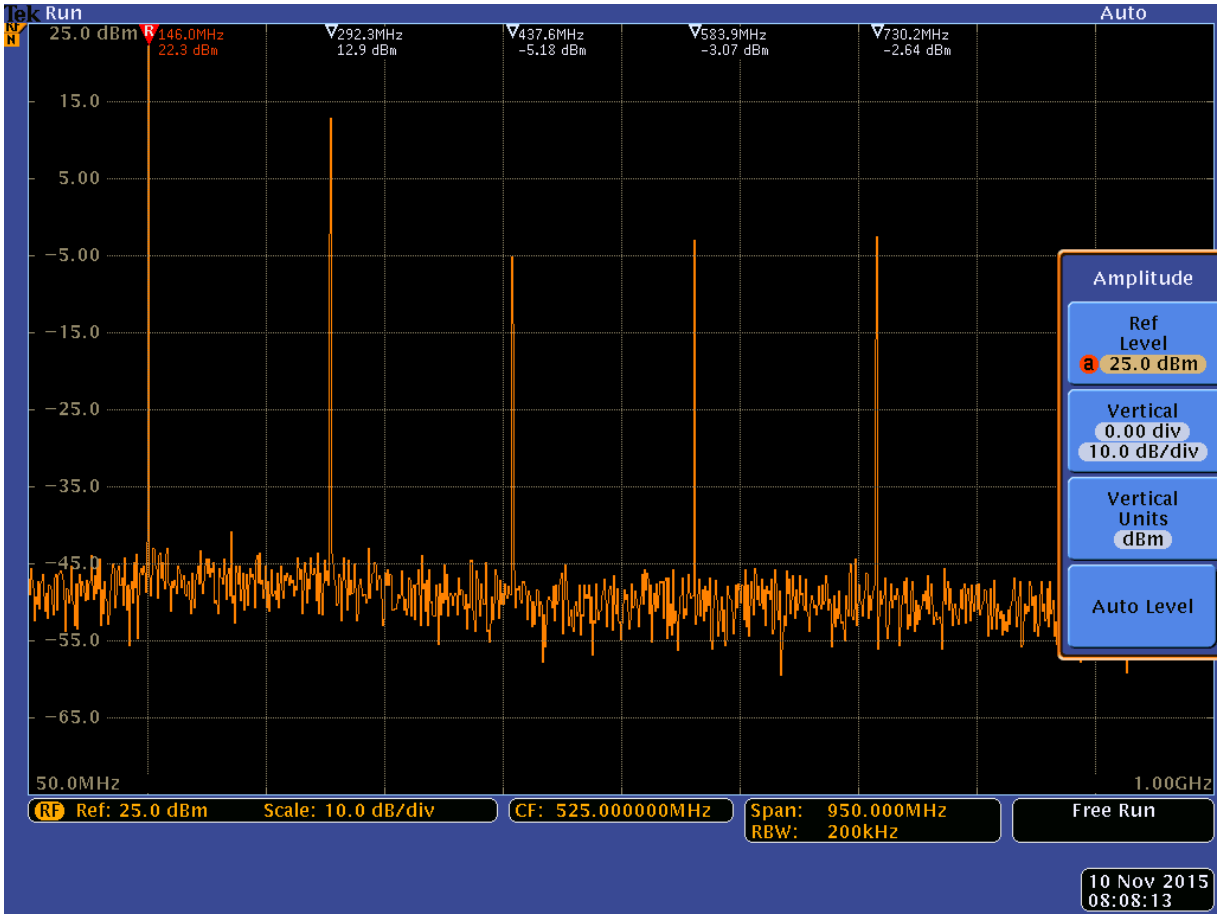

Figure 15.17: Observed Beacon Gain (While Functioning)

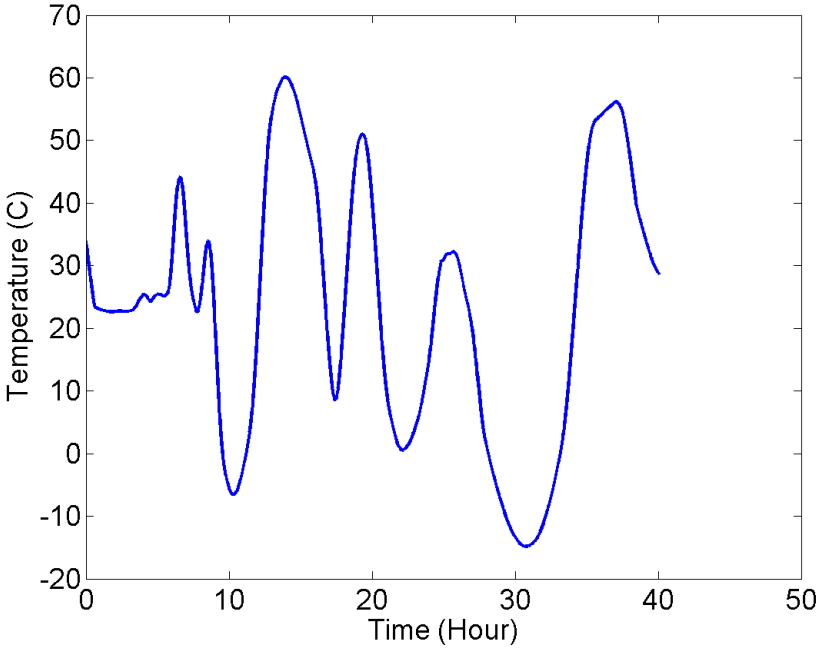

Figure 15.18: Beacon Power Amplifier temperature as observed on NI-DAQ

2. Whenever the beacon was working, the output of the Power Amplifier on the beacon board was, as expected, consistently between +21 to +23 dBm at the central frequency (145.98 MHz)

3. The output of the first harmonic (292 MHz) was 12 dBm, which is 10 dBm less than the central frequency. Subsequent harmonics have output less than 30 dBm from the central frequency.

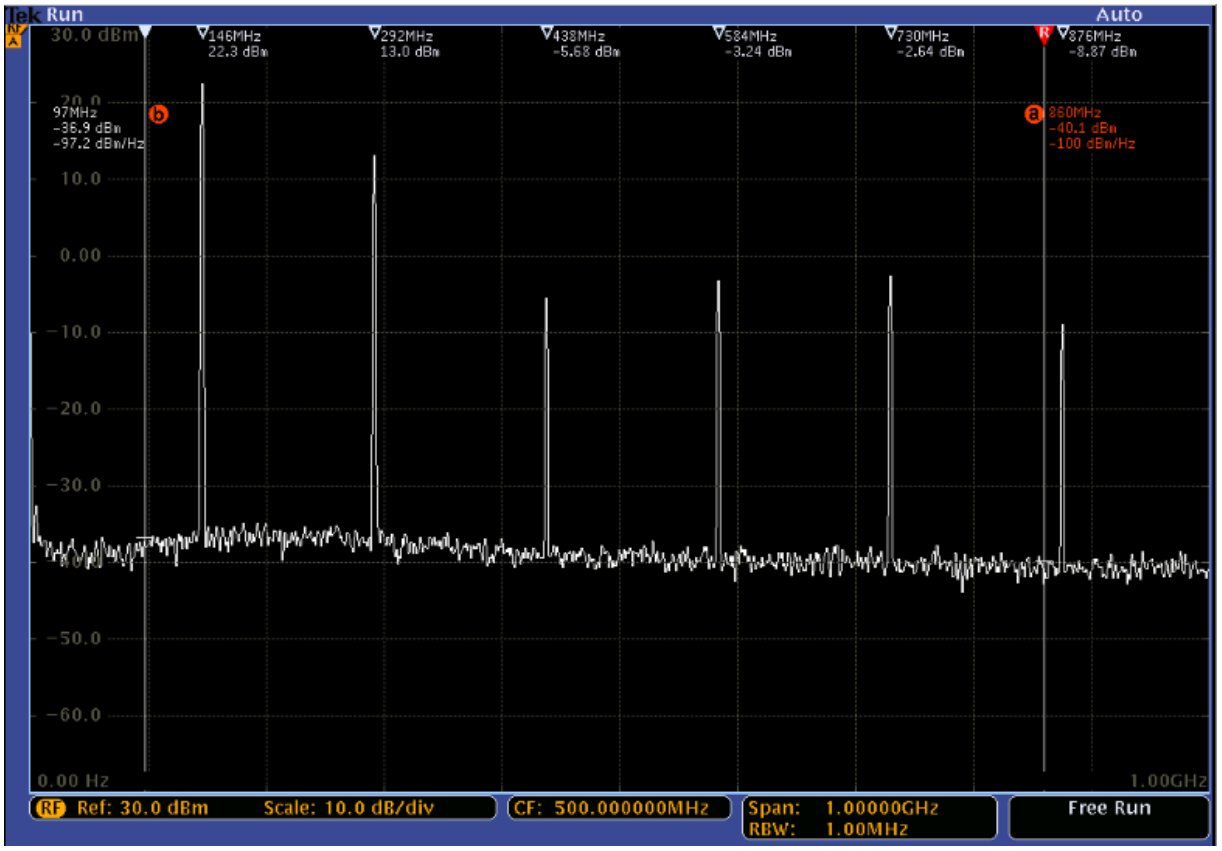

Figure 15.19: Beacon PA output during the HOT peak of first stress cycle

15.4.6 Downlink test

1. The data stored in the EEPROM was transmitted via the downlink to the uplink on the receiving side. The accuracy of the data was determined by comparing it with the corresponding house-keeping telemetry.

2. The temperature of the downlink Power Amplifier (PA) was observed using two thermistors. The output of one thermistor was a part of the house-keeping telemetry. The output of the other thermistor was measured separately and continuously using NI-DAQ.

Observations and inferences

1. Downlink board was switched on whenever commanded to do so from the GUI. Telemetry data was successfully received at the GUI end. It matched well with the housekeping data from OBC.
   Cold Soak

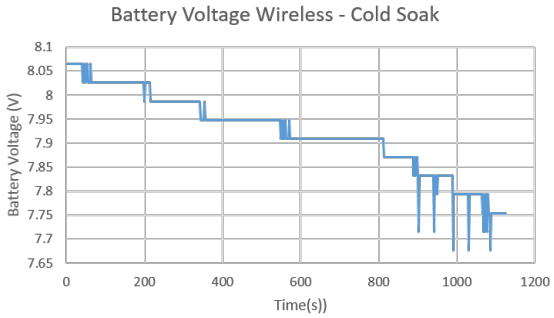

Figure 15.20: Battery Voltage - Payload Telemetry

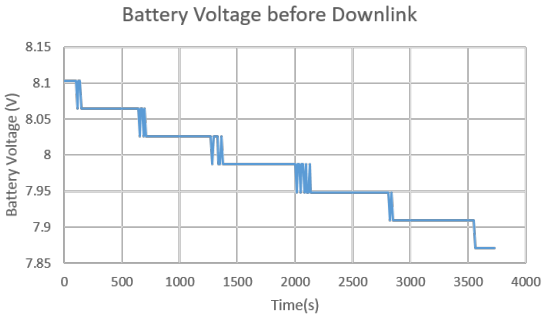

Figure 15.21: Battery Voltage - House-keeping telemetry

Hot Soak

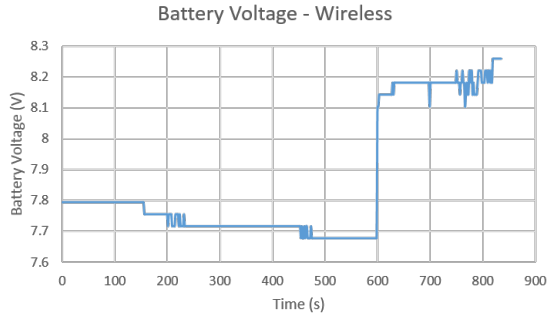

Figure 15.22: Battery Voltage - Payload Telemetry

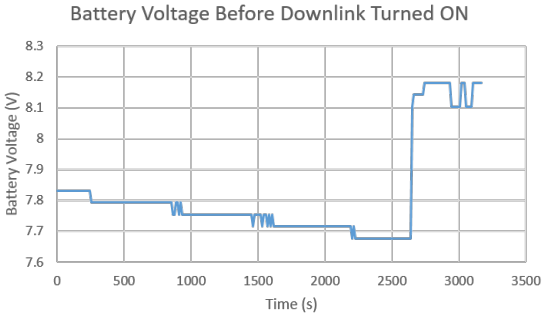

Figure 15.23: Battery Voltage - House-keeping telemetry

(a) The payload telemetry data matches well with the house-keeping telemetry data. A byte-by-byte check has also been done to check the same

(b) It appears that the payload telemetry is more informative. This is correct and the reason is that there is sub-sampling taking place. Only one of every five sets of data stored in the EEPROM is transmitted as house-keeping telemetry.

(c) Temperature was within the operational limits as expected. It worked in both Hot and Cold soak. Board is tested successfully for qualification level temperatures.

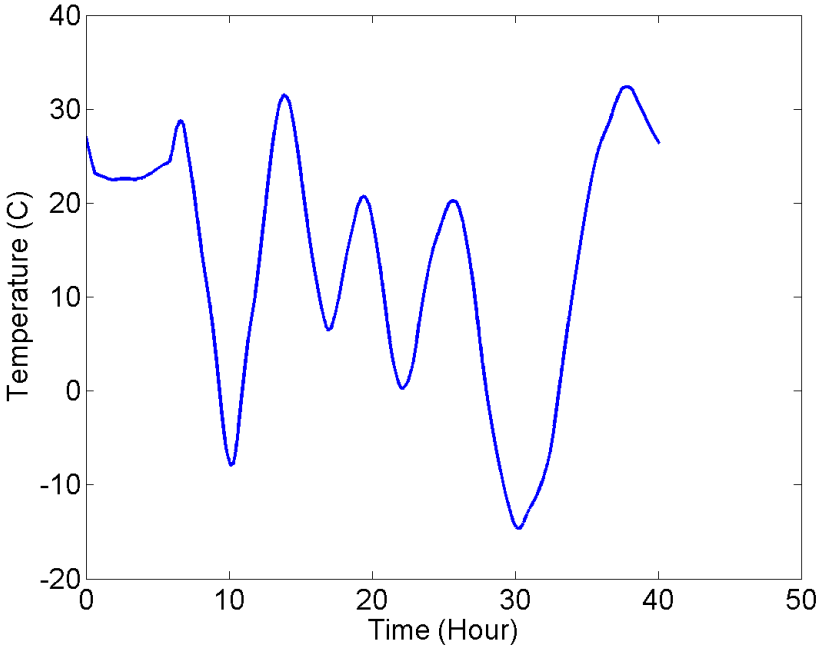

Figure 15.24: Downlink Power Amplifier temperature as observed on NI-DAQ

15.4.7 Uplink test

1. Reset Command was sent to the satellite when the Uplink was ON and the subsequent reset of the satellite was verified using house-keeping telemetry.

2. The temperature of the uplink Low Noise Amplifier (LNA) was observed using two thermistors. The output of one thermistor was a part of the house-keeping telemetry. The output of the other thermistor was measured separately and continuously using NI-DAQ.

Observations and inferences

1. Temperature was within the operational limits.

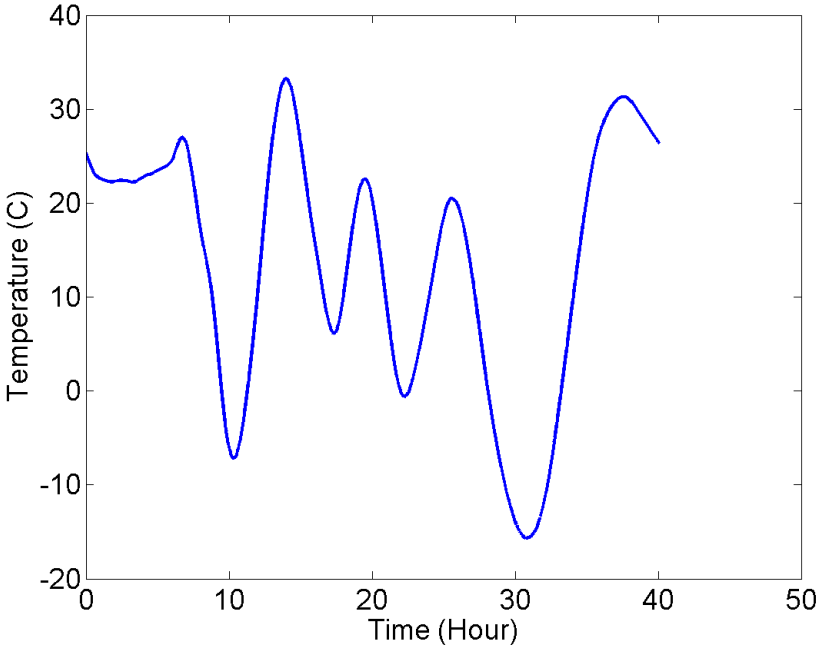

Figure 15.25: Temperature Variation: LNA on Uplink Board

2. Uplink was turned on by sending a wireless signal from the GUI. As expected it reset the whole satellite by turning off all the loads on the Power board and then turning them back on. It worked in both hot and cold soaks.

15.4.8 Component specifications

Component	**S11**	**S21**	**S12**	**S22**
Power Amplifier	-5.9 dBm	26 dBm	-70 dBm	-42 dBm
Co axial cable betwwen PA output and monopole input	-72 dBm	-0.32 dBm	-0.77 dBm	-75 dBm
Co axial cable from chamber to CC1101 at the GUI end	-70.7 dBm	-1.2 dBm	-2.15 dBm	-68.3 dBm
Monopole @ 145.98 MHz	-0.3 dBm	-	-	-
Monopole @ 437.45 MHz	-3 dBm	-	-	-

Table 15.6: Component Specification

NOTE: There was no difference in the co-cxial cable parameters in the bent mode. This might be due to our frequency been in the VHF range. The cable length is 3 inch which

is not comparable to the wavelength which is 2m.
The SWR of monopole at both the frequencies is not in the desirable range. This is because the monopole lengths are less than the recommended quarter-wavelength. Longer monopoles were not possible due to constraints of satellite envelope and structural strength. To ensure that the signal strength is enough we have tested the output power of the antenna. From the link budget calculations (in the "On-Board Communication" section) we are able to receive a positive system link margin. Moreover to validate this we are trying to receive signal from satellites whose EIRP is 40 - 100 mW which is close to our satellite's EIRP.

Appendices

Appendix A

Material Properties

A.1 Structural Properties

Property	Al 6016-T6	SS 304	FR04	GFRP
Density(kg/mˆ3)	2700	8000	1800	1800
Ultimate Tensile strength (MPa)	310	505	310	530
Tensile Yield Strength (MPa)	276	215	125	125
Modulus of elasticity(GPa)	68.9	193	24	26
Poisson's Ratio	0.33	0.29	0.136	0.28

Table A.1: Material properties

Material	Used in	Reason
Al 6061-T6	Satellite body, Solar panel backing plates Monopole antennae	Ductile, Lightweight, Easily machinable, Easily procurable,Cheap, Sufficiently stiff, Characterized for space applications
SS 304	Screws, Helocoils	Easy Availability Sufficiently stiff
FR 04	Base of Circuit Boards	
GFRP	Washers	

Table A.2: Materials Used

A.2 Thermal Properties

Property	Al T-6061	Solar Panel	FR-04	MLI	SS 304
Density(kg/m^3)	2700	2700	1900	0	8000
Conductivity(W/m-K)	155	0.192	0.23	0.05	16.2
Specific Heat Capacity(J/kg-K)	1256	755	1200	755	500
Absorptivity	0.2	0.75	0.65	0.36	
Emissivity	0.031	0.85	0.7	0.65	

Table A.3: Material properties: Thermal

Other emisivity values:

- Low emittance tape = 0.05
- OSR = 0.78

A.3 Thermal Conductivity Values

Object I	**Object II**	**Connected through**	**Total Conductance**
Solar Panel	Side	Screw and Washer	0.014
Side	Flange	Surface Contact	1.458
Side	Power Board	Stub and Screw	0.030
Side	OBC Board	Stub and Screw	0.030
Side	ADC Board	Stub and Screw	0.030
Side	Uplink Board	Stub and Screw	0.030
Side	Downlink Board	Stub and Screw	0.030
Side	Beacon Board	Stub and Screw	0.030
Side	Heat sink	Stub and Screw	0.066
PCB	Heat sink	Screw	0.070
Side	Magnetometer	Stub and Screw	6.597
Side	GPS	Stub and Screw	0.912
Side	MLI	Surface Contact	0.007
Beacon Board	Heat sink	Surface Contact	0.790
Downlink Board	Heat sink	Surface Contact	0.790
Uplink Board	Heat sink	Surface Contact	0.605
Side	Battery Box	Stub, Screw and Washer	0.013

Table A.4: Thermal Conductivity Values

A.4 Graphical User Interfaces

The following are the graphical user interfaces used for observing the house-keeping and payload telemetry and the critical temperatures during the thermo-vacuum test:

1. **House-Keeping Telemetry:**

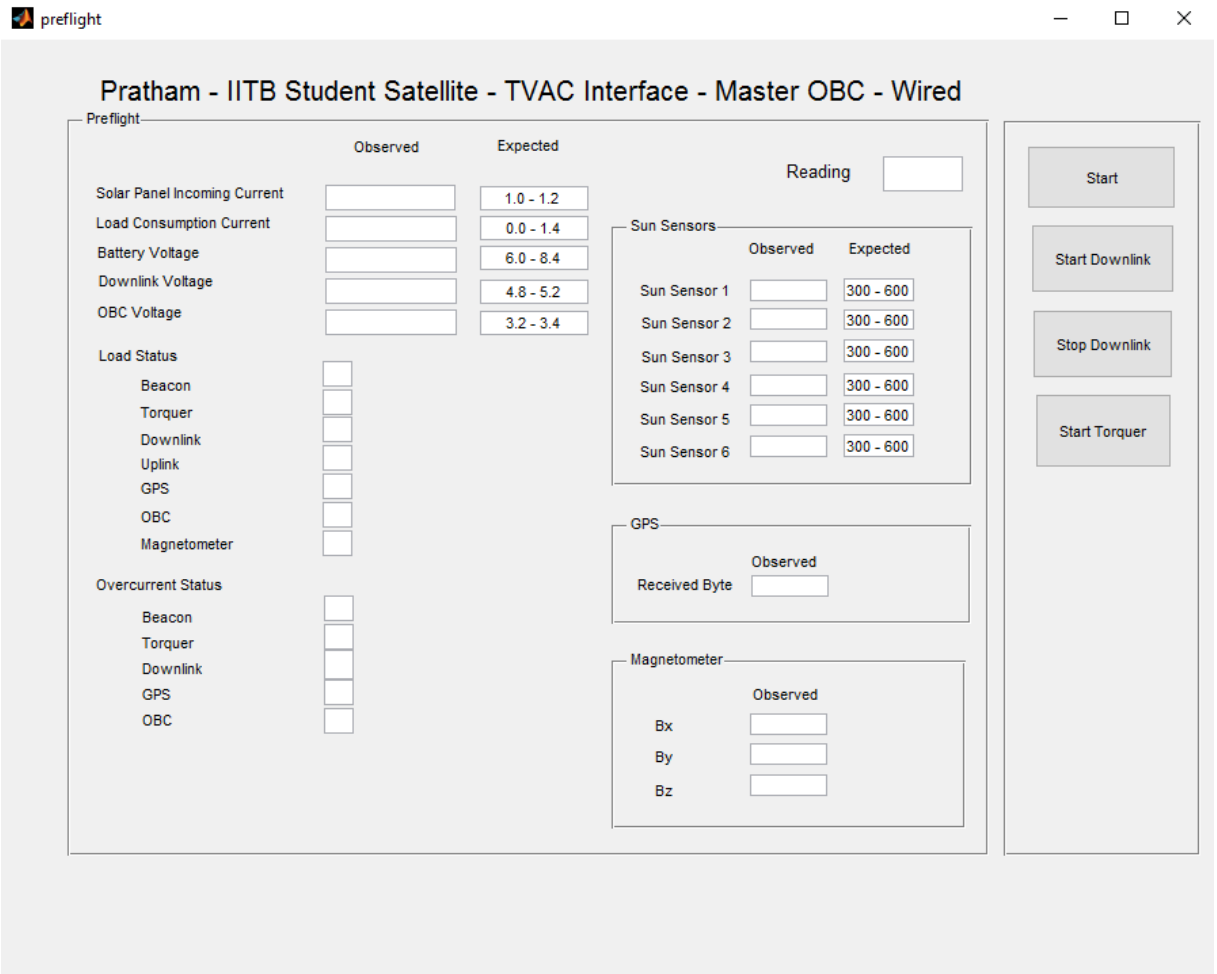

Figure A.1: GUI displaying the house-keeping telemetry received from the Master OBC

Notes:

- The left side of the GUI displays the HM data recieved from the Power Board. When a particular load is ON, the corresponding square is colored green in the Load Status section and when a particular load experiences overcurrent, the corresponding square is colored red in the Overcurrent Status section.
- The right side of the GUI shows the sensor readings.

- As discussed already, only the transmission of data by the GPS could be verified and hence, only one byte is taken from the GPS and displayed on the GUI

2. **Temperatures to be monitored in Flight:**

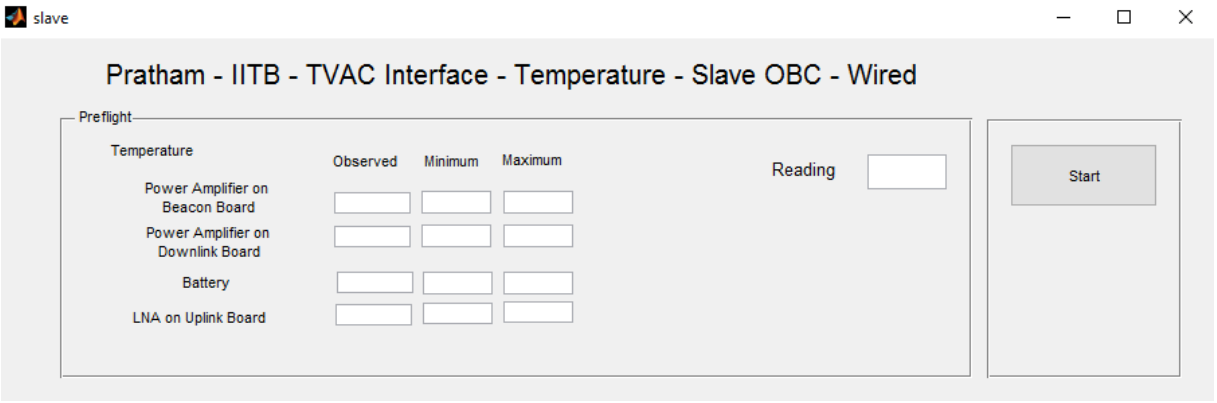

Figure A.2: GUI displaying the component temperatures that will be monitored in flight

Notes:

- The temperatures of four critical components will be recorded and stored in the EEPROM of the satellite in flight
- This GUI displays those temperatures as they are getting stored

3. **Payload Telemetry:**

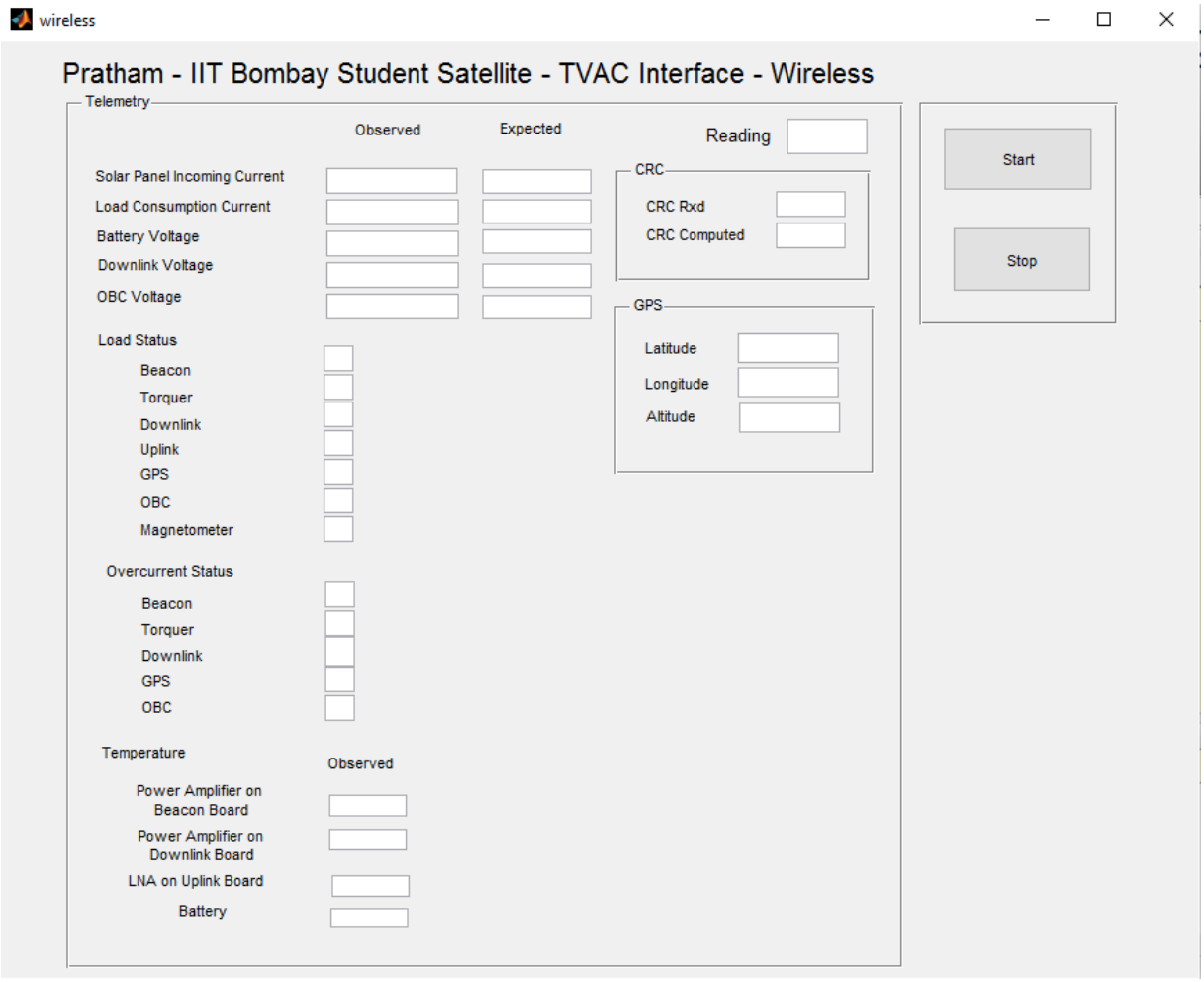

Figure A.3: GUI displaying the data received from the downlink

Notes:

- The health monitoring data and the temperature data along with real time latitude, longitude and altitude will be transmitted via downlink
- This GUI displays the data received and decoded by the uplink (Ground Station)

4. **Temperature monitoring during thermovac testing:**

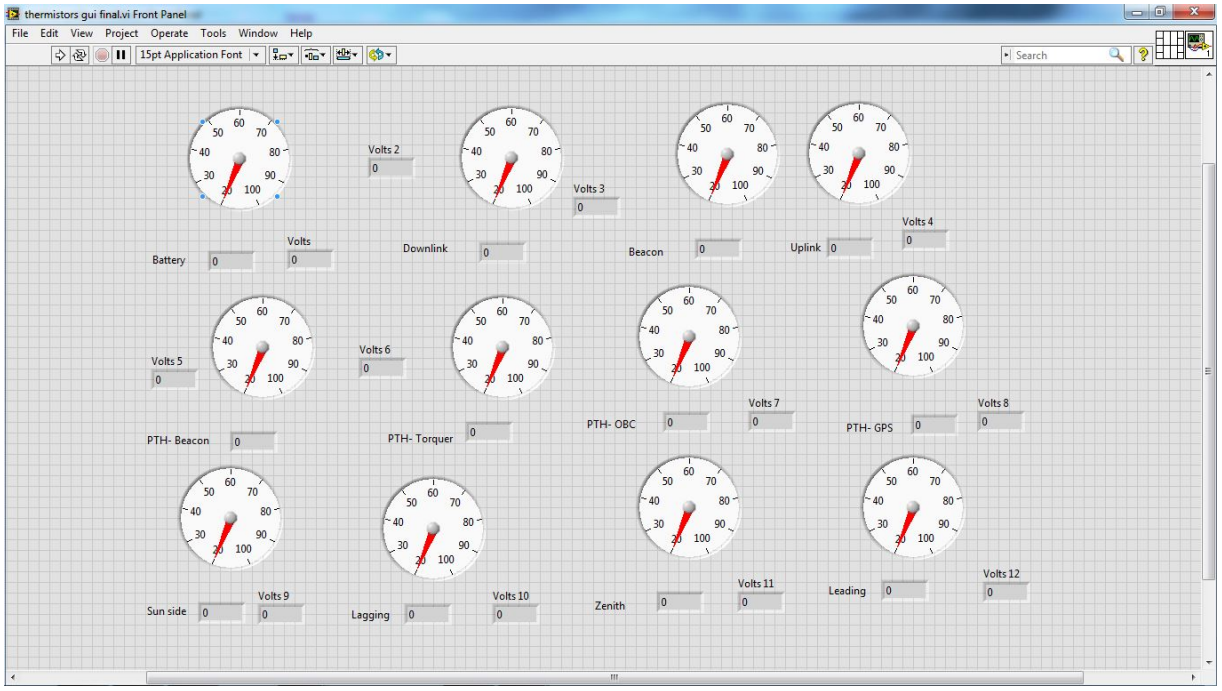

Figure A.4: A GUI showing the temperatures of many parts of the satellite.